The Efficacy of Using Small Molecule Ice Recrystallization Inhibitors to Enable the Frozen Storage of Livers

by

Nishaka Mevan William

A thesis submitted in partial fulfillment of the requirements for the degree of

Master of Science in Biopreservation

Department of Laboratory Medicine and Pathology
University of Alberta

Abstract:

The limited storage times afforded by hypothermic preservation at 0 °C to 4 °C imposes several logistic constraints on the organ transplant network. In the case of livers, two-thirds of wait listed patients do not receive transplants in Canada, which is partially attributed to the 12 h storage period under hypothermic conditions. Over the past seven decades, extensive research has gone into the development of methods to store organs at sub-zero temperatures in order to improving preservation standards. Emphasis is often placed on the avoidance of ice formation within tissues stored at sub-zero temperatures; however, these approaches come with their own respective challenges. Ice is not categorically damaging in tissues as evidenced by the survival strategies of several freeze tolerant organisms. Therefore, a preferable approach to sub-zero organ preservation may involve controlling the mechanisms through which ice damages tissues. Migratory recrystallization, the process through which large, more thermodynamically stable ice crystals grow at the expense of small ice crystals, is a major driving force for the cellular and structural damage that ice imparts. Thus, we sought to evaluate the efficacy using small molecule carbohydrate-derived ice recrystallization inhibitors (IRIs) our group has developed to minimize both intra- and extracellular ice recrystallization.

Hepatocytes comprise approximately 80% of the cellular mass of the liver and are highly prone to the formation of intracellular ice due to their high activation energy for water transport. Therefore, we evaluated the toxicity of three different IRIs as well as their ability to permeate and control intracellular ice recrystallization in HepG2 cells, a commonly used human liver cancer cell line. IRI 2 and IRI 3 demonstrated a significant reduction in the rate of intracellular ice recrystallization under a treatment condition where they did not prove to be toxic. The intracellular activity of each compound was further evaluated in the presence of permeating and non-permeating cryoprotective

agents (CPAs), which are vital to the recovery of cryopreserved cells and tissues. Generally, there was a loss of IRI activity in the presence of the four most commonly used permeating CPAs: ethylene glycol, glycerol, DMSO, and propylene glycol. IRI 2 demonstrated complete loss of intracellular activity in all cases, whereas IRI 3 retained activity in glycerol, DMSO, and propylene glycol. Interestingly, in the presence of trehalose, a commonly used non-permeating CPA, the activity of IRI 1 was improved while that of IRI 2 was diminished. IRI 3 activity, on the other hand, did not appeared to be altered in the presence of trehalose.

The liver consists of five different cell types, potentially leading to different toxicity outcomes than those seen in a single cell system. IRI 2 did not elicit any toxic effects following 30 min of subnormothermic machine perfusion (SNMP) in whole rat livers. Furthermore, this compound proved to be capable of permeating liver tissues and minimizing recrystallization, thus setting the stage for the implementation of this compound that has recently been designed to store livers in a frozen state at high sub-zero temperatures. The compound did not, however, improve post-thaw functional outcomes following 1 day of storage at -10 °C or 5 days of storage at -15 °C. Whether this is the result of a lack of IRI activity in the CPA solutions used or the result of other forms of freezing injury taking precedence over recrystallization injury, requires further investigation.

This work does not definitively establish the efficacy of small molecule IRIs in the frozen storage of livers; however, it highlights key considerations that need to be taken in future evaluations. Furthermore, it provides a better understanding of the ability of these compounds to control of intracellular ice recrystallization, which may prove valuable in the development of freezing protocols where intracellular ice formation (IIF) is probable.

Preface:

This thesis is an original work by Nishaka William. The research described in section 3.2.1 of Chapter 3, received research ethics approval from the University of Alberta Research Ethics Board, "Organ Preservation Techniques", AUP00003409, October 16th, 2019. The research described in section 3.2.2 of Chapter 3, received research ethics approval from the Institutional Animal Care and Use Committee (IACUC) at Massachusetts General Hospital (Boston, MA, USA), "High Subzero Preservation of Liver for Transplantation", 2017N000227, December 12th, 2017.

The method used to visualize ice crystals within frozen tissues as described in sections 3.2.1.3 and 3.2.1.4 has been published as L. Lautner, N. William, and J.P. Acker, High subzero cryofixation: A technique for observing ice within tissues. Cryobiology 95 (2020) 116-122. I contributed to the experimental design, data collection, and manuscript composition. L. Lautner assissted with the experimental design, data analysis, and manuscript composition. J.P. Acker was the supervisory author and was involved with concept formation and manuscript composition.

Experimental design, data collection, and data analysis described in Chapter 2 and Section 3.2.1 of Chapter 3 were performed by myself with input from Dr. Jason P. Acker. The work described in section 3.2.2 of Chapter 3 was part of an international research collaboration led by Dr. Jason P. Acker at the University of Alberta and Dr. Shannon N. Tessier at Harvard Medical School. This work was performed at Shriners Hospital for Children in Boston, MA, USA in Dr. Shannon N. Tessier's research lab. The experiment was based on a protocol developed by Dr. Shannon N. Tessier, Dr. Reinier de Vries, Stephanie E. J. Cronin, and Casie Pendexter (Shriners Hospital for Children, Boston, MA, USA and Center for Engineering in Medicine, Harvard Medical School & Massachusetts General Hospital, Boston, MA, USA). Casie Pendexter performed the liver procurements for these experiments. My role involved assisting Stephanie E. J. Cronin and Casie Pendexter in formulating the perfusion solutions, running the perfusion equipment, evaluating functional parameters during perfusion, and performing the data analysis.

Acknowledgements:

I would like to thank my supervisor Dr. Jason Acker for the unwavering support and guidance throughout every aspect of my graduate studies. I can say without a doubt that your mentorship has not only made me a better scientist, but also a better person. Your passion for research, brilliant problem solving, impeccable work ethic, integrity, and kindness, will always be a source of inspiration.

Thank you to all the members of both Dr. Jason Acker and Dr. Locksley McGann's research groups who made the lab an engaging place to do research and fostered a collaborative environment. I am incredibly grateful to Dr. Leah Marquez-Curtis, Tracey Turner, and April Xu, who consistently provided me with support in the lab. A very special gratitude also goes to my fellow graduate students Anusha Sajja, Wenhui Li, and Larissa Lautner for their help, support, and friendship. I want to particularly single out Larissa Lautner whose scientific insight, work ethic, and ambition has constantly pushed me to challenge myself. I am incredibly grateful to have had the opportunity to work alongside you.

I sincerely appreciate the insight and comments that members of my supervisory committee, Dr. Jayan Nagendran and Dr. Shannon Tessier, have provided throughout my degree. I especially want to thank Dr. Shannon Tessier, Dr. Reinier de Vries, Stephanie E. J. Cronin, and Casie Pendexter, for hosting me in their lab in Boston and showing me the utmost kindness. You allowed me to have a wonderful experience in a new city and take part in research that will inspire me for years to come.

A heartfelt thanks goes to my previous mentors, Dr. Judith Hugh, and Dr. Lacey Haddon. While you did not play a part in this project, it was the incredible experience I had doing research with the two of you which drove me to pursue this degree.

I would like to thank Cheryl Titus, and Dr. Monika Keelan, who both put incredible amounts effort into supporting graduate students in the Department of Laboratory Medicine and Pathology.

Finally, I will forever be grateful to my parents, Harindra William and Vijitha Silva, as well as my brother, Dilusha William. You push me to reach for the stars and have been a constant source of support and encouragement throughout this degree.

Table of Contents

List of Figures

List of Tables

Abbreviations:

AF(G)P	antifreeze (glyco)protein
ANOVA	analysis of variance
ECM	extracellular matrix
CPA	cryoprotective agent
DBD	donation after brain death
DCD	donation after cardiac death
DMEM	Dulbecco's modified eagle's medium
DMSO	dimethyl sulfoxide
DPBS	Dublecco's phosphate buffered saline
EG	ethylene glycol
HMP	hypothermic machine perfusion
HUVEC	human umbilical vein endothelial cells
IBP	ice binding protein
IIF	intracellular ice formation
INP	ice nucleating protein
IRI	ice recrystallization inhibitor
RBC	red blood cell
LT	liquidus tracking
PIP	paracellular ice penetration
PG	propylene glycol
SNMP	subnormothermic machine perfusion
TH	thermal hysteresis

Chapter 1 Introduction

1.1 Complex Tissue Preservation and "Ice Problem" at Sub-Zero Temperatures

Limitations in complex tissue preservation have proven to be a major bottleneck to the development and adoption of regenerative medicine therapies, ranging from tissue engineering to organ transplantation [87]. Standard organ preservation involves static cold storage (SCS) at 0-4 °C in acellular preservation solutions designed to combat the stressors of cold ischemia [28; 128; 167; 247]. The reduction in the kinetics of biochemical reactions at these temperatures reduces rates of aerobic metabolism by one-tenth at 4 °C, which enables storage anywhere from 6 hours for hearts to 24 hours for kidneys [175; 178; 215]. Despite the clinical efficacy of applying this method to standard criteria donor organs, marginal grafts have a diminished ability to tolerate SCS [177]. Furthermore, the limited preservation times offered by SCS additionally limit the utilization of human leukocyte antigen (HLA) matching and immune tolerance induction due to both geographical and logistical constraints [211].

The emergence of machine perfusion systems has invigorated researchers, entrepreneurs, and clinicians around the world to improve complex tissue preservation techniques. Their benefits are largely derived from their capacity to serve as a platform for pre-transplantation screening, functional augmentation, and immunomodulation [254]. Several of these technologies developed in the past two decades are additionally beginning to see translation from the experimental to the clinical realm [113]. Hypothermic machine perfusion (HMP) has become the clinical standard for extended criteria kidneys following randomized control trials showing significant improvements when compared to conventional SCS [113; 165; 166; 243]. Subnormothermic machine perfusion (SNMP) has shown some success in a pre-clinical setting and nomothermic machine perfusion (NMP) has been clinically applied to lungs, hearts, and livers [52; 158; 251]. Recapitulating several core metabolic functions has recently allowed researchers to maintain key functional parameters following a seven-day normothermic perfusion of human livers, proving to be the most promising results thus far [74].

Despite these advances, maintaining ex vivo physiologic function becomes increasingly complex with extended durations. Furthermore, the transportation of continuously perfused organs using even the most state-of-the art equipment remains a challenging endeavour. Static cold storage (SCS) persists primarily due to the expense and ease of this technique. As a result, there is significant value in exploring the preservation of complex tissues in a static state for long periods

of time at sub-zero temperatures. This topic has been the subject of numerous studies throughout the past six decades and has been the primary concern of the Organ Preservation Alliance established in 2015 [83; 110; 126; 182; 185]. The integration between machine perfusion and cryopreservation has recently shown significant promise and has been highlighted as the path forward in complex tissue preservation [87].

Ice formation during sub-zero storage is consistently deemed the most damaging factor in the sub-zero storage of structured tissues and therefore efforts are largely centered around storage in an ice-free state. The cryostasis strategy of the *Rana sylvatica* wood frog, which can survive for extended periods of time at high sub-zero temperatures with 60-75% of its water frozen extracellularly, is evidence that ice formation in tissues is not inherently damaging [123; 212; 225; 226; 230]. Complete avoidance of ice comes with many challenges, therefore modulating the location and distribution of ice could prove to be an effective means of cryopreserving complex tissues. Reviewing the mechanisms by which ice causes damage at a single cell and a multicellular level will prove invaluable in the development of an optimal approach to store complex tissues at low sub-zero temperatures.

1.2 Principles Governing the Cryobiology of Dilute Cell Suspensions

The complex three-dimensional architecture of tissues leads to a host of damage mechanisms that need not be considered in conventional cell cryopreservation. Furthermore, many of the challenges seen in cellular cryopreservation are exacerbated by several orders of magnitude in complex tissues. While the cryopreservation of isolated cells has been the subject of numerous excellent reviews [142; 144; 147; 159; 181], it is valuable to briefly address the freezing response and cryoprotective methodology for single cells prior to accounting for the complexities of tissues. Doing so will contextualize several of the challenges seen at the cellular level in tissue cryopreservation.

1.2.1 The Freezing of Biological Systems

It is thermodynamically favourable for liquid water to form a crystalline state at temperatures below -0.6 °C in isotonic biological systems [124; 268]. This phase transition proceeds through a supercooled state that becomes increasingly unstable as temperatures are lowered [124; 268]. Ice typically forms in biological systems between -5 °C to -30 °C through the action of heterophase

impurities (ie. foreign substances or surface structures) that promote the aggregation of water molecules into a stable crystal lattice [245; 268]. This heterogenous mechanism of nucleation can shift towards a homogenous mechanism involving the stochastic self-association of water molecules at lower temperatures (-38 °C to -44 °C) depending on the volume [258]. Thermodynamic and kinetic constraints can limit nucleation at high and low sub-zero temperatures, respectively, resulting in an intermediate temperature range between the equilibrium melting point and the glass transition temperature where nucleation rates peak [114]. The glass transition temperature is reached once there is an insufficient amount of kinetic energy for nucleation to occur, resulting in the formation of a non-crystalline amorphous phase. Controlling ice formation and growth by modulating nucleation temperatures, solution characteristics, and cooling rates, forms the basis of many approaches to cell cryopreservation.

The abundance of heterogeneous nucleators in the ionic environment surrounding cells, results in the formation of extracellular ice prior to the formation of intracellular ice [142]. Exclusion of solutes during crystal formation creates an increase in the solute concentration of the extracellular unfrozen fraction [142]. This in turn creates a difference in chemical potential between the extra- and intracellular medium, resulting in chemical equilibration through either osmotic cellular dehydration or a cytoplasmic phase transition. Maintaining equilibrium through osmotic dehydration relies on a rate of cooling that is sufficiently slow such that the cell is able to eliminate intracellular supercooling. The more rapid the cooling rate, the greater the degree of supercooling, and the higher the probability of a cytoplasmic phase transition [64; 141; 149; 152]. Cellular injury can ensue upon excessive osmotic dehydration or intracellular ice formation at sub- and supraoptimal cooling rates, respectively [141; 152]. Maintaining cell survival is therefore predicated on a balance between these two biophysical responses, which has historically been attained through identification of optimal cooling rates and the use of permeating and non-permeating cryoprotective agents (CPAs).

1.2.2 Injury at Sub-Optimal Cooling Rates and its Avoidance Using Permeating Cryoprotectants (CPAs)

The discovery of glycerol in 1949 by Polge et al. and DMSO in 1959 by Lovelock et al. were major milestones in cryobiology, enabling levels of post-thaw recovery that could not be attained through cooling rate optimizations alone [133; 189]. The protective efficacy of these compounds

has been largely attributed to a colligative mechanism, wherein the volume of unfrozen water is increased at any given temperature. This has enabled increased survival of cells cooled at sub-optimal rates; however, the impact this has on cells that undergo intracellular freezing is currently not well characterized. Rationalizing why this colligative mechanism renders protective effects was historically a subject of debate and called into question the ways in which cells are damaged at sub-optimal cooling rates [132; 153; 160; 161; 262; 263].

Lovelock ascribed this damage to increases in the salt concentration of the unfrozen fraction due to continual freezing out of extracellular water as temperatures are lowered [132]. Thus, the protective effects of permeating CPAs was a virtue of their ability to quell excessive increases in the intracellular KCl and extracellular NaCl concentration [132]. This was corroborated by the finding that red cells hemolyzed upon exposure to hypertonic NaCl and subsequent dilution in isotonic conditions in the absence of freezing [263]. Further investigations however demonstrated that the same post-hypertonic hemolysis phenomenon was seen following exposure to hypertonic solutions of sucrose [161; 262]. From these observations, Meryman proposed that damage was not due to the salt concentration per se, but instead a result of an inability of the cell to shrink to the extent required for osmotic equilibrium [160; 161]. In this view, the protective effects of a permeating CPA are twofold. Colligative reduction in the size of the extracellular unfrozen fraction at any given temperature will correspond to a reduction in osmotic shrinkage. The corresponding increase in intracellular osmolality following CPA permeation will cause the cell to have a higher volume under isotonic conditions. The presumption that the composition of the unfrozen fraction is the key determinant in cell damage was called into question by a series of seminal publications by Peter Mazur throughout the 1980's [151; 154; 155]. He suggested that it is the volume rather than the composition of the unfrozen fraction that is the predominant factor in cell injury. CPA permeation was additionally found not to be a prerequisite to the survival of red cells subject to slow cooling, suggesting that osmotic shrinkage can't wholly account for damage [153]. Rather, the primary mode of damage would involve the unfrozen channels distorting the cells at low temperatures which prevents them from shrinking in an isotropic fashion, a phenomenon that has been visualized at a microscopic level [144; 196].

This colligative mechanism is fundamental to the protection imparted by permeating CPAs; however, studies have also pointed to non-colligative interactions on both a solution and cellular

level that contribute to their effectiveness. The sulfinyl group of DMSO, the most commonly used permeating CPA, forms two strong hydrogen bonds with water , which reduces the number of water-water hydrogen bonds as well as the number of water molecules available to form a critical nucleus [90]. This can promote increased solution viscosity which would result in a reduction in the diffusion of water molecules and consequently the rate of nucleation [90]. In retarding the rate and onset of nucleation, the stability of the amorphous state will be increased at higher temperatures which can facilitate vitrification approaches to cryopreservation. At a cellular level, this can reduce the likelihood of intracellular ice formation (IIF) as the cell is being frozen. The presence of interactions between the CPA and the lipid bilayer has additionally been linked to cryoprotective efficacy [15]. In the case of DMSO, electrostatic interactions between the polar sulphoxide moiety and the phospholipid membrane is critical to the protection it imparts [14; 103]. Compounds that interact with the bilayer solely through a hydrophobic mechanism have also proven to render cytoprotective effects, albeit to a lesser extent [15]. Furthermore, both glycerol and DMSO have proven to lower the lipid transition temperature, which can promote membrane stability during freezing and rewarming [23; 195].

1.2.3 Intracellular Ice Formation (IIF) In Isolated Cells

Precluding IIF is a guiding principle in modern cryobiology due to the diminished survival that is often associated with freezing conditions that preferentially form intracellular ice. The primary requisites for IIF are (1) the presence of extracellular ice, (2) supercooling of intracellular water at the nucleation temperature, and (3) a water content greater than 10% of the isotonic volume [143]. IIF typically occurs between -5 °C and -20 °C following extracellular ice formation in a range of cell types [144]. The regular occurrence of IIF at temperatures well above the homogenous nucleation temperature infers a heterogenous mechanism of nucleation and overwhelming evidence has implicated extracellular ice in this process [13; 45; 145; 148; 222]. Extracellular ice-mediated nucleation of the intracellular milieu has been attributed to the stability of ice at temperatures below a critical temperature that have a radius of curvature equivalent to that of aqueous pores in the cell membrane (3 – 8 Å) [145; 149]. The lack of direct evidence to support this led to the modified hypothesis by Toner *et al.* that extracellular ice can alter the thermal, ionic, electrical, and mechanical properties of the cell membrane, thereby rendering it an effective heterogeneous nucleator [242].

A key presumption of these two theories is that the intracellular ice formation is a cause rather than a consequence of membrane injury, which has historically been a subject of debate. Studies by Steponkus and Dowgert on acclimated protoplasts using high-resolution video cryomicroscopy demonstrated mechanical failure of the membrane prior to IIF [221; 222; 223]. McGann and Muldrew explained this by demonstrating that the movement of water creates hydrostatic pressure gradients across the membrane [170; 171]. The hydrostatic pressure gradient will increase as nucleation temperatures are decreased [170; 171]. This is a virtue of a reduction in the hydraulic conductivity of membranes at lower temperatures combined with an increase in the osmotic gradient that develops when the volume of the extracellular unfrozen fraction is lowered. Furthermore, the tensile strength of the membrane is reduced as temperatures are lowered [170; 171]. Therefore, once a critical level of cytoplasmic supercooling is reached, the hydrostatic pressure gradient can exceed the tensile strength of the membrane. This will cause the membrane to rupture and extracellular ice to seed IIF through direct contact with the supercooled cytoplasm [170; 171].

While IIF has been established as a major mode of cryoinjury, reports of innocuous IIF in isolated cells suggest that the rate of rewarming and the volume of intracellular ice are important determinants in post-thaw recovery [18; 21; 96; 129; 136; 143; 149; 156; 164; 213]. Rapid rewarming has been proposed to decrease rates of migratory recrystallization and the temperature at which melting of the intracellular medium takes place [21; 136; 149; 213]. Intracellular ice melts at a faster rate than extracellular ice, therefore solute concentration in the intracellular unfrozen fraction takes place more rapidly [85]. This results in the development of osmotic gradient that promotes cellular rehydration [85]. Rapid rewarming rates would increase the temperature at which water begins to move across the membrane, thus creating less frictional drag due to the greater hydraulic conductivity of the membrane at higher temperatures [85]. Decreasing the relative volume of cell water using isothermal holding steps following extracellular nucleation or non-permeating CPAs have proven to promote recovery of cells that have undergone IIF [143]. Under the assumption that seeding of IIF is a consequence of mechanical failure of the membrane, cases of innocuous IIF suggest that a damaged membrane can repair itself [170; 171].

1.3 The Freezing Response of Cultured and Packed Cells

Investigating the cryobiological behavior of a tissue through characterizing the biophysical properties of its constituent cells can promote a general understanding of how the tissue would respond to freezing. However, attachment to an extracellular matrix combined with the presence of cell-cell contacts can significantly alter biophysical properties and nucleation characteristics [99; 104; 231; 232]. This results in a fundamentally different freezing response that creates a barrier in making these types of extrapolations. Cultured cells contain cell-cell and cell-matrix contacts that can be likened to those in tissues and thus provide insight into several tissue-specific mechanisms of IIF. Furthermore, densely packed cell suspensions have a vastly different response to slow-cooling injury, which may prove relevant when freezing tissues containing dense arrangements of cells.

1.3.1 Tissue-Specific Mechanisms of Intracellular Ice Formation (IIF)

Cell-substrate contacts yield profound impacts on the IIF kinetics of tissue systems [99; 104; 231; 232]. Investigation of micropatterned single-cell constructs revealed two novel forms of IIF initiation specific to adherent cells, termed paracellular ice penetration (PIP) and peripheral-zone initiation [104]. The peripheral zone refers to the region at the periphery of a flattened cell, which represents 10% of the surface area. The remaining surface area is accounted for by the interior zone. The surface catalyzed nucleation theory of IIF posits a uniform distribution of IIF initiation sites across the apical surface of the membrane, therefore IIF initiation sites should theoretically correspond to the relative area of each zone [13]. High-speed video cryomicroscopy however revealed a disproportionate probability of IIF initiation in the peripheral zone, thus representing a departure from the surface catalyzed nucleation theory [232]. Furthermore, a correlation was seen between IIF initiation sites and the location that extracellular ice dendrites penetrate the paracellular space between the substrate and the basal cell surface [231; 232]. Increasing the cell surface area and thus the size of the paracellular space coincides with an increase in the prevalence of this mode of nucleation [231]. A likely explanation is that the contact angle between extracellular ice and the plasma membrane is increased at the cell-substrate interface, making this region a more effective site of nucleation [2]. Furthermore, in accordance with the osmotic rupture hypothesis of freezing injury, it is possible that local adhesions to a substrate can render the plasma membrane more prone to rupture during osmotic shrinkage [2; 171]. While further investigation

into the exact mechanism of is warranted, paracellular ice penetration and peripheral-zone initiation together accounted for nearly all IIF events seen in this adherent single-cell model [104].

Previous studies have indicated that the kinetic parameters for IIF in cultured cells is higher than that of isolated cells, which has been attributed to a non-random mechanism of IIF predicated on the presence of ice in adjacent cells [2; 3; 4; 30; 45; 104; 121; 257]. The complete mechanism of intracellular ice propagation remains unresolved; however, gap junctions have demonstrated substantial involvement in this process. Applying low-calcium media or gap junction inhibitors, such as dinitrophenol, heptanol, and 18β-glycyrrhetinic acid, has proven to significantly depress the rate of intercellular ice propagation through precluding gap junction formation or uncoupling gap junctions, respectively [6; 24; 30]. Early studies characterizing this phenomenon additionally demonstrated a temperature-dependent effect on the kinetics of propagation. Ice propagation in confluent monolayers of Madin-Darby Canine Kidney (MDCK) cells was limited at temperatures above -3 °C; however, a marked increase in the incidence of IIF and a wave-like pattern of ice propagation were seen below this temperature [6]. Thermodynamic modeling of this phenomena suggests the equilibrium crystal curvature at temperatures above -3 °C is too large to permit propagation through gap junctions [6]. This infers the existence of a critical level of supercooling above which propagation is thermodynamically improbable.

Incomplete inhibition of intercellular ice propagation in the absence of gap junctions suggests there are concurrent mechanisms of ice propagation at play that do not require intercellular channels. It is possible that intracellular ice in an adjacent cell can function in a similar manner to extracellular ice in isolated cells, rendering the plasma membrane in the adjacent cell an effective nucleator of intracellular ice [99]. Furthermore, recent evidence suggests the existence of distinct domains of supercooled liquid trapped between apposing cell membranes [99]. Nucleation of these domains has been portrayed as a variant of PIP taking place at the cell-cell rather than the cell-substrate interface [99]. While ice dendrites in the paracellular space may enable surface-catalyzed nucleation of the adjacent cell, they may additionally penetrate pre-existing membrane pores [99; 242]. Irrespective of the exact mechanism, this mode of nucleation would be highly dependent on the type of cell-cell junction. Tight junctions have paracellular pores that are 0.5 nm in diameter, whereas gap junctions and adherens junctions have membrane separation distances of 3 nm and 25 nm, respectively [220; 253; 266]. Large pore sizes would result in cell-cell PIP at higher

temperatures; however, there have yet to be studies correlating the dependence this form of PIP with the architecture of the cell-cell interface.

Developing mathematical models that account for these tissue-specific mechanisms of IIF can enable prediction of freezing responses under varying freezing conditions, promoting more efficient optimization of freezing protocols and improvement of freezing outcomes. It has historically been common practice to apply mechanistic models for isolated cells to tissue systems, which has been met with varying degrees of success as their failure to incorporate non-random mechanisms of IIF renders them phenomenological in this application [55; 244]. Recently developed Markov chain models incorporating intercellular ice propagation with the traditional stochastic mechanism of nucleation have proven to accurately predict the kinetics of intracellular ice propagation [104]. They have effectively modeled experimental observations in micropatterned two-cell and one-dimensional multicellular constructs and could theoretically be applied to two and three-dimensional constructs [104].

While cell-cell contacts are an important determinant in the kinetics and patterns of IIF; however, Acker *et al.* have revealed that these contacts can mediate IIF-related membrane damage [5; 8; 9]. IIF in confluent cell monolayers has proven not to result in an immediate loss of membrane integrity, which is commonly the case in cell suspensions and individually attached cells [5; 8; 9]. This infers that intercellular ice propagation through gap junctions or cell-cell PIP can render IIF innocuous. In addition to dissociating IIF from membrane damage, IIF was found to yield protective effects during subsequent slow cooling [5; 10]. Survival of MDCK epithelial cells and V-79W fibroblasts cooled at 1 °C/min to -40 °C in the absence of a chemical cryoprotectant showed that the higher the incidence of IIF, the better the survival [5; 10]. This has been attributed to a substantial reduction in the osmotic efflux of water across the plasma membrane due to preferential osmotic equilibration through intracellular ice growth [5; 10]. Cells in tissues can prove to be more sensitive to volumetric excursions due to the need to maintain cell-cell and cell-matrix contact; therefore, circumventing cell shrinkage and osmotic dehydration during slow cooling through inducing IIF is an intriguing strategy that can be considered in the development of tissue cryopreservation strategies. Evidence has however suggested that while membrane integrity is retained, a high incidence of IIF in monolayers can diminish the proliferative ability of

constituent cells, thus further investigation into this phenomenon and its utility in tissue cryopreservation is warranted [267].

1.3.2 The Effect of Extracellular Matrices and Cell-Cell Contacts on Permeability and Nucleation Parameters

While it is clear that there are several tissue-specific mechanisms of IIF, many studies have additionally indicated that be biophysical parameters of freshly isolated cells and those maintained in culture differ significantly [7; 102; 191; 257]. Much of this initial work was performed on hepatocytes cultured in a collagen double gel matrix, which exhibited an increased propensity for IIF at any given cooling rate [102; 257]. This phenomenon was largely attributed to a reduction in the water permeability of these cultured cells, which corresponded to increased kinetic and thermodynamic nucleation parameters [102; 257].

A 1992 study by Yarmush *et al.* identified differences in water permeability and nucleation parameters in isolated hepatocytes, hepatocytes cultured in a collagen double gel matrix for 7 days, and hepatocytes digested from the matrix after 7 days [257]. While the hydraulic conductivity varied in all three of the tested conditions, it proved to be more closely related between digested and cultured cells than freshly isolated cells. This brings forth the possibility that functional differences in cultured hepatocytes caused by the physiologic environment of the extracellular collagen matrix could alter membrane characteristics in such a way that reduces hydraulic conductivity [102]. This is corroborated by the finding that the IIF kinetics varied not only based on the culture configuration but also on the time spent in culture [102]. Cells cultured for 7 days were able to tolerate more rapid cooling rates than those cultured for 3 days, which corresponded to a significant difference in functional parameters between these two time points [102]. However, differences in permeability parameters have not been thoroughly evaluated between these two time points making it possible that an increase in ECM-mediated stabilization of the plasma membrane after 7 days in culture can provide some level of protection against freezing stress [102]. Interestingly, the activation energy (ie. the temperature range that freeze-induced dehydration is active) in isolated cells was higher than that of digested and cultured cells, providing additional support to these differences in membrane characteristics brought forth by the physiologic environment [257]. Water transport in isolated hepatocytes is negligible at temperatures below -10 °C, making these cells more prone to IIF than most isolated mammalian cells [257]. Therefore,

it is simpler to limit cytoplasmic supercooling in the digested and cultured conditions evaluated. Furthermore, the theoretical maximum concentration of intracellular DMSO obtained through freeze-induced dehydration is significantly higher in digested and cultured cells [257].

While functional differences can impact permeability and nucleation characteristics, cell-cell interactions have proven to have a profound effect on the dehydration response. Morphological changes that ensue upon attachment to a substrate render an effective surface area for osmotic transport that is similar to that of cells in suspension; therefore, cell-matrix interactions play less of a role in this response than cell-cell interactions [16]. Based on these cell-cell mediated effects on permeability characteristics, several investigators have undertaken efforts to develop transport models for increasingly complex multicellular structures. Levin *et al.* have modeled transport in a one-dimensional array of closely packed erythrocytes [125]. Korniski and Hubel have characterized and modeled transport in hepatocyte spheroids, which retain morphology and function that is more representative of tissues than monolayer cultures [117]. Diller and Raymond developed one of the first transport models for multicellular tissues undergoing freezing, while more sophisticated models have used Krogh cylinder geometry to incorporate both the vascular and cellular space to model permeability and nucleation parameters in liver tissue [34; 59; 60; 63; 179; 206]. However, differences in the volume and geometry of the extracellular matrix, the nature of the cell-cell interaction, and the permeability of individual cells make these models highly specific to their system of interest.

1.3.3 The Effect of Cell Concentration on Mechanisms of Freezing Injury

The effect that cell density can have on the freezing response is pertinent to understanding the damage that ice causes in tissues and organs where cells tend to be more closely packed than in suspension. A cell packing effect was initially demonstrated in the 1960's, showing that red blood cell hemolysis was significantly higher when the hematocrit exceeded 60% [174]. One can envisage that mechanical stressors can be pronounced in packed cells where the overall size of the unfrozen fraction is significantly reduced. Interestingly, when the hematocrit was raised (<40%), damage caused by solute concentration is no longer independent of the size of the unfrozen fraction, which was previously proven to be the case in dilute suspensions of red cells [150]. Therefore, the solute composition component of damage is highly dependent on cell concentration, whereas this is less so the case for the mechanical component of damage. The ratio of the volume

of the unfrozen channels to the total volume of cells is higher at any given temperature in dense cell suspensions, therefore cell-cell contacts are more likely to occur upon freezing. It has been postulated that membrane protuberances in shrunken cells can interlock upon physical contact, leading to lysis following dispersal [150]. Therefore, an optimum cooling rate for packed cells may be higher than that for dilute cells. Treatment with glycerol has proven to ameliorate some of the damage seen in packed cells due to an increase in the fraction of unfrozen water [150; 174; 183]. More recent studies have however shown that compounds that promote membrane stabilization and fluidity can negate the packing effect in the absence of glycerol [246].

Hemolysis in packed red cells frozen at 1 °C/min was independent of the warming rate, whereas freezing rates of 200 °C/min increased susceptibility to damage during slow warming [183]. The porous nature of the red cell membrane typically precludes IIF at cooling rates less than 1000 °C/min [183]. In packed cells, it is possible that physical contacts can impede dehydration and therefore promote the formation of intracellular ice which can then recrystallize during rewarming. The probability of extracellular nucleation is reduced due to division of the extracellular space into small individual compartments rather than the large continuous network seen in dilute cell suspensions which can additionally promote IIF [65; 75]. Freeze-fracture studies however reveal an absence of IIF under the conditions studied. While this does not counter the possibility that the probability of IIF is higher in packed cells, it is likely in this case that rapid cooling rates created smaller and more metastable ice crystals extracellularly which were more prone to recrystallize under slow warming conditions. This could in turn cause shear stress on the membranes at low temperatures where they are more liable to fracture. It is also possible that non-equilibrium amounts of ice are formed upon cooling to the storage temperature, resulting an additional crystallization upon slow warming [36].

Characterizing the cell packing effect in nucleated cells would provide more insight into how these phenomena translate to the freezing of tissues and organs. Unfortunately, there has been limited work done on this front. McGrath *et al.* briefly investigated the packing effect in Hela S-3 cells and found that survival is in fact improved at slow cooling rates compared to unpacked cells, which is distinct from the findings in RBCs [157]. Preliminary data in their study appeared to demonstrate a decrease in survival at more rapid cooling rates, however limited control in the packing parameter made these results inconclusive [157]. Loecker *et al.* were able to demonstrate that a progressive

increase in the density of packed hepatocytes corresponded to a decrease in post-thaw survival at slow cooling rates [57]. While they did not study different cooling rates, their findings are in accordance with those seen in RBCs. It is certainly possible while cell density can influence the freezing response of nucleated cells, the outcomes can potentially be highly cell specific. It can additionally be challenging to ascertain the relevance of this phenomenon to complex tissue cryopreservation considering that the cell-cell interactions in packed cells are far removed from those seen in tissues. While the probability of IIF may prove to be higher in packed cells, the kinetics and damage mechanisms of IIF would likely manifest in a way that is considerably different due to the absence of junction proteins. However, it is possible that extracellular-ice damages packed cells through a mechanism that is similar to the damage it causes in tissues.

1.4. Organ and Tissue Preservation at Low Sub-Zero Temperatures

Historically, organ cryopreservation focused on either classical cryopreservation or vitrification to enable storage at low sub-zero temperatures (-80 °C to -196 °C). Both methods have enabled the low-temperature storage of small tissue sections, such as precision cut tissue slices; however, the physical dimensions of whole organs can lead to mass and heat transport issues that result in variable CPA distribution and thermal fluctuations throughout [56]. Ice has proven to perturb intercellular connections and extracellular contacts that are critical to retaining tissue function. As a result, vitrification has gained precedence in the field, however, this method comes with several of its own challenges.

1.4.1 Conventional Cryopreservation of Organs

Storage at low sub-zero temperatures using classical cryopreservation has been achieved in uterus, limbs, and ovaries of small animal models [66; 94; 162; 250]. Some of the most recent success demonstrated high rates of fertility following autotransplantation of frozen-thawed sheep ovaries following the use of anti-thrombotics to prevent clot formation during revascularization [41]. Efforts to apply conventional cryopreservation methodology to large vascularized tissues, such as the heart, liver, and kidney, have, however, been met with minimal success [17; 77; 111]. Perhaps the most promising results were that of Guttman *et al.* in 1977 [93]. Dog kidneys were perfused with 1.4 M DMSO, frozen to -80 °C, and thawed rapidly [93]. Of 16 kidneys tested and transplanted, 8 dogs showed survival ranging from 2-16 months on a single frozen kidney [93]. While promising, several researchers have failed in their attempts to replicate these results [92;

184]. The use of slow cooling rates was one of the key factors in the success of these early attempts to cryopreserve whole organs [32; 111; 235]. Rabbit kidneys perfused with 2 M glycerol and cooled to -80 °C at either 1 °C/hour showed improved revascularization than those frozen at 3 °C/min [111]. Freeze substitution and histological assessment revealed an absence of intracellular ice in the rapid cooling condition; however, interstitial ice was significantly more abundant and vascular damage, particularly to the glomerular capillaries, was eminent [111]. The distinct mechanisms through which ice grows and damages tissues can contextualize several of the challenges seen in the application of classical cryopreservation to tissues.

1.4.1.1 Ice Growth and Damage Mechanisms in Tissues

The thermal gradient that develops during freezing will promote ice formation at the periphery and progression of the ice front towards the center of the tissue [180; 202]. In normal physiologic solutions, ice grows in a dendritic fashion, with solutes becoming more concentrated between dendritic branches [100]. The extracellular matrix (ECM) of tissues is likely to impede the growth of ice, which contrasts with the unhindered growth of ice in cell suspensions [75; 108]. Crystals with successively smaller radii of curvature become increasingly thermodynamically stable at lower temperatures, as dictated by the Kelvin equation [75; 108; 146; 240]. The radius of curvature can impede crystal growth through capillary-like pores in the ECM, which becomes prevalent when considering growth at high temperatures through capillaries of submicron sizes.

If capillary size is insufficient to allow multiple dendrites to grow, a single dendrite will proceed through the capillary [75; 108]. In this case, the rate of growth will be limited because solutes will concentrate at the hemispherical head of the dendrite rather than in the gap between adjacent dendrites [75; 108]. Freezing point depression of the solution immediately adjacent to the ice front can occur if the rate of growth is slower than the diffusion of solutes. Accumulation of solutes in interstitial spaces at the phase change zone of the advancing front manifests as a non-homogeneous freezing pattern in newly frozen regions [203]. The thermal gradient that develops can cause these regions to supercool and freeze in sudden bursts upon subsequent cooling, a phenomenon known as constitutional supercooling [203]. As the degree of supercooling increases, the nucleation event becomes more damaging due to a reduction in degree of separation between ice dendrites and an increase in the curvature and, therefore, the speed of growth [100; 105].

Slow cooling can therefore cause damage due to both the concentration of solutes as well as mechanical damage that occurs due to this sudden freezing [180]. Rapid cooling rates would decrease the spacing between dendrites, which would in turn increase the speed at which the tissue would freeze, thus potentially limiting constitutional supercooling [100]. However, this would also increase the mechanical stress exerted by the advancing ice front and expose the organ to recrystallization injury during rewarming, as demonstrated by Pegg *et al.* in their cell packing effect research [183]. The tissue will be exposed to strong compressive stressors at the front of the phase change that are reduced to tensile stressors as the front advances [202]. In addition to the cooling rate, the overall magnitude of stress is a function of the material properties as well as the outer surface radius [202]. The relationship between the size of the tissue and the magnitude of stress makes the scale-up from rodent to human models particularly challenging [202].

Thermodynamics dictate that ice will preferentially form in interstitial aqueous cavities present throughout the tissue rather than small capillaries [75]. If ice formation is precluded in the surrounding capillaries, then water will flow to the growing crystal, forming an ice lens [75; 108]. Continued growth of this crystal can leave the surrounding tissue in a dehydrated state, causing osmotic stress on a cellular level [75; 172]. Furthermore, growth of the ice within the cavity can impose mechanical stressors which compromise the structural integrity of the surrounding tissue [75; 172]. In the process of drawing water to the growing ice lens, solutes will also be pulled from the surrounding capillaries [172]. This can potentially lead to hypotonic stress during rewarming.

The formation of ice lenses will dominate in the tissues composed primarily of extracellular matrix, such as articular cartilage [169]. In vascularized tissues, particularly those with a high ECM to cell ratio, a situation analogous to ice lensing predominates. Ice preferentially forms in and grows through the vasculature without impedance [32; 111; 204]. The vascular system assumes a similar role to the extracellular solution during the freezing of cell suspensions. An osmotic pressure gradient develops which causes dehydration of the surrounding interstitium and vessel distention [32; 111; 204]. The slower the cooling rate, the greater the vascular distension, and the higher the probability of rupture [32; 111; 204]. Under these slow cooling conditions, ice would be constrained to the vasculature. More rapid cooling rates would decrease the radius of curvature of individual dendrites and limit dehydration of cells lining the vasculature, which together increase the probability of IIF and the propagation of ice into the intersitium.

1.4.2 Vitrification of Organs

Research into vitrification approaches have severely outweighed efforts to develop a classical cryopreservation approach to whole organ preservation, which is largely a by-product of the notion that ice formation is inherently damaging to vascularized tissues. Studies have contrasted survival outcomes in smooth muscle, jugular veins, carotid arteries, and articular cartilage that had been either frozen or vitrified to low sub-zero temperatures [39; 217; 218; 219; 235; 236; 237]. Vitrified tissues on average retained ~60% higher viability than conventionally cryopreserved counterparts. Whether these benefits are due to an absence of ice or simply the lack of inadequate control of ice formation and growth is up for debate. Whole organ vitrification imposes several additional complications that result from the need to both place and recover the organ from an amorphous state. The traditional non-equilibrium approach to vitrification utilizes rapid cooling rates to place kinetic constraints on the nucleation event and CPAs to raise the glass transition temperature [81]. A stable amorphous state is reached once the homogeneous nucleation temperature intersects the glass transition temperature. Lower concentrations of CPAs are required to achieve vitrification as cooling rates are increased; however, rapid cooling rates are often unattainable in whole organs [81]. Furthermore, the size of these systems often hinders thermal uniformity, an issue which is intensified at increasingly rapid cooling and warming rates. Significant improvements in attainable speed and uniformity of warming rates have recently been demonstrated through the infusion of iron oxide nanoparticles throughout the organ followed by exposure to a low radiofrequency (RF) alternating magnetic field [31; 115; 137]. Marginal improvements in thermal uniformity under more rapid cooling conditions have been seen through the use of thermoelectric cooling devices and intraarterial helium circulation [91; 93; 109; 131; 184]. However, currently attainable cooling rates in whole organs do not preclude the use of high concentrations of CPAs. This introduces several issues relating to the addition and removal of highly viscous and toxic vitrification solutions. Two strategies being studied to mitigate these issues will be briefly discussed as they are not only relevant to whole organ vitrification, but they could prove to be relevant to any whole organ sub-zero storage strategy where CPA toxicity may prove to be an issue.

1.4.2.1 Cryoprotectant Toxicity Neutralization (CTN)

Fahy *et al.* have largely approached this issue from a solution manipulation perspective [80; 81]. Non-permeating sugars increase solution viscosity and, therefore, can reduce the concentration of

permeating CPAs required without significantly compromising the glass forming potential of the solution. The biochemical toxicity of permeating CPAs is distinct from osmotic toxicity and is attributed to specific interactions with biochemical constituents of the cell or non-specific alteration of the cellular environment [76]. Fahy *et al.* demonstrated these non-specific mechanisms of toxicity to be the result of the average hydrogen bonding strength associated with polar groups on the permeating CPA. This parameter, termed "qv", is the most dominant form of toxicity and is additionally the most predictive of glass forming potential [78; 79; 82]. Gene expression profiling has recently provided some insight into the transcriptional response of endothelial cells and precision cut liver slices to permeating CPAs [47; 88]. In line with this work, transposon-mediated mutagenesis has enabled the characterization of six genes in mouse embryonic stem cells whose inactivation conferred an improvement in survival following treatment with M22, a whole organ vitrification solution [53]. While much research has yet to be done to elucidate specific mechanisms associated with biochemical toxicity, inclusion of amides (urea, formamide, and acetamide) has proven to reduce the toxicity associated with 15-30% (w/v) DMSO, a phenomenon known as cryoprotectant toxicity neutralization (CTN) [78]. CTN has yet to be conclusively demonstrated in non-renal and non-hepatic tissues; however, inclusion of non-permeating CPAs and amides is now commonplace in commercially developed vitrification solutions [78; 79; 81].

1.4.2.2 Liquidus Tracking (LT)

The liquidus tracking (LT) method is an alternate approach to the toxicity issue which advantage of the reduced biochemical toxicity of permeating CPAs at low temperatures [138]. It is founded on the work of Farrant in 1965 and Elford et al. in 1970, who demonstrated the feasibility of incrementally increasing CPA concentration as cooling proceeds in such a way that follows the liquidus curve of the ternary (CPA-salt-H2O) phase diagram [71; 84]. Doing so prevents the formation of ice and negates the need to introduce high concentrations of CPAs at temperatures above 0 °C where they prove toxic. Furthermore, because LT is an equilibrium process, it significantly reduces the cooling rates required for vitrification to occur. Incremental introduction of the CPA additionally reduces osmotic shock; however, it is unclear how beneficial this is given that osmotic fluctuations tend to be more damaging at lower temperatures [11].

This method lay dormant for over 30 years before being revived by Pegg *et al.* for its application to articular cartilage vitrification [186; 249]. In order to streamline LT, they developed an automated system that enabled continuous programmed control of the cooling rate and the CPA concentration, which proved to overcome several of the challenges in traditional cartilage vitrification [186; 249]. Highly complex and expensive equipment would be needed to automate LT in large vascularized tissues. While manual LT would not require this complex equipment, lots of attention would need to be given to the various steps within the LT process, which could lead to significant operator-induced variability. Thus far, manual LT has only been applied to the vitrification of alginate encapsulated liver cells [194]. It should additionally be noted that while LT may preclude toxicity during the freezing phase, the tissue will still be exposed to high concentrations of CPAs during rewarming. Steps can be taken to continuously dilute the CPA as the tissue is being warmed; however, this would extend the warming process, causing it to last several hours [193]. Furthermore, in vascularized tissues, the perfusion of highly viscous solutions at low temperatures can promote shear stress to the endothelium. Slow flow rates can be used to curb this issue; however, this would further hamper the logistics of this approach.

In the context of whole organ vitrification, LT may have several benefits over the traditional non-equilibrium approach; however, the time-consuming nature of this process could limit its applicability in the real world. In spite of these limitations, additional thought should be given to its relevance in high sub-zero organ preservation where the organ can theoretically be stored at a temperature that is low enough to preclude biochemical toxicity under the desired storage times.

1.5 Organ and Tissue Preservation at High Sub-Zero Temperatures

Storage at high sub-zero temperatures (-2 °C to -20 °C) serves as an intermediate between deep sub-zero storage and the current hypothermic preservation standard. The increased storage times afforded by these high sub-zero preservation strategies may not enable the banking of organs for indefinite periods of time; however, they would significantly improve the logistical constraints currently in place with hypothermic preservation. Diverse arrays of phylogenetic groups have adapted cryostasis strategies that allow them to survive at sub-zero temperatures by tolerating ice formation in extracellular compartments [1; 27; 35; 95; 135; 173; 198; 212; 225]. This provides insurmountable evidence that ice formation alone is not damaging in tissues at high sub-zero

temperatures. Rather, it is inadequate control of the location of ice formation and its growth that results in damage. While ice-free approaches to high sub-zero organ preservation have seen the most success thus far, a nature-inspired freeze tolerance approach could overcome several of the limitations associated with ice-free preservation.

1.5.1 Supercooling – An Ice-Free Approach to High Sub-Zero Preservation

Supercooling preservation has shown promise in a number of bacterial, yeast, and mammalian cell types, and it has recently seen remarkable success at an organ level [89; 139; 140; 197; 199; 264; 265]. In natural systems, supercooling is predicated on 1) the synthesis of low-molecular weight carbohydrates that depress the supercooling point (ie. the temperature that spontaneous nucleation occurs during gradual cooling); 2) managing the abundance or potency of ice nucleating agents within the organism; or 3) synthesis of thermal hysteresis proteins that limit nucleation [134; 190]. These strategies are seen in several freeze avoidant insects, fish, amphibians, cold blooded vertebrates, and mammals [134; 190; 216; 260]. Much of the success seen in the supercooling preservation of mammalian organs is ascribed to the artificial implementation of these natural strategies.

Increased volumes, lower storage temperatures, and extended storage times all serve to increase the probability of nucleation in a supercooled state. Furthermore, while the probability of a nucleation event increases as the degree of supercooling is increased, so does the damage caused by the nucleation event [100; 105]. In a rodent model, Berendsen *et al.* leveraged subnormothermic machine perfusion (SNMP) to load and unload protective additives that depress the intravascular and intracellular supercooling point, which enabled preservation at -6 °C for 3 days in a supercooled state with promising transplantation outcomes [29; 40]. Translation from a rodent to human model proves challenging due to the increased liquid volume of the system, therefore additional measures are required to curb nucleation.

Theoretical and experimental studies have indicated that air-liquid interfaces are preferential sites for heterogeneous ice nucleation [67; 214; 233]. Huang *et al.* recently demonstrated that sealing the air-liquid interface with oils, pure alkanes, and primary alcohols, enabled the storage of large volumes (up to 100 mL) of water, for 100 days at -20 °C [101]. All sealing agents additionally demonstrated a substantial increase in the stability of the supercooled state following vibrational

and thermal disturbances that simulated real-world storage and transport conditions [101]. Extending this surface sealing approach to 1 mL RBC suspensions enabled storage for up to 100 days at -16 °C [101]. While this has yet to be extended to tissues and organs, minimization of air-liquid interfaces by de-airing the storage chamber was one of the key measures taken in a recent protocol developed to supercool human livers for 27 hours at -4 °C [58]. This was an extension of the previously developed rat liver supercooling protocol and has been one of the most promising high sub-zero organ preservation outcomes seen to date. Overcoming challenges associated with attaining CPA uniformity in a human organ add to the weight of this achievement. However, until more extensive surface sealing measures are able to be implemented in whole organs, the room for optimization in the supercooling approach is limited. Even with the most promising approaches to date, attempting to transport supercooled organs or increase storage times by reducing storage temperatures would invariably lead to a damaging nucleation event that would propagate throughout the organ.

1.5.2 Freezing Organs at High Sub-Zero Temperatures

Storing organs at a high sub-zero temperature in a frozen state can overcome several of the challenges that have rendered the classical cryopreservation approach to organ preservation largely elusive. The unfrozen fraction at higher temperatures would be greater, thus the organ would be in a "partially frozen" state. As a result, the mechanical stress imposed by ice would be significantly less than when the organ is frozen to low sub-zero temperatures. The increased unfrozen fraction afforded by a higher storage temperature would additionally cause less osmotic stress to constituent cells, therefore the required concentration of CPA would be significantly less. A reduction in the viscosity and toxicity that arise when CPA concentrations are lowered would improve the logistics associated with the perfusion and distribution of CPAs throughout the organ. Furthermore, a reduction in the temperature range transited during could additionally limit constitutional supercooling, IIF, and interstitial ice formation during the cooling phase, as well as mitigate recrystallization-mediated damage during the rewarming phase.

There have been a few notable attempts to store organs at high sub-zero temperatures. Moss *et al.* in 1965 revealed that canine livers perfused with 33% (w/v) glycerol and frozen down to -60 °C experienced significantly greater architectural damage than those frozen to -20 °C, however functional activity was nearly absent in both cases [168]. Kubota *et al.* in 1975 evaluated the effect

of freezing rates ranging from 0.1 °C/min to 10 °C/min in dog kidneys perfused with 12.5 (w/v) DMSO and frozen down to -20 °C [119]. Cooling rates between 2-4 °C/min showed optimal recovery. This is expected under the auspices that slow cooling rates would impose severe cellular dehydration and vascular distention, while rapid cooling rates would promote intracellular and interstitial ice formation. Despite the increased unfrozen fraction at this storage temperature, post-transplant function was severely limited, with recipients lasting marginally longer than bilaterally nephrectomised controls. Additional studies to freeze kidneys at higher sub-zero temperatures showed only marginal benefits compared to those stored at low sub-zero temperatures. These early high sub-zero preservation studies did not test different types of CPAs, concentrations of CPAs, perfusion protocols, or cooling and warming regimens. Thus, the poor results that were seen can likely be attributed to a lack of protocol optimization. Furthermore, strategies used by freeze-tolerant organisms to promote nucleation of intravascular ice at high sub-zero temperatures and prevent ice recrystallization were not implemented in these studies.

1.5.2.1 Freeze Tolerance Strategies in Nature

Freeze-tolerant organisms include intertidal bivalves, barnacles, annelids, gastropods, nematodes, and several terrestrial insects and amphibians [1; 27; 35; 95; 173; 198]. The wood frog (*Rana sylvatica*), the gray tree frog (*Hyla versicolor*), the chorus frog (*Pseudacris triseriata*), and the spring peeper (*Pseudacris crucifer*), are the only known vertebrates known to exhibit freeze tolerant capabilities [135; 212; 225]. The similarity between the organ systems of these amphibians and those of mammals has provided unique insight into overcoming the challenges that currently limit organ freezing. Perhaps the most extensive analyses thus far have been performed on the wood frog*, R. sylvatica*, which can survive for up to two weeks at temperatures as low as -8 °C with 65 % of extracellular water frozen (28). The ability to survive in this frozen state suggests there are mechanisms in place to control of extracellular ice formation, limit osmotic stress to constituent cells, and minimize intracellular ice formation.

1.5.2.1.1 Low-Molecular Weight CPAs in Freeze Tolerance

Low molecular weight carbohydrate cryoprotectants (CPAs) play a major role in the limiting these damage mechanisms, which is largely a virtue of their colligative effects [228]. Common CPAs include C3 polyols (glycerol), C4-C6 polyols (sorbitol, ribitol, threitol, erythritol), proline (C5), C6 sugars (glucose and fructose), and C12 sugars (sucrose and trehalose) [26; 68; 95; 163; 224].

Synthesis often begins in the early autumn, peaks midwinter, and begins to fall in the early spring, which create corresponding seasonal variations in the maximum tolerable ice content [229]. 50% lethality (LT_{50}) for the intertidal gastropod, *M. bidentatus*, in the winter is -13 °C and -3 °C in the summer, which correspond to ice contents of 75% and 3%, respectively [130]. Glycerol contents increased from 1.14 μmol/g to 2.96 μmol/g, therefore this decrease in tolerable ice content could be the result of intracellular nucleation [130]. In addition to colligative cryoprotection, polyols can function to stabilize the native state of proteins by hydrogen bonding to polar residues and stabilizing hydrophobic interactions [46; 50] In contrast, trehalose and proline offer limited colligative cryoprotection, but are responsible for stabilization of the lipid bilayer and inhibition of the lipid phase transition that occurs as temperatures are reduced [50; 51; 86; 208; 209].

Survival in the case of *R. sylvatica* is largely predicated on the synthesis and distribution of glucose throughout the organism, which glycerol-mediated cryoprotection of several other freeze-tolerant amphibians [212; 225; 229]. The liver contains glycogen reserves 10-fold greater than any other organ in the body, allowing it to synthesize sufficient amounts of glucose to enable survival [224; 225; 227; 229]. Initiation of ice formation in the extremities results triggers glucose synthesis in the liver through a currently unknown nervous or hormonal signalling pathway [224] This is unlike the anticipatory CPA synthesis that occurs in several other freeze tolerant organisms [224]. Maximal levels of glucose are attained 24-48 hr following the onset of synthesis, which typically correlates with the point at which the ice content reaches a maximum and blood flow ceases [122]. This slow rate of freezing (~2.8%/g) provides ample time for glucose equilibration on a micro- and macrostructural level, cell volume regulation, and minimization of freezing stress. Central tissues, such as the heart, brain, kidney, and liver have the highest amounts of glucose, ~200 μmol/g [49; 229]. The lung, stomach, and intestines have intermediate glucose levels (100-150 μmol/g), whereas skin, skeletal muscles, and gonads have the lowest levels (<60 μmol/g) [49; 229]. While the density of central tissues may necessitate increased glucose concentrations to minimize freezing stress, these differences also allow thawing to progress from central to the peripheral tissues, which ensures that the oxygenated blood supply is restored before exterior organs are thawed [207].

1.5.2.1.2 Ice Nucleating Agents and Thermal Hysteresis Proteins

Ice nucleating proteins (INPs) and thermal hysteresis (TH) proteins are two classes of ice binding proteins (IBPs) that govern freeze tolerance and freeze avoidance strategies, respectively [69; 116; 118; 248; 261]. Ice nucleating proteins (INPs) function by virtue of their ability to nucleate ice at high sub-zero temperatures (above -10 °C) [69]. Resulting outcomes can be likened to the physical events that take place when isolated cells in suspension are nucleated before a critical degree of intracellular supercooling is reached [65]. Ice formation is limited to the extracellular compartment and the application of osmotic stress to the surrounding cells is gradual. The propagation of ice throughout the vascular network will additionally prove to be less damaging when ice is nucleated close to the freezing point. Furthermore, the presence of INPs throughout the vasculature will ensure there is uniformity to this process and that constitutional supercooling is minimized [261]. Ice nucleating activity has been detected in heparinized whole blood, heparinized plasma, and serum of *R. sylvatica*, which correlates with studies characterizing the limited capacity of this organism to supercool [224; 255].

Ice binding proteins (IBPs) differ in levels of thermal hysteresis activity and can therefore be subclassified into high-TH antifreeze proteins (AFPs) and low-TH IBPs [68; 69; 70]. Thermal hysteresis activity relies on non-colligative suppression of the equilibrium freezing point through physical binding to the prism, basal, or pyramidal planes of the hexagonal crystal lattice such that a non-equilibrium freezing point is established [61]. While these TH proteins are extremely common in freeze avoidant organisms, the occurrence of low-TH IBPs has been reported in some species of freeze tolerant insects and the intertidal bivalve *Mytilus edulis* [19; 69]. The concurrent presence of low-TH IBPs with INPs indicates that thermal hysteresis and prevention of organismal freezing is not their primary function in this case. Rather their role can likely be attributed to the ice recrystallization inhibition (IRI) activity of TH proteins that results from adsorption to the crystal surface and prevention of water molecule addition to the growing ice crystal [62].

1.5.2.2 Developing a Nature-Inspired Strategy to Freeze Organs at High Sub-Zero Temperatures

The most notable efforts to implement freeze tolerant-inspired approaches to high sub-zero organ preservation were done by Rubinksy *et al.* in 1994 and Ishine *et al.* in 2000. Rubinksy *et al.* utilized a cryoprotective solution containing levels of glycerol similar to those found in freeze-tolerant

amphibians (0.5 M) as well as a low-TH IBP(1 mg/mL) to store whole rat livers at -3 °C for 6 hours [200]. While their results demonstrate a notable improvement over previous efforts to freeze livers, bile production proved to be significantly less than control livers that underwent hypothermic storage. The absence of either the antifreeze protein or glycerol, however, resulted in a near loss of function. Therefore, both components were crucial to their method. While AFGP's have ice recrystallization inhibition (IRI) activity, they can additionally promote retention of physiologic ion compositions as temperatures are reduced through passive blockage of Ca^{2+} and K^{+} channels [201; 205]. In this case, the mechanism by which they are imparting protection is unclear; however, it is unlikely that ice recrystallization would cause significant damage under the temperatures and storage times tested. Ishine *et al.* implemented a similar protocol to Rubinsky *et al*., using 0.5 M glycerol and 0.5 mg/mL of a low-TH IBP from a North Atlantic Cod [106; 107]. They attempted to store rat livers in a frozen state at -2 C° for 2 hours and assess transplantation outcomes. While all the livers retained high levels of bile production, only one animal survived up to 5 days while the remaining eight animals survived for 2 to 4 hours.

Directly translating an amphibian freeze-tolerance approach to a mammalian system may require degrees of optimization that were not present in the previously described studies. The structural architecture of mammalian rat liver differs significantly from that of *R. sylvatica*, with stereological measurements indicating that 26% of liver tissue in the frog accounting for vascular/extracellular space, in comparison to 15% in rat liver tissue [60]. More detailed assessment revealed 24% of hepatocytes in *R. sylvatica* liver tissue are not in direct contact with the vasculature, whereas 100% of hepatocytes in mammalian rat liver tissue are [60]. Furthermore, the radius of *R. sylvatica* sinusoids are approximately five times greater than those in rats. Differential scanning calorimetry has revealed that in the absence of any CPAs, cells in *R. sylvatica* liver tissue do not undergo complete dehydration at 5 °C/min, whereas they do in rat liver tissue, which indicates that these structural differences could impose a profound difference in the freezing response [59; 60; 179]. Therefore, perhaps it is a lack of cooling rate and CPA type/concentration optimization that led to the loss of function and poor transplantation outcomes seen by Rubinsky *et al.* and Ishine *et al.*

Higher concentrations of CPAs and ice nucleating agents will become particularly important when freezing organs at temperatures below -5 °C. A recent study in a simple blood vessel model showed

that inclusion of ice nucleating agents can alleviate endothelial injury, particularly following cooling to temperatures between -10 °C and -20 °C [239]. As previously mentioned, this is likely due to the prevention of IIF combined with the gradual application of osmotic stress; however, the prevalence of IIF was not examined in this study. Scanning electron cryomicroscopy has revealed that *R. sylvatica* liver slices containing peak levels of glucose (280 µmol/g) cells lining the vasculature retain 80% of their water content when cooled to -7 °C, whereas this is reduced to 6% at -20 °C [226]. This may explain why freeze tolerant frogs exposed to temperatures below their normal temperature range are unable to survive. The extent of dehydration incurred at -20 °C would likely result in irreparable cellular damage and possibly vascular damage due to excessive vessel distension; however, these issues could theoretically be ameliorated if higher concentrations of glucose were present. There have been recent promising efforts to use ice nucleating agents and increasingly complex cryoprotective cocktails with high concentrations of permeating and non-permeating CPAs to freeze rat livers at temperatures as low as -15 °C, however these results have not yet been published and will not be discussed in detail presently [238].

Previous literature on freeze-tolerance strategies and high sub-zero freezing of whole organ have pointed to ice recrystallization as a potential concern [106; 107; 200]. While recrystallization is a major form of intracellular ice-mediated damage, it can additionally prove to cause damage extracellularly [44; 183; 241]. In A594 cell monolayers, treatment with AFPIII produced a marked increase in the post-thaw when frozen at 1 °C/min down to 80 °C [241]. Interestingly, they conferred no benefit to A594 cells in suspension frozen under the same conditions, suggesting that extracellular ice recrystallization is likely more damaging in cell configurations containing cell-cell and cell-matrix contacts [241]. This is consistent with the reduction in viability seen in packed red cells frozen rapidly and warmed slowly in the absence of IIF [183].

Ice recrystallization would theoretically be rampant at temperatures above -20 °C where most freeze tolerant organisms survive. [228]. However, given that INP's trigger the nucleation of vascular ice between -2 °C and -3 °C, which is close to the equilibrium freezing point of -0.5 °C, the ice will likely be less prone to recrystallize due to its thermodynamic stability [48]. Recent identification of a xylomann-based AFGP in the European water frog *R. lessonae* was the first evidence of a large molecular mass antifreeze in a frog species [248]. Recrystallization inhibition was seen in tissue homogenates of muscle and skin but not in blood plasma, indicating possible

inhibition of interstitial recrystallization [248]. It remains unclear whether other freeze tolerant amphibians truly lack TH-proteins as this was the first study to isolate membrane associated TH proteins while previous studies have solely investigated plasma, serum, and whole blood [48].

The damage caused by recrystallization is typically attributed to amount of recrystallization that occurs [21; 22; 136; 149]. Irrespective of the rate of recrystallization, the relationship between the damage caused by a given amount of recrystallization and temperature is unclear. Theoretically, a given amount of recrystallization may be more damaging at lower temperatures where membranes are more liable to fracture; however, this assumes that the damage caused be recrystallization is either mechanical or osmotic when in fact the exact mechanisms of recrystallization-mediated damage are not known. There simply tends to be a correlation between inhibition of both intra- and extracellular ice recrystallization and survival [21; 22; 136; 149]. More thought should be given these points as it is certainly possible that while temperatures at the lower range of high sub-zero storage (ie. -20 C) may slow the rate of recrystallization, they may augment recrystallization-mediated damage under increased storage periods.

1.5.2.1 Using Small Molecule Ice Recrystallization Inhibitors (IRIs) to Inhibit Ice Recrystallization

The artificial implementation of low TH-IBPs in cell and tissue cryopreservation has revealed a delicate balance in AFP-induced enhancement of cell survival and AFP-induced enhancement of cell death [44; 192; 259]. This is the result of dynamic ice shaping (DIS) characteristics predicated on the irreversible adsorption of AFPs to the nonbasal planes of the hexagonal crystal lattice, a mechanism which guides their TH activity [176; 256]. DIS characteristics can change ice crystal morphology in such a way that exacerbates mechanical damage to the cell, an effect which becomes increasingly profound when these compounds are used at high concentrations or when temperatures depart extensively from the non-equilibrium freezing point [44; 105; 120].

The limited biological utility of AF(G)Ps has prompted the development of compounds that are more tenable to cryopreservation applications. Ice etching experiments have revealed that differences in TH activity between moderate and hyperactive AF(G)Ps is the result of differential binding to the basal and non-basal (prism and pyramidal) planes of the hexagonal lattice [25]. In several cases these variations in the DIS characteristics show minimal correlation to the compounds IRI activity, suggesting that these two antifreeze activities operate through distinct

mechanisms [210]. Eniate *et al.* in 2003 published the first evidence of carbon-linked (C-linked) AFGP analogs that, while deficient in TH activity, showed minimal variation in IRI activity when compared to the wild-type [72]. Further iterations of C-linked AFGP analogs developed in 2005 and 2008 demonstrated complete decoupling of TH and IRI activity, thus facilitating the biological utility of these compounds as ice recrystallization inhibitors (IRIs) [54; 127]. Structure-function studies on these C-linked AFGP analogs revealed a correlation between the hydration of carbohydrate moieties and IRI activity [54]. Consequently, a series of monosaccharides and disaccharides with known hydration parameters were shown to be effective at inhibiting recrystallization, which formed the foundation for the development of a series of small carbohydrate-based surfactants and hydrogelators retain similar levels of IRI activity to low TH-IBPs and lack dynamic ice shaping characteristics [43; 234]. Combined with the minimal toxicity several of these compounds have proven to elicit, they are unlikely to prove detrimental in cryopreservation applications, thereby significantly enhancing their biological utility relative to AF(G)Ps [20; 112; 252].

Small molecule IRIs have recently shown exceptional promise in a number of cell-based cryopreservation applications, conferring significant degrees of protection to cryopreserved red blood cells, umbilical cord blood (CD34+) cells, and platelets [37; 38; 42; 112; 188; 252]. Perhaps, the most promising results were those seen in RBCs where IRI supplementation enabled glycerol concentrations to be reduced from 40% to 15%; thus, minimizing the laboriousness of post-thaw deglycerolization procedures that are required to minimize intravascular hemolysis following transfusion [42]. Their applicability in most cell-based cryopreservation applications is based on their ability to minimize transient warming damage, which is correlated with the degree of extracellular ice recrystallization. 40% glycerol confers protection against transient warming injury in RBCs; however, in general the use of high concentrations of CPAs to protect against transient warming injury has limited applicability due to the several other stressors induced by simply by virtue of using a high concentration of CPAs [42]. The same notion can be applied to the frozen preservation of complex tissues.

Although these compounds have not yet been applied to tissue cryopreservation, perhaps the most promising indication of their utility to this effect is the 2018 study by Poisson *et al.* indicating their capacity for passive permeation into the membrane of endothelial cells and subsequent control of

intracellular ice recrystallization [187]. The ability to mitigate damage that results due to intracellular ice recrystallization can open several avenues for optimizing organ freezing protocols as this would promote increased flexibility in cooling rates and CPA concentrations. It is a fine balance between vascular rupture and cellular dehydration that dictate the recovery of frozen tissues [226]. Minimizing damage caused by vascular distension and cellular dehydration through either reducing concentrations of non-permeating and permeating CPAs perfused throughout the organ or increasing cooling rates could facilitate IIF. However, this may not prove to be problematic given that cell-cell contacts can render the initial nucleation of IIF innocuous, and IRIs can be used to mitigate recrystallization of intracellular ice [8; 9; 10; 187]. Furthermore, their capacity for passive permeation through cell membranes is a virtue of both their small size (300-400 Da compared to 3-12 KDa for AF(G)Ps) as well as their amphiphilicity, making it significantly easier for these compounds to permeate regions outside the vasculature when perfused.

1.6 Conclusions

Conventional cryopreservation and vitrification approaches to whole organ preservation are prone to several issues dictated primarily by the size of these systems. High sub-zero organ preservation methods, on the other hand, are much more likely to see translation into a clinical setting within the next two decades. While the supercooling approach has garnered significant interest due to its recent success, it is prone to several limitations that result from storage in a non-equilibrium state. In spite of this, the well-characterized damage that ice causes in tissues has caused ice-free sub-zero organ preservation strategies to gain precedence. This review has discussed the mechanisms through which ice causes damage at microscopic and macroscopic level in tissues and as well as both the necessity and difficulty in translating the principles used in cellular cryopreservation to complex tissues. However, emphasis has been placed on mechanisms and techniques that can render ice innocuous in tissues. A nature-inspired approach to freeze organs at high sub-zero temperatures warrants further investigation as it can be argued that the overcoming the challenges associated with controlling the formation and growth of ice in tissues can outweigh the challenges associated with avoiding ice formation at sub-zero temperatures. More work needs to be done on this front to optimize cryoprotective cocktails, cooling and warming regiments, as well as perfusion protocols, such that we can effectively store and recover frozen organs.

1.7 Rationale

1.7.1 Clinical Relevance

In Canada, 239 patients were active on the liver transplant wait list and 64 patients had died by the end of 2018 [12]. The Canadian Institute for Health Information (CIHI) 2019 organ donation statistics reveal that 60% of deceased donors had their livers used for transplantation [12]. Old age, high BMI, and diabetes are all independently associated with liver non-use; however, so is donation after cardiac death (DCD) [73]. In 2010, DCD accounted for one quarter of all non-use livers in the United States, as DCD organs experience extended warm ischemia, and as a result often fail to meet acceptable criteria for transplantation [177]. 10% of livers donated in Canada in 2019 were DCD livers and approximately 10.5% of DCD livers are discarded annually [12]. DCD organs have a limited capacity to tolerate SCS; therefore, the application of *ex vivo* machine perfusion could serve to increase the utilization of DCD livers by reducing the 10.5% discard rate [177]. Furthermore, the capacity of these systems to serve as a platform for functional augmentation could reduce the number of non-used livers [87].

The impacts of *ex vivo* machine perfusion on organ allocation would be strengthened substantially if these systems are to be paired with sub-zero preservation. This would not only apply to DCD livers, but additionally extend to donation after brain death (DBD) livers. Considering *in situ* cooling can be induced before circulation is ceased in DBD donors, warm ischemia is minimized, and therefore DBD livers account for 90% of liver transplants [177]. The limited preservation times afforded by the current preservation standards impose constraints in donor-recipient matching that fall disproportionately on those in rural communities with unequal access to transplants [97]. The aim of this thesis is to facilitate the application of small molecule IRIs to the high sub-zero storage of whole livers in a frozen state. Effective preservation of livers in a frozen state would invariably minimize the geographic and logistic constraints that currently plague the transplant network.

1.7.2 Justifying the Use of Small Molecule IRIs Based on the Current Status of Research

Efforts are currently ongoing at the University of Ottawa to understand how small molecule IRIs operate when solution characteristics as well as ice nucleation and growth conditions are varied. While the parameters under which these compounds operate in solution continues to be resolved, biological responses to these compounds can vary significantly between systems. Differences in

membrane characteristics can dictate the ability of the IRI to permeate the cell membrane and the extent to which they elicit a toxic response. Furthermore, the ability of a given IRI to permeate a cell may not directly correlate with its ability to control recrystallization due to physical and chemical differences in the intracellular environment of different cell types [33]. Thus, concurrent evaluations of how these compounds operate in solution as well as different biological systems is important. This thesis will characterize how small molecule IRIs operate intracellularly in hepatocytes and extracellularly in liver tissue. IRI-mediated toxicity will additionally be evaluated in each of these systems. Recent freeze tolerance-inspired strategies to liver preservation have been promising; however, a significant degree of optimization is required before successful long-term transplantation outcomes are possible. While current limitations in these strategies are multifaceted, the implementation of an IRI in this model could prove to be beneficial.

1.8 Hypothesis and Objectives

Small molecule ice recrystallization inhibitors (IRIs) can mitigate intra- and extracellular ice recrystallization in liver tissues without eliciting toxic effects.

The objectives of this thesis are to:

1. **Characterize IRI toxicity, permeation, and control of intracellular ice recrystallization in hepatocyte monolayers (Chapter 2).**

   Efforts to freeze complex tissues largely center around circumventing IIF; however, permitting IIF can curtail the stringency of freezing protocols. Adequate control of intracellular recrystallization can promote tolerance to IIF in multicellular systems where cell-cell contacts can render IIF innocuous [8; 9; 10]. Permeating and non-permeating CPAs can modulate intracellular nucleation parameters and recrystallization rates [33; 98]. Thus, evaluation of IRI-mediated control of intracellular recrystallization under conditions that vastly alter the intracellular milieu can promote confidence in the application of these compounds to more complex systems. Hepatocytes are the primary functional units of the liver and comprise approximately 80% of the liver's mass, making them an ideal candidate system to assess IRI efficacy. In this objective, the efficacy of a given IRI will be defined by its ability to permeate the hepatocyte membrane and control the recrystallization of intracellular ice without eliciting toxic effects.

2. **Evaluate IRI toxicity, permeation, control of recrystallization, and corresponding functional outcomes in liver tissue (Chapter 3).**

   While previously conducted splat cooling assays have established that the tested IRIs can effectively control ice recrystallization in solutions of 1X DPBS, it is unclear how this would translate to control of intravascular and interstitial recrystallization in liver tissue. This is due to the material properties of dense tissues create fundamentally different ice formation and growth characteristics than those seen in cell suspensions and monolayers [172; 180]. Furthermore, the presence of five different cell types in livers creates the potential for different toxic effects than those seen in objective 1. Evaluating toxicity, permeation, control of recrystallization within liver tissues, and post-thaw functional outcomes is vital for the continued application of these compounds to whole liver freezing strategies.

1.9 References

[1] A.V. Aarset, Freezing tolerance in intertidal invertebrates (a review). Comparative Biochemistry and Physiology Part A: Physiology 73 (1982) 571-580.

[2] J. Acker, A. Larese, H. Yang, A. Petrenko, and L. McGann, Intracellular ice formation is affected by cell interactions. Cryobiology 38 (1999) 363-371.

[3] J. Acker, and L. McGann, The role of cell-cell contact on intracellular ice formation. Cryo-letters 19 (1998) 367-374.

[4] J.P. Acker, Influence of cell adhesions on the freezing response of biological systems [Dissertation], Edmonton, AB: University of Alberta, 1998.

[5] J.P. Acker, Innocuous intracellular ice formation : mechanisms and implications [Dissertation], Edmonton, AB: University of Alberta, 2000.

[6] J.P. Acker, J.A.W. Elliott, and L.E. McGann, Intercellular Ice Propagation: Experimental Evidence for Ice Growth through Membrane Pores. Biophys J 81 (2001) 1389-1397.

[7] J.P. Acker, A. Larese, H. Yang, A. Petrenko, and L.E. McGann, Intracellular Ice Formation Is Affected by Cell Interactions. Cryobiology 38 (1999) 363-371.

[8] J.P. Acker, and L.E. McGann, Cell-cell contact affects membrane integrity after intracellular freezing. Cryobiology 40 (2000) 54-63.

[9] J.P. Acker, and L.E. McGann, Innocuous intracellular ice improves survival of frozen cells. Cell Transplant 11 (2002) 563-71.

[10] J.P. Acker, and L.E. McGann, Protective effect of intracellular ice during freezing? Cryobiology 46 (2003) 197-202.

[11] Y. Agca, J. Liu, J. McGrath, A. Peter, E. Critser, and J. Critser, Membrane permeability characteristics of metaphase II mouse oocytes at various temperatures in the presence of Me2SO. Cryobiology 36 (1998) 287-300.

[12] I. Alina, Annual statistics on organ replacement in Canada, 2017.

[13] S.M. Almdahl, M. Lie, P.E. Dahl, and D. Sorlie, [Aortic root reconstruction with homograft in bacterial endocarditis]. Tidsskr Nor Laegeforen 115 (1995) 2390-1.

[14] T.J. Anchordoguy, C.A. Cecchini, J.H. Crowe, and L.M. Crowe, Insights into the cryoprotective mechanism of dimethyl sulfoxide for phospholipid bilayers. Cryobiology 28 (1991) 467-473.

[15] T.J. Anchordoguy, A.S. Rudolph, J.F. Carpenter, and J.H. Crowe, Mode of interaction of cryoprotectants with membrane phospholipids during freezing. Cryobiology 24 (1987) 324-331.

[16] W. Armitage, and B. Juss, The influence of cooling rate on survival of frozen cells differs in monolayers and in suspensions. Cryo-Letters 17 (1996) 213-218.

[17] W.J. Armitage, and D.E. Pegg, The contribution of the cryoprotectant to total injury in rabbit hearts frozen with ethylene glycol. Cryobiology 16 (1979) 152-60.

[18] E. Asahina, K. Shimada, and Y. Hisada, A stable state of frozen protoplasm with invisible intracellular ice crystals obtained by rapid cooling. Exp Cell Res 59 (1970) 349-358.

[19] T. Aunaas, Nucleating agents in the haemolymph of an intertidal mollusc tolerant to freezing. Experientia 38 (1982) 1456-1457.

[20] A.K. Balcerzak, C.J. Capicciotti, J.G. Briard, and R.N. Ben, Designing ice recrystallization inhibitors: From antifreeze (glyco)proteins to small molecules. RSC Advances 80 (2014) 42682-96

[21] H. Bank, Freezing injury in tissue cultured cells as visualized by freeze-etching. Exp Cell Res 85 (1974) 367-76.

[22] H. Bank, Visualization of freezing damage. II. Structural alterations during warming. Cryobiology 10 (1973) 157-170.

[23] R.E. Barnett, The effects of dimethylsulfoxide and glycerol on Na+,K+-ATPase and membrane structure. Cryobiology 15 (1978) 227-229.

[24] E.L. Bastiaanse, H.J. Jongsma, A. van der Laarse, and B.R. Takens-Kwak, Heptanol-induced decrease in cardiac gap junctional conductance is mediated by a decrease in the fluidity of membranous cholesterol-rich domains. J Membrane Biol 136 (1993) 135-145.

[25] K. Basu, C.P. Garnham, Y. Nishimiya, S. Tsuda, I. Braslavsky, and P. Davies, Determining the ice-binding planes of antifreeze proteins by fluorescence-based ice plane affinity. JoVE (Journal of Visualized Experiments) (2014) e51185.

[26] J.G. Baust, and J.S. Edwards, Mechanisms of freezing tolerance in an Antarctic midge, Belgica antarctica. Physiol Entomol 4 (1979) 1-5.

[27] J.G. Baust, B. JG, and R. RA, The physiology and biochemistry of low temperature tolerance in insects and other terrestrial arthropods: a bibliography. (1982).

[28] F.O. Belzer, and J.H. Southard, Principles of solid-organ preservation by cold storage. Transplantation 45 (1988) 673-6.

[29] T.A. Berendsen, B.G. Bruinsma, C.F. Puts, N. Saeidi, O.B. Usta, B.E. Uygun, M.L. Izamis, M. Toner, M.L. Yarmush, and K. Uygun, Supercooling enables long-term transplantation survival following 4 days of liver preservation. Nat Med 20 (2014) 790-3.

[30] W.K. Berger, and B. Uhrik, Freeze-induced shrinkage of individual cells and cell-to-cell propagation of intracellular ice in cell chains from salivary glands. Experientia 52 (1996) 843-50.

[31] J. Bischof, 45. Nanowarming: A new concept in tissue and organ preservation. Cryobiology 71 (2015) 176.

[32] J. Bischof, C.J. Hunt, B. Rubinsky, A. Burgess, and D.E. Pegg, Effects of cooling rate and glycerol concentration on the structure of the frozen kidney: assessment by cryo-scanning electron microscopy. Cryobiology 27 (1990) 301-10.

[33] J.C. Bischof, and B. Rubinsky, Large ice crystals in the nucleus of rapidly frozen liver cells. Cryobiology 30 (1993) 597-603.

[34] J.C. Bischof, C.M. Ryan, R.G. Tompkins, M.L. Yarmush, and M. Toner, Ice formation in isolated human hepatocytes and human liver tissue. ASAIO J 43 (1997) 271-8.

[35] W. Block, Cold hardiness in invertebrate poikilotherms. Comp. Biochem. Physiol. Part A 73 (1982) 581-593.

[36] P. Boutron, More accurate determination of the quantity of ice crystallized at low cooling rates in the glycerol and 1, 2-propanediol aqueous solutions: comparison with equilibrium. Cryobiology 21 (1984) 183-191.

[37] J.G. Briard, S. Jahan, P. Chandran, D. Allan, N. Pineault, and R.N. Ben, Small-molecule ice recrystallization inhibitors improve the post-thaw function of hematopoietic stem and progenitor cells. ACS omega 1 (2016) 1010-1018.

[38] J.G. Briard, J.S. Poisson, T.R. Turner, C.J. Capicciotti, J.P. Acker, and R.N. Ben, Small molecule ice recrystallization inhibitors mitigate red blood cell lysis during freezing, transient warming and thawing. Sci Rep 6 (2016) 23619.

[39] K.G. Brockbank, Effects of cryopreservation upon vein function in vivo. Cryobiology 31 (1994) 71-81.

[40] B.G. Bruinsma, T.A. Berendsen, M.L. Izamis, H. Yeh, M.L. Yarmush, and K. Uygun, Supercooling preservation and transplantation of the rat liver. Nat Protoc 10 (2015) 484-94.

[41] B.K. Campbell, J. Hernandez-Medrano, V. Onions, C. Pincott-Allen, F. Aljaser, J. Fisher, A.S. McNeilly, R. Webb, and H.M. Picton, Restoration of ovarian function and natural fertility following the cryopreservation and autotransplantation of whole adult sheep ovaries. Hum Reprod 29 (2014) 1749-63.

[42] C.J. Capicciotti, J.D. Kurach, T.R. Turner, R.S. Mancini, J.P. Acker, and R.N. Ben, Small molecule ice recrystallization inhibitors enable freezing of human red blood cells with reduced glycerol concentrations. Sci Rep 5 (2015) 9692.

[43] C.J. Capicciotti, M. Leclere, F.A. Perras, D.L. Bryce, H. Paulin, J. Harden, Y. Liu, and R.N. Ben, Potent inhibition of ice recrystallization by low molecular weight carbohydrate-based surfactants and hydrogelators. Chem Sci 3 (2012) 1408-1416.

[44] J.F. Carpenter, and T.N. Hansen, Antifreeze protein modulates cell survival during cryopreservation: mediation through influence on ice crystal growth. Proc Natl Acad Sci U S A 89 (1992) 8953-7.

[45] R. Chambers, and H. Hale, The formation of ice in protoplasm. Proceedings of the Royal Society of London. Series B, Containing Papers of a Biological Character 110 (1932) 336-352.

[46] J.S. Clegg, P. Seitz, W. Seitz, and C.F. Hazlewood, Cellular responses to extreme water loss: the water-replacement hypothesis. Cryobiology 19 (1982) 306-16.

[47] R.M. Cordeiro, S. Stirling, G.M. Fahy, and J.P. de Magalhaes, Insights on cryoprotectant toxicity from gene expression profiling of endothelial cells exposed to ethylene glycol. Cryobiology 71 (2015) 405-12.

[48] J.P. Costanzo, and R.E. Lee, Jr., Avoidance and tolerance of freezing in ectothermic vertebrates. J Exp Biol 216 (2013) 1961-7.

[49] K.J. Cowan, and K.B. Storey, Freeze-thaw effects on metabolic enzymes in wood frog organs. Cryobiology 43 (2001) 32-45.

[50] J.H. Crowe, L.M. Crowe, J.F. Carpenter, and C. Aurell Wistrom, Stabilization of dry phospholipid bilayers and proteins by sugars. Biochem J 242 (1987) 1-10.

[51] J.H. Crowe, L.M. Crowe, and R. Mouradian, Stabilization of biological membranes at low water activities. Cryobiology 20 (1983) 346-356.

[52] M. Cypel, J.C. Yeung, M. Liu, M. Anraku, F. Chen, W. Karolak, M. Sato, J. Laratta, S. Azad, M. Madonik, C.W. Chow, C. Chaparro, M. Hutcheon, L.G. Singer, A.S. Slutsky, K. Yasufuku, M. de Perrot, A.F. Pierre, T.K. Waddell, and S. Keshavjee, Normothermic ex vivo lung perfusion in clinical lung transplantation. N Engl J Med 364 (2011) 1431-40.

[53] J.R. Cypser, W.S. Chick, G.M. Fahy, G.J. Schumacher, and T.E. Johnson, Genetic suppression of cryoprotectant toxicity. Cryobiology 86 (2019) 95-102.

[54] P. Czechura, R.Y. Tam, E. Dimitrijevic, A.V. Murphy, and R.N. Ben, The importance of hydration for inhibiting ice recrystallization with C-linked antifreeze glycoproteins. J Am. Chem. Soc. 130 (2008) 2928-2929.

[55] R.C. De Freitas, and K.R. Diller, Intracellular ice formation in three-dimensional tissues: pancreatic islets. Cell Pres Tech 2 (2004) 19-28.

[56] I.A. de Graaf, A.L. Draaisma, O. Schoeman, G.M. Fahy, G.M. Groothuis, and H.J. Koster, Cryopreservation of rat precision-cut liver and kidney slices by rapid freezing and vitrification. Cryobiology 54 (2007) 1-12.

[57] W. De Loecker, V.A. Koptelov, V.I. Grischenko, and P. De Loecker, Effects of Cell Concentration on Viability and Metabolic Activity during Cryopreservation. Cryobiology 37 (1998) 103-109.

[58] R. de Vries, S.N. Tessier, P.D. Banik, S. Ozer, S.E.J. Crorin, S. Nagpal, H. Yeh, and K. Uygun, Extending the Human Liver Preservation Time for Transplantation by Supercooling. Transplantation 102 (2018) S396.

[59] R.V. Devireddy, and J.C. Bischof, Measurement of water transport during freezing in mammalian liver tissue: Part II—The use of differential scanning calorimetry. (1998) 559-569.

[60] R.V. Devireddy, P.R. Barratt, K.B. Storey, and J.C. Bischof, Liver freezing response of the freeze-tolerant wood frog, Rana sylvatica, in the presence and absence of glucose. I. Experimental measurements. Cryobiology 38 (1999) 310-326.

[61] A.L. DeVries, S.K. Komatsu, and R.E. Feeney, Chemical and physical properties of freezing point-depressing glycoproteins from Antarctic fishes. J Biol Chem 245 (1970) 2901-8.

[62] A.L. Devries, and Y. Lin, Structure of a peptide antifreeze and mechanism of adsorption to ice. Biochim Biophys Acta 495 (1977) 388-92.

[63] K. Diller, and J. Raymond, Water transport through a multicellular tissue during freezing-a network thermodynamic modeling analysis. Cryo-Letters 11 (1990) 151-162.

[64] K.R. Diller, Intracellular freezing of glycerolized red cells. Cryobiology 16 (1979) 125-31.

[65] K.R. Diller, Intracellular freezing: effect of extracellular supercooling. Cryobiology 12 (1975) 480-5.

[66] R. Dittrich, T. Maltaris, A. Mueller, A. Dimmler, I. Hoffmann, F. Kiesewetter, and M.W. Beckmann, Successful uterus cryopreservation in an animal model. Horm Metab Res 38 (2006) 141-5.

[67] Y.S. Djikaev, A. Tabazadeh, P. Hamill, and H. Reiss, Thermodynamic Conditions for the Surface-Stimulated Crystallization of Atmospheric Droplets. J Phys Chem A 106 (2002) 10247-10253.

[68] J.G. Duman, Factors involved in overwintering survival of the freeze tolerant beetle, Dendroides canadensis. J Comp Phys 136 (1980) 52-59.

[69] J.G. Duman, Insect antifreezes and ice-nucleating agents. Cryobiology 19 (1982) 613-27.

[70] J.G. Duman, K.L. Horwarth, A. Tomchaney, and J.L. Patterson, Antifreeze agents of terrestrial arthropods. Comparative Biochemistry and Physiology Part A: Physiology 73 (1982) 545-555.

[71] B. Elford, and C. Walter, Effects of electrolyte composition and pH on the structure and function of smooth muscle cooled to− 79° C in unfrozen media. Cryobiology 9 (1972) 82-100.

[72] A. Eniade, M. Purushotham, R.N. Ben, J. Wang, and K. Horwath, A serendipitous discovery of antifreeze protein-specific activity in C-linked antifreeze glycoprotein analogs. Cell Biochem Biophys 38 (2003) 115-124.

[73] E.A. Eren, N. Latchana, E. Beal, D. Hayes Jr, B. Whitson, and S.M. Black, Donations after circulatory death in liver transplant. MESOT 14 (2016) 463.

[74] D. Eshmuminov, D. Becker, L. Bautista Borrego, M. Hefti, M.J. Schuler, C. Hagedorn, X. Muller, M. Mueller, C. Onder, R. Graf, A. Weber, P. Dutkowski, P. Rudolf von Rohr, and P.A. Clavien, An integrated perfusion machine preserves injured human livers for 1 week. Nat Biotechnol 38 (2020) 189-198.

[75] D. Everett, The thermodynamics of frost damage to porous solids. J Chem Soc Faraday Trans 57 (1961) 1541-1551.

[76] G. Fahy, Cryoprotectant toxicity-Biochemical or osmotic. Cryo-Letters 5 (1984) 79-90.

[77] G. Fahy, and A. Karow Jr, Ultrastructure-function correlative studies for cardiac cryopreservation. V. Absence of a correlation between electrolyte toxicity and cryoinjury in the slowly frozen, cryoprotected rat heart. Cryobiology 14 (1977) 418-427.

[78] G.M. Fahy, Cryoprotectant toxicity neutralization. Cryobiology 60 (2010) S45-53.

[79] G.M. Fahy, D. Levy, and S. Ali, Some emerging principles underlying the physical properties, biological actions, and utility of vitrification solutions. Cryobiology 24 (1987) 196-213.

[80] G.M. Fahy, T.H. Lilley, H. Linsdell, M.S. Douglas, and H.T. Meryman, Cryoprotectant toxicity and cryoprotectant toxicity reduction: in search of molecular mechanisms. Cryobiology 27 (1990) 247-68.

[81] G.M. Fahy, D.R. MacFarlane, C.A. Angell, and H.T. Meryman, Vitrification as an approach to cryopreservation. Cryobiology 21 (1984) 407-426.

[82] G.M. Fahy, B. Wowk, J. Wu, and S. Paynter, Improved vitrification solutions based on the predictability of vitrification solution toxicity. Cryobiology 48 (2004) 22-35.

[83] G.M. Fahy, B. Wowk, J. Wu, J. Phan, C. Rasch, A. Chang, and E. Zendejas, Cryopreservation of organs by vitrification: perspectives and recent advances. Cryobiology 48 (2004) 157-78.

[84] J. Farrant, Mechanism of cell damage during freezing and thawing and its prevention. Nature 205 (1965) 1284-1287.

[85] J. Farrant, and G.J. Morris, Thermal shock and dilution shock as the causes of freezing injury. Cryobiology 10 (1973) 134-140.

[86] B. Gaber, I. Chandrasekhar, and N. Pattiabiraman, Molecular Modeling of the Interaction of Trehalose with the Phospholipid-Bilayer, Biophysical Journal, BIOPHYSICAL SOCIETY 9650 ROCKVILLE PIKE, BETHESDA, MD 20814-3998, 1986, pp. A435-A435.

[87] S. Giwa, J.K. Lewis, L. Alvarez, R. Langer, A.E. Roth, G.M. Church, J.F. Markmann, D.H. Sachs, A. Chandraker, J.A. Wertheim, M. Rothblatt, E.S. Boyden, E. Eidbo, W.P.A. Lee, B. Pomahac, G. Brandacher, D.M. Weinstock, G. Elliott, D. Nelson, J.P. Acker, K. Uygun, B. Schmalz, B.P. Weegman, A. Tocchio, G.M. Fahy, K.B. Storey, B. Rubinsky, J. Bischof, J.A.W. Elliott, T.K. Woodruff, G.J. Morris, U. Demirci, K.G.M. Brockbank, E.J. Woods,

R.N. Ben, J.G. Baust, D. Gao, B. Fuller, Y. Rabin, D.C. Kravitz, M.J. Taylor, and M. Toner, The promise of organ and tissue preservation to transform medicine. Nat Biotechnol 35 (2017) 530-542.

[88] N. Guan, S.A. Blomsma, G.M. Fahy, G.M. Groothuis, and I.A. de Graaf, Analysis of gene expression changes to elucidate the mechanism of chilling injury in precision-cut liver slices. Toxicol In Vitro 27 (2013) 890-9.

[89] E.E. Guibert, L.L. Almada, M.E. Mamprin, C. Bellarosa, M.D. Pizarro, C. Tiribelli, and J.V. Rodriguez, Subzero nonfreezing storage of rat hepatocytes using UW solution and 1, 4-butanediol. II-functional testing on rewarming and gene expression of urea cycle enzymes. Annals of hepatology 8 (2009) 129-133.

[90] A.A. Gurtovenko, and J. Anwar, Modulating the structure and properties of cell membranes: the molecular mechanism of action of dimethyl sulfoxide. J Phys Chem B 111 (2007) 10453-60.

[91] F. Guttman, A. Khalessi, B. Huxley, R. Lee, and G. Savard, Whole organ preservation: I. A technique for in vivo freezing canine intestine using intraarterial helium and ambient nitrogen. Cryobiology 6 (1969) 32-36.

[92] F. Guttman, N. Segal, and J. Borzone, Cryopreservation of canine kidneys with dimethyl sulphoxide: further studies, Organ Preservation II, Churchill Livingstone Edinburgh, 1979, pp. 185.

[93] F.M. Guttman, J. Lizin, P. Robitaille, H. Blanchard, and C. Turgeon-Knaack, Survival of canine kidneys after treatment with dimethyl-sulfoxide, freezing at− 80° C, and thawing by microwave illumination. Cryobiology 14 (1977) 559-567.

[94] R. Hamilton, H.I. Holst, and H.B. Lehr, Successful preservation of canine small intestine by freezing. J Surg Res 14 (1973) 313-8.

[95] T. Hansen, Glycerol content and cold-hardiness in freeze tolerant insects. Eesti. NSV. Tead. Akad. Tiom. Biol 29 (1980) 113-118.

[96] C.L. Harris, M. Toner, A. Hubel, E.G. Cravalho, M.L. Yarmush, and R.G. Tompkins, Cryopreservation of isolated hepatocytes: Intracellular ice formation under various chemical and physical conditions. Cryobiology 28 (1991) 436-444.

[97] P.H. Hayashi, D.A. Axelrod, J. Galanko, P.R. Salvalaggio, and M. Schnitzler, Regional differences in deceased donor liver transplantation and their implications for organ utilization and allocation. Clin Tranplant 25 (2011) 156-163.

[98] J. Hey, and D. MacFarlane, Crystallization of ice in aqueous solutions of glycerol and dimethyl sulfoxide. 1. A comparison of mechanisms. Cryobiology 33 (1996) 205-216.

[99] A.Z. Higgins, and J.O. Karlsson, Effects of intercellular junction protein expression on intracellular ice formation in mouse insulinoma cells. Biophys J 105 (2013) 2006-15.

[100] P.V. Hobbs, Ice physics, Oxford university press, 2010.

[101] H. Huang, M.L. Yarmush, and O.B. Usta, Long-term deep-supercooling of large-volume water and red cell suspensions via surface sealing with immiscible liquids. Nat Commun 9 (2018) 3201.

[102] A. Hubel, M. Toner, E.G. Cravalho, M.L. Yarmush, and R.G. Tompkins, Intracellular ice formation during the freezing of hepatocytes cultured in a double collagen gel. Biotechnol Prog 7 (1991) 554-9.

[103] Z.E. Hughes, A.E. Mark, and R.L. Mancera, Molecular dynamics simulations of the interactions of DMSO with DPPC and DOPC phospholipid membranes. J Phys Chem B 116 (2012) 11911-23.

[104] D. Irimia, and J.O. Karlsson, Kinetics and mechanism of intercellular ice propagation in a micropatterned tissue construct. Biophys J 82 (2002) 1858-68.

[105] H. Ishiguro, and B. Rubinsky, Mechanical interactions between ice crystals and red blood cells during directional solidification. Cryobiology 31 (1994) 483-500.

[106] N. Ishine, B. Rubinsky, and C.Y. Lee, A histological analysis of liver injury in freezing storage. Cryobiology 39 (1999) 271-7.

[107] N. Ishine, B. Rubinsky, and C.Y. Lee, Transplantation of mammalian livers following freezing: vascular damage and functional recovery. Cryobiology 40 (2000) 84-9.

[108] K. Jackson, and B. Chalmers, Freezing of liquids in porous media with special reference to frost heave in soils. J App Phys 29 (1958) 1178-1181.

[109] S.W. Jacob, Studies in organ preservation by actual freezing and reduction of the freezing point. Cryobiology 1 (1964) 176-80.

[110] I.A. Jacobsen, and D.E. Pegg, Cryopreservation of organs: a review. Cryobiology 21 (1984) 377-84.

[111] I.A. Jacobsen, D.E. Pegg, H. Starklint, J. Chemnitz, C. Hunt, P. Barfort, and M.P. Diaper, Effect of cooling and warming rate on glycerolized rabbit kidneys. Cryobiology 21 (1984) 637-53.

[112] S. Jahan, M.K. Adam, J.K. Manesia, E. Doxtator, R.N. Ben, and N. Pineault, Inhibition of ice recrystallization during cryopreservation of cord blood grafts improves platelet engraftment. Transfusion 60 (2020) 769-778.

[113] I. Jochmans, C. Moers, J.M. Smits, H.G. Leuvenink, J. Treckmann, A. Paul, A. Rahmel, J.P. Squifflet, E. van Heurn, D. Monbaliu, R.J. Ploeg, and J. Pirenne, Machine perfusion versus cold storage for the preservation of kidneys donated after cardiac death: a multicenter, randomized, controlled trial. Ann Surg 252 (2010) 756-64.

[114] J.O. Karlsson, Effects of solution composition on the theoretical prediction of ice nucleation kinetics and thermodynamics. Cryobiology 60 (2010) 43-51.

[115] K. Khosla, L. Zhan, A. Bhati, A. Carley-Clopton, M. Hagedorn, and J. Bischof, Characterization of Laser Gold Nanowarming: A Platform for Millimeter-Scale Cryopreservation. Langmuir 35 (2019) 7364-7375.

[116] C.A. Knight, and J.G. Duman, Inhibition of recrystallization of ice by insect thermal hysteresis proteins: A possible cryoprotective role. Cryobiology 23 (1986) 256-262.

[117] B. Korniski, and A. Hubel, A model of low-temperature water transport for hepatocyte spheroids. Ann N Y Acad Sci 858 (1998) 183-90.

[118] E. Kristiansen, and K.E. Zachariassen, The mechanism by which fish antifreeze proteins cause thermal hysteresis, 2005.

[119] S. Kubota, F. Graham, B.G. Crabo, R.C. Lillehei, and R.H. Dietman, The effect of freeze rate, duration of phase transition, and warming rate on survival of frozen canine kidneys. Cryobiology 13 (1976) 455-62.

[120] A. Larese, J. Acker, K. Muldrew, H. Yang, and L. McGann, Antifreeze proteins induce intracellular nucleation. Cryo-Letters 17 (1996) 175-182.

[121] A. Larese, H. Yang, A. Petrenko, and L. McGann, Intracellular ice formation is affected by cell-to-cell contact. Cryobiology 29 (1992) 728.

[122] J.R. Layne Jr, and R.E. Lee Jr, Freeze tolerance and the dynamics of ice formation in wood frogs (Rana sylvatica) from southern Ohio. Can J Zool 65 (1987) 2062-2065.

[123] J.R. Layne, Jr., J.P. Costanzo, and R.E. Lee, Jr., Freeze duration influences postfreeze survival in the frog Rana sylvatica. J Exp Zool 280 (1998) 197-201.

[124] R.E. Lee, G.J. Warren, and L.V. Gusta, Biological ice nucleation and its applications, APS Press, St. Paul, Minn., 1995.

[125] R. Levin, E. Cravalho, and C. Huggins, Water transport in a cluster of closely packed erythrocytes at subzero temperatures. Cryobiology 14 (1977) 549-558.

[126] J.K. Lewis, J.C. Bischof, I. Braslavsky, K.G. Brockbank, G.M. Fahy, B.J. Fuller, Y. Rabin, A. Tocchio, E.J. Woods, B.G. Wowk, J.P. Acker, and S. Giwa, The Grand Challenges of Organ Banking: Proceedings from the first global summit on complex tissue cryopreservation. Cryobiology 72 (2016) 169-82.

[127] S. Liu, and R.N. Ben, C-linked galactosyl serine AFGP analogues as potent recrystallization inhibitors. Organic letters 7 (2005) 2385-2388.

[128] W.P. Liu, A.L. Humphries, Jr., R. Russell, L.D. Stoddard, and W.H. Moretz, 48-hour storage of canine kidneys after brief perfusion with Collins' solution. Ann Surg 173 (1971) 748-57.

[129] X. Liu, G. Zhao, Z. Shu, D. Niu, Z. Zhang, P. Zhou, Y. Cao, and D. Gao, Quantification of intracellular ice formation and recrystallization during freeze–thaw cycles and their relationship with the viability of pig iliac endothelium cells. Biopres Biobank 14 (2016) 511-519.

[130] S.H. Loomis, Seasonal changes in the freezing tolerance of the intertidal pulmonate gastropod Melampus bidentatus Say. Can J Zool 63 (1985) 2021-2025.

[131] P.A. Lotke, and M.F. Dolan, Thermoelectric cooler for whole organ freezing and thawing. Cryobiology 1 (1965) 289-91.

[132] J.E. Lovelock, Het mechanism of the protective action of glycerol against haemolysis by freezing and thawing. Bioch Biophys Acta 11 (1953) 28-36.

[133] J.E. Lovelock, and M.W. Bishop, Prevention of freezing damage to living cells by dimethyl sulphoxide. Nature 183 (1959) 1394-5.

[134] C.H. Lowe, P.J. Lardner, and E.A. Halpern, Supercooling in reptiles and other vertebrates. Comp Biochem Physiol A 39 (1971) 125-35.

[135] D. MacArthur, and J. Dandy, Physiological aspects of overwintering in the boreal chorus frog (Pseudacris triseriata maculata). Comp Biochem Physiol A 72 (1982) 137-141.

[136] A. MacKenzie, Death of frozen yeast in the course of slow warming, Ciba Foundation Symposium-The Frozen Cell, Wiley Online Library, 1970, pp. 89-96.

[137] N. Manuchehrabadi, Z. Gao, J. Zhang, H.L. Ring, Q. Shao, F. Liu, M. McDermott, A. Fok, Y. Rabin, K.G. Brockbank, M. Garwood, C.L. Haynes, and J.C. Bischof, Improved tissue cryopreservation using inductive heating of magnetic nanoparticles. Sci Transl Med 9 (2017) eaah4586.

[138] J. Matheny, A.M. Karow Jr, and O. Carrier Jr, Toxicity of dimethyl sulfoxide and magnesium as a function of temperature. Eur J Pharmacol 5 (1969) 209-212.

[139] S.F. Mathias, F. Franks, and R.H. Hatley, Preservation of viable cells in the undercooled state. Cryobiology 22 (1985) 537-46.

[140] N. Matsumoto, H. Yoshizawa, H. Kagamu, T. Abe, N. Fujita, S. Watanabe, H. Kuriyama, T. Ishiguro, J. Tanaka, and E. Suzuki, Successful liquid storage of peripheral blood stem cells at subzero non-freezing temperature. Bone Marrow Transplant 30 (2002) 777-784.

[141] P. Mazur, Causes of Injury in Frozen and Thawed Cells. Fed Proc 24 (1965) S175-82.

[142] P. Mazur, Cryobiology: The freezing of biological systems. Science (1970) 403-506

[143] P. Mazur, Equilibrium, quasi-equilibrium, and nonequilibrium freezing of mammalian embryos. Cell Biophys 17 (1990) 53-92.

[144] P. Mazur, Freezing of living cells: mechanisms and implications. Am J Physiol 247 (1984) C125-42.

[145] P. Mazur, Kinetics of water loss from cells at subzero temperatures and the likelihood of intracellular freezing. J Gen Physiol 47 (1963) 347-69.

[146] P. Mazur, Physical-chemical basis of injury from intracellular freezing in yeast. Cellular Injury and Resistance in Freezing Organisms: proceedings proceedings 2 (1967) 171-189.

[147] P. Mazur, Principles of cryobiology. Life in the frozen state (1984).

[148] P. Mazur, The role of cell membranes in the freezing of yeast and other single cells. Ann N Y Acad Sci 125 (1965) 658-76.

[149] P. Mazur, The role of intracellular freezing in the death of cells cooled at supraoptimal rates. Cryobiology 14 (1977) 251-272.

[150] P. Mazur, and K.W. Cole, Influence of cell concentration on the contribution of unfrozen fraction and salt concentration to the survival of slowly frozen human erythrocytes. Cryobiology 22 (1985) 509-536.

[151] P. Mazur, and K.W. Cole, Influence of cell concentration on the contribution of unfrozen fraction and salt concentration to the survival of slowly frozen human erythrocytes. Cryobiology 22 (1985) 509-36.

[152] P. Mazur, S.P. Leibo, and E.H. Chu, A two-factor hypothesis of freezing injury. Evidence from Chinese hamster tissue-culture cells. Exp Cell Res 71 (1972) 345-55.

[153] P. Mazur, and R.H. Miller, Survival of frozen-thawed human red cells as a function of the permeation of glycerol and sucrose. Cryobiology 13 (1976) 523-536.

[154] P. Mazur, W.F. Rall, and N. Rigopoulos, Relative contributions of the fraction of unfrozen water and of salt concentration to the survival of slowly frozen human erythrocytes. Biophys J 36 (1981) 653-75.

[155] P. Mazur, and N. Rigopoulos, Contributions of unfrozen fraction and of salt concentration to the survival of slowly frozen human erythrocytes: influence of warming rate. Cryobiology 20 (1983) 274-89.

[156] L.E. McGann, Differing actions of penetrating and nonpenetrating cryoprotective agents. Cryobiology 15 (1978) 382-90.

[157] J. McGrath, E. Cravalho, and C. Huggins, An experimental comparison of intracellular ice formation and freeze-thaw survival of HeLa S-3 cells. Cryobiology 12 (1975) 540-550.

[158] H. Mergental, M.T. Perera, R.W. Laing, P. Muiesan, J.R. Isaac, A. Smith, B.T. Stephenson, H. Cilliers, D.A. Neil, S.G. Hubscher, S.C. Afford, and D.F. Mirza, Transplantation of Declined Liver Allografts Following Normothermic Ex-Situ Evaluation. Am J Transplant 16 (2016) 3235-3245.

[159] H.T. Meryman, Cryopreservation of living cells: principles and practice. Transfusion 47 (2007) 935-45.

[160] H.T. Meryman, Freezing injury and its prevention in living cells. Ann Rev Biophys Bioeng 3 (1974) 341-363.

[161] H.T. Meryman, Osmotic stress as a mechanism of freezing injury. Cryobiology 8 (1971) 489-500.

[162] M. Milenkovic, C. Diaz-Garcia, A. Wallin, and M. Brannstrom, Viability and function of the cryopreserved whole rat ovary: comparison between slow-freezing and vitrification. Fertil Steril 97 (2012) 1176-82.

[163] L.K. Miller, and J.S. Smith, Production of threitol and sorbitol by an adult insect: association with freezing tolerance. Nature 258 (1975) 519-20.

[164] R.H. Miller, and P. Mazur, Survival of frozen-thawed human red cells as a function of cooling and warming velocities. Cryobiology 13 (1976) 404-414.

[165] C. Moers, J. Pirenne, A. Paul, R.J. Ploeg, and G. Machine Preservation Trial Study, Machine perfusion or cold storage in deceased-donor kidney transplantation. N Engl J Med 366 (2012) 770-1.

[166] C. Moers, J.M. Smits, M.H. Maathuis, J. Treckmann, F. van Gelder, B.P. Napieralski, M. van Kasterop-Kutz, J.J. van der Heide, J.P. Squifflet, E. van Heurn, G.R. Kirste, A. Rahmel, H.G. Leuvenink, A. Paul, J. Pirenne, and R.J. Ploeg, Machine perfusion or cold storage in deceased-donor kidney transplantation. N Engl J Med 360 (2009) 7-19.

[167] G. Moray, S. Sevmis, F. Karakayali, S. Gorur, and M. Haberal, Comparison of histidine-tryptophan-ketoglutarate and University of Wisconsin in living-donor liver transplantation, Transplantation proceedings, Elsevier, 2006, pp. 3572-3575.

[168] G.S. Moss, P. Reed, and A.G. Riddell, Observations on the effects of glycerol on the cold storage of the canine liver. J Surg Res 6 (1966) 147-51.

[169] K. Muldrew, M. Hurtig, K. Novak, N. Schachar, and L.E. McGann, Localization of freezing injury in articular cartilage. Cryobiology 31 (1994) 31-8.

[170] K. Muldrew, and L.E. McGann, Mechanisms of intracellular ice formation. Biophys J 57 (1990) 525-32.

[171] K. Muldrew, and L.E. McGann, The osmotic rupture hypothesis of intracellular freezing injury. Biophys J 66 (1994) 532-41.

[172] K. Muldrew, K. Novak, H. Yang, R. Zernicke, N.S. Schachar, and L.E. McGann, Cryobiology of articular cartilage: ice morphology and recovery of chondrocytes. Cryobiology 40 (2000) 102-9.

[173] D.J. Murphy, Freezing resistance in intertidal invertebrates. Annu Rev Physiol 45 (1983) 289-99.

[174] T. Nei, Mechanism of hemolysis of erythrocytes by freezing at near-zero temperatures: I. Microscopic observation of hemolyzing erythrocytes during the freezing and thawing process. Cryobiology 4 (1967) 153-156.

[175] J.M. O'Callaghan, S.R. Knight, R.D. Morgan, and P.J. Morris, Preservation solutions for static cold storage of kidney allografts: a systematic review and meta-analysis. Am J Transplant 12 (2012) 896-906.

[176] L.L. Olijve, K. Meister, A.L. DeVries, J.G. Duman, S. Guo, H.J. Bakker, and I.K. Voets, Blocking rapid ice crystal growth through nonbasal plane adsorption of antifreeze proteins. Proc Nat Acad Sci 113 (2016) 3740-3745.

[177] E.S. Orman, M.E. Mayorga, S.B. Wheeler, R.M. Townsley, H.H. Toro-Diaz, P.H. Hayashi, and A.S.t. Barritt, Declining liver graft quality threatens the future of liver transplantation in the United States. Liver Transpl 21 (2015) 1040-50.

[178] E. Ozcinar, E.N. Okatan, E. Tuncay, S. Eryilmaz, and B. Turan, Improvement of functional recovery of donor heart following cold static storage with doxycycline cardioplegia. Cardiovasc Toxicol 14 (2014) 64-73.

[179] P.V. Pazhayannur, and J.C. Bischof, Measurement and simulation of water transport during freezing in mammalian liver tissue. J Biomech Eng 119 (1997) 269-77.

[180] D.E. Pegg, Ice crystals in tissues and organs, The biophysics of organ cryopreservation, Springer, 1987, pp. 117-140.

[181] D.E. Pegg, -Principles of Cryopreservation, Preservation of Human Oocytes, CRC Press, 2009, pp. 34-46.

[182] D.E. Pegg, The relevance of ice crystal formation for the cryopreservation of tissues and organs. Cryobiology 60 (2010) S36-44.

[183] D.E. Pegg, M.P. Diaper, H.L. Skaer, and C.J. Hunt, The effect of cooling rate and warming rate on the packing effect in human erythrocytes frozen and thawed in the presence of 2 M glycerol. Cryobiology 21 (1984) 491-502.

[184] D.E. Pegg, C.J. Green, and C.A. Walter, Attempted canine renal cryopreservation using dimethyl sulphoxide helium perfusion and microwave thawing. Cryobiology 15 (1978) 618-626.

[185] D.E. Pegg, and A.M. Karow Jr, The biophysics of organ cryopreservation, Springer Science & Business Media, 2012.

[186] D.E. Pegg, L. Wang, and D. Vaughan, Cryopreservation of articular cartilage. Part 3: the liquidus-tracking method. Cryobiology 52 (2006) 360-8.

[187] J.S. Poisson, J.P. Acker, J.G. Briard, J.E. Meyer, and R.N. Ben, Modulating Intracellular Ice Growth with Cell-Permeating Small-Molecule Ice Recrystallization Inhibitors. Langmuir 35 (2018) 7452-7458.

[188] J.S. Poisson, J.G. Briard, T.R. Turner, J.P. Acker, and R.N. Ben, Hydroxyethyl Starch Supplemented with Ice Recrystallization Inhibitors Greatly Improves Cryopreservation of Human Red Blood Cells. Bioproc J 15 (2016).

[189] C. Polge, A.U. Smith, and A.S. Parkes, Revival of spermatozoa after vitrification and dehydration at low temperatures. Nature 164 (1949) 666.

[190] P. Popovic, and V. Popovic, Survival of newborn ground squirrels after supercooling or freezing. Am J Physiol 204 (1963) 949-52.

[191] A. Porsche, C. Körber, and G. Rau, Freeze thaw behavior of cultured (bovine corneal) endothelial cells: suspension vs. monolayer. Cryobiology 28 (1991) 545.

[192] P.D. Pudney, S.L. Buckley, C.M. Sidebottom, S.N. Twigg, M.P. Sevilla, C.B. Holt, D. Roper, J.H. Telford, A.J. McArthur, and P.J. Lillford, The physico-chemical characterization of a boiling stable antifreeze protein from a perennial grass (Lolium perenne). Arch Biochem Biophys 410 (2003) 238-45.

[193] E. Puschmann, C. Selden, S. Butler, and B. Fuller, Liquidus tracking: controlled rate vitrification for the cryopreservation of larger volumes and tissues. Cryo Letters 35 (2014) 345-55.

[194] E. Puschmann, C. Selden, S. Butler, and B. Fuller, Liquidus Tracking: Large scale preservation of encapsulated 3-D cell cultures using a vitrification machine. Cryobiology 76 (2017) 65-73.

[195] P.J. Quinn, A lipid-phase separation model of low-temperature damage to biological membranes. Cryobiology 22 (1985) 128-46.

[196] G. Rapatz, L. Menz, and B. Luyet, Anatomy of the freezing process in biological materials. Cryobiology 3 (1966) 139-162.

[197] D.H. Rasmussen, M.N. Macaulay, and A.P. MacKenzie, Supercooling and nucleation of ice in single cells. Cryobiology 12 (1975) 328-39.

[198] F. Riemann, M. Schrage, and H. Farke, High freezing tolerance of marine nematodes from intertidal sediments of the German Bight. Nematologica 30 (1984) 452-456.

[199] J.V. Rodríguez, L.L. Almada, M.E. Mamprin, E.E. Guibert, and G. Furno, Subzero nonfreezing storage of rat hepatocytes using modified University of Wisconsin solution (mUW) and 1, 4-butanediol. I-effects on cellular metabolites during cold storage. Ann Hepatol 8 (2009) 57-62.

[200] B. Rubinsky, A. Arav, J.S. Hong, and C.Y. Lee, Freezing of mammalian livers with glycerol and antifreeze proteins. Biochem Biophys Res Commun 200 (1994) 732-41.

[201] B. Rubinsky, A. Arav, M. Mattioli, and A.L. Devries, The effect of antifreeze glycopeptides on membrane potential changes at hypothermic temperatures. Biochem Biophys Res Com 173 (1990) 1369-1374.

[202] B. Rubinsky, E.G. Cravalho, and B. Mikic, Thermal stresses in frozen organs. Cryobiology 17 (1980) 66-73.

[203] B. Rubinsky, and M. Ikeda, A cryomicroscope using directional solidification for the controlled freezing of biological material. Cryobiology 22 (1985) 55-68.

[204] B. Rubinsky, C.Y. Lee, J. Bastacky, and G. Onik, The process of freezing and the mechanism of damage during hepatic cryosurgery. Cryobiology 27 (1990) 85-97.

[205] B. Rubinsky, M. Mattioli, A. Arav, B. Barboni, and G.L. Fletcher, Inhibition of Ca2+ and K+ currents by "antifreeze" proteins. Am J Physiol 262 (1992) R542-5.

[206] B. Rubinsky, and D.E. Pegg, A mathematical model for the freezing process in biological tissue. Proc R Soc Lond B Biol Sci 234 (1988) 343-58.

[207] B. Rubinsky, S. Wong, J. Hong, J. Gilbert, M. Roos, and K.B. Storey, 1H magnetic resonance imaging of freezing and thawing in freeze-tolerant frogs. Am J Physiol Regul Integr Comp Physiol 266 (1994) R1771-R1777.

[208] A.S. Rudolph, and J.H. Crowe, Membrane stabilization during freezing: the role of two natural cryoprotectants, trehalose and proline. Cryobiology 22 (1985) 367-77.

[209] A.S. Rudolph, J.H. Crowe, and L.M. Crowe, Effects of three stabilizing agents—proline, betaine, and trehalose—on membrane phospholipids. Arch Biochem Biophys 245 (1986) 134-143.

[210] O.Y. Sally, A. Brown, A.J. Middleton, M.M. Tomczak, V.K. Walker, and P.L. Davies, Ice restructuring inhibition activities in antifreeze proteins with distinct differences in thermal hysteresis. Cryobiology 61 (2010) 327-334.

[211] J.D. Scandling, S. Busque, J.A. Shizuru, E.G. Engleman, and S. Strober, Induced immune tolerance for kidney transplantation. N Engl J Med 365 (2011) 1359-60.

[212] W.D. Schmid, Survival of frogs in low temperature. Science 215 (1982) 697-8.

[213] S. Seki, and P. Mazur, Effect of warming rate on the survival of vitrified mouse oocytes and on the recrystallization of intracellular ice. Biol Reprod 79 (2008) 727-37.

[214] R.A. Shaw, A.J. Durant, and Y. Mi, Heterogeneous surface crystallization observed in undercooled water. J Phys Chem B 109 (2005) 9865-8.

[215] A. Sicular, and F.D. Moore, The postmortem survival of tissues: the effect of time and temperature on the survival of liver as measured by glucose oxidation rate. J Surg Res 1 (1961) 16-22.

[216] L. Sømme, Supercooling and winter survival in terrestrial arthropods. Comparative Biochemistry and Physiology Part A: Physiology 73 (1982) 519-543.

[217] Y.C. Song, Y.H. An, Q.K. Kang, C. Li, J.M. Boggs, Z. Chen, M.J. Taylor, and K.G. Brockbank, Vitreous preservation of articular cartilage grafts. J Invest Surg 17 (2004) 65-70.

[218] Y.C. Song, P.O. Hagen, F.G. Lightfoot, M.J. Taylor, A.C. Smith, and K.G. Brockbank, In vivo evaluation of the effects of a new ice-free cryopreservation process on autologous vascular grafts. J Invest Surg 13 (2000) 279-88.

[219] Y.C. Song, B.S. Khirabadi, F. Lightfoot, K.G. Brockbank, and M.J. Taylor, Vitreous cryopreservation maintains the function of vascular grafts. Nat Biotechnol 18 (2000) 296-9.

[220] G.E. Sosinsky, and B.J. Nicholson, Structural organization of gap junction channels. Biochimica et Biophysica Acta (BBA)-Biomembranes 1711 (2005) 99-125.

[221] P. Steponkus, and M. Dowgert, Phenomenology of intracellular ice nucleation in isolated protoplasts. Plant Physiol 67 (1981) S, 58.

[222] P.L. Steponkus, Role of the plasma membrane in freezing injury and cold acclimation. Annual Review of Plant Physiology 35 (1984) 543-584.

[223] P.L. Steponkus, M.F. Dowgert, and W.J. Gordon-Kamm, Destabilization of the plasma membrane of isolated plant protoplasts during a freeze-thaw cycle: the influence of cold acclimation. Cryobiology 20 (1983) 448-65.

[224] J.M. Storey, and K.B. Storey, Triggering of cryoprotectant synthesis by the initiation of ice nucleation in the freeze tolerant frog, Rana sylvatica. J Comp Phys B 156 (1985) 191-195.

[225] K.B. Storey, Freeze tolerance in the frog,Rana sylvatica. Experientia 40 (1984) 1261-1262.

[226] K.B. Storey, J. Bischof, and B. Rubinsky, Cryomicroscopic analysis of freezing in liver of the freeze-tolerant wood frog. Am J Physiol 263 (1992) R185-94.

[227] K.B. Storey, and J.M. Storey, Biochemical adaption for freezing tolerance in the wood frog, Rana sylvatica. J Comp Phys B 155 (1984) 29-36.

[228] K.B. Storey, and J.M. Storey, Freeze tolerance in animals. Physiol Rev 68 (1988) 27-84.

[229] K.B. Storey, and J.M. Storey, Freeze tolerant frogs: cryoprotectants and tissue metabolism during freeze–thaw cycles. Canadian Journal of Zoology 64 (1986) 49-56.

[230] K.B. Storey, and J.M. Storey, Natural Freezing Survival in Animals. Annual Review of Ecology and Systematics 27 (1996) 365-386.

[231] S.L. Stott, and J.O.M. Karlsson, 29. Cell perimeter modulates the kinetics of intracellular ice formation and frequency of paracellular ice formation in micropatterned endothelial cells. Cryobiology 53 (2006) 379-380.

[232] S.L. Stott, and J.O.M. Karlsson, Visualization of intracellular ice formation using high-speed video cryomicroscopy. Cryobiology 58 (2009) 84-95.

[233] A. Tabazadeh, Y.S. Djikaev, and H. Reiss, Surface crystallization of supercooled water in clouds. Proc Natl Acad Sci U S A 99 (2002) 15873-8.

[234] R.Y. Tam, S.S. Ferreira, P. Czechura, J.L. Chaytor, and R.N. Ben, Hydration Index · A Better Parameter for Explaining Small Molecule Hydration in Inhibition of Ice Recrystallization. J Am Chem Soc 130 (2008) 17494-17501.

[235] M. Taylor, and D. Pegg, The effect of ice formation on the function of smooth muscle tissue following storage at− 21 C and− 60 C. Cryobiology 20 (1982) 36-40.

[236] M. Taylor, Y. Song, K. Brockbank, B. Fuller, N. Lane, and E. Benson, 22 Vitrification in Tissue Preservation: New Developments. Life in the Frozen State, BJ Fuller, N. Lane, and EE Benson, eds., CRC Press, Boca Raton, FL (2004) 604-641.

[237] M.J. Taylor, Y. Song, B. Kheirabadi, F. Lightfoot, and K. Brockbank, Vitrification fulfills its promise as an approach to reducing freeze-induced injury in a multicellular tissue. ASME-PUBLICATIONS-HTD 363 (1999) 93-102.

[238] S.N. Tessier, S.E.J. Cronin, C.A. Pendexter, S. Özer, R.J. de Vries, S. Nagpal, P.D. Banik, K. Uygun, and M. Toner, Partial freezing: A nature-inspired strategy for organ banking. Cryobiology 81 (2018) 220.

[239] S.N. Tessier, L. Weng, W.D. Moyo, S.H. Au, K.H.K. Wong, C. Angpraseuth, A.E. Stoddard, C. Lu, L.T. Nieman, R.D. Sandlin, K. Uygun, S.L. Stott, and M. Toner, Effect of Ice Nucleation and Cryoprotectants during High Subzero-Preservation in Endothelialized Microchannels. ACS Biomater Sci Eng 4 (2018) 3006-3015.

[240] W. Thomson, LX. On the equilibrium of vapour at a curved surface of liquid. The London, Edinburgh, and Dublin Philosophical Magazine and Journal of Science 42 (2009) 448-452.

[241] R.M.F. Tomas, T.L. Bailey, M. Hasan, and M.I. Gibson, Extracellular Antifreeze Protein Significantly Enhances the Cryopreservation of Cell Monolayers. Biomacromolecules 20 (2019) 3864-3872.

[242] M. Toner, E.G. Cravalho, and M. Karel, Thermodynamics and kinetics of intracellular ice formation during freezing of biological cells. J App Phys 67 (1990) 1582-1593.

[243] J. Treckmann, C. Moers, J.M. Smits, A. Gallinat, M.H. Maathuis, M. van Kasterop-Kutz, I. Jochmans, J.J. Homan van der Heide, J.P. Squifflet, E. van Heurn, G.R. Kirste, A. Rahmel, H.G. Leuvenink, J. Pirenne, R.J. Ploeg, and A. Paul, Machine perfusion versus cold storage for preservation of kidneys from expanded criteria donors after brain death. Transpl Int 24 (2011) 548-54.

[244] T. Tsuruta, Y. Ishimoto, and T. Masuoka, Effects of Glycerol on Intracellular Ice Formation and Dehydration of Onion Epidermis a. Annals of the New York Academy of Sciences 858 (1998) 217-226.

[245] J. van der Elsken, J. Dings, and J.C.F. Michielsen, The freezing of supercooled water. J Mol Struct 250 (1991) 245-251.

[246] C.T. Wagner, M.B. Burnett, S.A. Livesey, and J. Connor, Red blood cell stabilization reduces the effect of cell density on recovery following cryopreservation. Cryobiology 41 (2000) 178-194.

[247] J.A. Wahlberg, J.H. Southard, and F.O. Belzer, Development of a cold storage solution for pancreas preservation. Cryobiology 23 (1986) 477-82.

[248] K.R. Walters, Jr., A.S. Serianni, Y. Voituron, T. Sformo, B.M. Barnes, and J.G. Duman, A thermal hysteresis-producing xylomannan glycolipid antifreeze associated with cold tolerance is found in diverse taxa. J Comp Physiol B 181 (2011) 631-40.

[249] L. Wang, D.E. Pegg, J. Lorrison, D. Vaughan, and P. Rooney, Further work on the cryopreservation of articular cartilage with particular reference to the liquidus tracking (LT) method. Cryobiology 55 (2007) 138-147.

[250] Z. Wang, B. He, Y. Duan, Y. Shen, L. Zhu, X. Zhu, and Z. Zhu, Cryopreservation and replantation of amputated rat hind limbs. Eur J Med Res 19 (2014) 28.

[251] G. Warnecke, D. Van Raemdonck, M.A. Smith, G. Massard, J. Kukreja, F. Rea, G. Loor, F. De Robertis, J. Nagendran, K.K. Dhital, F.J. Moradiellos Diez, C. Knosalla, C.A. Bermudez, S. Tsui, K. McCurry, I.W. Wang, T. Deuse, G. Leseche, P. Thomas, I. Tudorache, C. Kuhn, M. Avsar, B. Wiegmann, W. Sommer, A. Neyrinck, M. Schiavon, F. Calabrese, N. Santelmo, A. Olland, P.E. Falcoz, A.R. Simon, A. Varela, J.C. Madsen, M. Hertz, A. Haverich, and A. Ardehali, Normothermic ex-vivo preservation with the portable Organ Care System Lung device for bilateral lung transplantation (INSPIRE): a randomised, open-label, non-inferiority, phase 3 study. Lancet Respir Med 6 (2018) 357-367.

[252] L. Waters, R. Ben, J.P. Acker, M.P. Padula, D.C. Marks, and L. Johnson, Characterizing the ability of an ice recrystallization inhibitor to improve platelet cryopreservation. Cryobiology (2020).

[253] C. Watson, M. Rowland, and G. Warhurst, Functional modeling of tight junctions in intestinal cell monolayers using polyethylene glycol oligomers. Am J Physiol Cell Physiol 281 (2001) C388-C397.

[254] B.A. Whitson, and S.M. Black, Organ assessment and repair centers: The future of transplantation is near. World J Transplant 4 (2014) 40-2.

[255] J.P. Wolanczyk, K.B. Storey, and J.G. Baust, Ice nucleating activity in the blood of the freeze-tolerant frog, Rana sylvatica. Cryobiology 27 (1990) 328-35.

[256] D. Yang, M. Sax, A. Chakrabartty, and C. Hew, Crystal structure of an antifreeze polypeptide and its mechanistic implications. Nature 333 (1988) 232-237.

[257] M.L. Yarmush, M. Toner, J.C. Dunn, A. Rotem, A. Hubel, and R.G. Tompkins, Hepatic tissue engineering. Development of critical technologies. Ann N Y Acad Sci 665 (1992) 238-52.

[258] P. Yi, and G.C. Rutledge, Molecular origins of homogeneous crystal nucleation. Annu Rev Chem Biomol Eng 3 (2012) 157-82.

[259] S.O. Yu, A. Brown, A.J. Middleton, M.M. Tomczak, V.K. Walker, and P.L. Davies, Ice restructuring inhibition activities in antifreeze proteins with distinct differences in thermal hysteresis. Cryobiology 61 (2010) 327-34.

[260] K.E. Zachariassen, Physiology of cold tolerance in insects. Physiol Rev 65 (1985) 799-832.

[261] K.E. Zachariassen, The role of polyols and nucleating agents in cold-hardy beetles. J Comp Phys 140 (1980) 227-234.

[262] A.M. Zade-Oppen, Posthypertonic hemolysis in a sucrose system. Experientia 26 (1970) 1087-8.

[263] A.M.M. Zade-Oppen, Posthypertonic Hemolysis in Sodium Chloride Systems. Acta Physiologica Scandinavica 73 (1968) 341-364.

[264] P.M. Zavos, and E.F. Graham, Effects of various degrees of supercooling and nucleation temperatures on fertility of frozen turkey spermatozoa. Cryobiology 20 (1983) 553-559.

[265] P.M. Zavos, and E.F. Graham, Preservation of turkey spermatozoa by the use of emulsions and supercooling methods. Cryobiology 18 (1981) 497-505.

[266] K. Zheng, M. Trivedi, and T.J. Siahaan, Structure and function of the intercellular junctions: barrier of paracellular drug delivery. Current pharmaceutical design 12 (2006) 2813-2824.

[267] M. Zhurova, E.J. Woods, and J.P. Acker, Intracellular ice formation in confluent monolayers of human dental stem cells and membrane damage. Cryobiology 61 (2010) 133-41.

[268] B. Zobrist, C. Marcolli, T. Peter, and T. Koop, Heterogeneous ice nucleation in aqueous solutions: the role of water activity. J Phys Chem A 112 (2008) 3965-75.

Chapter 2 Characterization of IRI Toxicity and Control of Intracellular Ice Recrystallization in Hepatocyte Monolayers

2.1 Introduction

Ice recrystallization is a major source of damage in the cryopreservation of single-cell and multicellular systems [21; 41; 54; 55; 56]. Recently developed small carbohydrate-based surfactants and hydrogelators have proven to exhibit potent IRI activity and lack the DIS characteristics of AF(G)Ps [20]. The application of these compounds to the cryopreservation of red blood cells (RBCs) and hematopoietic stem and progenitor cells (HSPCs) in umbilical cord blood has been highly successful; however, they have yet to be applied to the cryopreservation of tissues [14; 15; 19; 58]. Maintaining intercellular connections and extracellular contacts is one of the leading challenges in tissue cryopreservation [54; 56; 63; 69]. These interactions increase susceptibility to damage caused by extracellular and interstitial ice recrystallization, which has been a major impediment to the success of tissue cryopreservation protocols. Recent studies have additionally demonstrated that the size and amphiphilic nature of these small molecule IRIs can enable passive permeation into endothelial cells and control of intracellular ice recrystallization, one of the primary mechanisms governing intracellular ice formation (IIF)-mediated damage [9; 10; 44; 46; 47; 49; 50; 52; 57].

Permitting IIF in multicellular systems while reducing the amount of recrystallization could prove beneficial in comparison to the traditional equilibrium approaches to cryopreservation. Cell-cell contacts increase the probability of IIF in multicellular systems; however, Acker *et al.* have demonstrated that gap junction mediated propagation of intracellular ice or paracellular ice penetration (PIP) at the cell-cell interface can render intracellular ice innocuous [1; 4; 5; 6; 34; 36; 65]. Preferential equilibration through intracellular ice growth rather than osmotic dehydration has additionally proven beneficial in tissues, where cell-cell and cell-matrix contacts confer a heightened degree of sensitivity to volumetric excursions [5]. Furthermore, the use of permeating CPAs to depress the heterogenous nucleation temperature and therefore the onset of IIF, has proven challenging in tissues and model tissue systems [38]. For example, studies on sandwich cultured hepatocytes demonstrate that the predicted heterogeneous nucleation temperature curve lie 7-10 °C below, yet parallel to the liquidus curve at DMSO concentrations up to 3 M [38]. The implication is that only a limited degree of supercooling is permitted prior to intracellular nucleation; therefore, cells must either be cooled at very slow rates to prevent intracellular

nucleation, or high concentrations of permeating CPAs must be used [38]. Given the biochemical toxicity of CPAs at high temperatures, both cases may prove deleterious to cell survival [24].

Small molecule IRI-mediated inhibition of intracellular ice recrystallization has thus far only been assessed in the absence of CPAs under freezing conditions that would invariably result in cell death [57]. The effect that permeating CPAs have on the survival of cells that have already undergone intracellular freezing is not well characterized [49]. However, it is likely that their membrane stabilization capabilities in combination with their ability to increase the intracellular unfrozen fraction can improve survival following IIF [7; 8; 11; 29; 35; 59]. In contrast, non-permeating CPAs reduce the relative volume of water inside the cell prior to nucleation, which has proven to reduce the extent of IIF-mediated damage [31]. These compounds will be vital in efforts to cryopreserve tissues; however, treatment with both permeating and non-permeating CPAs can significantly alter the amount of frozen water inside the cell at any given temperature. This can have significant effects on solution characteristics of the intracellular milieu and, as a result, the dynamics of the recrystallization process [32].

This work sought to evaluate the ability of three small molecule IRIs to control intracellular ice recrystallization in hepatocyte monolayers treated with common permeating and non-permeating CPAs. Hepatocytes are more prone to IIF than other mammalian cell types and comprise 80% of the mass of the liver. IRI permeation, control of intracellular recrystallization, and retention of intracellular IRI activity in the presence of permeating and non-permeating CPAs will make them highly amenable to hepatocyte cryopreservation and facilitate their application to liver tissues.

2.2 Methods

2.2.1 Cell Culture

HepG2 (human liver hepatocellular carcinoma cells, HB8065, ATCC, Manassas, VA, USA) were cultured in Dulbecco's modified eagle medium (DMEM; D1145, Sigma-Aldrich, Oakville, ON, Canada) supplemented with 10% fetal bovine serum (FBS; F1015, Gibco, Billings, MT, USA) in 75 cm^2 Corning® flasks (CLS430720, Corning, NY, USA). Flasks were incubated in a Thermo Scientific Forma 370 Steri-Cycle CO2 Incubator (ThermoFisher Scientific, Mississauga, ON, Canada) set at 37 °C and supplied with 5% CO_2. Culture medium was renewed every 3-4 days. Cells were harvested upon reaching 70-80 % confluency in accordance with previously described

protocols [51]. HepG2 cells were seeded onto 12 mm collagen-coated glass coverslips (89015-725, VWR, Radnor, PA, USA) at a density of 40,000 cells/cm^2 and given six days to reach 70-80% confluency for all experiments described. Culture medium was renewed every 2 days to promote optimal growth on the substrate. Culture conditions (ie. cell density and time in culture) was consistent for all experiments to limit differences in cell-cell adhesion molecule expression which has proven to affect IIF patterns [12; 64]. Cell passage numbers were 7-8 for all experiments described.

2.2.2 Collagen Reconstitution and Monolayer Substrate Preparation

A solution of 1 M HCl (SA48-1, Fisher Scientific, Waltham, MA, USA) was diluted to 0.01 mM using molecular grade water (SH30538.02, HyClone, Logan, UT, USA). This solution was used to reconstitute 15 mg of lyophilized type I collagen from rat tail (5006, PureCol, Carlsbad, CA, USA) to create a final concentration of 3 mg/mL. The stock solution was diluted to 200 µg/mL using 1X Dulbecco's phosphate buffered saline (1X DPBS; 14190235, Gibco). To promote attachment of cells, 12 mm glass coverslips (89015-725, VWR) were placed into individual wells of a 24-well plate (930186, ThermoFisher Scientific) and coated with 100 µL of the 200 µg/mL dissolved type I collagen solution for a minimum of 1 h at 22 °C. Immediately before cells were seeded, collagen was removed using pasteur pipette connected to an in-line vacuum and coverslips were rinsed twice with 300 µL of 1 X DPBS to remove residual HCl.

2.2.3 Preparation of CPA Solutions

The IRIs depicted in Figure 2.1 were used at the following concentrations: 10 mM (IRI 1), 11 mM (IRI 2), and 160 mM (IRI 3) for the purposes of this study. The different evaluations conducted, and the solutions prepared for each evaluation are shown in Table 2.1. IRIs were reconstituted in DMEM + 10% FBS for evaluation 1, while 1X DPBS was the base solution for all CPA mixtures prepared for evaluations 2-4. Evaluation 1 was conducted in a 37 °C incubator supplied with 5% CO_2; therefore, growth medium (DMEM + 10% FBS) is was the ideal buffer under these conditions. However, FBS functions as a non-permeating CPA, and thus the use of growth medium could confound results of the ice control evaluations (eval. 2-4) [27]. While DMEM without FBS supplementation could have been used for evaluations 2-4, 1X DPBS was chosen due to cost.

2.2.3.1 Permeating CPA Solution Preparation:

Permeating CPAs were all in a hydrated form with >99.5% purity. Equation 2.1 and 2.2 were used to interconvert between molarity (Cm) and percentage (Cp) using the molecular weight (M) and density (D) of the substance. 50 mL solutions of all permeating CPAs were made and from these, 10 mL solutions of each IRI were prepared using a 10 mL volumetric flask.

$$\mathrm{Cm} = \frac{\mathrm{Cp} \times \mathrm{D}}{100 \times \mathrm{M}} \qquad \text{Eq 2.1}$$

$$\mathrm{Cp} = \mathrm{Cm} \times \frac{\mathrm{M}}{\mathrm{D}} \times 100 \qquad \text{Eq 2.2}$$

2.2.3.2 Non-Permeating CPA Solution Preparation:

Ten grams of trehalose (BP2687-25, Fisher Scientific) was used to make a 100 mL solution of 5% trehalose in a 100 mL volumetric flask. This was subsequently diluted with 50 mL of 1X DPBS to make 2.5% trehalose. 10 mL solutions of each IRI were prepared using a 10 mL volumetric flask from these base solutions.

2.2.4 Metabolic Activity Measurements for IRI Toxicity Screening

Monolayers were incubated with 350 µL of either IRI 1, IRI 2, or IRI 3 for 15 min, 30 min, 45 min, and 60 min in a 37 °C incubator supplied with 5% CO_2 (n = 4). Following the incubation period, the IRI treatment was removed and replaced with 500 µL of DMEM + 10% FBS. Monolayers were placed back in the incubator and given 12 hours to recover, after which the alamarBlue™ metabolic activity assay was performed in accordance with previously described protocols [53]. In brief, the commercial stock solution (Invitrogen, Life Technologies Inc., Eugene, OR) was diluted 10-fold using the DMEM + 10% FBS. 600 µL of this working solution was added to each well of the 24-well plate and absorbance measurements were carried out after a 3 h incubation period. Three 150 µL aliquots were taken from each replicate and transferred to individual wells of a 96-well plate. A SpectraMax 364 Microplate Reader (Molecular Devices, San Jose, CA, USA) interfaced with SoftMax Pro 5.2.4 software (Molecular Devices) was used to measure absorbance of alamarBlue™ at λ = 570 nm and λ = 600 nm. Formula 2.3 used to calculate the % reduction of alamarBlue™ and formula 2.4 was used to normalize the % reduction of the experimental conditions to the control condition. The negative control in this case is a 10%

alamarBlue™ solution incubated in the absence of cells under the conditions as the experimental groups. The positive control was not treated with an IRI.

$$\%\ \text{alamarBlue}^{TM}\ \text{Reduction} = \frac{[(117216)A570nm - (80586)A600nm]\ \text{Experimental Condition or Positive Control}}{[(155677)A600nm - (14652)A570nm]\ \text{Negative Control}} \quad \text{Eq 2.3}$$

$$\text{Normalized metabolic activity} = \frac{\%\ \text{alamarBlue Reduction of Experimental Condition}}{\%\ \text{alamarBlue reduction of Positive Control}} \times 100 \quad \text{Eq 2.4}$$

2.2.5 Evaluation of Intracellular IRI Activity

A 5 mM stock solution of the nucleic acid fluorophore, SYTO13 (S7575, Molecular Probes, Eugene, OR, USA), was diluted in 1X DPBS to 50 µM. HepG2 monolayers were treated with 110 µL of 50 µM SYTO13 in the dark for 10 min at 22 °C prior to application of the treatment. This method of visualizing patterns of intracellular ice formation and growth has been previously described [2; 3]. Permeating CPA and trehalose treatments were performed at 22 °C for 10 min. IRI incubations were carried out at 37 °C for 15 min. For monolayers treated with IRIs in combination with a permeating or non-permeating CPA, an initial IRI-only incubation was carried out for 37 °C for 15 min. This solution was then removed using a Pasteur pipette connected to an in-line vacuum and the CPA-IRI treatment was performed at 22 °C for 10 min. Membrane permeability increases with temperature; therefore, this two-step treatment was done to facilitate permeation of the IRI and minimize CPA toxicity at 37 °C [67]. The volume of solution used was 350 µl for all treatments and IRI concentrations were kept the same between these two steps.

Monolayers were transferred to a Linkam FDCS196 convection cryomicroscopic stage (Linkam Scientific Instruments, Tadworth, England) set up on a Nikon Eclipse 80i inverted microscope (Nikon, Tokyo, Japan). Monolayers were frozen at 90 °C/min from 4 °C to -15 °C, at which point nucleation was induced. Conditions treated with a permeating CPA were nucleated at -16 °C to account for depression of the intracellular freezing point. Nucleation at these temperatures was confirmed to induce 100% intracellular ice under all treatment conditions evaluated. Samples were held at the nucleation temperature in order to exacerbate isothermal recrystallization of intracellular ice. All parameters of the freezing profile were input into Lynksis 32 software

(Linkam Scientific Instruments). A Hamamatsu digital camera (C4742-80, Hamamatsu, Japan) interfaced with NIS elements AR 3.22.14 software (Nikon) was used to capture images of intracellular ice using a Nikon LU Plan 50X objective lens with a working distance of 0.55 mm. Images were captured immediately after nucleation at -15 °C and every 0.5 min after nucleation up to 5 min. Two independent replicates were ran for each treatment condition evaluated.

2.2.6 Quantifying Mean Grain Size and Rates of Recrystallization

Figure 2.2 demonstrates the process of intracellular ice recrystallization under a 5 min isothermal hold following nucleation at -15 °C, where dark regions within the nuclei of cells are indicative of intracellular ice crystals. The average mean grain size of ice crystals within the nucleus of each cell was manually calculated using NIS elements AR 3.22.14 software (Nikon) on images taken 1 min, 2.5 min, and 5 min after nucleation as shown by the green highlighted region of the cell in Figure 2.2. Mean grain size 0 min after nucleation was assumed to be 0.2 μm^3 for all conditions as this was the minimum mean grain size that could be resolved. The number of cells counted would vary from 15 to 30 cells per replicate (n = 2) depending on the number of cells in the field of view and the resolution of intracellular ice within the cell. The Laplacian of Gaussian (LoG) operation was executed at a power of 1.4 (range 1.02 to 2) on each image prior to analysis such that the resolution of intracellular ice could be enhanced.

In order to calculate differences in the rates of isothermal recrystallization, the Lifshitz-Slyozov-Wagner (LSW) theory of Ostwald ripening (Equation 2.5) was used, where r^3 represents the cube of the ice grain radius, r_0^3 is the radius of an ice grain 0 min after nucleation (ie. t = 0), and k is the isothermal recrystallization rate, which is determined form the slope of the r^3 values between t = 0 to t = 5 [17; 30; 40; 43; 60; 66; 70]. Linear regression aggression analysis was performed using GraphPad Prism 8.1.0 to determine the rate of recrystallization (k) in each given cell in the field of view from t = 0 to t = 5.

$$r^3 = r_0^3 + kt \qquad \text{Eq 2.5}$$

2.2.7 Statistical Analysis:

All statistical analysis was performed using GraphPad Prism 8.1.0. Toxicity data was analyzed using a two-way analysis of variance (ANOVA) followed by a Tukey's post hoc test to evaluate a significant reduction in metabolic activity relative to an untreated control. For ice control

evaluations, a nested one-way ANOVA followed by Dunnet's post hoc test to evaluate differences in recrystallization rates relative to the control condition. Data for this analysis was log transformed to approximate normality prior to statistical analysis. Standard $y = \log(y)$ transformation was done for all analyses, except for the IRI-mediated control of intracellular ice recrystallization evaluation in the presence of 5% trehalose (Fig. 1.12) where a $y = \log(y + 0.01)$ was used as several cells demonstrated no evidence of recrystallization over the 5 min period at -15 °C. Differences for both toxicity and ice control evaluations were considered significant when $p < 0.05$.

2.3 Results

2.3.1 Metabolic Activity Measurements for IRI Toxicity Screening

IRI toxicity was evaluated at 37 °C as this temperature was preferable for the subsequent permeation studies and would exacerbate potential toxic effects. Toxicity was solely investigated at concentrations where each IRI has demonstrated optimal activity in previously performed splat cooling assays (Robert N. Ben, personal communication, July 23, 2019). There was a significant reduction ($p = 0.036$) in metabolic activity after a 60 min incubation with IRI 2, while IRI 1 did not significantly impact metabolic activity under the conditions that were studied ($p > 0.05$) (Fig 2.3). IRI 3 does not significantly impact metabolic activity following a 45 min treatment; however, there is a marked reduction in metabolic activity following a 60 min treatment ($p = 0.0029$; 18.63% ± 3.03%) (Fig. 2.3). This level of toxicity is substantially greater than that exhibited with IRI 2 after 60 min treatment, where the normalized metabolic activity was 79.15% ± 1.09% (Fig. 2.3).

2.3.2 Intracellular IRI Activity

Inhibition of intracellular ice recrystallization was used as an indirect measure for IRI permeation. Figure 2.4 demonstrates a clear reduction in the mean grain size of ice crystals within the cells 5 min after nucleation in the conditions treated with IRI 2 and IRI 3. Quantifying r^3 values and corresponding recrystallization rates (k) indicated that both IRI 2 and IRI 3 are capable of reducing rates of recrystallization (IRI 2: p = 0.0046; IRI 3: p = 0.0020) relative to the untreated control (Fig. 2.5).

The cryoprotective efficacy of a given IRI is largely predicated on its ability to control recrystallization in the presence of permeating CPAs, which prove to be fundamental in modern

cryobiology. Therefore, evaluating how commonly used permeating CPAs alter intracellular IRI activity is pertinent to the subsequent utilization of these compounds in cryopreservation applications where IIF would be expected to occur. Figure 2.6 indicates the activity of the three IRIs relative to a CPA-only (ie. non-IRI) controls. IRI 1 and IRI 2 did not demonstrate any significant reduction in rates of intracellular ice recrystallization in the presence of all four of the tested permeating CPAs. Rates of recrystallization were significantly increased when IRI 1 was in the presence of DMSO ($p = 0.0033$) and ethylene glycol ($p = 0.019$), as well as when IRI 2 was in the presence of each of the four permeating CPAs (glycerol: $p = 0.0022$; PG: $p = 0.0018$; DMSO: 0.0008; EG: $p = 0.0010$). Considering that treatment with 0.2 M glycerol, propylene glycol, ethylene glycol, and DMSO did not prove to significantly alter recrystallization rates relative to untreated (ie. non IRI) controls, the increase in the rate of recrystallization can be attributed to a loss of IRI activity. This is particularly the case for IRI 2 which demonstrated a significant reduction ($p = 0.0046$) in recrystallization rates in the absence of a CPA (Fig. 2.5). There was additionally significant increase in the presence of all four permeating CPAs for IRI 3 ($p < 0.0001$). However, IRI 3 did significantly reduce recrystallization rates in the presence of glycerol ($p = 0.0473$), DMSO ($p = 0.0135$), and propylene glycol ($p = 0.0002$), suggesting that it may prove to be effective when utilized with these CPAs.

Dehydration of a cell reduces the ratio of freezable to unfreezable (bound) intracellular water, thus reducing the volume of frozen water inside the cell and improving the recovery of cells that have undergone IIF. Figure 2.8 and 2.9 indicate that treatment with trehalose, a commonly used non-permeating CPA, can significantly reduce rates of intracellular recrystallization when used at concentrations of 2.5% ($p = 0.0002$) and 5% ($p < 0.0001$), thereby suggesting a potential relationship between cellular dehydration and intracellular ice recrystallization. In the presence of 2.5% trehalose, all three IRIs proved so significantly reduce recrystallization rates (IRI 1: $p = 0.041$; IRI 2: $p = 0.020$; IRI 3: $p = 0.0026$) relative to a trehalose-only (ie. non IRI) control (Fig. 2.10 and Fig. 2.11). In the presence of 5% trehalose, only IRI 1 ($p = 0.0040$) and IRI 3 ($p = 0.0024$) reduced rates of recrystallization, while IRI 2 did not (Fig. 2.12 and Fig. 2.13). This suggests a reduction in activity for IRI 2 and potential augmentation in activity of IRI 1, considering that in the absence of a CPA, IRI 2 proved to be effective ($p = 0.0046$), while IRI 1 did not (Fig. 2.4 and Fig. 2.5).

2.4 Discussion

2.4.1 Small Molecule IRIs Can Permeate Hepatocytes and Control Intracellular Ice Recrystallization

Results suggest all three IRIs are capable of permeating the hepatocyte membrane following a pre-incubation period and controlling intracellular ice recrystallization under conditions where they elicit no toxic effects (Fig. 2.3 and Fig. 2.5). This aligns with previous work suggesting that IRI 3 can permeate and control intracellular ice recrystallization in Human Umbilical Vein Endothelial Cells (HUVECs), thereby further establishing small molecule IRIs as the first IRI active compounds capable of permeating cell membranes in the absence of membrane permeabilization techniques [57]. Furthermore, it correlates with results seen in splat cooling assays suggesting that each of the three compounds are functional at the tested concentrations (Robert N. Ben, personal communication, July 23, 2019). Albeit promising, the role of IRIs in cryopreservation protocols that favor the formation of intracellular ice is largely dependent on their ability to function in the presence of permeating and non-permeating CPAs, which vastly alter intracellular solution characteristics.

2.4.2 Loss of IRI Activity in the Presence of Permeating CPAs

The role of permeating CPAs in promoting the survival of cells that undergo intracellular freezing has not previously been well characterized. However, our group has generated data suggesting that increasing concentrations of permeating CPAs decrease the sensitivity of cells to damage (unpublished results) caused by intracellular freezing, which prompted us to evaluate IRI activity in the four most commonly used permeating CPAs. For the most part, our results convey a loss of IRI activity in the presence of permeating CPAs as well as variability in activity between CPAs (Fig 2.6 and Fig. 2.7). Numerous studies have demonstrated how permeating CPAs modulate rates of ice nucleation and crystal growth as a function of both temperature and concentration [16; 32; 33; 37; 45]. Furthermore, the strength of the interaction between water molecules and the solute makes crystallization and recrystallization characteristics highly CPA specific [26]. Therefore, while these results are not unexpected, the extent to which IRI activity is lost is surprising, particularly given that none of CPAs had significant effects on intracellular recrystallization rates at the tested concentration of 0.2 M (Fig. 2.6A-B).

There has previously been evidence suggesting that the IRI activity of AF(G)Ps can be diminished in 50% w/w glycerol and 40% w/w DMSO [25; 33]. High concentrations of CPAs can interact with the crystal lattice; thus, this phenomenon has been ascribed to competitive binding between the AF(G)P and the CPA [25; 33]. Considering that small molecule IRIs do not bind to the crystal surface and that low concentrations of CPAs were used; the mechanism of inhibition is vastly different in this case. Small molecule IRIs are thought to inhibit recrystallization through disrupting the order of the semi-ordered quasi-liquid layer (QLL) that exists between the crystal lattice and the bulk water, thus limiting the transfer water molecules to the growing ice crystal [18; 68]. The ability of the IRI to disrupt the pre-ordering of water at the bulk water-QLL interface has proven to be dependent on the hydration index of the compound (ie. the number of tightly bound water molecules per volume of carbohydrate) [68]. Although it is challenging to ascertain how the presence of a permeating CPA in the bulk-water could affect IRI activity, evaluating a three-way relationship between compound hydration, IRI activity, and CPA concentration may prove informative in this regard. CPAs could additionally be directly interacting with the IRI in such a way that limits their ability to function. There has been preliminary data suggesting that the activity of IRI 2 is inhibited at low concentrations (<1%) of DMSO in spat cooling assays, which alludes to this possibility given that modification of solution characteristics is nominal at these low concentrations (Robert N. Ben, personal communication, July 23, 2019). Direct evaluation of a binding interaction between the three tested IRIs and the four permeating CPAs is warranted.

Given the physical and chemical differences that exist between the intracellular and extracellular environment, evaluating how each of the three IRIs operate in splat cooling assays in the presence of permeating CPAs can confirm whether results seen intracellularly correlate with those seen extracellularly. The addition of IRI 1 and IRI 3 to a 15% glycerol solution has proven beneficial to post-thaw RBC integrity under slow cooling conditions, which has corresponded to outcomes seen in splat cooling assessments [19]. IIF likely did not occur under the freezing conditions studied, which, in concert with the results of the present study, suggests that IRI function may be distinct between the intra- and extracellular environments.

Ice nucleation and growth conditions were kept constant in this study in order to evaluate the effects of different treatments on IRI activity. However, an intimate interaction between the thermodynamic stability of the ice crystal formed and the kinetic energy of the system dictates the

rate at which ice will recrystallize, which may in turn affect the ability of the IRI to control recrystallization [39; 42]. Ice nucleated at increasingly low temperatures would be more prone to recrystallize at any given temperature, and thus visible IRI activity may be diminished as temperatures are increased. In contrast, if ice is nucleated at a high temperature, IRI activity may only be evident as temperatures are lowered, despite the relative thermodynamic stability of the crystal. Therefore, loss of IRI activity in the presence of permeating CPAs should be interpreted in the context of the ice nucleation and growth conditions implemented in this study. Altering these parameters would allow for conclusive assessment of differences in IRI activity as a function of ice growth dynamics. Ultimately, a thorough understanding of the mechanism through which small molecule IRIs function would inform how such studies would best be implemented, however significantly more work has yet to be done on this front.

2.4.3 Dehydration Can Modulate Intracellular IRI Activity

The relationship between the water content of the cell and the rate of intracellular recrystallization has not previously been explored; however, our work demonstrates an inverse relationship between these two factors (Fig. 2.8 and Fig. 2.9). Distortion of the plasma membrane and increased proximity of cellular constituents in dehydrated cells could, however, result in excess damage with any given amount of recrystallization. Therefore, while further studies are needed to evaluate how this phenomenon corresponds to viability outcomes, a reduction in the water volume of the cell has been undoubtedly associated with an increase in the recovery following IIF [48]. Thus, confirmation of IRI activity in dehydrated cells was pertinent.

Theoretically IRI efficacy would be improved in dehydrated cells given that (1) the overall rate of recrystallization is reduced, and that (2) there is an increase in the amount of IRI for any given amount of ice. IRI 1 did not alter rates of recrystallization in the absence of a CPA (Fig. 2.4 and Fig. 2.5); however, it did in the presence of 2.5% and 5% trehalose (Fig. 2.12 and 2.13). This raises the possibility that the presence of a dehydrating agent may promote IRI activity under cases where activity had previously been lost in the presence of a permeating CPA (Fig 2.7). Alternatively, IRI 2 did not reduce rates of recrystallization in the presence of 5% trehalose (Fig. 2.12 and Fig. 2.13), which contrasts with the efficacy that it demonstrated in both the absence of a CPA (Fig. 2.4 and 2.5) and in the presence of 2.5% trehalose (Fig. 2.10 and Fig. 2.11). It is possible that the well characterized effects of trehalose on the lipid bilayer could limit IRI permeation; however, if this

was the case, a similar loss in activity would be expected for IRI 2 and IRI 3 [22; 23; 28; 61; 62]. This additionally proves to be unlikely given that an initial IRI-only incubation was carried out prior to the trehalose + IRI treatment. In solution, IRI concentration does not directly correspond to an improvement in IRI activity. IRI 2 functions optimally at concentrations of 11 mM, although it is soluble at concentrations up to 15 mM (Robert N. Ben, personal communication, July 23, 2019). Thus, increasing the ratio of the IRI to ice may amount to a similar loss of activity seen when IRI concentration is increased.

Continual improvement in the activity of IRI 1 and the loss in activity of IRI 2 as concentrations of non-permeating CPAs are increased suggest that an absence of intracellular IRI activity may not necessarily be indicative of a lack of permeation and should not be interpreted as such. This will prove important when assessing permeation and control of intracellular recrystallization in different cell types where the water content may differ to that of hepatocytes [13].

2.5 Conclusions

These results have further established small molecule carbohydrate-based IRIs as the first IRI active compounds capable of passively permeating the cell membrane. In addition, it is the first study to demonstrate small molecule IRI permeation in hepatocytes, a cell type which proves to be highly prone to IIF [71]. However, it is clear that CPAs can modulate intracellular IRI activity, which highlights the need to evaluate activity in any given CPA cocktail prior to their implementation in the associated cryopreservation protocol. Considering IRI 3 proves to be effective in the presence of commonly used permeating and non-permeating CPAs, there is value in assessing whether this compound can improve post-thaw outcomes in hepatocytes under conditions where IIF is prominent. Furthermore, despite the ineffectiveness of IRI 1 and IRI 2 in the presence of permeating CPAs, control of intracellular recrystallization in the absence of CPAs and the presence of non-permeating CPAs can still prove efficacious in tissue cryopreservation efforts where the presence of a permeating CPA, while preferable, may not be vital [5; 6]. Ultimately, it is pertinent to assess how the findings of this study translate to the extracellular environment given that cell-cell and cell-matrix contacts in tissue systems can accentuate the damage posed by extracellular ice recrystallization.

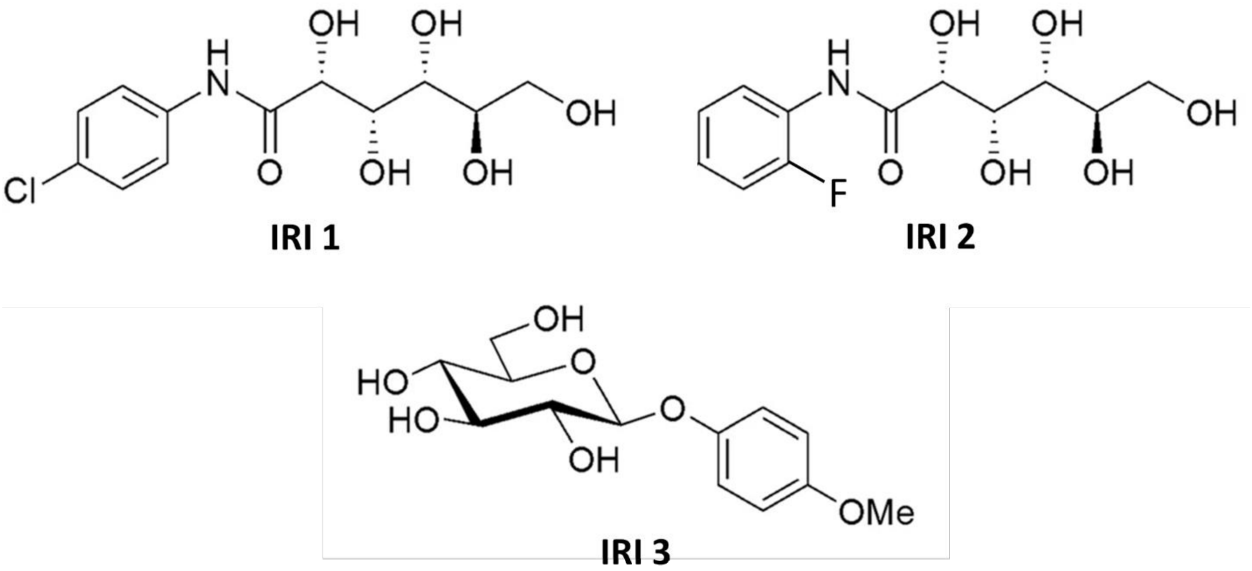

Figure 2.1 Structures of small molecule ice recrystallization inhibitors (IRIs). N-(4-chlorophenyl)-D-gluconamide (IRI 1), N-(2-fluorophenyl)-D-gluconamide (IRI 2), and para-methoxyphenyl-β-D-glycoside (IRI 3).

Table 2.1 Overview of conducted evaluations

Evaluations	Control Treatments	Experimental Treatments
Eval 1. IRI Toxicity **Eval 2.** Permeation of IRI and Control of Intracellular Ice Recrystallization	No CPA	IRI 1
		IRI 2
		IRI 3
Eval 3. Retention of IRI activity presence of permeating CPAs	0.2 M DMSO (CP-100, CryoPur, Paris, France)	0.2 M DMSO + IRI 1
		0.2 M DMSO + IRI 2
		0.2 M DMSO + IRI 3
	0.2 M Ethylene Glycol (102466-500, Sigma-Aldrich)	0.2 M Ethylene Glycol + IRI 1
		0.2 M Ethylene Glycol + IRI 2
		0.2 M Ethylene Glycol + IRI 3
	0.2 M Propylene Glycol (P355-1, Fisher Scientific)	0.2 M Propylene Glycol + IRI 1
		0.2 M Propylene Glycol + IRI 2
		0.2 M Propylene Glycol + IRI 3
	0.2 M Glycerol (G153-1, Fisher Scientific)	0.2 M Glycerol + IRI 1
		0.2 M Glycerol + IRI 2
		0.2 M Glycerol + IRI 3
Eval 4. Retention of IRI activity in the presence of non-permeating CPAs	2.5 % Trehalose (BP2687-25, Fisher Scientific)	2.5% Trehalose + IRI 1
		2.5% Trehalose + IRI 2
		2.5% Trehalose + IRI 3
	5% Trehalose (BP2687-25, Fisher Scientific)	5% Trehalose + IRI 1
		5% Trehalose + IRI 2
		5% Trehalose + IRI 3

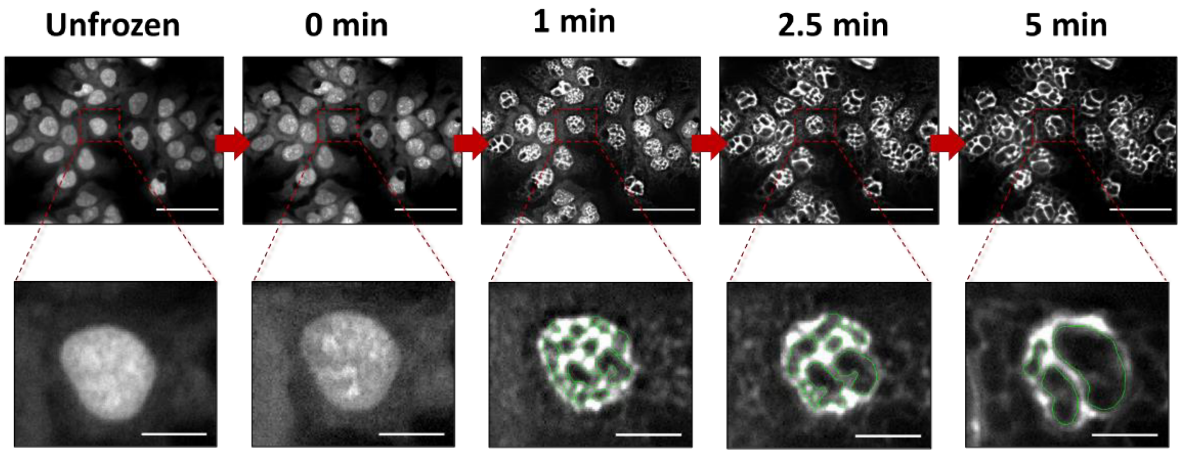

Figure 2.2 Method for determination of mean grain size of ice crystals in cells. (A) Isothermal recrystallization over 5 min period following nucleation at -15 °C in a 1X DPBS-treated monolayer. Images displayed obtained prior to nucleation (unfrozen), immediately (0 min), 1 min, 2.5 min, and 5 min after nucleation. Green highlighted regions in the magnified images at the 1 min, 2.5 min, and 5 min timepoint offer an example of how intracellular ice was quantified. Scale bar = 50 μm on original images. Scale bar = 10 μm on magnified images.

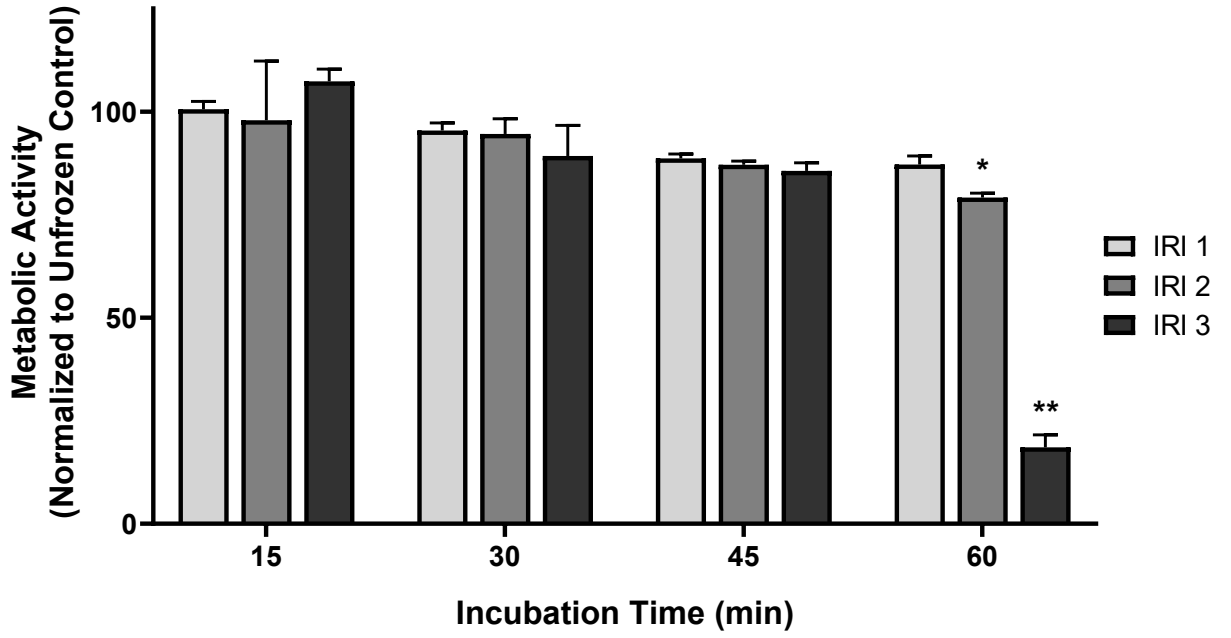

Figure 2.3 Metabolic activity assessment for evaluation of IRI toxicity. alamarBlue™ metabolic activity assay was performed 12 hours after removal of treatment. Percent alamarBlue™ reduction values calculated using equation 2.3 were normalized to the untreated control using equation 2.4. Error bars represent the standard error of the mean of four samples per condition (n = 4). Significance differences relative to the untreated control were calculated using a two-way ANOVA followed by a Dunnet's post hoc test: *$p < 0.05$, **$p < 0.01$.

\

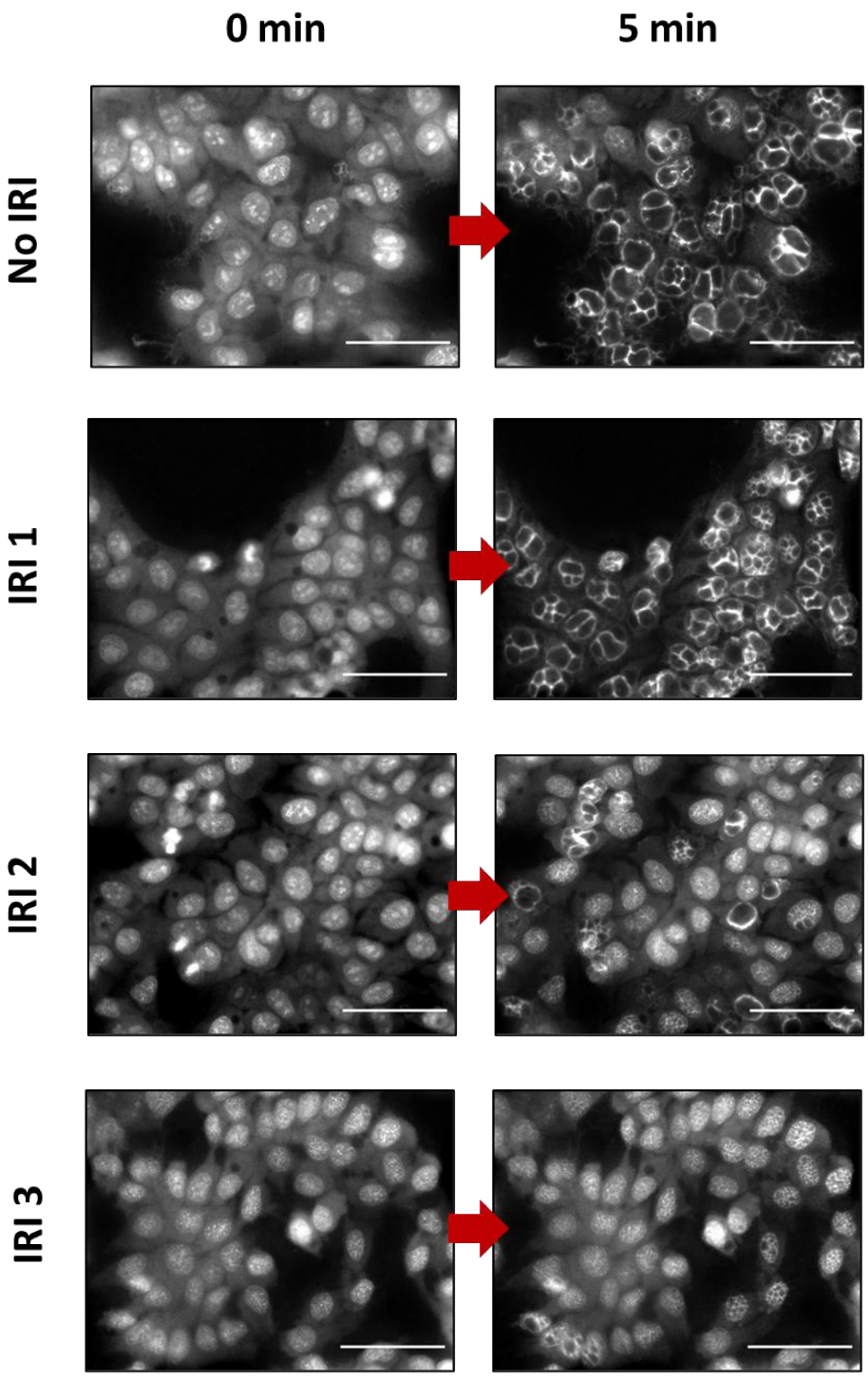

Figure 2.4 IRI permeation and control of recrystallization: representative images. Images displayed taken immediately (0 min) and 5 min after nucleation at -15 °C. Scale bar = 50 μm.

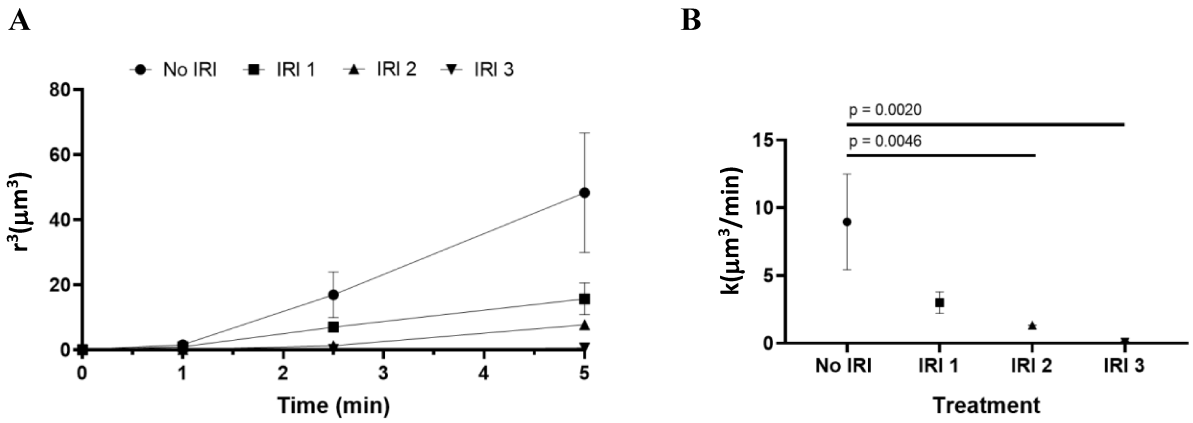

Figure 2.5 IRI permeation and control of intracellular ice recrystallization. (A) r^3 values were determined from the mean grain size per cell calculated in 15 to 30 cells per replicate at 1 min, 2.5 min, and 5 min after nucleation. (B) Rates of recrystallization (k) values were determined from the r^3 values as indicated in equation 2.5. Error bars represent the standard error of the mean between replicates. Significance differences from the control were calculated using a nested one-way ANOVA followed by a Dunnet's post-hoc test on log transformed data. Differences where $p < 0.05$ were considered to be statistically significant.

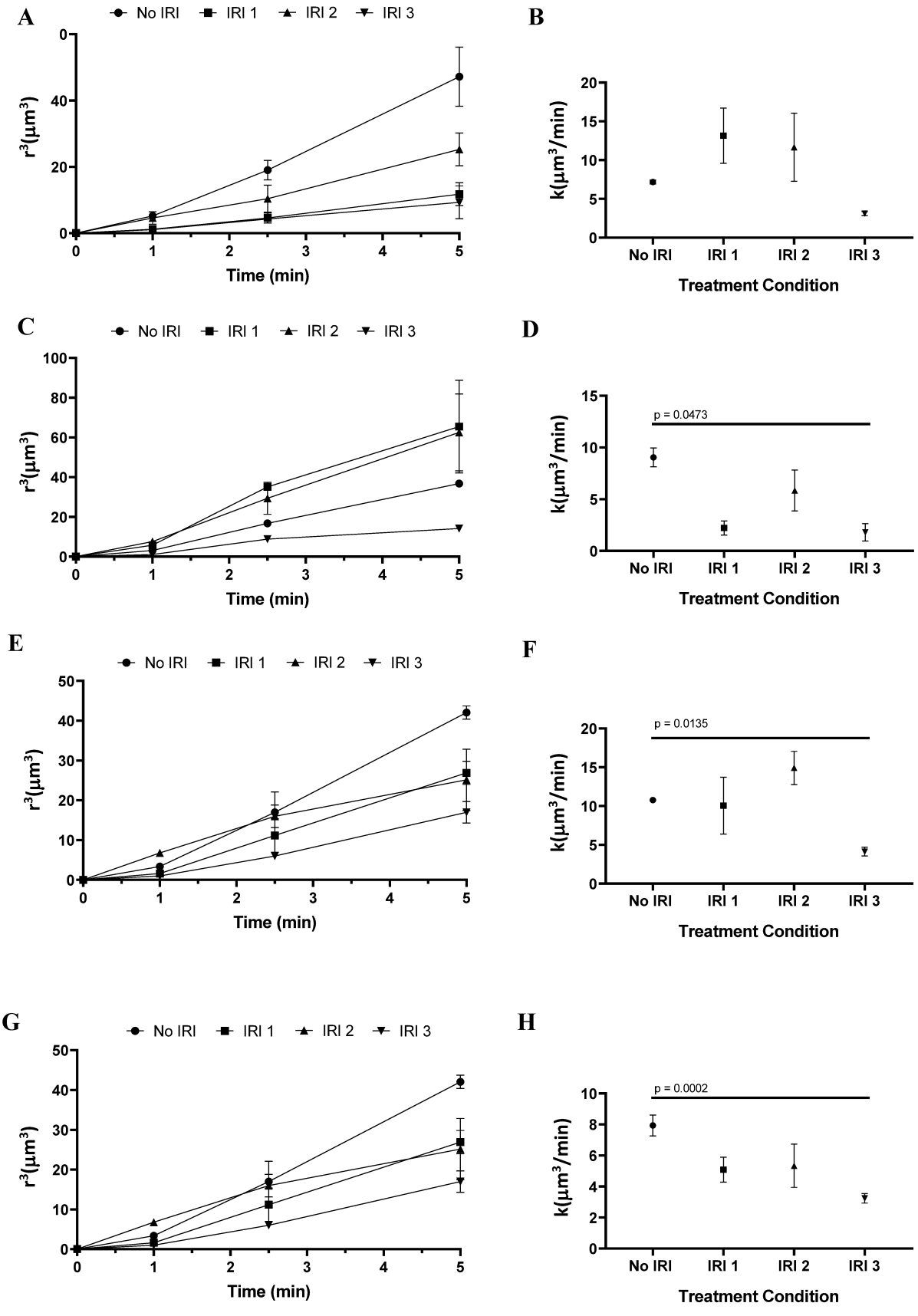
A
No IRI
IRI 1
IRI 2
IRI 3
r³(µm³)
Time (min)
B
k(µm³/min)
No IRI
IRI 1
IRI 2
IRI 3
Treatment Condition
C
D
p = 0.0473
E
F
p = 0.0135
G
H
p = 0.0002

Figure 2.6 IRI-mediated control of intracellular ice recrystallization in the presence of permeating CPAs relative to CPA-only controls. Figures respectively represent the r^3 and k values indicating the activity of the three tested IRIs relative to CPA-only controls in (A-B) ethylene glycol, (C-D) glycerol, (E-F) DMSO, and (G-H) propylene glycol. r^3 values were determined from the mean grain size per cell calculated in 15 to 30 cells per replicate at 1 min, 2.5 min, and 5 min after nucleation. Rates of recrystallization (k) values were determined from the r^3 values as indicated in equation 2.5. Error bars represent the standard error of the mean between replicates. Significance differences from the control were calculated using a nested one-way ANOVA followed by a Dunnet's post-hoc test on log transformed data. Differences where $p < 0.05$ were considered to be statistically significant.

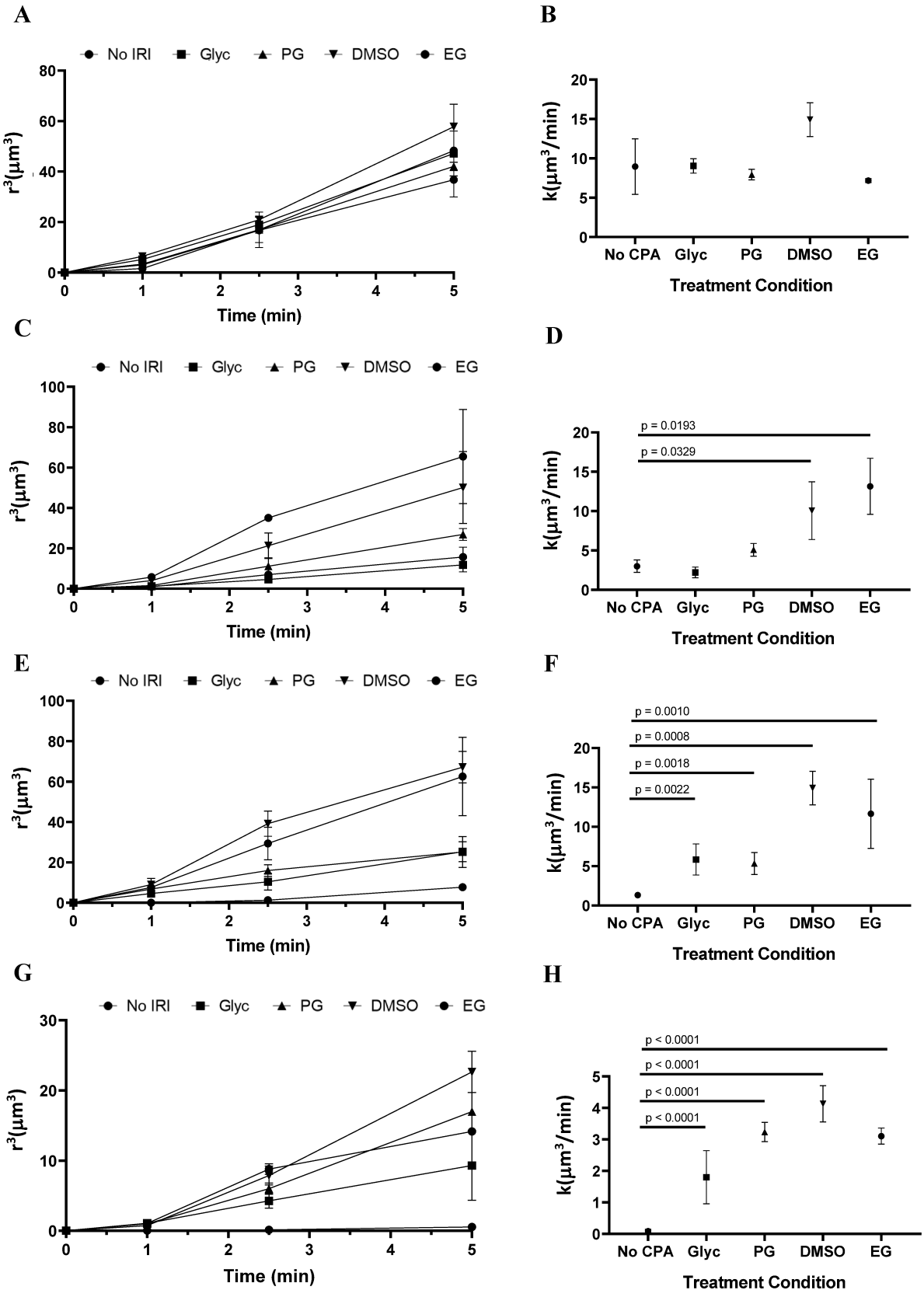
A
No IRI
Glyc
PG
DMSO
EG
r³(µm³)
Time (min)
B
k(µm³/min)
No CPA
Glyc
PG
DMSO
EG
Treatment Condition
C
D
p = 0.0193
p = 0.0329
E
F
p = 0.0010
p = 0.0008
p = 0.0018
p = 0.0022
G
H
p < 0.0001
p < 0.0001
p < 0.0001
p < 0.0001

Figure 2.7 IRI-mediated control of intracellular ice recrystallization in the presence of permeating CPAs relative to no CPA controls. Data is the same as that presented in Figure 2.4; however, it has been graphed and analyzed to demonstrate change in recrystallization rates relative to a no CPA control in order to evaluate changes in IRI activity in the presence of ethylene glycol, glycerol, DMSO, and propylene glycol. Figures respectively represent the r^3 and k values in (A-B) the absence of an IRI (ie. No IRI), (C-D) IRI 1, (E-F) IRI 2, and (G-H) IRI 3. r^3 values were determined from the mean grain size per cell calculated in 15 to 30 cells per replicate at 1 min, 2.5 min, and 5 min after nucleation. Rates of recrystallization (k) values were determined from the r^3 values as indicated in equation 2.5. Error bars represent the standard error of the mean between replicates. Significance differences from the control were calculated using a nested one-way ANOVA followed by a Dunnet's post-hoc test on log transformed data. Differences where $p < 0.05$ were considered to be statistically significant.

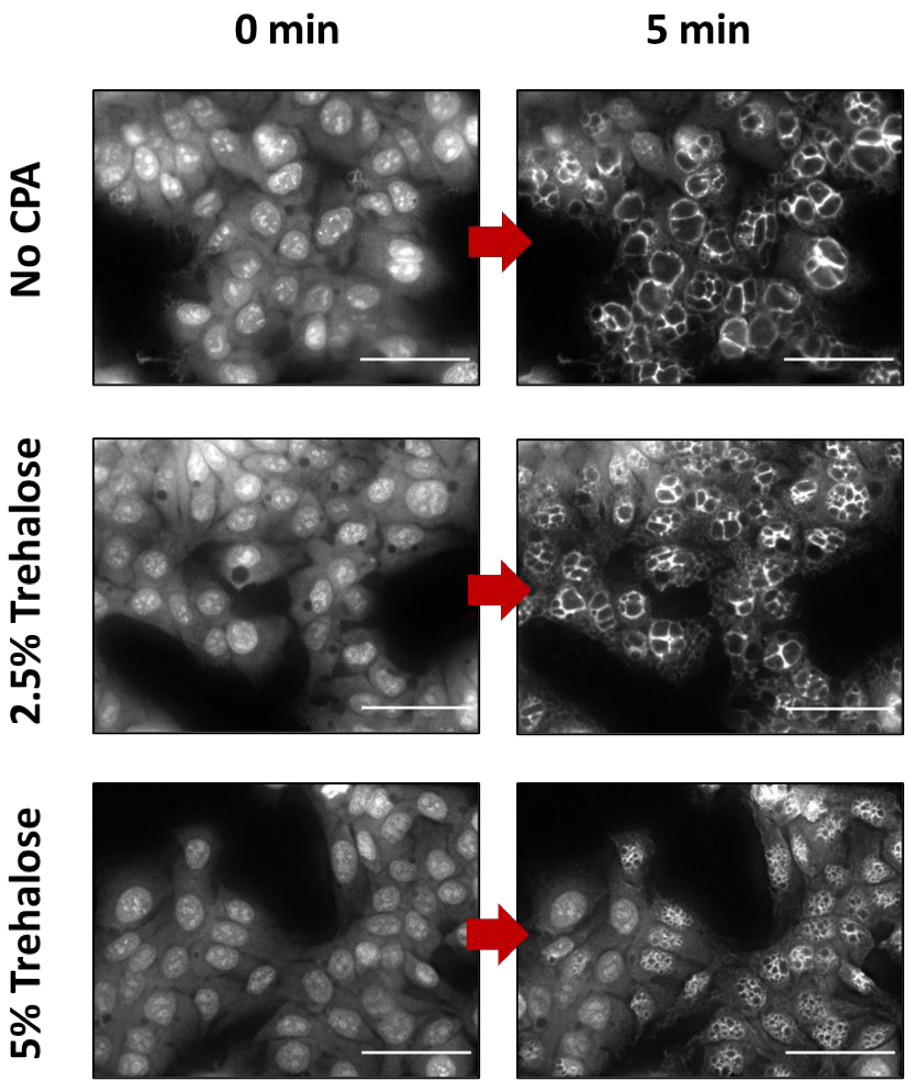

Figure 2.8 The impact of trehalose on intracellular ice recrystallization: representative images. Images displayed taken immediately (0 min) and 5 min after nucleation at -15 °C. Scale bar = 50 μm.

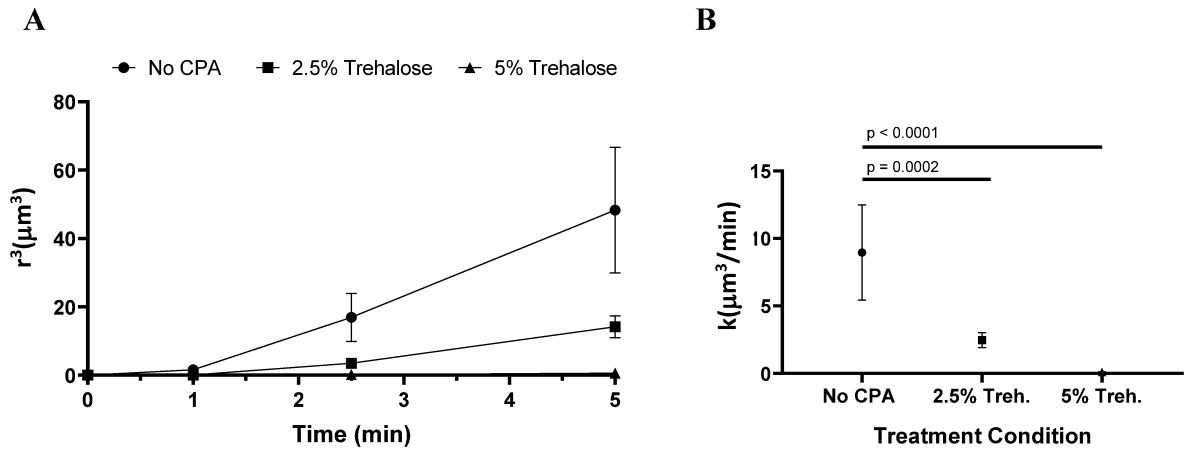

Figure 2.9 The impact of trehalose on intracellular ice recrystallization. (A) r^3 values were determined from the mean grain size per cell calculated in 15 to 30 cells per replicate at 1 min, 2.5 min, and 5 min after nucleation. (B) Rates of recrystallization (k) values were determined from the r^3 values as indicated in equation 2.5. Error bars represent the standard error of the mean between replicates. Significance differences from the control were calculated using a nested one-way ANOVA followed by a Dunnet's post-hoc test on log transformed data. Differences where $p < 0.05$ were considered to be statistically significant.

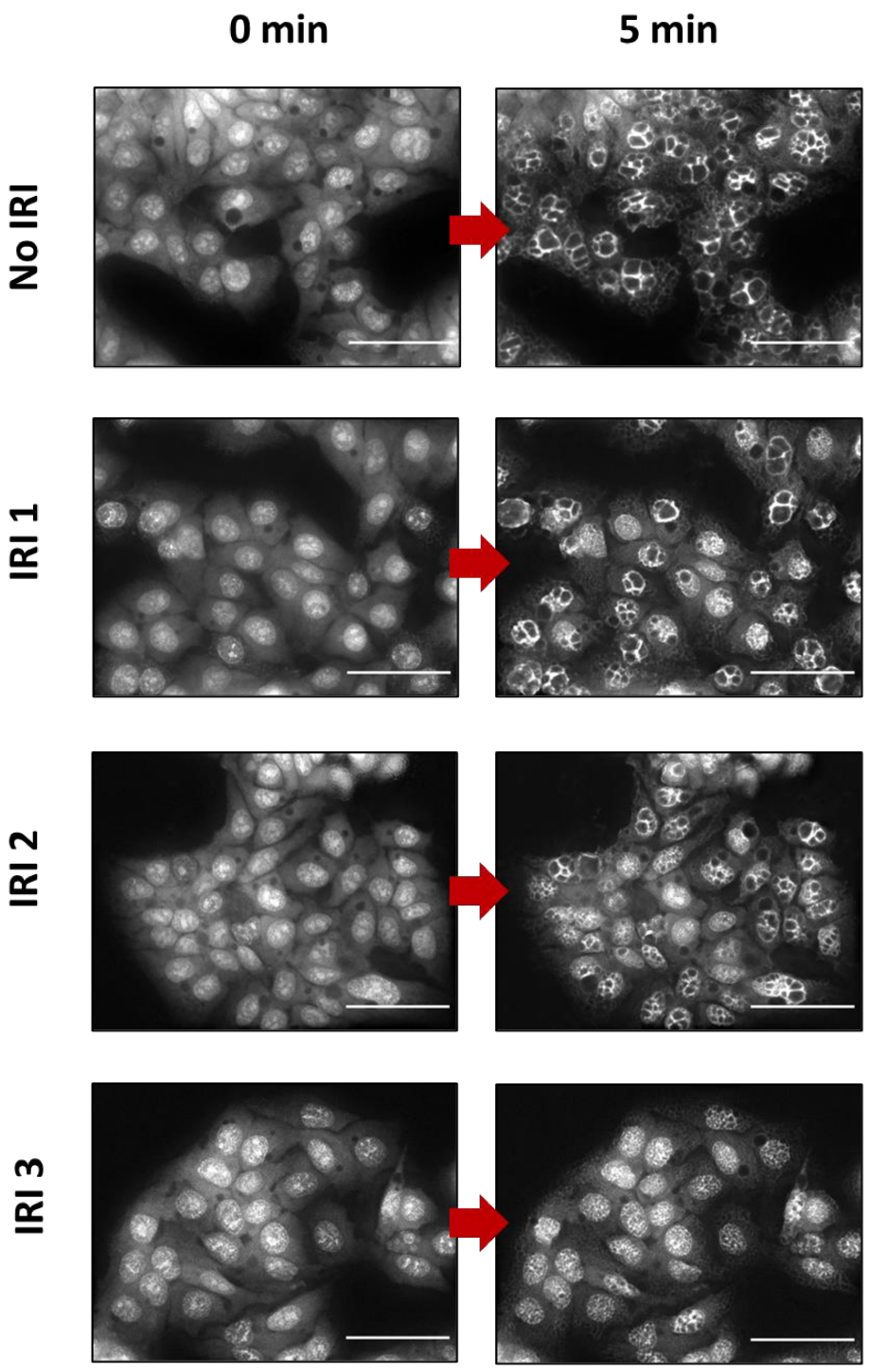

Figure 2.10 IRI-mediate control of intracellular ice recrystallization in cells treated with 2.5% trehalose: representative images. Images displayed taken immediately (0 min) and 5 min after nucleation at -15 °C. Scale bar = 50 µm.

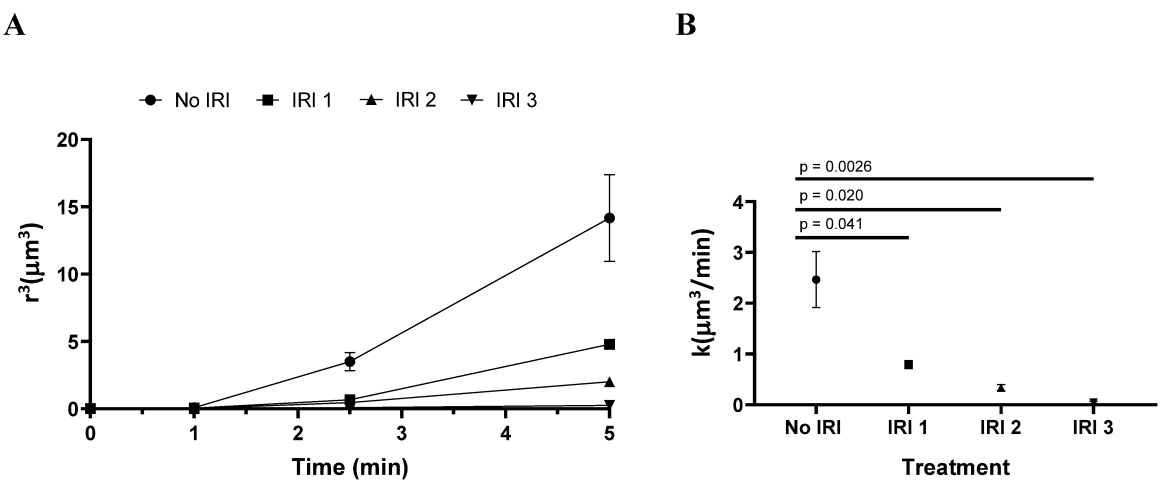

Figure 2.11 IRI-mediate control of intracellular ice recrystallization in cells treated with 2.5% trehalose. (A) r^3 values were determined from the mean grain size per cell calculated in 15 to 30 cells per replicate at 1 min, 2.5 min, and 5 min after nucleation. (B) Rates of recrystallization (k) values were determined from the r^3 values as indicated in equation 2.5. Error bars represent the standard error of the mean between replicates. Significance differences from the control were calculated using a nested one-way ANOVA followed by a Dunnet's post-hoc test on log transformed data. Differences where $p < 0.05$ were considered to be statistically significant.

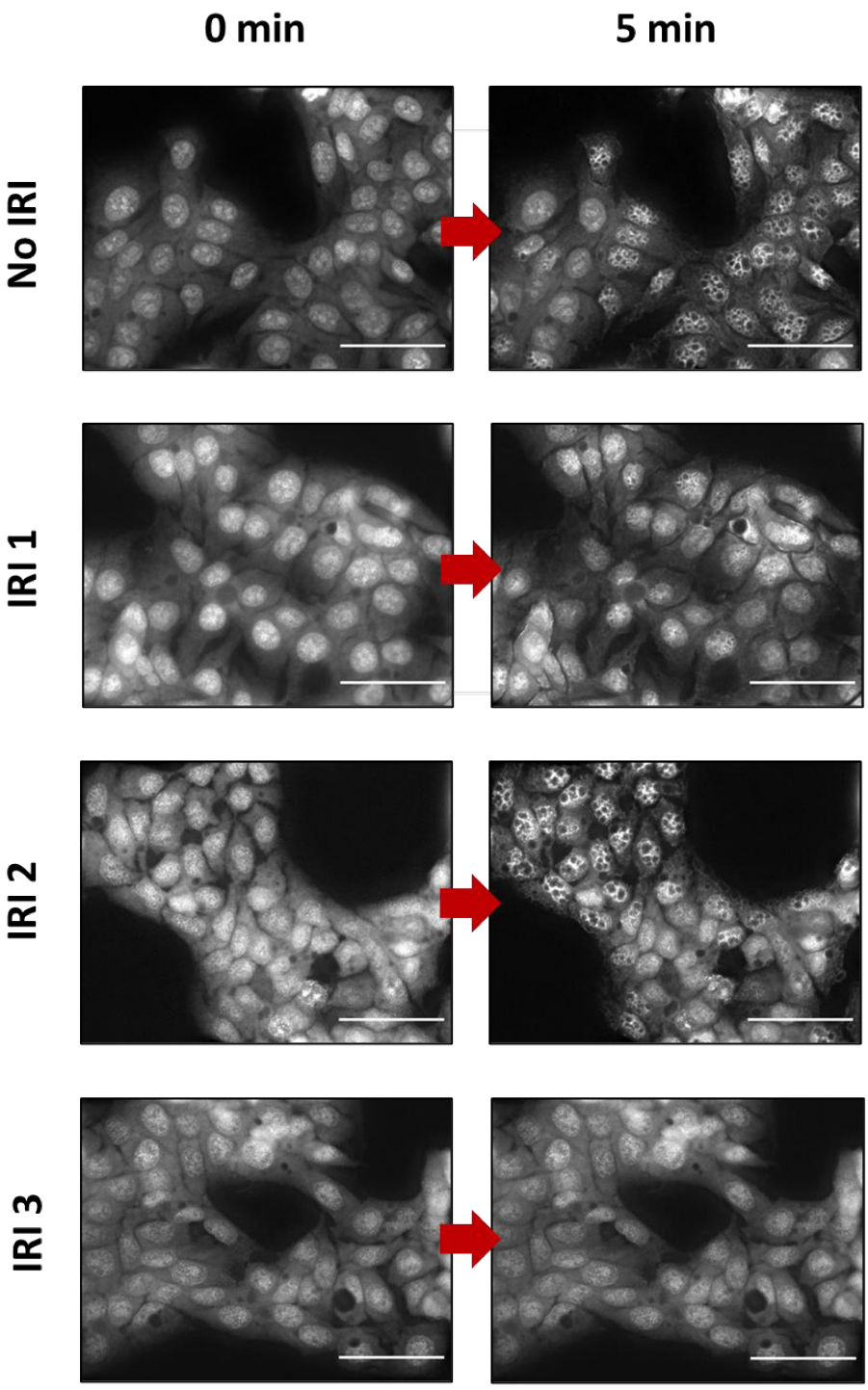

Figure 2.12 IRI-mediate control of intracellular ice recrystallization in cells treated with 5% trehalose: representative images. Images displayed taken immediately (0 min) and 5 min after nucleation at -15 °C. Scale bar = 50 μm.

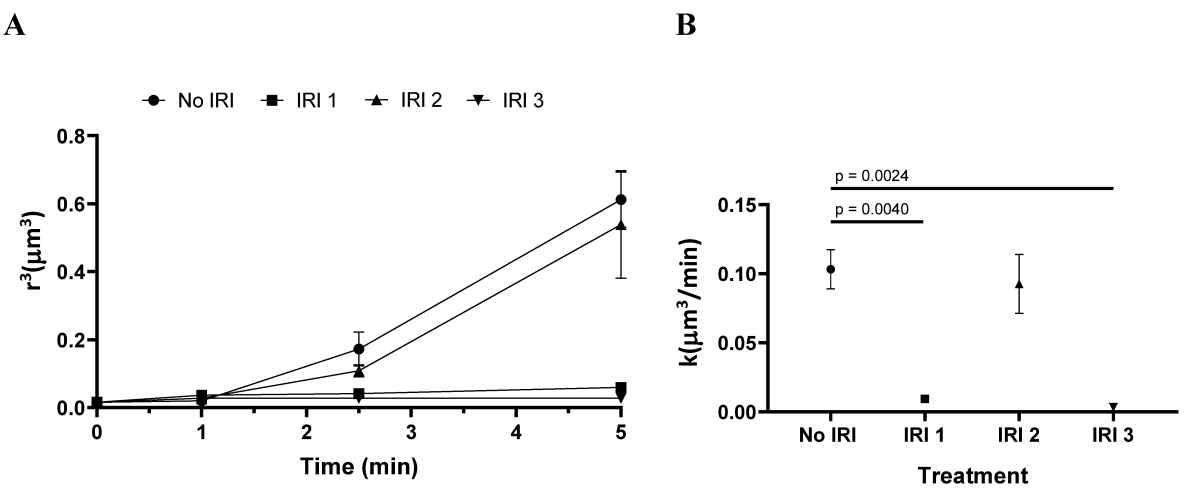

Figure 2.13 IRI-mediate control of intracellular ice recrystallization in cells treated with 5% trehalose. (A) r^3 values were determined from the mean grain size per cell calculated in 15 to 30 cells per replicate at 1 min, 2.5 min, and 5 min after nucleation. (B) Rates of recrystallization (k) values were determined from the r^3 values as indicated in equation 2.5. Error bars represent the standard error of the mean between replicates. Significance differences from the control were calculated using a nested one-way ANOVA followed by a Dunnet's post-hoc test on log transformed data. Differences where $p < 0.05$ were considered to be statistically significant.

2.6 References

[1] J.P. Acker, Influence of cell adhesions on the freezing response of biological systems [Dissertation], Edmonton, AB: University of Alberta, 1998.

[2] J.P. Acker, Innocuous intracellular ice formation : mechanisms and implications [Dissertation], Edmonton, AB: University of Alberta, 2000.

[3] J.P. Acker, and I.M. Croteau, Pre- and post-thaw assessment of intracellular ice formation. J Microsc 215 (2004) 131-8.

[4] J.P. Acker, and L.E. McGann, Cell-cell contact affects membrane integrity after intracellular freezing. Cryobiology 40 (2000) 54-63.

[5] J.P. Acker, and L.E. McGann, Innocuous intracellular ice improves survival of frozen cells. Cell Transplant 11 (2002) 563-71.

[6] J.P. Acker, and L.E. McGann, Protective effect of intracellular ice during freezing? Cryobiology 46 (2003) 197-202.

[7] T.J. Anchordoguy, C.A. Cecchini, J.H. Crowe, and L.M. Crowe, Insights into the cryoprotective mechanism of dimethyl sulfoxide for phospholipid bilayers. Cryobiology 28 (1991) 467-473.

[8] T.J. Anchordoguy, A.S. Rudolph, J.F. Carpenter, and J.H. Crowe, Mode of interaction of cryoprotectants with membrane phospholipids during freezing. Cryobiology 24 (1987) 324-331.

[9] H. Bank, Freezing injury in tissue cultured cells as visualized by freeze-etching. Exp Cell Res 85 (1974) 367-76.

[10] H. Bank, Visualization of freezing damage. II. Structural alterations during warming. Cryobiology 10 (1973) 157-70.

[11] R.E. Barnett, The effects of dimethylsulfoxide and glycerol on Na+, K+-ATPase and membrane structure. Cryobiology 15 (1978) 227.

[12] R.C. Bates, N.S. Edwards, and J.D. Yates, Spheroids and cell survival. Crit Rev Oncol Hematol 36 (2000) 61-74.

[13] J.C. Bischof, and B. Rubinsky, Large ice crystals in the nucleus of rapidly frozen liver cells. Cryobiology 30 (1993) 597-603.

[14] J.G. Briard, S. Jahan, P. Chandran, D. Allan, N. Pineault, and R.N. Ben, Small-Molecule Ice Recrystallization Inhibitors Improve the Post-Thaw Function of Hematopoietic Stem and Progenitor Cells. ACS Omega 1 (2016) 1010-1018.

[15] J.G. Briard, J.S. Poisson, T.R. Turner, C.J. Capicciotti, J.P. Acker, and R.N. Ben, Small molecule ice recrystallization inhibitors mitigate red blood cell lysis during freezing, transient warming and thawing. Sci Rep 6 (2016) 23619.

[16] V.L. Bronshteyn, and P.L. Steponkus, Nucleation and growth of ice crystals in concentrated solutions of ethylene glycol. Cryobiology 32 (1995) 1-22.

[17] C. Budke, C. Heggemann, M. Koch, N. Sewald, and T. Koop, Ice recrystallization kinetics in the presence of synthetic antifreeze glycoprotein analogues using the framework of LSW theory. J Phys Chem B 113 (2009) 2865-2873.

[18] C.J. Capicciotti, M. Doshi, and R.N. Ben, Ice recrystallization inhibitors: From biological antifreezes to small molecules. Recent developments in the study of recrystallization. 177 (2013) 224.

[19] C.J. Capicciotti, J.D. Kurach, T.R. Turner, R.S. Mancini, J.P. Acker, and R.N. Ben, Small molecule ice recrystallization inhibitors enable freezing of human red blood cells with reduced glycerol concentrations. Sci Rep 5 (2015) 9692.

[20] C.J. Capicciotti, M. Leclere, F.A. Perras, D.L. Bryce, H. Paulin, J. Harden, Y. Liu, and R.N. Ben, Potent inhibition of ice recrystallization by low molecular weight carbohydrate-based surfactants and hydrogelators. Chem Sci 3 (2012) 1408-1416.

[21] J.L. Chaytor, J.M. Tokarew, L.K. Wu, M. Leclere, R.Y. Tam, C.J. Capicciotti, L. Guolla, E. von Moos, C.S. Findlay, D.S. Allan, and R.N. Ben, Inhibiting ice recrystallization and optimization of cell viability after cryopreservation. Glycobiology 22 (2012) 123-33.

[22] J.H. Crowe, L.M. Crowe, J.F. Carpenter, and C. Aurell Wistrom, Stabilization of dry phospholipid bilayers and proteins by sugars. Biochem J 242 (1987) 1-10.

[23] J.H. Crowe, L.M. Crowe, and R. Mouradian, Stabilization of biological membranes at low water activities. Cryobiology 20 (1983) 346-356.

[24] G. Fahy, Cryoprotectant toxicity-Biochemical or osmotic. Cryo-Letters 5 (1984) 79-90.

[25] G. Fahy, The role of nucleation in cryopreservation. Biological Ice Nucleation and its Applications, APS Press, St. Paul (1995) 315-336.

[26] G.M. Fahy, D.R. MacFarlane, C.A. Angell, and H.T. Meryman, Vitrification as an approach to cryopreservation. Cryobiology 21 (1984) 407-426.

[27] R. Fujisawa, M. Mizuno, H. Katano, K. Otabe, N. Ozeki, K. Tsuji, H. Koga, and I. Sekiya, Cryopreservation in 95% serum with 5% DMSO maintains colony formation and chondrogenic abilities in human synovial mesenchymal stem cells. BMC Musculoskelet Disord 20 (2019) 316-316.

[28] B. Gaber, I. Chandrasekhar, and N. Pattiabiraman, Molecular Modeling of the Interaction of Trehalose with the Phospholipid-Bilayer, Biophysical Journal, BIOPHYSICAL SOCIETY 9650 ROCKVILLE PIKE, BETHESDA, MD 20814-3998, 1986, pp. A435-A435.

[29] A.A. Gurtovenko, and J. Anwar, Modulating the structure and properties of cell membranes: the molecular mechanism of action of dimethyl sulfoxide. J Phys Chem B 111 (2007) 10453-60.

[30] T. Hagiwara, R.W. Hartel, and S. Matsukawa, Relationship between recrystallization rate of ice crystals in sugar solutions and water mobility in freeze-concentrated matrix. Food Biophys 1 (2006) 74-82.

[31] C.L. Harris, M. Toner, A. Hubel, E.G. Cravalho, M.L. Yarmush, and R.G. Tompkins, Cryopreservation of isolated hepatocytes: intracellular ice formation under various chemical and physical conditions. Cryobiology 28 (1991) 436-444.

[32] J. Hey, and D. MacFarlane, Crystallization of ice in aqueous solutions of glycerol and dimethyl sulfoxide. 1. A comparison of mechanisms. Cryobiology 33 (1996) 205-216.

[33] J.M. Hey, and D.R. Macfarlane, Crystallization of ice in aqueous solutions of glycerol and dimethyl sulfoxide 2: Ice crystal growth kinetics. Cryobiology 37 (1998) 119-130.

[34] A.Z. Higgins, and J.O. Karlsson, Effects of intercellular junction protein expression on intracellular ice formation in mouse insulinoma cells. Biophys J 105 (2013) 2006-15.

[35] Z.E. Hughes, A.E. Mark, and R.L. Mancera, Molecular dynamics simulations of the interactions of DMSO with DPPC and DOPC phospholipid membranes. J Phys Chem B (2012).

[36] D. Irimia, and J.O. Karlsson, Kinetics and mechanism of intercellular ice propagation in a micropatterned tissue construct. Biophys J 82 (2002) 1858-68.

[37] H. Ishiguro, and B. Rubinsky, Mechanical interactions between ice crystals and red blood cells during directional solidification. Cryobiology 31 (1994) 483-500.

[38] J.O. Karlsson, E.G. Cravalho, I.H. Borel Rinkes, R.G. Tompkins, M.L. Yarmush, and M. Toner, Nucleation and growth of ice crystals inside cultured hepatocytes during freezing in the presence of dimethyl sulfoxide. Biophys J 65 (1993) 2524-36.

[39] J.O.M. Karlsson, Effects of solution composition on the theoretical prediction of ice nucleation kinetics and thermodynamics. Cryobiology (2010).

[40] P. Klinmalai, M. Shibata, and T. Hagiwara, Recrystallization of ice crystals in trehalose solution at isothermal condition. Food Biophysics 12 (2017) 404-411.

[41] C.A. Knight, and J.G. Duman, Inhibition of recrystallization of ice by insect thermal hysteresis proteins: A possible cryoprotective role. Cryobiology 23 (1986) 256-262.

[42] R.E. Lee, G.J. Warren, and L.V. Gusta, Biological ice nucleation and its applications, APS Press, St. Paul, Minn., 1995.

[43] I.M. Lifshitz, and V.V. Slyozov, The kinetics of precipitation from supersaturated solid solutions. J Phys Chem Sol 19 (1961) 35-50.

[44] X. Liu, G. Zhao, Z. Shu, D. Niu, Z. Zhang, P. Zhou, Y. Cao, and D. Gao, Quantification of intracellular ice formation and recrystallization during freeze–thaw cycles and their relationship with the viability of pig iliac endothelium cells. Biopres Biobank 14 (2016) 511-519.

[45] F. Lv, B. Liu, W. Li, and G.K. Jaganathan, Devitrification and recrystallization of nanoparticle-containing glycerol and PEG-600 solutions. Cryobiology 68 (2014) 84-90.

[46] A. MacKenzie, Death of frozen yeast in the course of slow warming, Ciba Foundation Symposium-The Frozen Cell, Wiley Online Library, 1970, pp. 89-96.

[47] P. Mazur, 2. Roles of intracellular ice formation, vitrification of cell water, and recrystallization of intracellular ice on the survival of mouse embryos and oocytes. Cryobiology 65 (2012) 339.

[48] P. Mazur, Equilibrium, quasi-equilibrium, and nonequilibrium freezing of mammalian embryos. Cell Biophys 17 (1990) 53-92.

[49] P. Mazur, Freezing of living cells: mechanisms and implications. Am J Physiol 247 (1984) C125-42.

[50] P. Mazur, The role of intracellular freezing in the death of cells cooled at supraoptimal rates. Cryobiology 14 (1977) 251-272.

[51] E. Metzen, M. Wolff, J. Fandrey, and W. Jelkmann, Pericellular PO2 and O2 consumption in monolayer cell cultures. Respir Physiol 100 (1995) 101-6.

[52] R.H. Miller, and P. Mazur, Survival of frozen-thawed human red cells as a function of cooling and warming velocities. Cryobiology 13 (1976) 404-414.

[53] J. O'Brien, I. Wilson, T. Orton, and F. Pognan, Investigation of the Alamar Blue (resazurin) fluorescent dye for the assessment of mammalian cell cytotoxicity. Eur J Biochem 267 (2000) 5421-6.

[54] D.E. Pegg, Ice crystals in tissues and organs, The biophysics of organ cryopreservation, Springer, 1987, pp. 117-140.

[55] D.E. Pegg, M.P. Diaper, H.L. Skaer, and C.J. Hunt, The effect of cooling rate and warming rate on the packing effect in human erythrocytes frozen and thawed in the presence of 2 M glycerol. Cryobiology 21 (1984) 491-502.

[56] D.E. Pegg, I.A. Jacobsen, M.P. Diaper, and J. Foreman, The effect of cooling and warming rate on cortical cell function of glycerolized rabbit kidneys. Cryobiology 21 (1984) 529-35.

[57] J.S. Poisson, J.P. Acker, J.G. Briard, J.E. Meyer, and R.N. Ben, Modulating Intracellular Ice Growth with Cell-Permeating Small-Molecule Ice Recrystallization Inhibitors, Langmuir, 2018.

[58] J.S. Poisson, J.G. Briard, T.R. Turner, J.P. Acker, and R.N. Ben, Hydroxyethyl Starch Supplemented with Ice Recrystallization Inhibitors Greatly Improves Cryopreservation of Human Red Blood Cells. Bioproc J 15 (2016).

[59] P.J. Quinn, A lipid-phase separation model of low-temperature damage to biological membranes. Cryobiology (1985).

[60] A.T. Rahman, T. Arai, A. Yamauchi, A. Miura, H. Kondo, Y. Ohyama, and S. Tsuda, Ice recrystallization is strongly inhibited when antifreeze proteins bind to multiple ice planes. Sci Rep 9 (2019) 1-9.

[61] A.S. Rudolph, and J.H. Crowe, Membrane stabilization during freezing: the role of two natural cryoprotectants, trehalose and proline. Cryobiology 22 (1985) 367-77.

[62] A.S. Rudolph, J.H. Crowe, and L.M. Crowe, Effects of three stabilizing agents—proline, betaine, and trehalose—on membrane phospholipids. Arch Biochem Biophys 245 (1986) 134-143.

[63] T. Rutt, N. Eskandari, M. Zhurova, J.A. Elliott, L.E. McGann, J.P. Acker, and J.A. Nychka, Thermal expansion of substrate may affect adhesion of Chinese hamster fibroblasts to surfaces during freezing. Cryobiology 86 (2019) 134-139.

[64] J.P. Stegemann, H. Hong, and R.M. Nerem, Mechanical, biochemical, and extracellular matrix effects on vascular smooth muscle cell phenotype. J Appl Physiol (1985) 98 (2005) 2321-7.

[65] S.L. Stott, and J.O.M. Karlsson, Visualization of intracellular ice formation using high-speed video cryomicroscopy. Cryobiology 58 (2009) 84-95.

[66] R.L. Sutton, A. Lips, G. Piccirillo, and A. Sztehlo, Kinetics of ice recrystallization in aqueous fructose solutions. Journal of food science 61 (1996) 741-745.

[67] E.A. Szurek, and A. Eroglu, Comparison and avoidance of toxicity of penetrating cryoprotectants. PLoS One 6 (2011) e27604.

[68] R.Y. Tam, S.S. Ferreira, P. Czechura, R.N. Ben, and J.L. Chaytor, Hydration index-a better parameter for explaining small molecule hydration in inhibition of ice recrystallization. J Am Chem Soc 130 (2008) 17494-17501.

[69] R.M.F. Tomas, T.L. Bailey, M. Hasan, and M.I. Gibson, Extracellular Antifreeze Protein Significantly Enhances the Cryopreservation of Cell Monolayers. Biomacromolecules 20 (2019) 3864-3872.

[70] C. Wagner, Theorie der alterung von niederschlägen durch umlösen (Ostwald-reifung). Zeitschrift für Elektrochemie, Berichte der Bunsengesellschaft für physikalische Chemie 65 (1961) 581-591.

[71] M.L. Yarmush, M. Toner, J.C. Dunn, A. Rotem, A. Hubel, and R.G. Tompkins, Hepatic tissue engineering. Development of critical technologies. Ann N Y Acad Sci 665 (1992) 238-52.

Chapter 3 Investigation of IRI Efficacy in Liver Tissue

3.1 Introduction

Freeze tolerant organisms capable of surviving temperatures as low as -20 °C, rely on the synthesis of: (1) low molecular weight CPAs do depress the equilibrium freezing point, and (2) ice nucleating proteins (INPs) to promote intravascular nucleation within 2-3 °C of the equilibrium freezing point [3; 8; 14; 23; 33; 48; 63; 65; 66; 67; 68]. Together these mechanisms limit the total volume of ice formed, constrain ice to the vascular network, and enable the gradual application of osmotic stress to cells in the surrounding interstitium [56; 65; 67]. Mitigating vascular damage has, however, been the crux of freeze tolerance-inspired approaches to artificially cryopreserve mammalian organs, such as the heart, liver, and kidney, *in vitro* [4; 17; 20; 21; 22; 31; 51; 52; 56; 69]. Loss of vascular integrity causes an organ to fail even when other structural components remain intact [54; 56]. This issue is multifaceted and the development of improved perfusion protocols to load and unload CPAs, as well as pre-conditioning the organ can aid in this effect [10; 71]. However, ice-induced damage within the vasculature is not only a product of the total volume of ice formed, but is additionally related to the amount of recrystallization that occurs [33; 35].

The damage posed by intracellular ice recrystallization does not differ between single cell and multicellular systems; however, the degree to which the recrystallization of extracellular ice proves damaging is highly dependent on the spatial proximity of cells [41; 53; 64]. Pegg *et al.* eloquently demonstrated this through identifying a correlation between red cell hematocrit and susceptibility to extracellular ice recrystallization [53]. The architecture of increasingly dense and complex multicellular systems not only enhances this mode of cellular damage, but also introduces cell-cell and cell-matrix contacts as targets for extracellular ice recrystallization. The use of IRI-active antifreeze proteins has proven valuable in the cryopreservation of monolayer systems due to the need to maintain these contacts [73]. Further corroborating this notion are several studies demonstrating improved histologic and functional outcomes in frozen tissues following the use of rapid rewarming to minimize recrystallization [22; 30; 36].

The formation of ice outside the vasculature is commonly associated with diminished functional outcomes [31; 64]. Recrystallization injury can be augmented in these cases due to the reduced size of extracellular compartments external to the vascular network. In livers, endothelial cells lining the sinusoids lack a basement membrane and are attached to the loose matrix in the perisinusoidal space of disse, positioned between the hepatocytes and the sinusoid [25].

Recrystallization of ice within the perisinusoidal space of disse would result in endothelial cell detachment and ensuing vascular failure. The same notion can be applied to the formation and recrystallization of intracellular ice within these endothelial cells [1; 2; 38; 40; 42; 43; 44; 49; 55]. High nucleation temperatures and slow cooling rates can constrain ice to the vasculature; however, these strategies can promote excessive dehydration of cells in the surrounding interstitium [4; 61]. The corollary of this is excessive vessel distension and rupture [4; 61]. CPAs can be used to limit these volumetric excursions; however, the concentration of CPA used would need to increase proportionally as storage temperatures are lowered [39; 45; 46; 47; 75; 76]. Perfusing high concentrations of CPAs can compromise endothelial integrity and give rise to toxicity issues; thereby, effectively limiting the temperatures that frozen organs can be stored at using current technologies [70]. Measures to minimize interstitial or intracellular ice formation will likely be of less importance given that corresponding measures are taken to limit the amount of recrystallization that occurs.

The purpose of this chapter is to evaluate the toxicity and permeation of small molecule ice recrystallization inhibitors (IRIs) in rat liver tissue. Furthermore, it aims to offer insight into the efficacy of using these IRIs in a freeze tolerance-inspired approach to sub-zero liver preservation. There are currently no studies that have categorically investigated the utility of controlling recrystallization in a freeze tolerance-inspired organ preservation strategy. Evidence has pointed to the benefits of perfusing IRI-active antifreeze proteins throughout the organ prior to storage, which suggests that if a small molecule IRIs are capable of permeating liver tissue and additionally prove to be non-toxic, then it may be valuable in a freeze tolerance-inspired approach to sub-zero liver preservation. However, there are several alternate mechanisms unrelated to recrystallization through which antifreeze proteins can render protective effects and ice can damage complex tissues [28; 29; 59]. Thus, this chapter additionally aims to offer further insight and discussion into how recrystallization might be damaging when storing organs in a frozen state at high sub-zero temperatures, rather than simply a discussion on the efficacy of small molecule IRIs.

3.2 Methods

3.2.1 Evaluation of IRI-Mediated Control of Recrystallization in Rat Liver Tissue Sections

3.2.1.1 Study Design Overview

The purpose of experiment 1 was to utilize control of recrystallization as a measure to assess IRI permeation into rat liver tissue as the freezing and fixation conditions described in the subsequent condition would likely elucidate a condition where the IRI prove to be effective. Experiment 2 was performed to evaluate the ability of an IRI to control recrystallization under conditions that are more representative of a high sub-zero organ preservation strategy. N-(2-fluorophenyl)-D-gluconamide was the only IRI evaluated in this chapter. It should be noted that the IRI was used at a concentration of 15 mM for experiment 1 and 11 mM for experiment 2. This is the result of evaluations conducted at the University of Ottawa following experiment 1 that revealed that 11 mM is optimal concentration for this compound (Robert N. Ben, personal communication, July 23, 2019). Ideally, experiment 1 would be redone with 11 mM such that comparisons could be made between the two experiments, however this was not performed due to time constraints related to the COVID-19 global pandemic. Figure 3.1 outlines the general study design for the two experiments performed to assess IRI efficacy in rat liver tissue sections.

3.2.1.2 Liver Sectioning and Treatment

Liver was excised from male Sprague-Dawley rats immediately after the animal was euthanized following an unrelated surgical procedure. This procedure received ethics approval from the University of Alberta Research Ethics Board. Liver was placed in ice cold 1X Dulbecco's phosphate buffered saline (14190235, Gibco) to mitigate deterioration and sections were obtained from the median lobe. 0.5 mm^2 sections were obtained for experiment 1, whereas 0.25 mm^2 sections were obtained for experiment 2. Each section was placed into separate wells of a 24-well plate and 1.5 mL of either the IRI treatment or the control treatment (1X DPBS) was added to each well. Following a 6 h incubation at 22 °C, the sections were frozen as described in the subsequent sections. The IRI solutions were prepared in 1X DPBS as described in Chapter 2, section 2.2.3. Each condition was performed in replicates of 2.

3.2.1.3 Experiment 1 – Freezing, Fixation, and Preparation for Optical Microscopy

Sections were placed into glass vials (45 × 15 mm, 60965D-1, Kimble Chase, Rochester, NY, USA), plunged in liquid nitrogen (-196 °C), and held for 1 hour. The glass vials were subsequently

placed on dry ice and 1.5 mL of fixative consisting of 85 parts 70% ethanol, 10 parts 38% formaldehyde, 5 parts glacial acetic acid was immediately applied. Fixative was pre-cooled to -80 °C prior to use, which ensured that ice crystals within the tissue did not melt or recrystallize due to fixative exposure. The sections were stored in a -80 °C freezer for 1 h to enable temperature equilibration. Freeze substitution for evaluation of cellular ultrastructure is typically performed at -80 °C following a liquid nitrogen plunge; thus, it can be assumed that limited recrystallization would take place under these conditions [16; 64]. Following the 24 h storage period, the glass vials were transferred onto dry ice and allowed to rewarm over the course 48 h after which they were transferred to a 4 °C fridge. Tissues were Paraffin embedded using a HistoCore PEARL tissue processor (Leica Biosystems, Buffalo Grove, IL, USA) and 5 μm sections were obtained from the center and base of each block using a HistoCore AUTOCUT microtome (Leica Biosystems). Hematoxylin (3801561, Sigma-Aldrich) and eosin (3801602, Sigma-Aldrich) staining and subsequent mounting using Surgipath MM 24 Mounting Medium (3801120, Leica Biosystems) was performed to enable visualization through light microscopy. Embedding, sectioning, and staining was performed in accordance with the prior protocols [18; 19].

3.2.1.4 Experiment 2 – Freezing, Fixation, and Preparation for Optical Microscopy

Sections were placed onto 12 mm glass coverslips (VWR, 89015-725) and transferred to a Linkam FDCS196 cryostage (Linkam Scientific Instruments, Tadworth, England) pre-set to 4 °C. Samples were frozen at a rate of either 1 °C/min or 90 °C/min to -20 °C and held at this temperature for 5 min to facilitate temperature equilibration throughout the tissue. All freezing profiles were input into Lynksis 32 software (Linkam Scientific, Tadworth, England). For conditions frozen at 1 °C/min, residual liquid surrounding the base of the tissue section was manually nucleated at -5 °C using a copper wire pre-cooled in liquid nitrogen. This was done to promote consistency in both the localization and metastability of ice formed between individual tissue sections. Manual nucleation of sections frozen at 90 °C/min was not performed as the aim in this condition was to nucleate as close to -20 °C as possible to facilitate intracellular ice formation (IIF) and maximize crystal metastability. This temperature was chosen as it would theoretically be at the lower temperature range for a sub-zero organ preservation strategy [67; 71; 72]. Furthermore, nucleation would regularly take place at -15 °C to -20 C under a 90 °C/min cooling rate. This was the fastest cooling rate that could be attained by the Linkam FDCS196 cryostage; therefore, it was not

possible to increase the metastability of the ice crystals that were formed using this method of freezing.

Following the 5 min hold at -20 °C, coverslips were transferred into a 24-well plate in a -20 °C freezer. In order to minimize temperature fluctuations during the transition between the cryostage and the freezer, coverslips were transported on a 15 mm Petri dish suspended on methanol pre-cooled to -20 °C in a -20 °C freezer. Significant care was taken to ensure that methanol did not enter the Petri dish and contact the tissue section as this would interfere with subsequent fixation efforts and evaluations of ice grain size. A 1.5 mL volume of fixative consisting of 85 parts 70% ethanol, 10 parts 38% formaldehyde, 5 parts glacial acetic acid, was applied immediately after transfer to the -20 °C freezer, or following 5 days of storage at -20 °C. Similar to experiment 1, fixative was pre-cooled to -20 °C in a -20 °C freezer prior to use to ensure ice crystals did not melt or recrystallize due to fixative exposure. Sections were held in fixative for a period of 24 h and then transferred to 4 °C fridge. The 24 h duration of fixation has been confirmed to enable permeation of the fixative through 1 mm of liver tissue at -20 °C; promoting confidence that complete fixation of the 0.25 mm^2 tissue sections used in this study took place during this 24 h period [37]. Tissues were Paraffin embedded, sectioned, and stained as described in section 3.2.1.3 with the only variation being that the sections were solely obtained from the center of each block rather the center and the base.

3.2.1.5 Image Acquisition and Analysis

Images were taken on a Nikon Eclipse TE2000-U inverted microscope (Nikon, Tokyo, Japan) connected to NIS elements AR 3.22.14 software (Nikon). A 4X Nikon LU Plan Fluor objective lens with a working distance of 0.14 mm was used to obtain images for experiment 1 to visualize differences between the edge and the center of the tissue section. A 20X Nikon LU Plan Fluor objective lens with a working distance of 0.45 mm was used to obtain images in experiment 1 and 2 for subsequent thresholding segmentation. All images subject to thresholding did not have large vessel structures (ie. they solely contained hepatocytes and sinusoids). For experiment 1, a total of four 20X images from the interior region of each section were obtained per replicate. Two images were taken from section taken from the center and base of each block, which were then compiled for analysis. For experiment 2, four images were obtained per replicate at random regions throughout the section. Thresholding segmentation was performed using NIS elements AR 3.22.14

software. It is well-accepted that opaque regions in freeze substituted tissues are representative of ice crystal ghosts [26]. Our group has generated data correlating the patterns and morphology of ice crystals formed within liver tissues fixed using the aforementioned fixative with those seen following freeze substitution [37]. Thus, opaque regions seen within tissues were classified as ice crystals. Both the average area of each opaque region as well as the total fraction of the image that was opaque were reported.

Pixel intensity limits for thresholding were set at 167 to 255 on a 0 (black) to 255 (white) scale. Objects equal to or less than 10 μm^2 were not included in the analysis as these objects did not have clear opacity or defined borders. A 5X smoothening filter was ran on each image prior to analysis in order to depress small holes and depressions, thereby promoting homogeneity within identified objects. In addition, the number of bins was increased from 20 to 25 for each image in order to effectively differentiate object borders. Prior to exporting thresholding data, objects touching the border of the image were removed. These processes are all detailed in the NIS-Elements Advanced Research User's Guide Ver. 3.00 [50]. Figure 3.2 offers a representative image of how these processes impact image thresholding.

3.2.2 Evaluating IRI Efficacy in Frozen Whole Rat Livers[1]

3.2.2.1 Rat Liver Procurement

The health and welfare of the animals was maintained by Massachusetts General Hospital Center of Comparative Medicine (CCM), and the experimental protocols were approved by the Institutional Animal Care and Use Committee (IACUC) of Massachusetts General Hospital (Boston, MA, USA). Procurement of the rat liver was performed in accordance with previously describe protocols on 200 g to 250 g male Lewis rats [6]. In brief, the rat is anesthetized in 5% isofluorane accompanied by oxygen flow at 8 mL/min during the introduction phase. Isofluorane is lowered to 2-3% for the maintenance phase. A transverse abdominal incision is made and transparent membranes securing each lobe of the liver to surrounding organs were cut to mobilize the organ. A 16-guage catheter was then used to cannulate the portal vein (PV) past the

[1] All the work performed in section 3.2.2 was conducted in Shannon N. Tessier's lab at Shriners Hospital for Children in Boston, MA, USA. Rat liver procurement described in section 3.2.2.1 was performed by Casie A. Pendexter. The work described in sections 3.2.2.2 and 3.2.2.4 was done with the assistance of Casie A. Pendexter and Stephanie E. J. Cronin. Both individuals, including Shannon N. Tessier, are affiliated with Shriners Hospital for Children, Boston, MA, USA and Center for Engineering in Medicine, Harvard Medical School & Massachusetts General Hospital, Boston, MA, USA.

gastroduodenal and splenic branches. The bile duct (BD) was dissected and cannulated with a 28-guage cannula. Both cannulas were secured using 3.0 silk. The hepatic artery, renal vein, splenic vein, and adrenal veins were dissected and ligated with 6.0 silk. The inferior vena cava (IHVC) was transected and the liver was flushed with 30 mL of lactated Ringer solution (LR) with 30 units of heparin at a rate of ~7 mL/min. The suprahepatic inferior vena cava and hepatoduodenal ligament were transected in order to remove the liver from the abdominal cavity. The liver was placed on ice and flushed with an additional 20 mL of LR solution with 30 units of heparin.

3.2.2.2 Machine Perfusion and CPA Loading

The loading solution, storage solution 1, storage solution 2, the thawing solution, and the recovery solution are abbreviated as L, S1, S2, T, and R, respectively. Components of these different solutions can be found in Table 3.1.

Perfusate is consecutively pumped from a 500 mL bottle through an oxygenator (Radnoti, Monrovia, CA, USA), bubble trap (Radnoti), pressure sensor (Living Systems Instrumentation, Albans City, VT, USA), and sampling port (Cole-Parmer, Vernon Hills, IL, USA). Perfusate flowed through all these components and into the 16-guage cannula connected to the portal vein of the liver which was housed in a glass chamber (Radnoti). The different components within the system were all connected using size-16 masterflex platinum-cured silicone tubing (Cole-Parmer). Prior to initiation of perfusion, the system was primed with 500 mL of solution L, during which the gas flow to the oxygenator (95% O_2 and 5% CO_2) was set at 1 L/min. To calibrate the pressure sensor, a 16-guage catheter was connected to the system and the pressure was recorded at flow rates ranging from 0 mL/min to 30 mL/min. Once the solution had perfused for a minimum of 15 min, 95 μL inflow samples were analyzed in using a i-Stat blood analyser (Abbot Laboratories, Chicago, IL, USA) to confirm adequate oxygenation and pH. pH was adjusted accordingly using $NaHCO_3$ or HCl to correct for acidosis or alkalosis, respectively. Pressure calibrations were only performed for solution L, which may have introduced some error to the portal resistance calculations performed following the addition of solutions S1 and S2 due to their varying viscosity.

Prior to connecting the liver, the bubble trap was completely filled, and the tubing was bubble free. The controlled rate chiller was set at 21 °C and the flow rate at 5 mL/min once the liver was connected to the system (Fig 3.3, step 1). The target flow rate for subnormothermic machine

perfusion (SNMP) was 25 mL/min. Flow rate was increased as fast as 1 mL/min every 20 to 30 seconds if portal pressure could be maintained within 3-4 mmHg. This was done to minimize deterioration of the tissue. The maximum allotted portal pressure was 4-5 mmHg; therefore, if pressure exceeded these values, the increase in flow rate was decreased. A gradual switch to solution S1 began following 30 min of SNMP with solution L, at which point the circulating-controlled rate chiller was set to 4 °C (Fig. 3.3, step 2). 50 mL of solution was in the perfusion system at any given time; therefore, 50 mL of a 1 to 5 ratio of S1 to L was prepared in a 50 mL conical tube and added to the system. Once the entire 50 mL of this solution was in the perfusion system, the solution was switched to 50 mL of a 2 to 5 ratio of S1 to L. This was done until solution S1 comprised 100% of the solution in the system. This manner of increasing the concentration of solution S1 in 20% increments limited osmotic stress and was confirmed to be crucial to enabling the successful perfusion of the solutions used (Shannon N. Tessier, personal communication, December 20, 2019). Due to the viscosity of solution S1 in combination with the reduction in temperature, flow rates were decreased to 6-8 mL/min to keep the portal pressure within 4-5 mmHg once the temperature of the system had reached 4 °C. This lasted 30 min, after which a gradual switch to solution S2 began (Fig. 3.3, step 3). This was done in the same manner as the incremental addition of solution S1. Flow rates were decreased accordingly to accommodate the increase in portal pressure caused by the increased viscosity of solution S2. The flow rate was reduced to 0.5 mL/min once the system contained 100% solution S2. Perfusion at this flow rate continued for 30 min, after which the liver was placed in a sealable sterile bag containing 50 mL of S2. This bag was then placed in a freezer pre-cooled to either -10 °C or -15 °C.

Inflow and outflow samples (95 μL) for pH, pO_2, HCO_3^-, lactate, Na^+, K^+, Ca^{2+}, Cl^-, glucose, and Hb were taken at the onset of steps 1 and 2, as well as at the beginning and end of step 3. All samples were analyzed using an iStat blood analyzer (Abbot Laboratories).

3.2.2.3 CPA Unloading, Recovery, and Reperfusion

Prior to connecting the thawed liver to the perfusion circuit, pressure calibrations were performed for solution T and solution R similar to the method described in section 3.2.2.2. Calibrations were performed at 1 mL/min increments up to 10 mL/min and 30 mL/min for T and R, respectively.

Livers were removed from the freezer and gently swirled in a 37 °C water bath for 5 min to allow for complete thawing. The liver was then connected to the perfusion circuit and solution T was perfused at a flow rate of 2 mL/min for 30 min at 4 °C (Fig. 3.3, step 4). The temperature was then raised at a rate of 1 °C/min up to 22 °C, and flow rates were raised accordingly in 1 mL/min increments up to 7 mL/min. Portal pressure was kept within 3-4 mmHg during this process. 30 min after initiation of the temperature increase, incremental addition of solution R began in the same manner described in section 3.2.2.2, except the addition was performed in 10% rather than 20% increments (Fig. 3.3, step 5). Once solution R comprised 100% of the solution in the system, the liver was perfused for 3 hours at 22 °C (Fig. 3.3, step 6). Flow rates were kept at 25 mL/min during the 3-hour period given that portal pressure was below 3-4 mmHg. Blood reperfusion began after the 3-hour recovery period. The temperature of the system was raised to 37 °C at a rate of 1 °C/min and flow rates were increased in 1 mL/min increments up to 30 mL/min (Fig. 3.3, step 7). Reperfusion was carried out for 2 hours and portal pressures were kept within 11 mmHg during this phase.

Inflow and outflow samples (95 µL) for pH, pO_2, HCO_3^-, lactate, Na^+, K^+, Ca^{2+}, Cl^-, glucose, and Hb were taken at the end of step 4, step 5, every 60 min during step 6, and every 60 min during step 7. All samples for analyzed using an iStat blood analyzer (Abbot Laboratories).

3.2.2.4 Data Processing for Vascular Resistance and Oxygen Consumption

Vascular resistance was calculated using equation 3.1:

$$Vascular\ Resistance = \frac{\frac{portal\ pressure}{flow\ rate}}{initial\ liver\ weight} \qquad \text{Eq 3.1}$$

Oxygen consumption was calculated using equation 3.2:

$$
\begin{aligned}
&Oxygen\ Consumption \\
&\quad = coeff O_2 \\
&\quad \times \Bigg(((art_{pO_2} + port_{pO_2} - ven_{pO_2}) \times (art_{flow} + port_{flow})) \\
&\quad + (Hb \times cHb) \\
&\quad \times \Bigg(\left(\frac{art_{sO_2}}{100} \times art_{flow} \right) + \left(\frac{port_{sO_2}}{100} \times port_{flow} \right) \\
&\quad - \frac{ven_{sO_2}}{100} \times (art_{flow} + port_{flow}) \Bigg) \Bigg) \\
&\quad \overline{\qquad\qquad\qquad\qquad\qquad\qquad\qquad\qquad\qquad\qquad\qquad\qquad} \\
&\quad liver\ weight
\end{aligned}
\qquad \text{Eq 3.2}
$$

$CoeffO_2$ is the oxygen solubility coefficient: 3.14×10^{-5} mL O_2/mmHgO_2/mL; art_{pO2} is the arterial partial oxygen solubility coefficient (mmHg); $port_{O2}$ is the portal partial oxygen pressure (mmHg); $venP_{O2}$ is the venous partial oxygen pressure (mmHg); art_{flow} is the arterial flow rate (mL/min); $port_{flow}$ is the portal flow rate (mL/min); art_{sO2} is the arterial oxygen saturation (%); $port_{SO2}$ is the portal hemoglobin saturation (%); ven_{sO2} is the venous hemoglobin saturation (%); cHb is the hemoglobin oxygen binding capacity (1.34 mL O_2/g); Hb is hemoglobin concentration; and liver weight is the initial weight of the liver (kg).

3.2.3 Statistical analysis

All statistical analysis was performed using GraphPad Prism 8.1.0. Thresholding data form the image analysis performed on liver tissue sections was normalized using a log transformation and analyzed using a nested one-way ANOVA followed by a Tukey's post hoc test to evaluate differences between conditions. Differences were considered significant when $p < 0.05$.

For the evaluation of IRI efficacy in whole rat livers, differences were evaluated between the two storage conditions at each given timepoint as well as between timepoints for each storage condition. Analysis was done using a repeated-measures two-way ANOVA followed by the Sidak post-hoc test. Differences were considered significant when $p < 0.05$.

3.3 Results

3.3.1 IRI-Mediated Control of Recrystallization in Liver Tissues

3.3.1.1 Evaluation 1

Plunging liver tissues in liquid nitrogen resulted in a cooling rate of 550 °C/min (Fig 3.4). Concurrent fixation and recrystallization during rewarming promoted a gradient of increasing crystal size from the edge to the center of the tissue section in the untreated control; however, no such gradient was seen in IRI-treated liver tissue sections (Fig. 3.5A-B). This was consistent between sections obtained from both the base and center of each block (Fig. 3.5A-B). In the interior region of the IRI-treated condition, small perforations seen within the nucleus and cytoplasm of constituent cells are indicative of small ice crystals as these are clearly absent in the unfrozen tissue section (Fig. 3.5C). Previous literature has additionally characterized such perforations seen under light microscopy to be correlated with small intracellular ice crystals seen under low temperature scanning electron microscopy [5]. The presence of these small ice crystals in the IRI-treated condition clearly contrasts with the vascular expansion and large ice crystals evident within constituent cells of the untreated condition (Fig. 3.5C). Image segmentation by thresholding revealed no significant differences in the mean grain size between the IRI-treated and untreated conditions (Fig. 3.6A). However, there was a significant difference in the fraction of the area that was thresholded between the two conditions ($p = 0.0048$), which is not surprising considering the small ice crystals within the hepatocytes of the IRI-treated condition did not appear opaque (Fig. 3.3C and Fig 3.4B).

3.3.1.2 Evaluation 2

Evaluating the ability of the IRI to control recrystallization in liver tissues at high sub-zero temperatures is pertinent to understanding their utility in a freeze tolerance-inspired organ preservation strategy. In tissue sections frozen at 1 °C/min, hepatocytes appear dehydrated and large ice crystals appear to have formed in the surrounding vasculature (Fig 3.7A-B). This was the case regardless of whether the sections were fixed immediately upon freezing or after the 5-day storage period (Fig. 3.5A). Image segmentation by thresholding revealed no significant differences in mean grain size between IRI-treated and untreated conditions at the 0-day and 5-day timepoints (Fig. 3.8A). Furthermore, there were no significant differences in mean grain size between the two storage periods for either treatment condition (Fig. 3.8A). This also proved to be the case for the

fraction of the area that was thresholded, and therefore the absence of significant differences in mean grain size was not simply due to an inability to detect ice crystals via image thresholding (Fig. 3.8).

Minimal dehydration of hepatocytes is apparent in tissue sections frozen at 90 °C/min as they clearly retain circular morphology and the surrounding vasculature does not appear distended (Fig. 3.7B). The opaque regions within the cytoplasm and nucleus of the hepatocytes are indicative of intracellular ice (Fig. 3.7B). The mean grain size in both the IRI-treated and untreated conditions frozen at 90 °C/min were significantly smaller than those frozen at 1 °C/min at both the 0-day and 5-day storage periods (Fig. 3.8) (IRI 0 d: $p < 0.0001$; IRI 5 d: $p = 0.0011$; No IRI 0 d: $p < 0.0001$; No IRI 5 d: $p = 0.0005$) However, there were no significant differences between the two treatment conditions, which additionally proved to be the case at the 5-day storage period (Fig. 3.8). Interestingly, both treatment conditions stored for 5 days demonstrated a significant increase in mean grain size relative to those fixed immediately (Fig. 3.8A) (IRI: $p = 0.0041$; No IRI: $p = 0.0019$). Significant differences in mean grain size were not reflected in the fraction of thresholded area, where no difference was detected between either of the two treatment conditions or storage periods assessed for sections frozen at 90 °C/min (Fig. 3.8B). However, this is likely due to intracellular ice being picked up by the thresholding as it is large enough to appear opaque (Fig. 3.7B).

3.3.2 Functional Parameters Following IRI Loading in Whole Rat Livers

Considering the perfusion protocol and CPA loading regimen had previously been optimized to minimize endothelial injury and CPA toxicity, adverse outcomes during the initial loading phase would be indicative of IRI toxicity. Figure 3.9 A-C represents functional parameters assessed during the loading phase, with dashed lines indicating reference values recently published by De Vries *et al.* for the 30 min timepoint during SNMP pre-conditioning [9] (Table 3.2). Non-IRI controls were not performed as part of this study and have not yet been published; therefore, comparisons to these controls were not made due to the data being proprietary. The lack of post-perfusion weight gain is indicative of minimal hepatocellular edema during the loading phase (Fig. 3.9D). Portal resistance reference values are well-below the reference values, further indicating a lack of hepatocellular edema as well as a lack of endothelial injury (Fig. 3.9C) [6; 10]. Oxygen uptake rates are highly correlated with liver specific functions (Fig 3.9A) [7]. The significant

increase in oxygen consumption from 0 to 30 min following SNMP is normal during SNMP pre-conditioning under this protocol and the 30 min values did not depart extensively from the reference values (Fig. 3.9A) [9]. Furthermore, the potassium concentration in the portal outflow was lower than the reference values; thus, hepatocellular injury was likely minimal (Fig. 3.9B) [6; 10].

3.3.3 Reperfusion of Rat Livers Frozen with IRI

As was previously mentioned, non-IRI controls for both storage conditions were not performed as part of this study and have not yet been published, therefore comparisons to these controls were not made. While non-IRI control data has not been included as a part of this thesis, personal correspondence on the outcomes of these controls will be form a basis for discussion in the sections 3.4.2 and 3.4.3 (Shannon N. Tessier, personal communication, December 20, 2019). Reference values for fresh, non-preconditioned livers undergoing normothermic reperfusion have been given to contextualize some of the results obtained in this study (Table 3.3).

Normothermic machine perfusion with blood has recently been used as a model for transplantation and is traditionally used to assess the viability of livers prior to transplant [74]. Considering that an increase in vascular resistance infers the presence of endothelial injury and hepatocellular edema, a stable vascular resistance profile is preferable [6; 10]. Results indicate that the vascular resistance of both storage conditions is stable throughout reperfusion, with no significant differences between timepoints or between storage conditions at each timepoint (Fig. 3.10D). The error in these measures are substantial, making it challenging to compare this parameter to reference values for fresh livers (Fig 3.10D, Table 3.3). However, weight gain is additionally indicative of hepatocellular edema and both storage conditions have a clear difference in % weight gain when compared to reference values for fresh livers post reperfusion (Fig 3.10E, Table 3.3). The pre- and post-reperfusion weights of the IRI frozen livers are not significant, which suggests that livers did not become more edematous during reperfusion (Fig 3.10E). Hepatocellular injury is demonstrated by aspartate aminotransferase (AST), alanine aminotransferase (ALT), and potassium concentrations in the portal outflow [6; 10]. In regard to potassium concentrations, there is again no significant difference between storage conditions. However, there is a clear discrepancy when compared to the reference values for fresh livers (Fig 3.10B, Table 3.3). ALT and AST concentrations are significantly higher at the 120 min and 180 min timepoints for the -15 °C, 5 d

storage condition, when compared to the -10 °C, 1 d storage condition (ALT 120 min; $p = 0.0003$; ALT 180 min: $p = 0.0003$; AST 120 min: $p = 0.0187$; AST 180 min: $p = 0.0107$) (Fig. 3.10F-G). ALT and AST concentrations for both storage conditions, however, appear to be substantially higher than the fresh control (Fig. 3.10F-G). There was no significant difference between storage conditions or timepoints for lactate clearance, another important measure of liver function (Fig. 3.10C). Error in the values makes it challenging to ascertain how the values for this measure compare to the fresh control (Fig. 3.10C, Table 3.3).

3.4 Discussion

3.4.1 IRI-Mediated Inhibition of Recrystallization in Liver Tissues

Determining that the IRI is capable of permeating liver tissues was a vital first-step in demonstrating the efficacy of these compounds in the frozen storage of whole livers. A liquid nitrogen plunge resulted in cooling rates of 550 °C/min at the base of the liver tissue blocks, promoting the formation of highly metastable nuclei (Fig 3.4). Application of a fixative at -80 °C, followed by slow rewarming period to 22 °C over the course of 48 hours, resulted in a gradient of increasing crystal size from the exterior towards the interior of untreated blocks (Fig. 3.5 and Fig. 3.6). This is not unexpected as the melting point of the fixative used is -80 °C, and thus it can be assumed that fixation and recrystallization would be taking place concurrently. However, this gradient was absent in the IRI treated condition, suggesting the IRI permeated throughout the tissue under the 6 h incubation period at 22 °C (Fig 3.5 and Fig. 3.6). It should be noted that the aforementioned freezing and fixation process created vastly different recrystallization characteristics than would be seen in a freeze tolerance-inspired approach to high sub-zero organ preservation This ultimately formed the basis for the subsequent study.

Freeze-fixation and evaluation of mean grain size revealed an absence of IRI-mediated control of recrystallization in liver tissue sections frozen at 90 °C/min to -20 °C (Fig 3.7 and Fig. 3.8). The previous experiment demonstrates that the IRI is capable of permeating a 0.5 mm^2 liver tissue section following a 6 h, 22 °C incubation; thus, inadequate permeation in this case is not the culprit (Fig 3.5 and Fig. 3.6). Furthermore, given that the conditions under which nucleation occurred were in the range of -15 °C to -20 °C for sections frozen at 90 °C/min, IRI activity would be expected based on the findings of Chapter 2. The lack of detectable IRI activity is more likely a

result of recrystallization in both the IRI-treated and untreated condition plateauing following 5 days of storage at -20 °C. This warrants further investigation; however, given the increase in mean grain size from 0 to 5 days of storage at -20 °C is significant in tissues frozen at 90 °C/min, it is possible that IRI activity could be seen if these tissues were instead stored for 1-4 days prior to fixation (Fig 3.8A). Furthermore, the IRI was used at a concentration of 11 mM in this experiment, while the previous evaluation demonstrated IRI efficacy at a concentration of 15 mM. 11 mM has been deemed the optimal concentration of this compound based on data from splat cooling assays; therefore, this is unlikely to be the culprit for the lack of activity seen, although this would additionally require further investigation (Robert N. Ben, personal communication, July 23, 2019).

Whole organs will invariably need to be frozen at relatively slow rates (< 3 °C/min) in order to achieve thermal uniformity and limit constitutional supercooling [24; 27; 32]. Thus, the absence of detectable IRI activity in all liver tissue sections frozen at 1 °C/min and the apparent absence of recrystallization between the 0 d and 5 d storage periods is more relevant to a discussion on the role of recrystallization and small molecule IRI's in the high sub-zero preservation of frozen organs (Fig 3.5 and Fig. 3.6). It is possible that recrystallization plateaued before fixation that the 0 d condition took place, which would suggest that recrystallization either took place during handling (ie. the transfer to the tissue section from the Linkam cryostage to the -20 °C freezer), or during the initial freezing event to -20 °C. Replication of these conditions in a thin film solution on a Linkam cryostage could provide insight to this effect; however, the latter is more likely given the rapid kinetics of recrystallization at temperatures between -5 °C and -15 °C [11; 12].

3.4.2 No IRI-Mediated Improvement of Functional Outcomes in Frozen Rat Livers

While the IRI did not demonstrate any toxic effects during its initial loading in whole rat livers (Fig 3.9), it is challenging to draw conclusions regarding its efficacy in a freeze tolerance-inspired approach to liver preservation. Several of the measured parameters during post-thaw reperfusion indicate a marked reduction in viability relative to a fresh, non-preconditioned liver (Fig 3.10). However, such a comparison is fraught as it does not account for or characterize additional damage that ensued during the CPA loading and unloading phases. Therefore, it offers minimal insight into the cryoprotective efficacy of the CPAs or the IRI as it does not isolate injury incurred during the freezing and thawing process. Transaminase levels are significantly increased 120 min and 180 min following reperfusion in the -15 °C, 5-day storage condition in comparison to the -10 °C, 1-

day storage condition (Fig. 3.10F-G). However, it is challenging to ascertain the extent to which this is the result of the storage temperature or the storage time. Furthermore, a discussion on the difference between the two storage conditions does not offer significant insight into the efficacy of the IRI. Therefore, the remainder of the discussion will be dedicated to personal correspondence with Dr. Shannon N. Tessier's at Massachusetts General Hospital (personal communication, December 20, 2019) suggesting that addition of the IRI does not substantially improve reperfusion parameters following storage at -10 °C for 1 day or -15 °C for 5 days.

The lack of IRI efficacy in this model could be narrowed down to IRI inactivation in storage solution 2 (S2) (Table 3.1) or an inability to detect the benefits of using an IRI due to a lack of optimization of the freezing protocol. Propylene glycol is used at a concentration of 12% in the freezing protocol implemented and results from the previous chapter suggest that intracellular activity of this IRI is lost in the presence of 0.2 M propylene glycol [71]. However, given the high concentration of permeating and non-permeating CPAs used, in combination with the high vascular nucleation temperature, the incidence of IIF is likely minimal. Thus, the absence of intracellular IRI activity may be inconsequential. Certainly, more relevant in this application would be the minimization of extracellular ice recrystallization; therefore, splat cooling assessment of IRI activity in S2 is warranted. There has been evidence that this IRI does not function extracellularly in DMSO and glycerol, making such evaluations increasingly important (Robert N. Ben, personal communication, July 23, 2019). Furthermore, while the freezing protocol leveraged in this study has demonstrated immense improvements over previously developed methods to freeze whole livers, there is considerable room for optimization [28; 29; 59; 71]. Functional parameters assessed during reperfusion indicate livers frozen to -10 °C or -15 °C for 1 day, or those frozen to -15 °C for 5 days, are far from transplantable (Shannon N. Tessier, personal communication, December 20, 2019). Increased transaminase levels and decreased oxygen uptake during reperfusion of livers frozen to -15 °C for 1 day compared to those frozen to -10 °C for 1 day is not surprising considering that an increase in the concentration of colligative CPAs does not accommodate the decrease in temperature (Fig. 3.10E-F) (Shannon N. Tessier, personal communication, December 20, 2019). The volume of vascular ice in livers frozen to -15 °C will be greater than those frozen to -10 °C; therefore, one could expect increased vascular distension and dehydration of the surrounding interstitium. As a result, other forms of freezing injury may

take precedence over recrystallization injury, limiting the extent to which IRI efficacy can be detected.

3.4.3 Recrystallization Injury in a Freeze Tolerance-Inspired Organ Preservation Method

Ultimately, the damage caused by recrystallization in a freeze tolerance-inspired approach to organ preservation is debatable. In other words, if the IRI was active in S2 and the freezing protocol was optimized to abrogate alternate mechanisms of freezing injury, this compound may have afforded minimal benefits. The freezing protocol leveraged in this study used Snomax, a commercially produced ice nucleating protein isolated from the bacterium *Pseudomonas syringae*, to achieve vascular nucleation between -5 °C and -6 °C (Table 3.1). Nucleation at these temperatures results in rapid rates of crystal growth; however, the overall magnitude of recrystallization will not be substantial given the relative thermodynamic stability of the ice formed. The fact that several freeze tolerant organisms contain RI active antifreeze proteins does not implicate RI activity as a requirement for freeze tolerance [8; 15]. The addition of antifreeze proteins in the storage of whole rat livers at -3 °C for 6 hours has proven beneficial; however, these compounds can promote retention of physiologic ion compositions during the freezing process through passive blockage of Ca^{2+} and K^{+} channels [57; 58; 59; 60; 62]. Furthermore, they can halt the migration of liquid water inclusions within ice that can ensue as a response to temperature gradients [35]. Both processes can respectively promote cellular and mechanical tissue damage; therefore, recrystallization inhibition is unlikely to be the dominant mechanism through which RI active antifreeze proteins impart protection in freeze tolerant organisms [33; 35]. This is corroborated by the absence of RI active antifreeze proteins in the hemolymph of freeze tolerant amphibians, who's organ systems are similar to those in mammals [8].

Although the survival of freeze tolerant organisms may not be predicated on the inhibition of recrystallization, RI activity may provide a selective advantage in response to seasonal temperature fluctuations. For example, if an organ is stored at -10 °C and the temperature increases by 1 °C, ice crystals can partially melt causing the volume of the unfrozen fraction to increase. A subsequent drop back down to -10 °C could promote additional nucleation and growth within the unfrozen fraction. These ice crystals would have a higher radius of curvature and be more thermodynamically unstable than the ice crystals that were initially nucleated at -5 °C or -6 °C, thereby facilitating recrystallization. Thus, in the event that complete melting does not occur,

temperature fluctuations may augment recrystallization. Studies on recrystallization in ice cream have revealed that the amplitude and frequency of temperature oscillations are correlated with the magnitude and rate of recrystallization, respectively [12; 13]. Furthermore, the effect of temperature fluctuations on the rate of recrystallization is highly dependent on the storage temperature [12; 13]. The 1 °C oscillations at storage temperatures below -15 °C prove to have a minimal impact on recrystallization rates, whereas the impact is substantial between -10 °C and -5 °C [13]. Ultimately, the utilization of RI active compounds to counter recrystallization that results from temperature fluctuations is secondary to the use of storage devices that can maintain static temperatures.

Recrystallization is not only dependent on the temperature and initial grain size, but also on the solute concentration. Migratory recrystallization (ie. grain boundary migration) occurs when individual molecules transfer from small convex ice grains to large concave ice grains. The presence of impurities between ice grains has proven to interfere with the migration process [34]. Therefore, minimizing this form of recrystallization is not predicated on the presence of an RI active compound. The relationship between the size of the impurity and the interference of the migration process has not been clearly delineated; however, it is likely that this interference is due to a reduction in the overall grain boundary area [34]. Therefore, there may be a correlation between the size of the compound and the extent to which it inhibits recrystallization. The presence of several large molecular weight compounds such as hydryoxyethyl starch (HES), raffinose, polyethylene glycol (PEG), and bovine serum albumin (BSA), may therefore provide some protection against recrystallization injury despite not having explicit RI activity (Table 3.2). As a virtue of their size, these compounds will solely preside in the vasculature. Given that this was the only region where ice formed within the organ, the ability of the IRI to render clear benefits may have been further hampered due solute mediated inhibition of recrystallization.

3.5 Conclusions

This chapter highlights that the IRI studied is capable of permeating rat liver tissue and additionally does not prove to whole rat livers. However, it fails to effectively demonstrate the efficacy of this compound in a freeze tolerance-inspired approach to high sub-zero liver preservation. This could be due to either (1) limited recrystallization taking place under the freezing conditions implemented, (2) an inability of the IRI to minimize recrystallization due to an appreciable extent

due to CPA-mediated inactivation of the compound, or (3) other forms of freezing injury taking precedence over recrystallization. Further studies are warranted to investigate these different factors. Given that the IRI tested is not toxic in whole rat livers, freezing under conditions where recrystallization injury is explicit may highlight their utility. However, the most pressing concern is to evaluate if the compound retains its activity in the presence of different permeating and non-permeating CPAs. These points will be further discussed in the subsequent chapter.

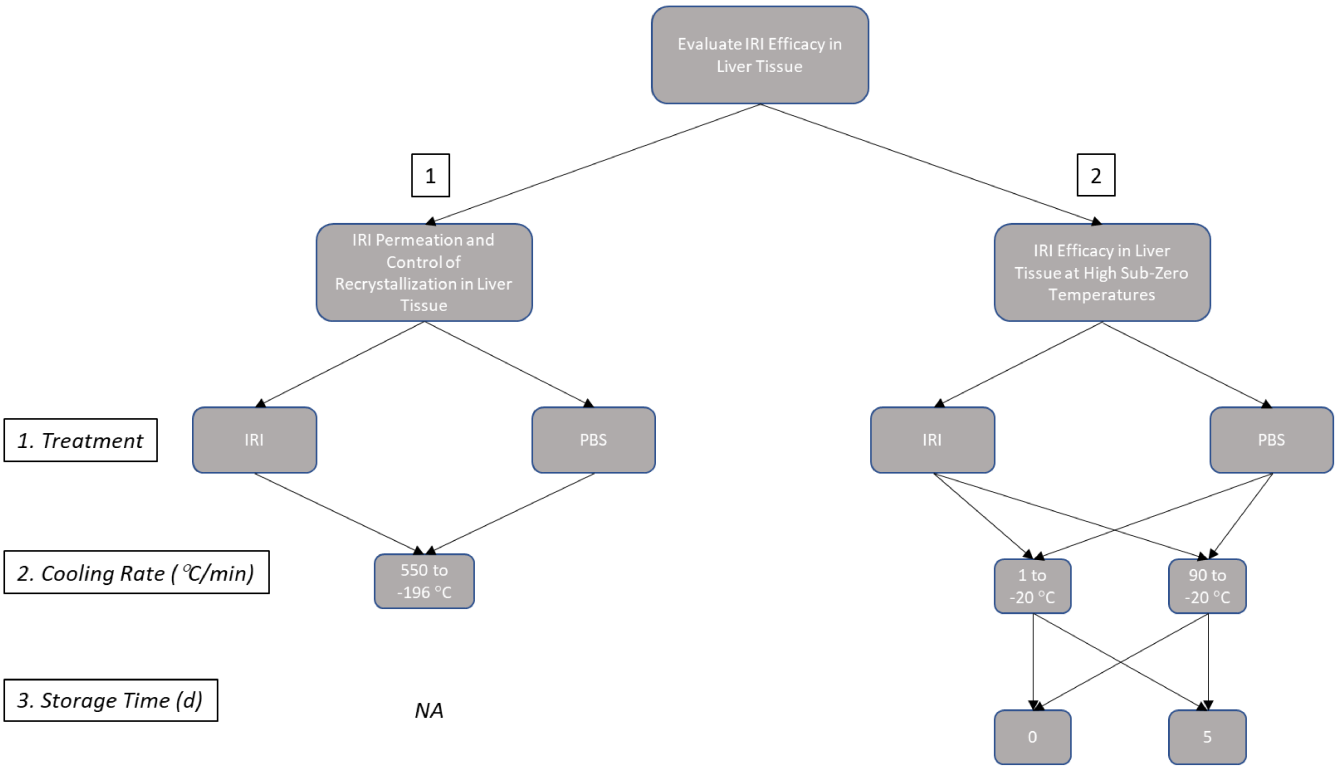

Figure 3.1 Overview of liver tissue experiment 1 and 2.

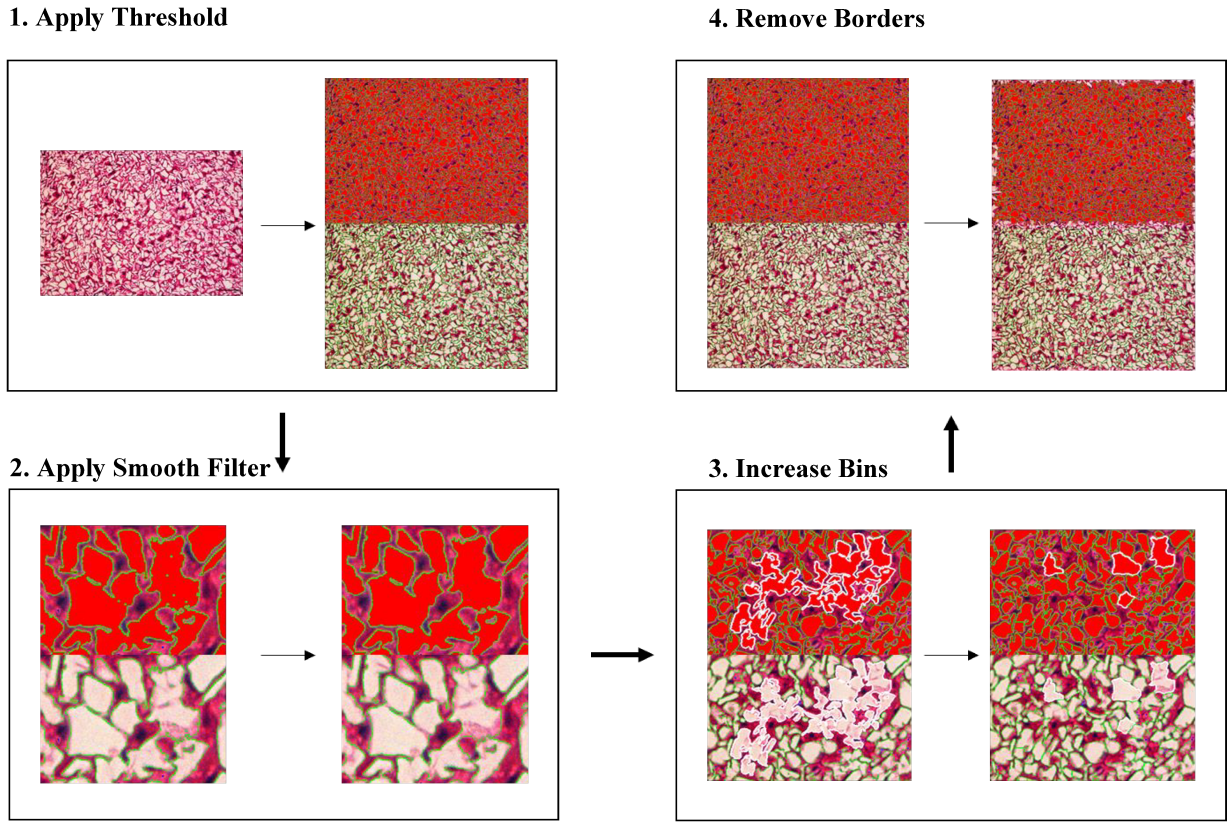

Figure 3.2 Workflow of thresholding analysis.

Table 3.1 Composition of the different solutions used in the whole rat liver freezing protocol described in sections 3.1.2.2 and 3.1.3.3.

Step	Solution	Solution Components
CPA Loading (Steps 1-3)	Loading Solution **(L)**	Williams E, 100 mM 3-OMG, 2%PEG, 10 mg/mL BSA, 2500 U/250 mL heparin, 500 μL/250 mL insulin, 12 mg/500 mL dexamethasone, 50 μL/250 mL hydrocortisone
	Storage Solution 1 **(S1)**	Williams E, 2% PEG, 100 mM 3-OMG, 6% PG, 3% HES, 30 mM raffinose, 12 mg/500mL dexamethasone, 500 μL/250 mL insulin, 1000 U/250 mL heparin, 2.5 g/250 mL BSA, 50 μL/250 mL hydrocortisone
	Storage Solution 2 **(S2)**	UW solution, 5% PEG, 100 mM 3-OMG, 12% PG, 50 mM trehalose, 12 mg/500mL dexamethasone, 10 μL/100 mL insulin, 1000 U/250 mL heparin, 2.5 g/250 mL BSA, 50 μL/250 mL hydrocortisone
CPA Unloading (Step 4)	Thawing Solution **(T)**	Williams E, 2% PEG, 100 mM 3-OMG, 6% PG, 3% HES, 30 mM raffinose, trehalose (50 mM), 12 mg/500 mL dexamethasone, 50 μL/250 mL insulin, 1000 U/250 mL heparin, 2.5 g/250 mL BSA, 50 μL/250 mL hydrocortisone
Recovery (Step 5)	Recovery Solution **(R)**	Williams E, 2% PEG, 12 mg/500 mL dexamethasone, 50 μL/250 mL insulin, 1000 U/250 mL heparin, 2.5 g/250 mL BSA, 50 μL/250 mL hydrocortisone, 5 mM glutathione

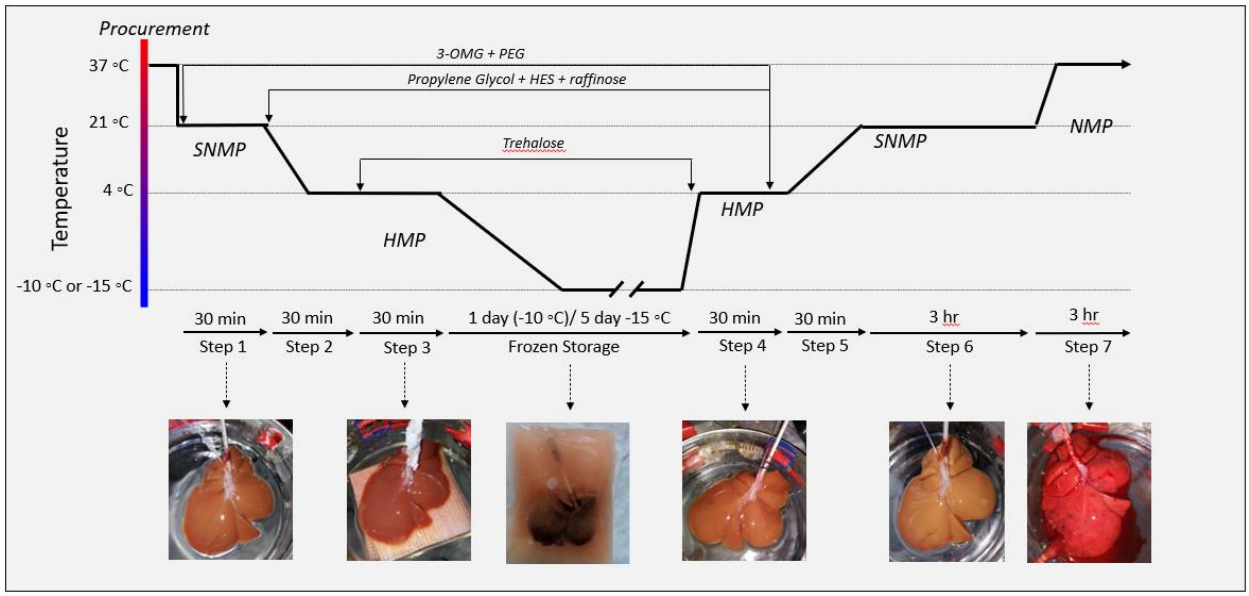

Figure 3.3 Overview of high sub-zero freezing protocol implemented for rat livers.[2] The solutions loaded in the different steps are indicated in Table 3.1.

[2]Figure was provided by Shannon N. Tessier, Casie Pendexter, Stephanie E. J. Cronin, and Reinier J. de Vries. All members are affiliated with Shriners Hospital for Children, Boston, MA, USA and Center for Engineering in Medicine, Harvard Medical School & Massachusetts General Hospital, Boston, MA, USA.

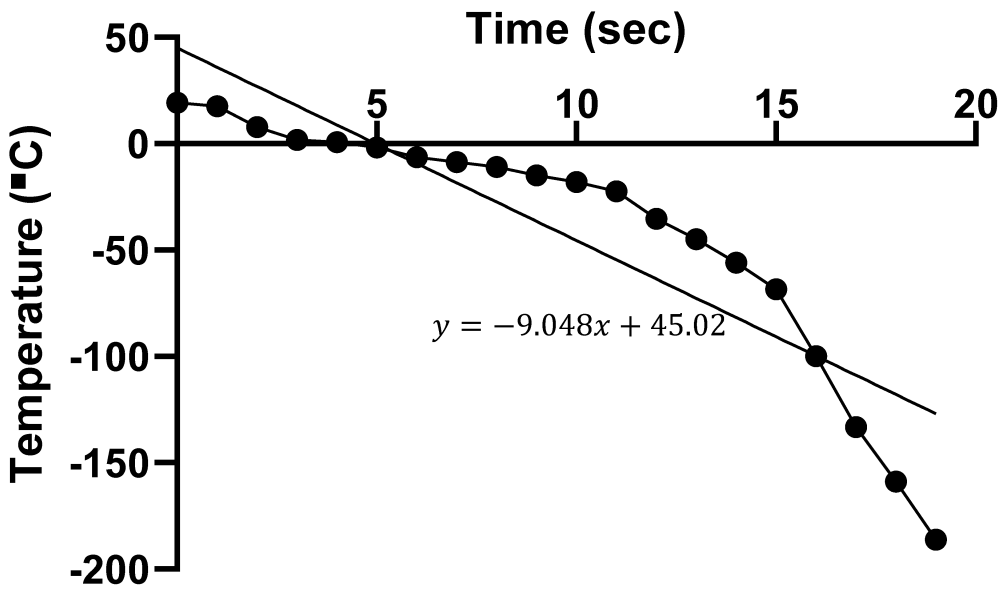

Figure 3.4 Cooling rate for liver tissue experiment 1. Linear regression analysis performed to determine the average slope of the temperature profile, which was used for calculating the cooling rate.

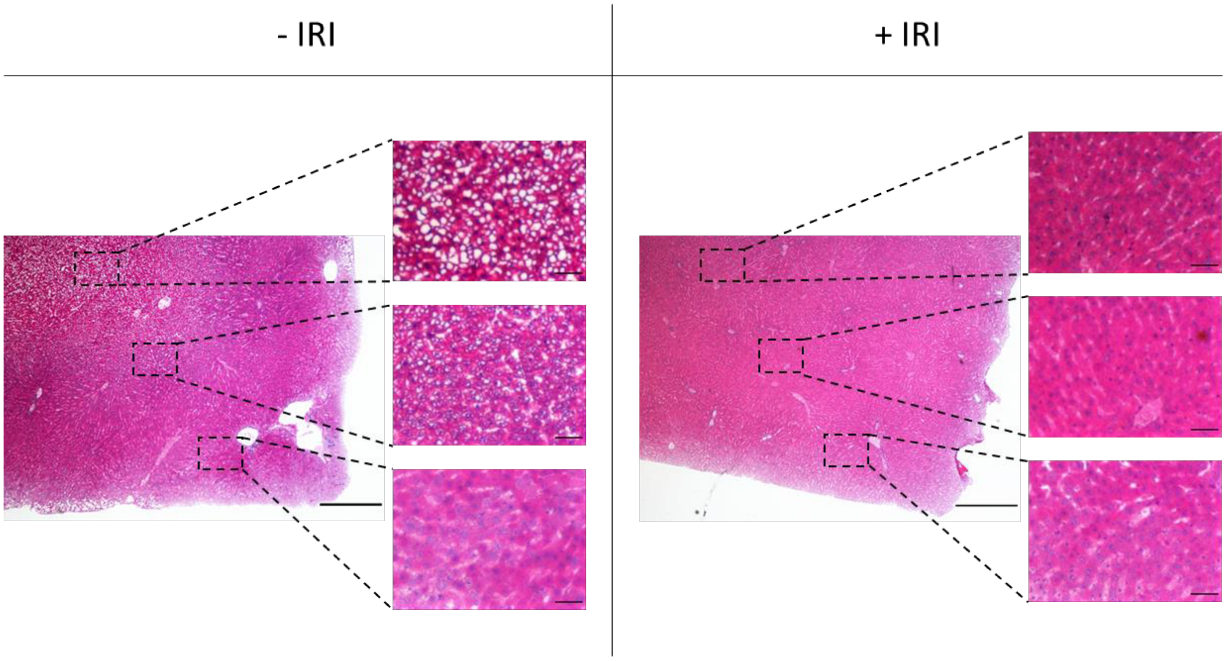

Figure 3.5A Representative images from liver tissue experiment 1. Gradient of recrystallization from the edge to the center of the tissue for IRI-treated and untreated conditions. Scale 25 μm on magnified images.

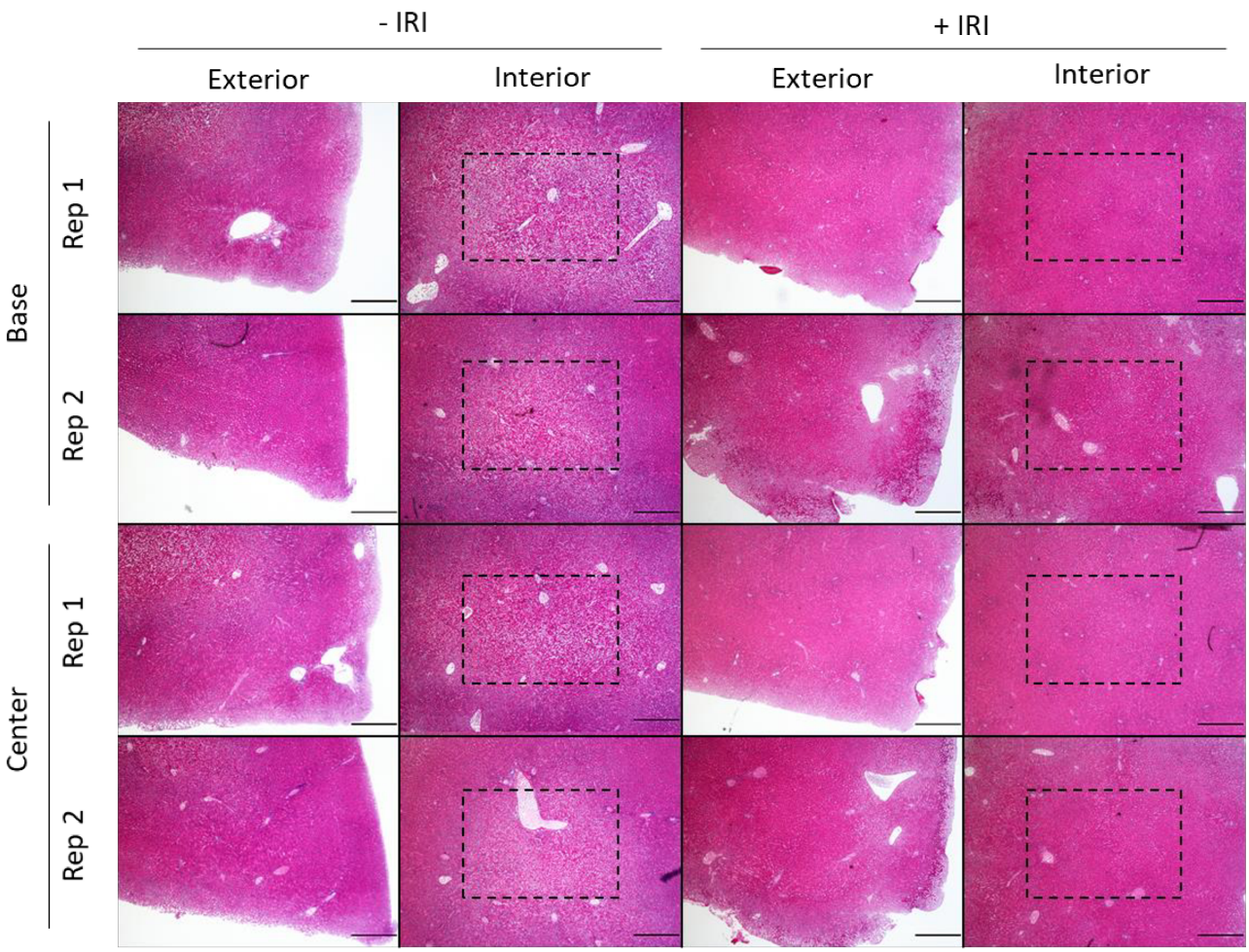

Figure 3.5B Representative images from liver tissue experiment 1. 4X images obtained from the edge and center at two different depths of IRI-treated and untreated liver tissue sections. Dashed boxes indicate regions where 20X images were obtained for thresholding analysis. Scale bar = 500 μm.

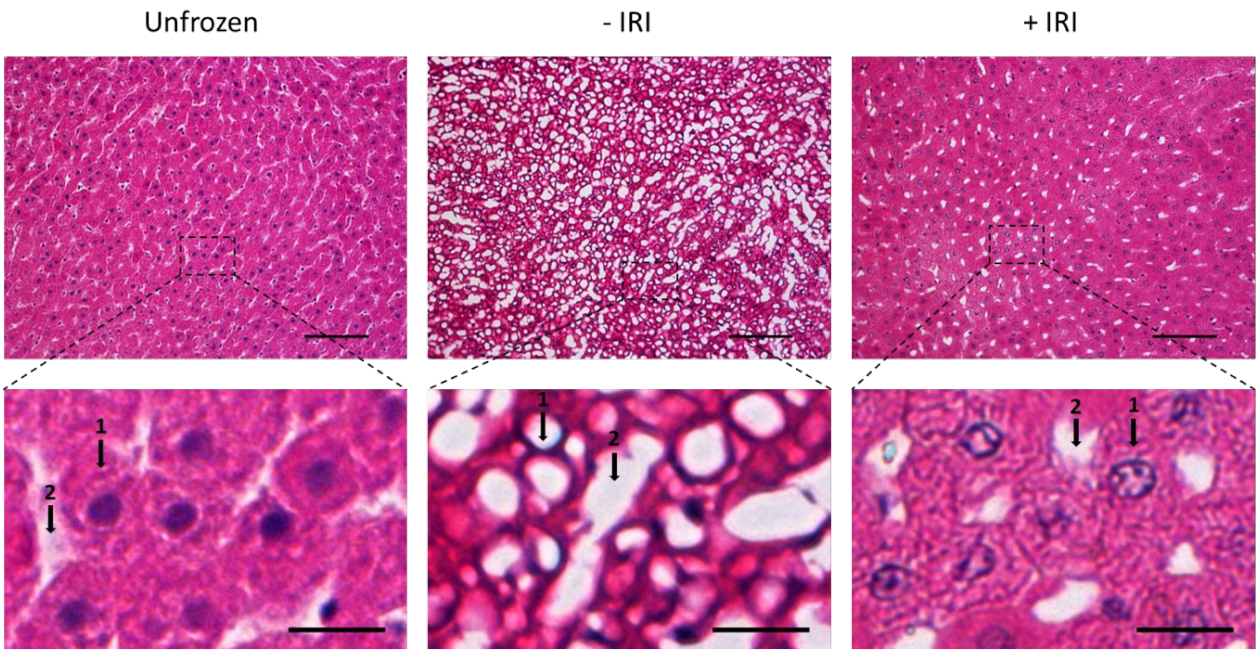

Figure 3.5C Representative images from liver tissue experiment 1: differences in ice crystals between IRI-treated and untreated liver tissue blocks. Arrow 1: Hepatocytes. Arrow 2: Vascular space. Images obtained from the interior regions of sections taken at the base of the blocks. Scale bar = 100 μm on original 20x images. Scale bar = 20 μm on magnified images.

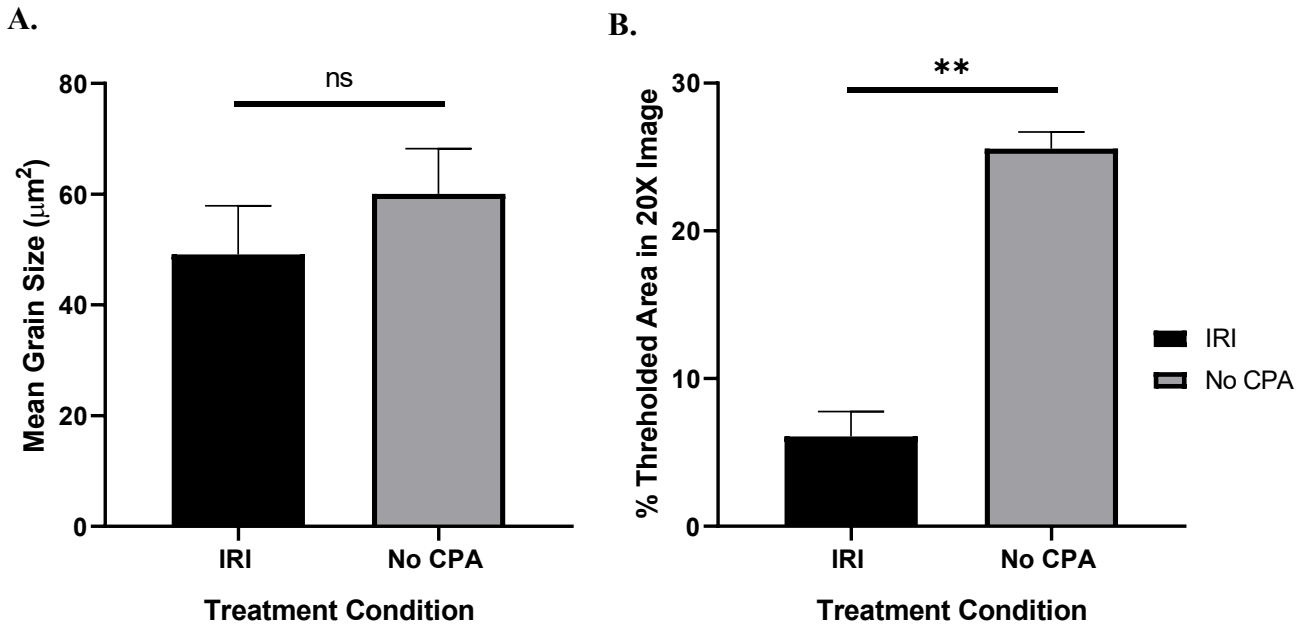

Figure 3.6 Image thresholding for liver tissue experiment 1. Analysis performed on four random 20X images obtained from two independent replicates. (A) Average mean grain size. (B) % of the area thresholded within the entire image (ie. percent of the image that was opaque). Error bars represent the standard error of the mean between replicates. Statistical significance was calculated using a nested one-way ANOVA on log transformed data followed by a Tukey's post hoc test to evaluate differences between treatments. $^{**}p < 0.01$; ns = no significance.

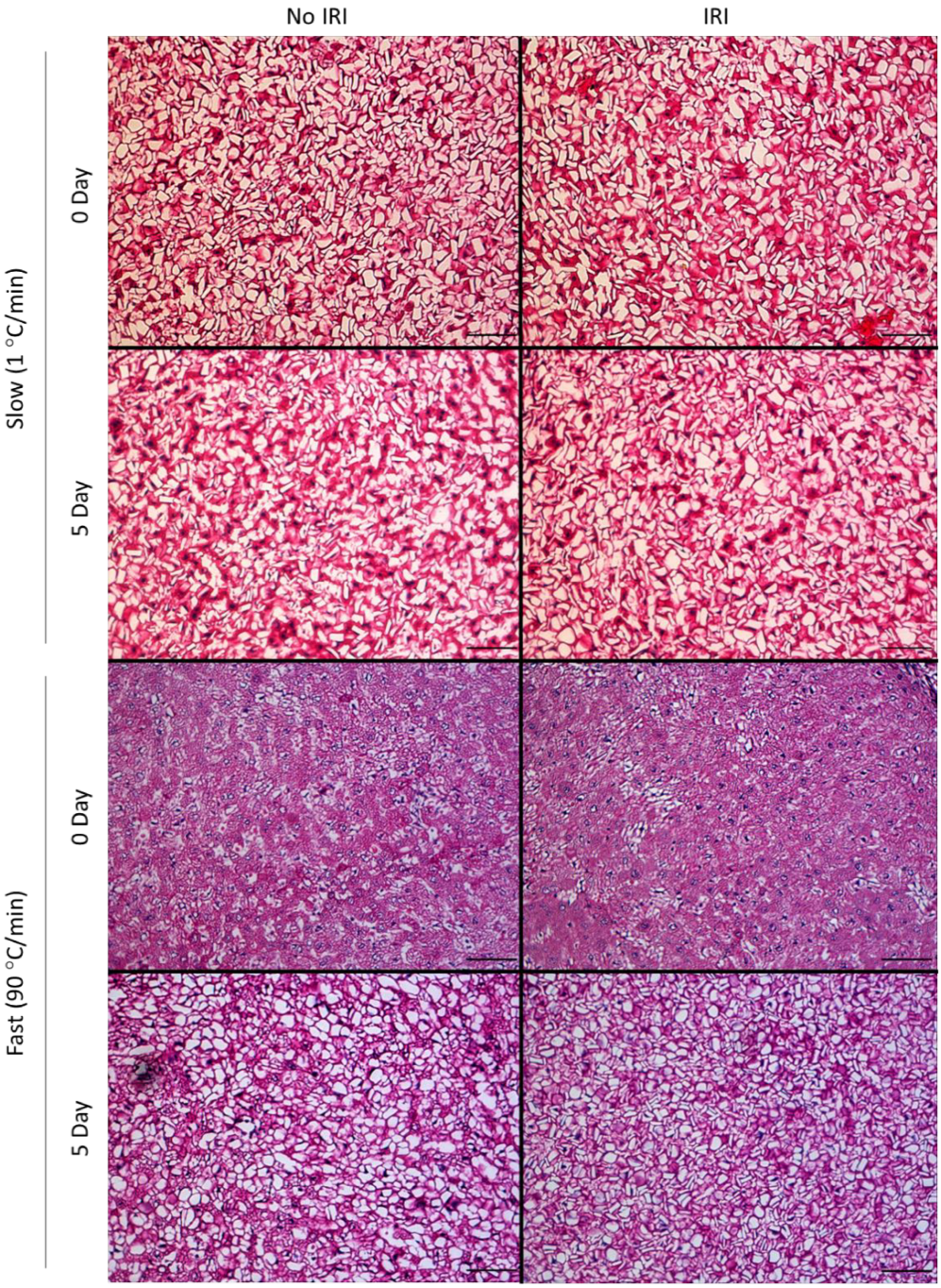

Figure 3.7A Representative images from liver tissue experiment 2. Representative 20X images. Scale bar = 100 μm

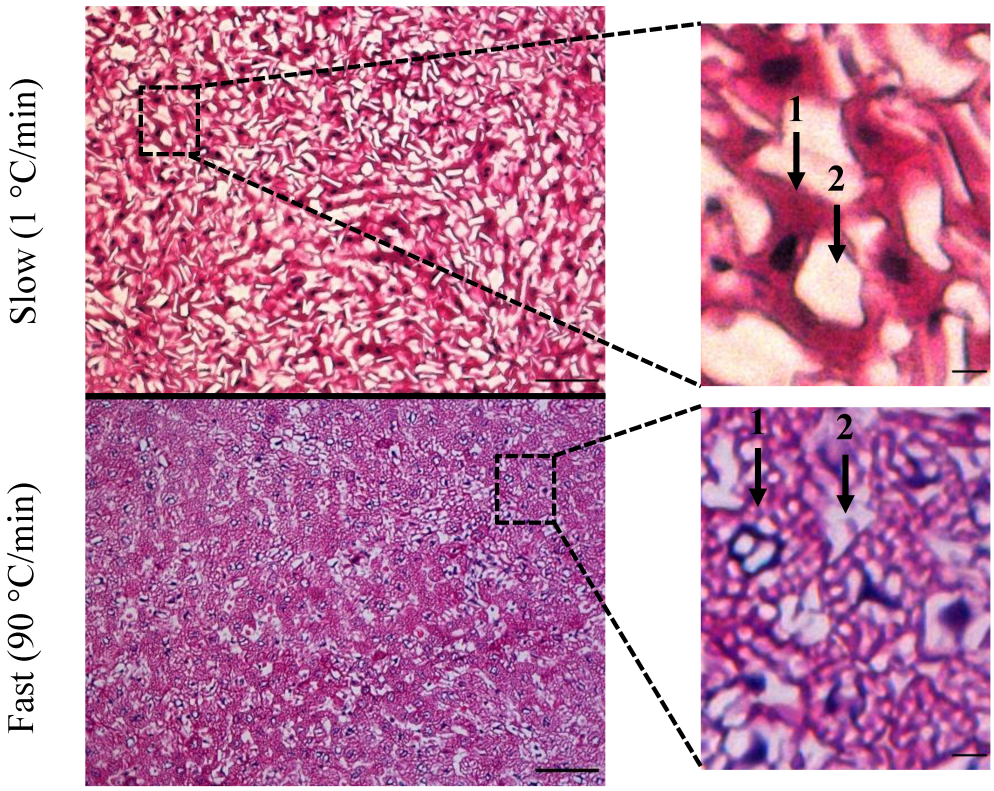

Figure 3.7B Representative images from liver tissue experiment 2: differences in ice crystals between slow and rapid cooled liver tissue sections. Images taken from the 0-day, non-IRI conditions. Arrow 1: Hepatocytes. Arrow 2: Vascular space. Scale bar = 100 μm on original 20x images. Scale bar = 10 μm on magnified images.

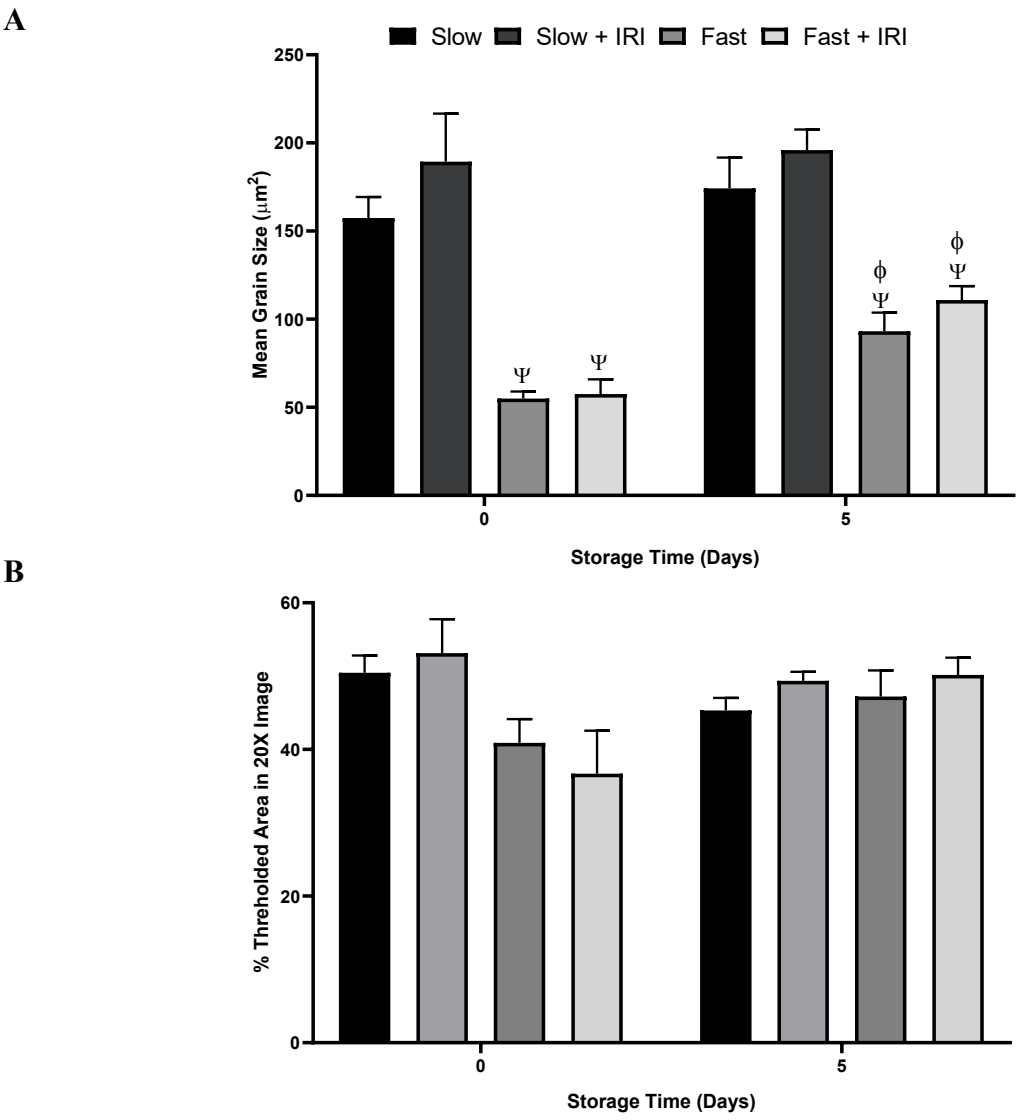

Figure 3.8 Image thresholding for liver tissue experiment 2. Analysis performed on four random 20X images obtained from two independent replicates. (A) Average mean grain size. (B) % of the area thresholded within the entire image (ie. percent of the image that was opaque). "S" represents the slow cooling condition (1 °C/min), while "F" represents the rapid cooling condition (90 °C/min). Error bars represent the standard error of the mean between replicates. Statistical significance was calculated nested one-way ANOVA on log transformed data followed by a Tukey's post hoc test to evaluate differences between treatments, timepoints, and storage times. Ψ - significant difference from slow cooling condition ($p < 0.05$); ϕ - significant difference from 0 d condition ($p < 0.05$).

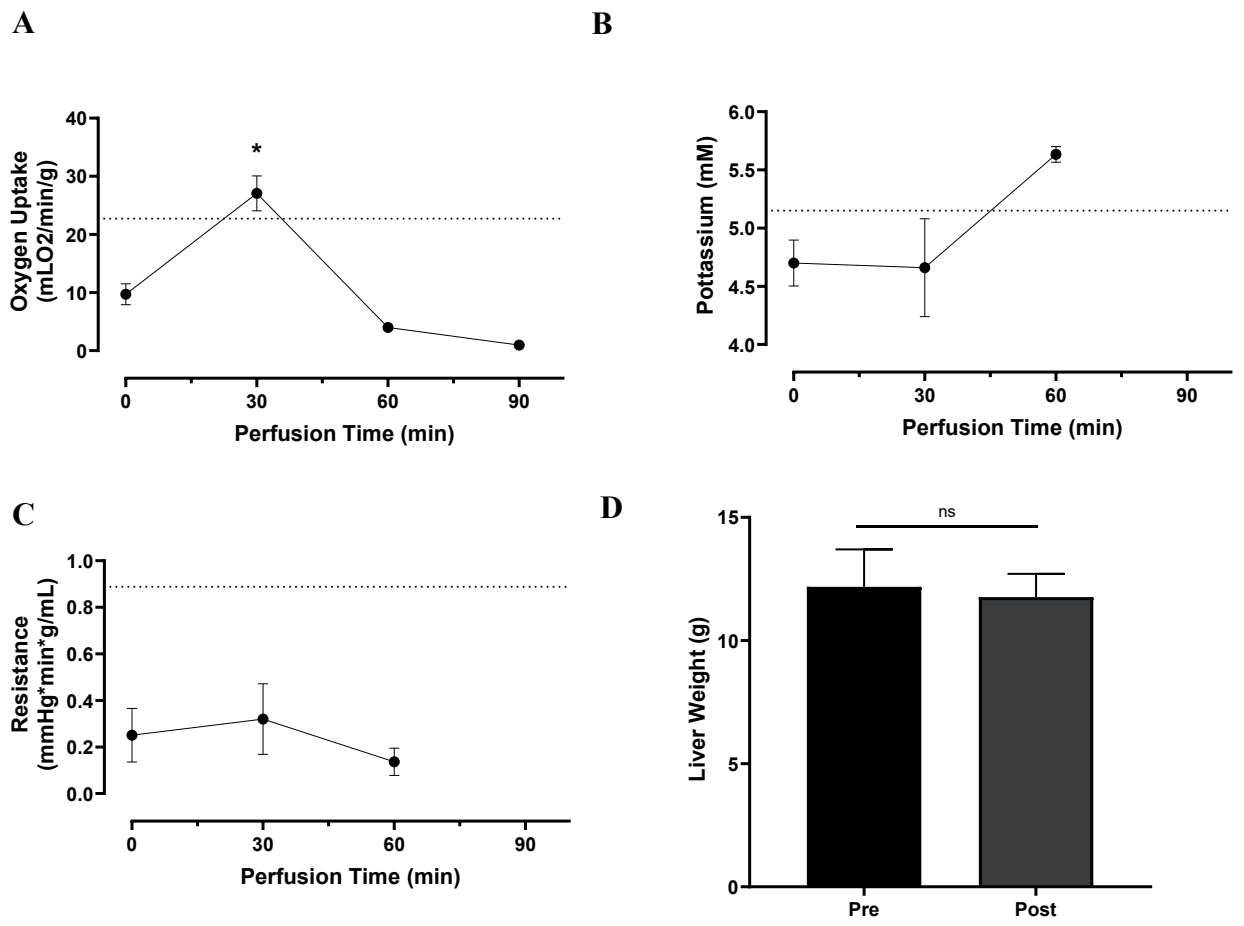

Figure 3.9 Pre-freeze loading with IRI: evaluation of IRI toxicity in whole livers. (A) Oxygen uptake calculated using equation 3.2 (section 3.2.2.4). (B) Potassium concentration in the hepatic vein. (C) Resistance of the portal vein calculated using equation 3.1 (section 3.2.2.4). (D) Liver weight pre- and post- CPA loading. Error bars represent standard error of the mean of four independent replicates. Dashed lines represent reference values following 30 min of SNMP pre-conditioning in the absence of an IRI. 60 min and 90 min HMP values were not available and were therefore not included. The reference values can be found in Table 3.3. Significant differences between the 0 min and 30 min timepoints as well as the pre- and post- perfusion weight were calculated using an unpaired two-tailed Student's *t*-test: $*p < 0.05$, ns = no significance. The 60 min timepoint was not included significance calculations because the change in parameters could be attributed to the transition from SNMP to HMP.

Table 3.2 SNMP pre-conditioning non-IRI reference values.

	0 min	**30 min**
Oxygen Uptake (mLO_2/min/g)	6.24	22.7
Potassium (mM)	5.13	5.15
Resistance (mmHg*min*g/mL)	1.88	0.889

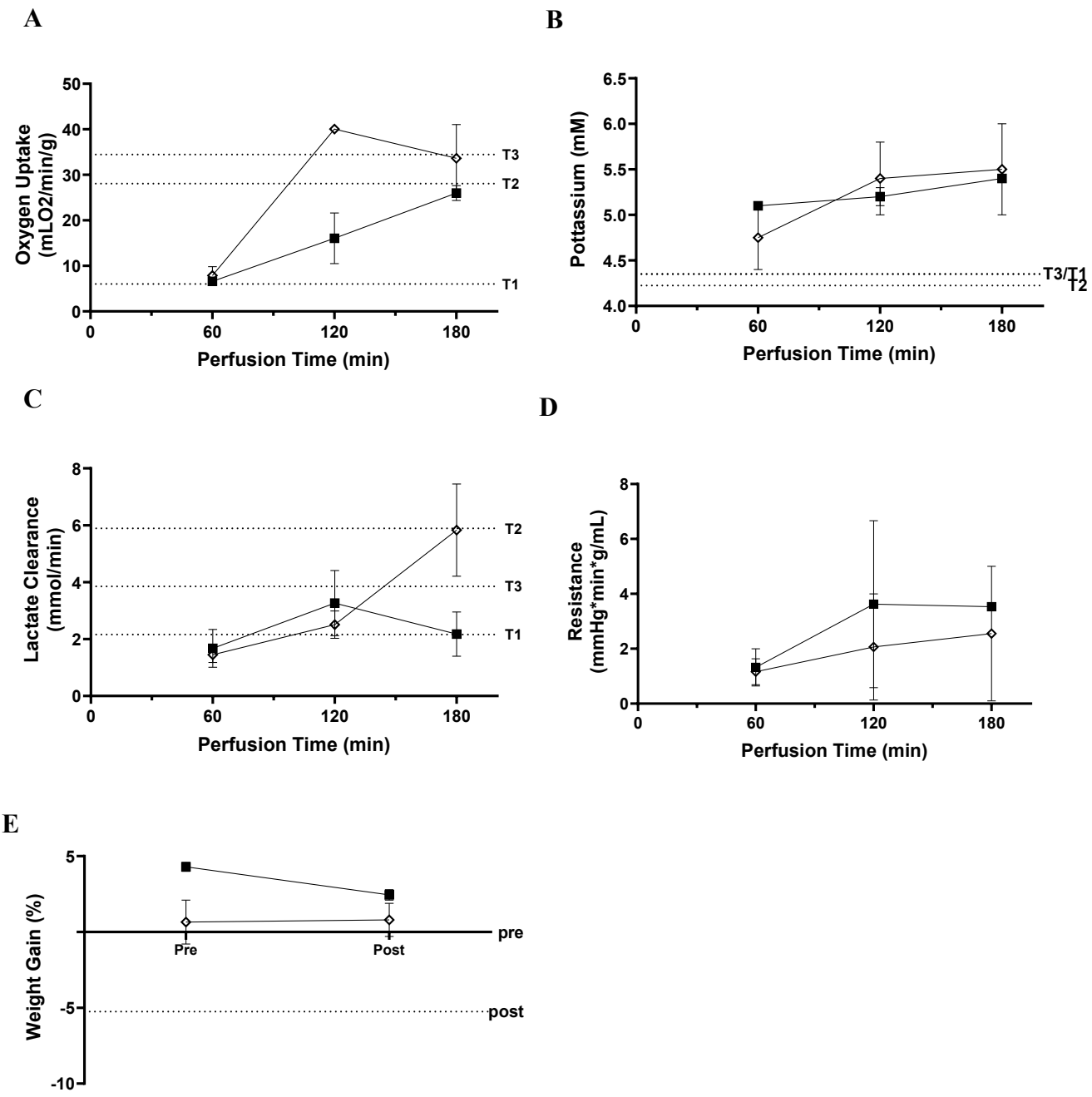

Figure 3.10 Post-thaw functional parameters during normothermic reperfusion. (◇) -10 °C, 1 day (■) -15 °C, 5 day. Figure description on next page.

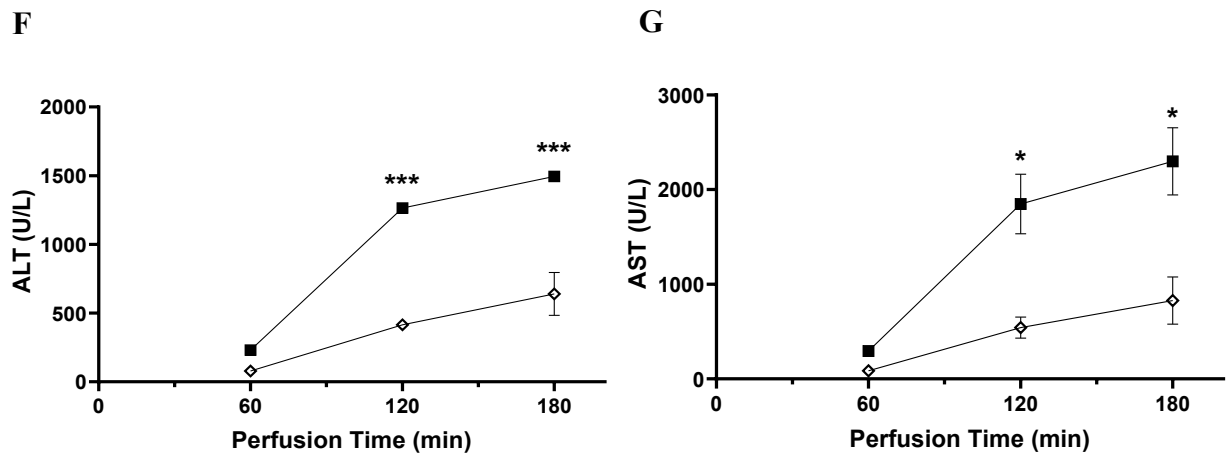

Figure 3.10 Post-thaw functional parameters during normothermic reperfusion. (◇) -10 °C, 1 day (■) -15 °C, 5 day. (A) Oxygen uptake calculated using equation 3.2 (section 3.2.2.4). (B) Potassium concentration in the hepatic vein. (C) Lactate concentration in the hepatic vein. (D) Resistance of the portal vein calculated using equation 3.1 (section 3.2.2.4). (E) Percent of weight gained pre- and post- reperfusion. (F) Aspartate aminotransferase (AST) concentration in the hepatic vein. (G) Alanine aminotransferase (ALT) concentration in the hepatic vein. Error bars represent standard error of the mean of two independent replicates. Dashed lines represent reference values of fresh controls that were not pre-conditioned or stored prior to reperfusion (T1: 60 min, T2: 120 min, T3: 180 min). Reference values can be found in Table 3.3. Reference values for graphs E, F, and G were not visually informative and were therefore not depicted on the graphs. Significant differences between storage conditions at each timepoint were calculated using a repeated measures two-way ANOVA, followed by Sidak's post-hoc test: $^{**}p < 0.01$, $^{***}p < 0.001$.

Table 3.3 Reperfusion reference values for fresh non-preconditioned controls

	T0 (0 min)	T1 (60 min)	T2 (120 min)	T3 (180 min)
Oxygen Uptake (mLO_2/min/g)	NA	6.02	28.07	34.5
Potassium (mM)	NA	4.35	4.225	4.35
Lactate Clearance (mM/min)	NA	2.16	5.89	3.85
Resistance (mmHg*min*g/mL)	NA	0.0438	0.041	0.0162
Weight Gain (%)	0	NA	NA	-5.25
ALT (U/L)	NA	39.25	60	92
AST (U/L)	NA	44.5	70.5	132.3

3.6 References

[1] H. Bank, Freezing injury in tissue cultured cells as visualized by freeze-etching. Exp Cell Res 85 (1974) 367-76.

[2] H. Bank, Visualization of freezing damage. II. Structural alterations during warming. Cryobiology 10 (1973) 157-70.

[3] J.G. Baust, and J.S. Edwards, Mechanisms of freezing tolerance in an Antarctic midge, Belgica antarctica. Physiol Entomol 4 (1979) 1-5.

[4] J. Bischof, C.J. Hunt, B. Rubinsky, A. Burgess, and D.E. Pegg, Effects of cooling rate and glycerol concentration on the structure of the frozen kidney: assessment by cryo-scanning electron microscopy. Cryobiology 27 (1990) 301-10.

[5] J.C. Bischof, and B. Rubinsky, Large ice crystals in the nucleus of rapidly frozen liver cells. Cryobiology 30 (1993) 597-603.

[6] B.G. Bruinsma, T.A. Berendsen, M.L. Izamis, H. Yeh, M.L. Yarmush, and K. Uygun, Supercooling preservation and transplantation of the rat liver. Nat Protoc 10 (2015) 484-94.

[7] C.H. Cho, J. Park, D. Nagrath, A.W. Tilles, F. Berthiaume, M. Toner, and M.L. Yarmush, Oxygen uptake rates and liver-specific functions of hepatocyte and 3T3 fibroblast co-cultures. Biotech Bioeng 97 (2007) 188-199.

[8] J.P. Costanzo, and R.E. Lee, Jr., Avoidance and tolerance of freezing in ectothermic vertebrates. J Exp Biol 216 (2013) 1961-7.

[9] R.J. de Vries, C.A. Pendexter, S.E.J. Cronin, B. Marques, E.O.A. Hafiz, A. Muzikansky, T.M. van Gulik, J.F. Markmann, S.L. Stott, H. Yeh, M. Toner, K. Uygun, and S.N. Tessier, Cell release during perfusion reflects cold ischemic injury in rat livers. Sci Rep 10 (2020) 1102.

[10] R.J. de Vries, S.N. Tessier, P.D. Banik, S. Nagpal, S.E. Cronin, S. Ozer, E.O. Hafiz, T.M. van Gulik, M.L. Yarmush, and J.F. Markmann, Supercooling extends preservation time of human livers. Nat Biotechnol 37 (2019) 1131-1136.

[11] D. Donhowe, R. Hartel, and R. Bradley, Ice crystallization processes during manufacture and storage of ice cream. J Dairy Sci 74 (1991) 3334-3344.

[12] D.P. Donhowe, and R.W. Hartel, Recrystallization of ice during bulk storage of ice cream. Int Dairy J 6 (1996) 1209-1221.

[13] D.P. Donhowe, and R.W. Hartel, Recrystallization of ice in ice cream during controlled accelerated storage. Int Dairy J 6 (1996) 1191-1208.

[14] J.G. Duman, Factors involved in overwintering survival of the freeze tolerant beetle, Dendroides canadensis. J Comp Phys 136 (1980) 52-59.

[15] J.G. Duman, Insect antifreezes and ice-nucleating agents. Cryobiology 19 (1982) 613-627.

[16] P. Echlin, Freeze Substitution and Low-Temperature Embedding. in: P. Echlin, (Ed.), Low-Temperature Microscopy and Analysis, Springer US, Boston, MA, 1992, pp. 223-264.

[17] G. Fahy, and A. Karow Jr, Ultrastructure-function correlative studies for cardiac cryopreservation. V. Absence of a correlation between electrolyte toxicity and cryoinjury in the slowly frozen, cryoprotected rat heart. Cryobiology 14 (1977) 418-427.

[18] A.H. Fischer, K.A. Jacobson, J. Rose, and R. Zeller, Hematoxylin and eosin staining of tissue and cell sections. CSH Protocols 2008 (2008) pdb. prot4986.

[19] A.H. Fischer, K.A. Jacobson, J. Rose, and R. Zeller, Paraffin embedding tissue samples for sectioning. CSH Protocols 2008 (2008) pdb. prot4989.

[20] F. Guttman, A. Khalessi, B. Huxley, R. Lee, and G. Savard, Whole organ preservation: I. A technique for in vivo freezing canine intestine using intraarterial helium and ambient nitrogen. Cryobiology 6 (1969) 32-36.

[21] F. Guttman, N. Segal, and J. Borzone, Cryopreservation of canine kidneys with dimethyl sulphoxide: further studies, Organ Preservation II, Churchill Livingstone Edinburgh, 1979, pp. 185.

[22] F.M. Guttman, J. Lizin, P. Robitaille, H. Blanchard, and C. Turgeon-Knaack, Survival of canine kidneys after treatment with dimethyl-sulfoxide, freezing at− 80° C, and thawing by microwave illumination. Cryobiology 14 (1977) 559-567.

[23] T. Hansen, Glycerol content and cold-hardiness in freeze tolerant insects. Eesti. NSV. Tead. Akad. Tiom. Biol 29 (1980) 113-118.

[24] P.V. Hobbs, Ice physics, Oxford university press, 2010.

[25] R.C. Huebert, and V.H. Shah, Hepatic Sinusoidal Endothelial Cells. in: J.-F. Dufour, and P.-A. Clavien, (Eds.), Signaling Pathways in Liver Diseases, Springer Berlin Heidelberg, Berlin, Heidelberg, 2010, pp. 79-91.

[26] C. Hunt, Studies on cellular structure and ice location in frozen organs and tissues: the use of freeze-substitution and related techniques. Cryobiology 21 (1984) 385-402.

[27] H. Ishiguro, and B. Rubinsky, Mechanical interactions between ice crystals and red blood cells during directional solidification. Cryobiology 31 (1994) 483-500.

[28] N. Ishine, B. Rubinsky, and C.Y. Lee, A histological analysis of liver injury in freezing storage. Cryobiology 39 (1999) 271-7.

[29] N. Ishine, B. Rubinsky, and C.Y. Lee, Transplantation of mammalian livers following freezing: vascular damage and functional recovery. Cryobiology 40 (2000) 84-9.

[30] I.A. Jacobsen, and D.E. Pegg, Cryopreservation of organs: a review. Cryobiology 21 (1984) 377-84.

[31] I.A. Jacobsen, D.E. Pegg, H. Starklint, J. Chemnitz, C. Hunt, P. Barfort, and M.P. Diaper, Effect of cooling and warming rate on glycerolized rabbit kidneys. Cryobiology 21 (1984) 637-653.

[32] J.O.M. Karlsson, and M. Toner, Long-term storage of tissues by cryopreservation: Critical issues. Biomaterials 17 (1996) 243-256.

[33] C.A. Knight, and J.G. Duman, Inhibition of recrystallization of ice by insect thermal hysteresis proteins: a possible cryoprotective role. Cryobiology 23 (1986) 256-262.

[34] C.A. Knight, J. Hallett, and A. DeVries, Solute effects on ice recrystallization: an assessment technique. Cryobiology 25 (1988) 55-60.

[35] C.A. Knight, D. Wen, and R.A. Laursen, Nonequilibrium antifreeze peptides and the recrystallization of ice. Cryobiology 32 (1995) 23-34.

[36] S. Kubota, F. Graham, B.G. Crabo, R.C. Lillehei, and R.H. Dietman, The effect of freeze rate, duration of phase transition, and warming rate on survival of frozen canine kidneys. Cryobiology 13 (1976) 455-62.

[37] L. Lautner, N. William, and J.P. Acker, High subzero cryofixation: A technique for observing ice within tissues. Cryobiology 95 (2020) 116-122.

[38] X. Liu, G. Zhao, Z. Shu, D. Niu, Z. Zhang, P. Zhou, Y. Cao, and D. Gao, Quantification of intracellular ice formation and recrystallization during freeze–thaw cycles and their relationship with the viability of pig iliac endothelium cells. Biopres Biobank 14 (2016) 511-519.

[39] J.E. Lovelock, Het mechanism of the protective action of glycerol against haemolysis by freezing and thawing. Bioch Biophys Acta 11 (1953) 28-36.

[40] A. MacKenzie, Death of frozen yeast in the course of slow warming, Ciba Foundation Symposium-The Frozen Cell, Wiley Online Library, 1970, pp. 89-96.

[41] M.N. Martino, and N.E. Zaritzky, Ice recrystallization in a model system and in frozen muscle tissue. Cryobiology 26 (1989) 138-48.

[42] P. Mazur, 2. Roles of intracellular ice formation, vitrification of cell water, and recrystallization of intracellular ice on the survival of mouse embryos and oocytes. Cryobiology 65 (2012) 339.

[43] P. Mazur, Freezing of living cells: mechanisms and implications. Am J Physiol 247 (1984) C125-42.

[44] P. Mazur, The role of intracellular freezing in the death of cells cooled at supraoptimal rates. Cryobiology 14 (1977) 251-272.

[45] P. Mazur, and R.H. Miller, Survival of frozen-thawed human red cells as a function of the permeation of glycerol and sucrose. Cryobiology 13 (1976) 523-536.

[46] H.T. Meryman, Freezing injury and its prevention in living cells. Ann Rev Biophys Bioeng 3 (1974) 341-363.

[47] H.T. Meryman, Osmotic stress as a mechanism of freezing injury. Cryobiology 8 (1971) 489-500.

[48] L. Miller, and J. Smith, Production of threitol and sorbitol by an adult insect: association with freezing tolerance. Nature 258 (1975) 519-520.

[49] R.H. Miller, and P. Mazur, Survival of frozen-thawed human red cells as a function of cooling and warming velocities. Cryobiology 13 (1976) 404-414.

[50] N. Nikon, Elements Advanced Research, 2014. User's Guide-ver 4.

[51] D.E. Pegg, Ice crystals in tissues and organs, The biophysics of organ cryopreservation, Springer, 1987, pp. 117-140.

[52] D.E. Pegg, The relevance of ice crystal formation for the cryopreservation of tissues and organs. Cryobiology (2010).

[53] D.E. Pegg, M.P. Diaper, H.L. Skaer, and C.J. Hunt, The effect of cooling rate and warming rate on the packing effect in human erythrocytes frozen and thawed in the presence of 2 M glycerol. Cryobiology 21 (1984) 491-502.

[54] D.E. Pegg, I.A. Jacobsen, M.P. Diaper, and J. Foreman, The effect of cooling and warming rate on cortical cell function of glycerolized rabbit kidneys. Cryobiology 21 (1984) 529-35.

[55] J.S. Poisson, J.P. Acker, J.G. Briard, J.E. Meyer, and R.N. Ben, Modulating Intracellular Ice Growth with Cell-Permeating Small-Molecule Ice Recrystallization Inhibitors. Langmuir 35 (2018) 7452-7458.

[56] G.A. Pollock, D.E. Pegg, and I.R. Hardie, An isolated perfused rat mesentery model for direct observation of the vasculature during cryopreservation. Cryobiology 23 (1986) 500-511.

[57] P.J. Quinn, A lipid-phase separation model of low-temperature damage to biological membranes. Cryobiology (1985).

[58] B. Rubinsky, A. Arav, and G.L. Fletcher, Hypothermic protection - A fundamental property of "Antifreeze" proteins. Biochem Biophys Res Comm 180 (1991) 566-571.

[59] B. Rubinsky, A. Arav, J.S. Hong, and C.Y. Lee, Freezing of mammalian livers with glycerol and antifreeze proteins. Biochem Biophys Res Comm 200 (1994) 732-741.

[60] B. Rubinsky, A. Arav, M. Mattioli, and A.L. Devries, The effect of antifreeze glycopeptides on membrane potential changes at hypothermic temperatures. Biochem Biophys Res Comm 173 (1990) 1369-1374.

[61] B. Rubinsky, C.Y. Lee, J. Bastacky, and G. Onik, The process of freezing and the mechanism of damage during hepatic cryosurgery. Cryobiology 27 (1990) 85-97.

[62] B. Rubinsky, M. Mattioli, A. Arav, B. Barboni, and G.L. Fletcher, Inhibition of Ca2+ and K+ currents by "antifreeze" proteins. Am J Physiol 262 (1992) R542-5.

[63] W.D. Schmid, Survival of frogs in low temperature. Science 215 (1982) 697-8.

[64] R. Steinbrecht, Recrystallization and ice-crystal growth in a biological specimen, as shown by a simple freeze substitution method. J Microsc 140 (1985) 41-46.

[65] J.M. Storey, and K.B. Storey, Triggering of cryoprotectant synthesis by the initiation of ice nucleation in the freeze tolerant frog, Rana sylvatica. J Comp Phys B 156 (1985) 191-195.

[66] K.B. Storey, Freeze tolerance in the frog,Rana sylvatica. Experientia 40 (1984) 1261-1262.

[67] K.B. Storey, and J.M. Storey, Freeze tolerance in animals. Physiol Rev 68 (1988) 27-84.

[68] K.B. Storey, and J.M. Storey, Freeze tolerant frogs: cryoprotectants and tissue metabolism during freeze–thaw cycles. Can J Zool 64 (1986) 49-56.

[69] M. Taylor, and D. Pegg, The effect of ice formation on the function of smooth muscle tissue following storage at− 21 C and− 60 C. Cryobiology 20 (1982) 36-40.

[70] M.J. Taylor, B.P. Weegman, S.C. Baicu, and S.E. Giwa, New Approaches to Cryopreservation of Cells, Tissues, and Organs. Transfusion medicine and hemotherapy : offizielles Organ der Deutschen Gesellschaft fur Transfusionsmedizin und Immunhamatologie 46 (2019) 197-215.

[71] S.N. Tessier, S.E.J. Cronin, C.A. Pendexter, S. Özer, R.J. de Vries, S. Nagpal, P.D. Banik, K. Uygun, and M. Toner, Partial freezing: A nature-inspired strategy for organ banking. Cryobiology 81 (2018) 220.

[72] S.N. Tessier, L. Weng, W.D. Moyo, S.H. Au, K.H.K. Wong, C. Angpraseuth, A.E. Stoddard, C. Lu, L.T. Nieman, R.D. Sandlin, K. Uygun, S.L. Stott, and M. Toner, Effect of Ice Nucleation and Cryoprotectants during High Subzero-Preservation in Endothelialized Microchannels. ACS Biomater Sci Eng 4 (2018) 3006-3015.

[73] R.M.F. Tomas, T.L. Bailey, M. Hasan, and M.I. Gibson, Extracellular Antifreeze Protein Significantly Enhances the Cryopreservation of Cell Monolayers. Biomacromolecules 20 (2019) 3864-3872.

[74] C.J. Watson, V. Kosmoliaptsis, C. Pley, L. Randle, C. Fear, K. Crick, A.E. Gimson, M. Allison, S. Upponi, and R. Brais, Observations on the ex situ perfusion of livers for transplantation. Am J Transplant 18 (2018) 2005-2020.

[75] A.M. Zade-Oppen, Posthypertonic hemolysis in a sucrose system. Experientia 26 (1970) 1087-8.

[76] A.M.M. Zade-Oppen, Posthypertonic Hemolysis in Sodium Chloride Systems. Acta Physiologica Scandinavica 73 (1968) 341-364.

Chapter 4 General Discussion and Concluding Remarks

4.1 Overview – The Use of Small Molecule IRIs to Tackle Recrystallization Injury in Complex Tissues

Historical attempts to freeze complex tissues and whole organs failed to effectively optimize freezing parameters, storage conditions, CPA cocktails, and perfusion protocols [2; 20; 25; 26; 27; 40; 60; 62; 64; 80]. This is not surprising given the complexity of such an endeavor; however, as a result, post-thaw functional outcomes were often subpar. This spurred the notion that ice formation is lethal in tissues, prompting ice-free approaches to high and low sub-zero organ preservation to gain precedence [18; 22; 68; 90]. However, methods to avoid ice formation come with their own respective challenges and the ability of several phylogenetic groups to tolerate ice formation is evidence that ice is not inherently lethal [1; 6; 9; 28; 61; 70; 75; 76; 77; 78]. The Organ Preservation Alliance which was established in 2015 highlighted the localization, volume, stability, and recrystallization of ice, as prime determinants for ice-induced damage in complex tissues [24; 42]. The development of technologies to abrogate recrystallization injury has received considerable attention the past few decades [3; 11; 12; 14; 17; 29; 37; 39; 66; 67; 79].

Historically, inhibition of recrystallization was pursued using AF(G)P's; however, at high concentrations and low sub-zero temperatures, AF(G)Ps can promote the formation of spicular ice crystals [15; 30; 86]. This has proven to exacerbate mechanical damage to cell membranes and, in some cases, promote IIF [41]. Challenges associated with the large-scale isolation and synthesis of AF(G)Ps, further hamper the artificial implementation of these compounds in commercial cryopreservation applications [33]. Small molecule ice recrystallization inhibitors (IRIs), on the other hand, are amenable to large-scale synthesis [3; 33]. While this can additionally be stated for recently developed synthetic IRI-active polymers, small molecule IRIs lack dynamic ice shaping (DIS) characteristics that facilitate the previously stated modulation of ice crystal morphology [12; 79]. Furthermore, their small size can enhance permeation kinetics throughout large tissue systems as well as enable membrane permeation and control of intracellular ice recrystallization [66].

The need to control recrystallization injury in tissues, combined with the ideal characteristics of these small molecule IRIs, formed the basis for the work conducted throughout this thesis. Livers are currently the only organ where a nature-inspired freeze tolerance approach to sub-zero preservation has been implemented; therefore, this was an ideal model system for investigation of IRI efficacy [31; 32; 71; 82]. In Chapter 2, we evaluated the ability of three different IRIs to

permeate the HepG2 cells and subsequently control rates of intracellular ice recrystallization. This was assessed in the presence of several different commonly used permeating CPAs (DMSO, glycerol, propylene glycol, and ethylene glycol) as well as in the presence of trehalose, a commonly used non-permeating CPA. Hepatocytes comprise 80% of the cellular mass of the liver and the incidence of IIF tends to be higher in dense tissues, making these evaluations pertinent. Our findings indicated that two of the three tested compounds were effective at minimizing recrystallization in the absence of any other cryoprotective agents under conditions where they did not elicit toxic effects. However, the activity of each of the compounds was modulated substantially in the presence of both permeating and non-permeating CPAs. Generally, there was a loss of IRI activity in the presence of permeating CPAs. Whereas, in the presence of trehalose, some compounds saw an improvement in activity, while others demonstrated diminished activity. In chapter 3, we tested a single compound and found it to be capable of permeating liver tissues and controlling both intra- and extracellular recrystallization. While the IRI additionally did not prove to be toxic in liver tissues, it did not render any functional benefits when implemented in a high sub-zero freezing approach to liver preservation. This, in combination with the alteration of IRI activity in the presence of CPA, will form the basis for much of the discussion in this chapter.

4.2 Developing an Improved Screening Procedure for New IRIs

The IRIs used in this study have demonstrated activity in splat cooling assays, which is measured as the ratio of mean grain size (MGS) in the IRI solution to MGS in a solution of phosphate buffered saline (PBS) [3]. IRI activity is subject to change upon alteration of solution characteristics as well as ice nucleation and growth conditions; however, evaluations on this front have been limited. As a result, this has diminished our ability to fully interpret several of the results presented in this thesis. It is unclear whether the loss of intracellular IRI activity in the presence of permeating CPAs presented in Chapter 2 is specific to the intracellular environment due to differences in water content and inorganic ion composition or whether it is the result of limited IRI activity in the solutions and freezing conditions implemented [8; 44]. Furthermore, while the lack of IRI-mediated improvement of functional outcomes in rat livers presented in Chapter 3 was likely multifaceted, it is again possible that IRI activity was simply diminished in the solutions that were used.

These evaluations should be performed retroactively for IRIs currently in use; however, they should become part of a refined screening process during the IRI development stage. Ideally this would involve evaluating IRI activity as a function of IRI concentration, CPA-type, CPA concentration, and thermodynamic stability of the ice formed. While IRI activity is currently evaluated as a function of IRI concentration, the latter three parameters are not regularly assessed. Altering the thermodynamic stability of ice would involve modification of currently conducted splat cooling assays for IRI activity assessment, which involve nucleation of ice at -80 °C and evaluation of IRI-mediated control of isothermal recrystallization at -6.4 °C [3]. This is far removed from the nucleation and growth conditions that would occur in real world cryopreservation applications. These current screening methods could lead to an IRI that demonstrates exceptional activity in splat cooling assays being investigated further and implemented in biological systems when its activity may be limited in the presence of CPAs. However, a compound that demonstrates limited activity in a splat cooling assay but retains activity in either the presence of CPAs or under conditions where ice is increasingly stable, would be sidelined.

These types of evaluations can inform whether the implementation of an IRI is appropriate in a given biological system, making downstream assessments significantly more informative. For example, if the activity of an IRI is limited in glycerol but active in DMSO, it should not be used in red blood cell (RBC) cryopreservation applications, where glycerol is the optimal CPA. Considering the toxicological effects of any given IRI will differ between cell types, evaluating toxicity in RBCs would not be highly informative in this case. The same notion can undoubtedly be applied to permeation assessments. Permeation should be assessed in conjunction with toxicity if the goal is to minimize intracellular ice formation or cryopreserve tissues. The method described in this thesis of visualizing control of ice recrystallization as an indicator of permeation into cells or tissues requires confidence that the compound would function in the solutions and ice nucleation and growth conditions evaluated. Otherwise an absence of detectable IRI activity is not necessarily indicative of a lack of permeation. With an improved understanding of IRI activity parameters, this method would be valuable under the presumption that the intracellular milieu or the material properties of tissues alter IRI activity. However, more direct assessments of permeation, such as Raman spectroscopy, NMR, or HPLC, are warranted [62; 65; 85; 89].

Ongoing efforts to identify or isolate IRI active compounds use similar screening procedures to those used in the development of small molecule IRIs [38; 84]. This discussion has been targeted at small molecule IRIs due to evidence suggesting that the activity of some of these compounds can be diminished in the presence of CPAs (Robert N. Ben, personal communication, July 23, 2019). However, perhaps the standard method used among cryobiologists for assessing whether different compounds have IRI activity should be revisited. From a funding perspective, there is significantly more interest in seeing positive outcomes arising from the biological application of small molecule IRIs; therefore, the parameters under which IRI activity is assessed may need to be prioritized for efficiency's sake. Considering the widespread use of CPAs in modern cryobiology, evaluation of IRI activity in the presence of commonly used permeating and non-permeating CPAs should be performed at the very least.

4.3 The Effects Permeating and Non-Permeating CPAs on Recrystallization Injury and the Role of IRIs

There is value in considering how the combined use of CPAs and IRIs can impact recrystallization injury from a theoretical and mechanistic perspective rather than simply considering how CPAs can modulate the activity of IRIs. If recrystallization injury is thought to be mechanical (ie. mechanical damage to cell membranes or extracellular interactions), then it is possible that while commonly used CPAs may not directly elicit RI activity, an increase in the unfrozen fraction at any given temperature may diminish recrystallization injury [53; 55; 56]. This can consider in the context of both extracellular and intracellular recrystallization injury, with the latter specific to permeating CPAs. Furthermore, the presence of CPAs at the grain boundary can limit rates of recrystallization, despite these compounds lacking explicit IRI activity [38]. While the presence of any impurities at the grain boundary would limit recrystallization, the hydration of several commonly used CPAs further impedes molecular mobility at this interface [16; 36; 46; 47; 79]. Due to these processes, reducing the concentration of CPAs may abrogate recrystallization injury; however, this can be countered by supplementing an IRI to the preservation medium. This should be approached with caution as there are several unrelated mechanisms through which permeating and non-permeating CPAs render protection; therefore, there may need to be modifications to the freezing protocol to account for reduced CPA concentration. The use of certain small molecule IRIs has enabled a reduction in the concentration of glycerol required for the cryopreservation of red blood cells under freezing conditions where the incidence of IIF was likely minimal [10; 13].

Several commercial cryopreservation applications would benefit from reduced concentrations of permeating CPAs due to their osmotic and biochemical toxicity [21]. DMSO, the most widely used permeating CPA, has proven to alter the epigenetic landscape, potentially confounding research and corresponding patient outcomes [83]. In the context of organ cryopreservation, a reduction in the overall concentration of CPAs may minimize the potential for endothelial damage during the initial perfusion and unloading phase.

Permeating CPAs would likely impact rates of intracellular ice recrystallization; however, there have been no studies evaluating the impact of non-permeating CPAs in this regard. This thesis demonstrated a reduction in the rate of intracellular recrystallization as the concentration of impermeant solute is increased, suggesting a correlation between the osmotically active volume of water frozen inside the cell and the rate of intracellular recrystallization. While the water content of the cell was not measured, decreasing the total number of ice crystals inside the cell would certainly decrease the overall magnitude of recrystallization and one can envision how this could in turn decrease the rate of recrystallization. However, it is unclear how reducing intracellular recrystallization rates through dehydration would correspond to improved viability outcomes. It is possible that distortion of the plasma membrane and increased proximity of cellular constituents could augment recrystallization injury, therefore this mechanism of protection warrants further study. Dehydrating cells with trehalose did however prove to modulate intracellular IRI activity in some cases. IRI 1 demonstrated improved intracellular IRI activity in the presence of a non-permeating CPA. Given, that intracellular IRI activity was diminished in the presence of permeating CPAs, perhaps pairing a permeating and a non-permeating CPA could improve intracellular IRI activity. This notion is specific to IRI 1, as IRI 2 lost activity in the presence of a non-permeating CPA, while the activity of IRI 3 was unmodified.

Understanding how commonly used permeating and non-permeating CPAs impact recrystallization is not only pertinent to a broader understanding of recrystallization injury in cryobiology but will inform the continued implementation of IRIs in different biological systems.

4.4 The Continued Application of Small Molecule IRIs to Sub-Zero Organ Preservation

The findings of chapter 3 demonstrated IRI 2 is capable of permeating liver tissue sections and controlling recrystallization. Furthermore, it did not appear to be toxic in whole rat livers; however, it failed to demonstrate any post-thaw functional benefits to rat livers frozen at high sub-zero

temperatures. This was ascribed to either a lack of IRI activity in the solutions used, other forms of freezing injury taking precedence over recrystallization injury, limited recrystallization occurring in the freezing protocol, or a combination of the three. While it is vital that IRI activity be assessed in the solutions utilized in this protocol, the future implementation of IRIs in whole organ preservation should be performed under conditions where recrystallization injury is explicit.

As storage temperatures are lowered, the concentration of permeating CPA will need to be increased in order to (1) limit excessive dehydration in cells surrounding the vasculature, (2) limit the volume of ice formed within the vasculature, and (3) constrain ice to the vasculature [45; 54; 57; 87; 88]. The corresponding increase in solution viscosity will require the development of complex perfusion protocols to minimize endothelial injury and toxicity during perfusion. The benefits of small molecule IRIs in this application may be a virtue of their ability to reduce the required concentration of CPA. While this can be viewed from the solution perspective described in the previous section, it is important to additionally consider it in terms of ice crystal localization in vascularized tissues. A decrease in the concentration of permeating CPA would likely need to be accompanied by an increase in the cooling rate to minimize vascular distension and dehydration of the surrounding interstitium [7; 35; 72]. However, the corresponding formation of interstitial and intracellular ice would allow recrystallization injury to gain prominence, which small molecule IRIs can be used to mitigate [4; 5; 34; 43; 48; 49; 50; 51; 52; 59; 63; 66; 74]. This notion can additionally be applied to the Tessier *et al.* protocol leveraged in Chapter 3 of this thesis [82]. The perfusion of high concentrations of non-permeating CPAs to limit extravascular ice formation may, in fact, promote damage during perfusion or freezing phases. Again, the emphasis on minimizing extravascular ice formation may not be necessary if the recrystallization of extravascular ice is minimized. However, it should be stated that this is largely theoretical, particularly given the increase in the total volume of ice formed as CPA concentrations are reduced. Thus, there are several more appropriate approaches to optimizing the Tessier *et al.* protocol that may not concern the use of an IRI.

IRIs could additionally be considered as a supplement to ice-free approaches to tissue and organ preservation due to their lack of toxicity and limited contributions to solution viscosity. Recrystallization following nucleation would undeniably exacerbate damage due to the thermodynamic instability of ice formed in supercooled or vitrified systems. However, the damage

associated with the nucleation event in these non-equilibrium systems would take precedence over recrystallization injury, thus emphasis should be placed on the inhibition of nucleation. The liquidus tracking (LT) approach sub-zero preservation involves a sequential increase in the CPA concentration in stepwise manner during the cooling phase in such a way that the system does not depart from the liquidus curve [19; 23]. Nucleation in this system would likely occur near the equilibrium freezing point and, as a result, the nucleation event will prove less damaging than in non-equilibrium approaches to ice-free preservation. While the magnitude of recrystallization will be diminished when ice is nucleated near the equilibrium freezing point, the absence of controlled vascular nucleation would result in an increased probability of interstitial and intracellular ice formation. While this would augment recrystallization injury, the high concentration of CPAs in the LT approach may enable sufficient solute mediated inhibition of recrystallization, thereby diminishing the effect of the IRI [38].

4.5 Next Steps for a Nature-Inspired High Sub-Zero Liver Preservation Strategy

Assessing the location and extent of ice formation throughout the tissue under the freezing and treatment conditions implemented would prove exceptionally informative to the whole liver freezing protocol leveraged in Chapter 3. Given that ice formation is not constrained to the vasculature, it is unclear whether efforts to inhibit recrystallization rather than the implementation of reduced cooling rates and higher CPA concentrations to constrain ice to the vasculature would prove more beneficial. On the opposing end of the spectrum, this form of analysis could reveal extensive dehydration of cells surrounding the vasculature, promoting not only cellular damage, but also raising the possibility of extensive vascular distention and subsequent rupture [58; 73]. Modeling vascular distention and cellular dehydration using Krogh cylinder models could help inform whether critical limits are surpassed on each of these ends [73]. However, while the biophysics of the freezing response would certainly be the dominant concern in any approach to freeze whole organs, optimizing this method of preservation through solely a biophysical lens is bound to yield limited outcomes. For example, the protocol implemented in Chapter 3 uses polyethylene glycol (PEG) to serve not only as a colligative CPA, but because this compound is additionally known to stabilize the vascular endothelium and minimize lipid peroxidation [69]. It is in this vein that organ preservation protocols must be designed, with more initiative taken to include compounds that may enhance stress tolerance or actively depress metabolic rates [81].

Facilitating the preservation of organs in a frozen state will ultimately require a concatenation of technologies that together tackle multiple sources of injury.

4.6 Conclusion

Continued research and implementation of IRIs into organ cryopreservation efforts should be form part of a larger body of research that seeks to further understand recrystallization injury. Specifically, how it differs based on the location of ice within tissues, the temperature it takes place at, the types of CPAs present, and concentrations of different CPAs. While there is no doubt that recrystallization is damaging, effectively tackling this issue requires a better understanding of mechanisms through which it causes damage. Concurrent research into the mechanisms through which small molecule IRIs operate and the conditions under which they prove effective, will open several avenues in the development of sub-zero complex tissue and whole organ preservation techniques. Ultimately, the combination of sub-zero organ preservation and *ex vivo* machine perfusion systems describe throughout this thesis will substantially improve organ allocation through ceasing geographical and logistic constraints within the transplant network as well as facilitating the use of extended criteria organs.

4.7 References

[1] A.V. Aarset, Freezing tolerance in intertidal invertebrates (a review). Comp Biochem Physiol A 73 (1982) 571-580.

[2] W.J. Armitage, and D.E. Pegg, The contribution of the cryoprotectant to total injury in rabbit hearts frozen with ethylene glycol. Cryobiology 16 (1979) 152-60.

[3] A.K. Balcerzak, C.J. Capicciotti, J.G. Briard, and R.N. Ben, Designing ice recrystallization inhibitors: From antifreeze (glyco)proteins to small molecules. RSC Advances 80 (2014) 42682-96

[4] H. Bank, Freezing injury in tissue cultured cells as visualized by freeze-etching. Exp Cell Res 85 (1974) 367-76.

[5] H. Bank, Visualization of freezing damage. II. Structural alterations during warming. Cryobiology 10 (1973) 157-70.

[6] J.G. Baust, B. JG, and R. RA, The physiology and biochemistry of low temperature tolerance in insects and other terrestrial arthropods: a bibliography. (1982).

[7] J. Bischof, C.J. Hunt, B. Rubinsky, A. Burgess, and D.E. Pegg, Effects of cooling rate and glycerol concentration on the structure of the frozen kidney: assessment by cryo-scanning electron microscopy. Cryobiology 27 (1990) 301-10.

[8] J.C. Bischof, and B. Rubinsky, Large ice crystals in the nucleus of rapidly frozen liver cells. Cryobiology 30 (1993) 597-603.

[9] W. Block, Cold hardiness in invertebrate poikilotherms. Comp Biochem Biophys A 73 (1982) 581-593.

[10] J.G. Briard, J.S. Poisson, T.R. Turner, C.J. Capicciotti, J.P. Acker, and R.N. Ben, Small molecule ice recrystallization inhibitors mitigate red blood cell lysis during freezing, transient warming and thawing. Sci Rep 6 (2016) 23619.

[11] C. Budke, and T. Koop, Ice recrystallization inhibition and molecular recognition of ice faces by poly(vinyl alcohol). ChemPhysChem 7 (2006) 2601-2606.

[12] A.A. Burkey, C.L. Riley, L.K. Wang, T.A. Hatridge, and N.A. Lynd, Understanding Poly(vinyl alcohol)-Mediated Ice Recrystallization Inhibition through Ice Adsorption Measurement and pH Effects. Biomacromolecules 19 (2018) 248-255.

[13] C.J. Capicciotti, J.D. Kurach, T.R. Turner, R.S. Mancini, J.P. Acker, and R.N. Ben, Small molecule ice recrystallization inhibitors enable freezing of human red blood cells with reduced glycerol concentrations. Sci Rep 5 (2015) 9692.

[14] C.J. Capicciotti, M. Leclere, F.A. Perras, D.L. Bryce, H. Paulin, J. Harden, Y. Liu, and R.N. Ben, Potent inhibition of ice recrystallization by low molecular weight carbohydrate-based surfactants and hydrogelators. Chemical Science 3 (2012) 1408-1416.

[15] J.F. Carpenter, and T.N. Hansen, Antifreeze protein modulates cell survival during cryopreservation: mediation through influence on ice crystal growth. Proc Nat Acad Sci U S A (1992).

[16] J.L. Chaytor, J.M. Tokarew, L.K. Wu, M. Leclere, R.Y. Tam, C.J. Capicciotti, L. Guolla, E. von Moos, C.S. Findlay, D.S. Allan, and R.N. Ben, Inhibiting ice recrystallization and optimization of cell viability after cryopreservation. Glycobiology 22 (2012) 123-33.

[17] J.L. Chaytor, J.M. Tokarew, L.K. Wu, M. Leclre, R.Y. Tam, C.J. Capicciotti, L. Guolla, E. Von Moos, C.S. Findlay, D.S. Allan, and R.N. Ben, Inhibiting ice recrystallization and optimization of cell viability after cryopreservation. Glycobiology 22 (2012) 123-133.

[18] R.J. de Vries, S.N. Tessier, P.D. Banik, S. Nagpal, S.E. Cronin, S. Ozer, E.O. Hafiz, T.M. van Gulik, M.L. Yarmush, and J.F. Markmann, Supercooling extends preservation time of human livers. Nature Biotechnol 37 (2019) 1131-1136.

[19] B. Elford, and C. Walter, Effects of electrolyte composition and pH on the structure and function of smooth muscle cooled to− 79° C in unfrozen media. Cryobiology 9 (1972) 82-100.

[20] G. Fahy, and A. Karow Jr, Ultrastructure-function correlative studies for cardiac cryopreservation. V. Absence of a correlation between electrolyte toxicity and cryoinjury in the slowly frozen, cryoprotected rat heart. Cryobiology 14 (1977) 418-427.

[21] G.M. Fahy, The relevance of cryoprotectant “toxicity” to cryobiology. Cryobiology 23 (1986) 1-13.

[22] G.M. Fahy, D.R. MacFarlane, C.A. Angell, and H.T. Meryman, Vitrification as an approach to cryopreservation. Cryobiology 21 (1984) 407-426.

[23] J. Farrant, Mechanism of cell damage during freezing and thawing and its prevention. Nature 205 (1965) 1284-1287.

[24] S. Giwa, J.K. Lewis, L. Alvarez, R. Langer, A.E. Roth, G.M. Church, J.F. Markmann, D.H. Sachs, A. Chandraker, J.A. Wertheim, M. Rothblatt, E.S. Boyden, E. Eidbo, W.P.A. Lee, B. Pomahac, G. Brandacher, D.M. Weinstock, G. Elliott, D. Nelson, J.P. Acker, K. Uygun, B. Schmalz, B.P. Weegman, A. Tocchio, G.M. Fahy, K.B. Storey, B. Rubinsky, J. Bischof, J.A.W. Elliott, T.K. Woodruff, G.J. Morris, U. Demirci, K.G.M. Brockbank, E.J. Woods, R.N. Ben, J.G. Baust, D. Gao, B. Fuller, Y. Rabin, D.C. Kravitz, M.J. Taylor, and M. Toner, The promise of organ and tissue preservation to transform medicine. Nat Biotechnol 35 (2017) 530-542.

[25] F. Guttman, A. Khalessi, B. Huxley, R. Lee, and G. Savard, Whole organ preservation: I. A technique for in vivo freezing canine intestine using intraarterial helium and ambient nitrogen. Cryobiology 6 (1969) 32-36.

[26] F. Guttman, N. Segal, and J. Borzone, Cryopreservation of canine kidneys with dimethyl sulphoxide: further studies, Organ Preservation II, Churchill Livingstone Edinburgh, 1979, pp. 185.

[27] F.M. Guttman, J. Lizin, P. Robitaille, H. Blanchard, and C. Turgeon-Knaack, Survival of canine kidneys after treatment with dimethyl-sulfoxide, freezing at− 80° C, and thawing by microwave illumination. Cryobiology 14 (1977) 559-567.

[28] T. Hansen, Glycerol content and cold-hardiness in freeze tolerant insects. Eesti. NSV. Tead. Akad. Tiom. Biol 29 (1980) 113-118.

[29] M. Hasan, A.E. Fayter, and M.I. Gibson, Ice Recrystallization Inhibiting Polymers Enable Glycerol-Free Cryopreservation of Microorganisms. Biomacromolecules 19 (2018) 3371-3376.

[30] H. Ishiguro, and B. Rubinsky, Mechanical interactions between ice crystals and red blood cells during directional solidification. Cryobiology 31 (1994) 483-500.

[31] N. Ishine, B. Rubinsky, and C.Y. Lee, A histological analysis of liver injury in freezing storage. Cryobiology 39 (1999) 271-7.

[32] N. Ishine, B. Rubinsky, and C.Y. Lee, Transplantation of mammalian livers following freezing: vascular damage and functional recovery. Cryobiology 40 (2000) 84-9.

[33] C. J, M. Doshi, and R. N, Ice Recrystallization Inhibitors: From Biological Antifreezes to Small Molecules, 2013.

[34] I.A. Jacobsen, D.E. Pegg, H. Starklint, J. Chemnitz, C. Hunt, P. Barfort, and M.P. Diaper, Effect of cooling and warming rate on glycerolized rabbit kidneys. Cryobiology (1984).

[35] I.A. Jacobsen, D.E. Pegg, H. Starklint, J. Chemnitz, C. Hunt, P. Barfort, and M.P. Diaper, Effect of cooling and warming rate on glycerolized rabbit kidneys. Cryobiology 21 (1984) 637-53.

[36] P. Klinmalai, M. Shibata, and T. Hagiwara, Recrystallization of ice crystals in trehalose solution at isothermal condition. Food Biophysics 12 (2017) 404-411.

[37] C.A. Knight, and J.G. Duman, Inhibition of recrystallization of ice by insect thermal hysteresis proteins: A possible cryoprotective role. Cryobiology 23 (1986) 256-262.

[38] C.A. Knight, J. Hallett, and A. DeVries, Solute effects on ice recrystallization: an assessment technique. Cryobiology 25 (1988) 55-60.

[39] C.A. Knight, D. Wen, and R.A. Laursen, Nonequilibrium antifreeze peptides and the recrystallization of ice. Cryobiology (1995).

[40] S. Kubota, F. Graham, B.G. Crabo, R.C. Lillehei, and R.H. Dietman, The effect of freeze rate, duration of phase transition, and warming rate on survival of frozen canine kidneys. Cryobiology 13 (1976) 455-62.

[41] A. Larese, J. Acker, K. Muldrew, H. Yang, and L. McGann, Antifreeze proteins induce intracellular nucleation. Cryo-Letters 17 (1996) 175-182.

[42] J.K. Lewis, J.C. Bischof, I. Braslavsky, K.G. Brockbank, G.M. Fahy, B.J. Fuller, Y. Rabin, A. Tocchio, E.J. Woods, B.G. Wowk, J.P. Acker, and S. Giwa, The Grand Challenges of Organ Banking: Proceedings from the first global summit on complex tissue cryopreservation. Cryobiology 72 (2016) 169-82.

[43] X. Liu, G. Zhao, Z. Shu, D. Niu, Z. Zhang, P. Zhou, Y. Cao, and D. Gao, Quantification of intracellular ice formation and recrystallization during freeze–thaw cycles and their relationship with the viability of pig iliac endothelium cells. Biopres Biobank 14 (2016) 511-519.

[44] H. Lodish, A. Berk, S.L. Zipursky, P. Matsudaira, D. Baltimore, and J. Darnell, Intracellular ion environment and membrane electric potential, Molecular Cell Biology. 4th edition, WH Freeman, 2000.

[45] J.E. Lovelock, Het mechanism of the protective action of glycerol against haemolysis by freezing and thawing. Bioch Biophys Acta 11 (1953) 28-36.

[46] B. Luyet, D. Rasmussen, and C. Kroener, Successive crystallization and recrystallization, during rewarming, of rapidly cooled solutions of glycerol and ethylene glycol. Biodynamica 10 (1966) 53-60.

[47] F. Lv, B. Liu, W. Li, and G.K. Jaganathan, Devitrification and recrystallization of nanoparticle-containing glycerol and PEG-600 solutions. Cryobiology 68 (2014) 84-90.

[48] A. MacKenzie, Death of frozen yeast in the course of slow warming, Ciba Foundation Symposium-The Frozen Cell, Wiley Online Library, 1970, pp. 89-96.

[49] M.N. Martino, and N.E. Zaritzky, Ice recrystallization in a model system and in frozen muscle tissue. Cryobiology 26 (1989) 138-48.

[50] P. Mazur, 2. Roles of intracellular ice formation, vitrification of cell water, and recrystallization of intracellular ice on the survival of mouse embryos and oocytes. Cryobiology 65 (2012) 339.

[51] P. Mazur, Freezing of living cells: mechanisms and implications. Am J Physiol 247 (1984) C125-42.

[52] P. Mazur, The role of intracellular freezing in the death of cells cooled at supraoptimal rates. Cryobiology 14 (1977) 251-272.

[53] P. Mazur, and K.W. Cole, Influence of cell concentration on the contribution of unfrozen fraction and salt concentration to the survival of slowly frozen human erythrocytes. Cryobiology 22 (1985) 509-36.

[54] P. Mazur, and R.H. Miller, Survival of frozen-thawed human red cells as a function of the permeation of glycerol and sucrose. Cryobiology 13 (1976) 523-536.

[55] P. Mazur, W.F. Rall, and N. Rigopoulos, Relative contributions of the fraction of unfrozen water and of salt concentration to the survival of slowly frozen human erythrocytes. Biophys J 36 (1981) 653-75.

[56] P. Mazur, and N. Rigopoulos, Contributions of unfrozen fraction and of salt concentration to the survival of slowly frozen human erythrocytes: influence of warming rate. Cryobiology 20 (1983) 274-89.

[57] H.T. Meryman, Freezing injury and its prevention in living cells. Annual Rev Biophys Bioeng 3 (1974) 341-363.

[58] H.T. Meryman, Osmotic stress as a mechanism of freezing injury. Cryobiology 8 (1971) 489-500.

[59] R.H. Miller, and P. Mazur, Survival of frozen-thawed human red cells as a function of cooling and warming velocities. Cryobiology 13 (1976) 404-414.

[60] G.S. Moss, P. Reed, and A.G. Riddell, Observations on the effects of glycerol on the cold storage of the canine liver. J Surg Res 6 (1966) 147-51.

[61] D.J. Murphy, Freezing resistance in intertidal invertebrates. Annu Rev Physiol 45 (1983) 289-99.

[62] D.E. Pegg, Ice crystals in tissues and organs, The biophysics of organ cryopreservation, Springer, 1987, pp. 117-140.

[63] D.E. Pegg, M.P. Diaper, H.L. Skaer, and C.J. Hunt, The effect of cooling rate and warming rate on the packing effect in human erythrocytes frozen and thawed in the presence of 2 M glycerol. Cryobiology 21 (1984) 491-502.

[64] D.E. Pegg, I.A. Jacobsen, M.P. Diaper, and J. Foreman, The effect of cooling and warming rate on cortical cell function of glycerolized rabbit kidneys. Cryobiology 21 (1984) 529-35.

[65] D.E. Pegg, L. Wang, D. Vaughan, and C.J. Hunt, Cryopreservation of articular cartilage. Part 2: mechanisms of cryoinjury. Cryobiology 52 (2006) 347-359.

[66] J.S. Poisson, J.P. Acker, J.G. Briard, J.E. Meyer, and R.N. Ben, Modulating Intracellular Ice Growth with Cell-Permeating Small-Molecule Ice Recrystallization Inhibitors. Langmuir 35 (2018) 7452-7458.

[67] J.S. Poisson, J.G. Briard, T.R. Turner, J.P. Acker, and R.N. Ben, Hydroxyethyl Starch Supplemented with Ice Recrystallization Inhibitors Greatly Improves Cryopreservation of Human Red Blood Cells. Bioproc J 15 (2016).

[68] M.J. Powell-Palm, Y. Zhang, J. Aruda, and B. Rubinsky, Isochoric conditions enable high subfreezing temperature pancreatic islet preservation without osmotic cryoprotective agents. Cryobiology 86 (2019) 130-133.

[69] C. Puts, T. Berendsen, B. Bruinsma, S. Ozer, M. Luitje, O.B. Usta, M. Yarmush, and K. Uygun, Polyethylene glycol protects primary hepatocytes during supercooling preservation. Cryobiology 71 (2015) 125-129.

[70] F. Riemann, M. Schrage, and H. Farke, High freezing tolerance of marine nematodes from intertidal sediments of the German Bight. Nematologica 30 (1984) 452-456.

[71] B. Rubinsky, A. Arav, J.S. Hong, and C.Y. Lee, Freezing of mammalian livers with glycerol and antifreeze proteins. Biochem Biophys Res Comm 200 (1994) 732-741.

[72] B. Rubinsky, C.Y. Lee, J. Bastacky, and G. Onik, The process of freezing and the mechanism of damage during hepatic cryosurgery. Cryobiology 27 (1990) 85-97.

[73] B. Rubinsky, D. Pegg, and R.Y. Calne, A mathematical model for the freezing process in biological tissue. Proceedings of the Royal Society of London. Series B. Biological Sciences 234 (1988) 343-358.

[74] R. Steinbrecht, Recrystallization and ice-crystal growth in a biological specimen, as shown by a simple freeze substitution method. J Microsc 140 (1985) 41-46.

[75] K.B. Storey, Freeze tolerance in the frog,Rana sylvatica. Experientia 40 (1984) 1261-1262.

[76] K.B. Storey, and J.M. Storey, Freeze tolerance in animals. Physiol Rev 68 (1988) 27-84.

[77] K.B. Storey, and J.M. Storey, Freeze tolerant frogs: cryoprotectants and tissue metabolism during freeze–thaw cycles. Can J Zool 64 (1986) 49-56.

[78] K.B. Storey, and J.M. Storey, Natural Freezing Survival in Animals. Annual Review of Ecology and Systematics 27 (1996) 365-386.

[79] R.Y. Tam, S.S. Ferreira, P. Czechura, R.N. Ben, and J.L. Chaytor, Hydration index-a better parameter for explaining small molecule hydration in inhibition of ice recrystallization. J Am Chem Soc 130 (2008) 17494-17501.

[80] M. Taylor, and D. Pegg, The effect of ice formation on the function of smooth muscle tissue following storage at− 21 C and− 60 C. Cryobiology 20 (1982) 36-40.

[81] M.J. Taylor, B.P. Weegman, S.C. Baicu, and S.E. Giwa, New Approaches to Cryopreservation of Cells, Tissues, and Organs. Transfusion medicine and hemotherapy : offizielles Organ der Deutschen Gesellschaft fur Transfusionsmedizin und Immunhamatologie 46 (2019) 197-215.

[82] S.N. Tessier, S.E.J. Cronin, C.A. Pendexter, S. Özer, R.J. de Vries, S. Nagpal, P.D. Banik, K. Uygun, and M. Toner, Partial freezing: A nature-inspired strategy for organ banking. Cryobiology 81 (2018) 220.

[83] M. Verheijen, M. Lienhard, Y. Schrooders, O. Clayton, R. Nudischer, S. Boerno, B. Timmermann, N. Selevsek, R. Schlapbach, H. Gmuender, S. Gotta, J. Geraedts, R. Herwig, J. Kleinjans, and F. Caiment, DMSO induces drastic changes in human cellular processes and epigenetic landscape in vitro. Sci Rep 9 (2019) 4641.

[84] D.A. Wharton, P.W. Wilson, J.S. Mutch, C.J. Marshall, and M. Lim, Recrystallization inhibition assessed by splat cooling and optical recrystallometry. CryoLetters 28 (2007) 61-68.

[85] G. Yu, R. Li, and A. Hubel, Interfacial interactions of sucrose during cryopreservation detected by raman spectroscopy. Langmuir 35 (2018) 7388-7395.

[86] S.O. Yu, A. Brown, A.J. Middleton, M.M. Tomczak, V.K. Walker, and P.L. Davies, Ice restructuring inhibition activities in antifreeze proteins with distinct differences in thermal hysteresis. Cryobiology 61 (2010) 327-334.

[87] A.M. Zade-Oppen, Posthypertonic hemolysis in a sucrose system. Experientia 26 (1970) 1087-8.

[88] A.M.M. Zade-Oppen, Posthypertonic Hemolysis in Sodium Chloride Systems. Acta Physiologica Scandinavica 73 (1968) 341-364.

[89] S.-z. Zhang, X.-y. Yu, and G.-m. Chen, Permeation of dimethyl sulfoxide into articular cartilage at subzero temperatures. Journal of Zhejiang University SCIENCE B 13 (2012) 213-220.

[90] Y. Zhang, G. Ukpai, A. Grigoropoulos, M.J. Powell-Palm, B.P. Weegman, M.J. Taylor, and B. Rubinsky, Isochoric vitrification: An experimental study to establish proof of concept. Cryobiology 83 (2018) 48-55.

Bibliography

A.V. Aarset, Freezing tolerance in intertidal invertebrates (a review). Comparative Biochemistry and Physiology Part A: Physiology 73 (1982) 571-580.

J.P. Acker, A. Larese, H. Yang, A. Petrenko, and L. McGann, Intracellular ice formation is affected by cell interactions. Cryobiology 38 (1999) 363-371.

J.P. Acker, and L. McGann, The role of cell-cell contact on intracellular ice formation. Cryo-letters 19 (1998) 367-374.

J.P. Acker, Influence of cell adhesions on the freezing response of biological systems [Dissertation], Edmonton, AB: University of Alberta, 1998.

J.P. Acker, Innocuous intracellular ice formation : mechanisms and implications [Dissertation], Edmonton, AB: University of Alberta, 2000.

J.P. Acker, and I.M. Croteau, Pre- and post-thaw assessment of intracellular ice formation. J Microsc 215 (2004) 131-8.

J.P. Acker, J.A.W. Elliott, and L.E. McGann, Intercellular Ice Propagation: Experimental Evidence for Ice Growth through Membrane Pores. Biophys J 81 (2001) 1389-1397.

J.P. Acker, and L.E. McGann, Cell-cell contact affects membrane integrity after intracellular freezing. Cryobiology 40 (2000) 54-63.

J.P. Acker, and L.E. McGann, Innocuous intracellular ice improves survival of frozen cells. Cell Transplant 11 (2002) 563-71.

J.P. Acker, and L.E. McGann, Protective effect of intracellular ice during freezing? Cryobiology 46 (2003) 197-202.

Y. Agca, J. Liu, J. McGrath, A. Peter, E. Critser, and J. Critser, Membrane permeability characteristics of metaphase II mouse oocytes at various temperatures in the presence of Me2SO. Cryobiology 36 (1998) 287-300.

I. Alina, Annual statistics on organ replacement in Canada, 2017.

S.M. Almdahl, M. Lie, P.E. Dahl, and D. Sorlie, [Aortic root reconstruction with homograft in bacterial endocarditis]. Tidsskr Nor Laegeforen 115 (1995) 2390-1.

T.J. Anchordoguy, C.A. Cecchini, J.H. Crowe, and L.M. Crowe, Insights into the cryoprotective mechanism of dimethyl sulfoxide for phospholipid bilayers. Cryobiology 28 (1991) 467-473.

T.J. Anchordoguy, A.S. Rudolph, J.F. Carpenter, and J.H. Crowe, Mode of interaction of cryoprotectants with membrane phospholipids during freezing. Cryobiology 24 (1987) 324-331.

W. Armitage, and B. Juss, The influence of cooling rate on survival of frozen cells differs in monolayers and in suspensions. Cryo-Letters 17 (1996) 213-218.

W.J. Armitage, and D.E. Pegg, The contribution of the cryoprotectant to total injury in rabbit hearts frozen with ethylene glycol. Cryobiology 16 (1979) 152-60.

E. Asahina, K. Shimada, and Y. Hisada, A stable state of frozen protoplasm with invisible intracellular ice crystals obtained by rapid cooling. Exp Cell Res 59 (1970) 349-358.

T. Aunaas, Nucleating agents in the haemolymph of an intertidal mollusc tolerant to freezing. Experientia 38 (1982) 1456-1457.

A.K. Balcerzak, C.J. Capicciotti, J.G. Briard, and R.N. Ben, Designing ice recrystallization inhibitors: From antifreeze (glyco)proteins to small molecules. RSC Advances 80 (2014) 42682-96

H. Bank, Freezing injury in tissue cultured cells as visualized by freeze-etching. Exp Cell Res 85 (1974) 367-76.

H. Bank, Visualization of freezing damage. II. Structural alterations during warming. Cryobiology 10 (1973) 157-170.

R.E. Barnett, The effects of dimethylsulfoxide and glycerol on Na+, K+-ATPase and membrane structure. Cryobiology 15 (1978) 227.

E.L. Bastiaanse, H.J. Jongsma, A. van der Laarse, and B.R. Takens-Kwak, Heptanol-induced decrease in cardiac gap junctional conductance is mediated by a decrease in the fluidity of membranous cholesterol-rich domains. J Membrane Biol 136 (1993) 135-145.

K. Basu, C.P. Garnham, Y. Nishimiya, S. Tsuda, I. Braslavsky, and P. Davies, Determining the ice-binding planes of antifreeze proteins by fluorescence-based ice plane affinity. JoVE (Journal of Visualized Experiments) (2014) e51185.

R.C. Bates, N.S. Edwards, and J.D. Yates, Spheroids and cell survival. Crit Rev Oncol Hematol 36 (2000) 61-74.

J.G. Baust, and J.S. Edwards, Mechanisms of freezing tolerance in an Antarctic midge, Belgica antarctica. Physiol Entomol 4 (1979) 1-5.

J.G. Baust, B. JG, and R. RA, The physiology and biochemistry of low temperature tolerance in insects and other terrestrial arthropods: a bibliography. (1982).

J.M. Baust, M.J. Vogel, R. Van Buskirk, and J.G. Baust, A molecular basis of cryopreservation failure and its modulation to improve cell survival. Cell Transplant 10 (2001) 561-71.

F.O. Belzer, and J.H. Southard, Principles of solid-organ preservation by cold storage. Transplantation 45 (1988) 673-6.

T.A. Berendsen, B.G. Bruinsma, C.F. Puts, N. Saeidi, O.B. Usta, B.E. Uygun, M.L. Izamis, M. Toner, M.L. Yarmush, and K. Uygun, Supercooling enables long-term transplantation survival following 4 days of liver preservation. Nat Med 20 (2014) 790-3.

W.K. Berger, and B. Uhrik, Freeze-induced shrinkage of individual cells and cell-to-cell propagation of intracellular ice in cell chains from salivary glands. Experientia 52 (1996) 843-50.

J. Bischof, 45. Nanowarming: A new concept in tissue and organ preservation. Cryobiology 71 (2015) 176.

J. Bischof, C.J. Hunt, B. Rubinsky, A. Burgess, and D.E. Pegg, Effects of cooling rate and glycerol concentration on the structure of the frozen kidney: assessment by cryo-scanning electron microscopy. Cryobiology 27 (1990) 301-10.

J.C. Bischof, and B. Rubinsky, Large ice crystals in the nucleus of rapidly frozen liver cells. Cryobiology 30 (1993) 597-603.

J.C. Bischof, C.M. Ryan, R.G. Tompkins, M.L. Yarmush, and M. Toner, Ice formation in isolated human hepatocytes and human liver tissue. ASAIO J 43 (1997) 271-8.

W. Block, Cold hardiness in invertebrate poikilotherms. Comp. Biochem. Physiol. Part A 73 (1982) 581-593.

K.G. Brockbank, Effects of cryopreservation upon vein function in vivo. Cryobiology 31 (1994) 71-81.

V.L. Bronshteyn, and P.L. Steponkus, Nucleation and growth of ice crystals in concentrated solutions of ethylene glycol. Cryobiology 32 (1995) 1-22.

B.G. Bruinsma, T.A. Berendsen, M.L. Izamis, H. Yeh, M.L. Yarmush, and K. Uygun, Supercooling preservation and transplantation of the rat liver. Nat Protoc 10 (2015) 484-94.

C. Budke, C. Heggemann, M. Koch, N. Sewald, and T. Koop, Ice recrystallization kinetics in the presence of synthetic antifreeze glycoprotein analogues using the framework of LSW theory. J Phys Chem B113 (2009) 2865-2873.

C. Budke, and T. Koop, Ice recrystallization inhibition and molecular recognition of ice faces by poly(vinyl alcohol). ChemPhysChem (2006).

A.A. Burkey, C.L. Riley, L.K. Wang, T.A. Hatridge, and N.A. Lynd, Understanding Poly(vinyl alcohol)-Mediated Ice Recrystallization Inhibition through Ice Adsorption Measurement and pH Effects. Biomacromolecules 19 (2018) 248-255.

B.K. Campbell, J. Hernandez-Medrano, V. Onions, C. Pincott-Allen, F. Aljaser, J. Fisher, A.S. McNeilly, R. Webb, and H.M. Picton, Restoration of ovarian function and natural fertility following the cryopreservation and autotransplantation of whole adult sheep ovaries. Hum Reprod 29 (2014) 1749-63.

C.J. Capicciotti, M. Doshi, and R.N. Ben, Ice recrystallization inhibitors: From biological antifreezes to small molecules. Recent developments in the study of recrystallization 177 (2013) 224.

C.J. Capicciotti, J.D. Kurach, T.R. Turner, R.S. Mancini, J.P. Acker, and R.N. Ben, Small molecule ice recrystallization inhibitors enable freezing of human red blood cells with reduced glycerol concentrations. Sci Rep 5 (2015) 9692.

C.J. Capicciotti, M. Leclere, F.A. Perras, D.L. Bryce, H. Paulin, J. Harden, Y. Liu, and R.N. Ben, Potent inhibition of ice recrystallization by low molecular weight carbohydrate-based surfactants and hydrogelators. Chem Sci 3 (2012) 1408-1416.

J.F. Carpenter, and T.N. Hansen, Antifreeze protein modulates cell survival during cryopreservation: mediation through influence on ice crystal growth. Proc Natl Acad Sci U S A (1992)

R. Chambers, and H. Hale, The formation of ice in protoplasm. Proceedings of the Royal Society of London. Series B, Containing Papers of a Biological Character 110 (1932) 336-352.

J.L. Chaytor, J.M. Tokarew, L.K. Wu, M. Leclere, R.Y. Tam, C.J. Capicciotti, L. Guolla, E. von Moos, C.S. Findlay, D.S. Allan, and R.N. Ben, Inhibiting ice recrystallization and optimization of cell viability after cryopreservation. Glycobiology 22 (2012) 123-33.

C.H. Cho, J. Park, D. Nagrath, A.W. Tilles, F. Berthiaume, M. Toner, and M.L. Yarmush, Oxygen uptake rates and liver-specific functions of hepatocyte and 3T3 fibroblast co-cultures. Biotech Bioeng 97 (2007) 188-199.

J.S. Clegg, P. Seitz, W. Seitz, and C.F. Hazlewood, Cellular responses to extreme water loss: the water-replacement hypothesis. Cryobiology 19 (1982) 306-16.

R.M. Cordeiro, S. Stirling, G.M. Fahy, and J.P. de Magalhaes, Insights on cryoprotectant toxicity from gene expression profiling of endothelial cells exposed to ethylene glycol. Cryobiology 71 (2015) 405-12.

J.P. Costanzo, and R.E. Lee, Jr., Avoidance and tolerance of freezing in ectothermic vertebrates. J Exp Biol 216 (2013) 1961-7.

K.J. Cowan, and K.B. Storey, Freeze-thaw effects on metabolic enzymes in wood frog organs. Cryobiology 43 (2001) 32-45.

J.H. Crowe, L.M. Crowe, J.F. Carpenter, and C. Aurell Wistrom, Stabilization of dry phospholipid bilayers and proteins by sugars. Biochem J 242 (1987) 1-10.

J.H. Crowe, L.M. Crowe, and R. Mouradian, Stabilization of biological membranes at low water activities. Cryobiology 20 (1983) 346-356.

M. Cypel, J.C. Yeung, M. Liu, M. Anraku, F. Chen, W. Karolak, M. Sato, J. Laratta, S. Azad, M. Madonik, C.W. Chow, C. Chaparro, M. Hutcheon, L.G. Singer, A.S. Slutsky, K. Yasufuku, M. de Perrot, A.F. Pierre, T.K. Waddell, and S. Keshavjee, Normothermic ex vivo lung perfusion in clinical lung transplantation. N Engl J Med 364 (2011) 1431-40.

J.R. Cypser, W.S. Chick, G.M. Fahy, G.J. Schumacher, and T.E. Johnson, Genetic suppression of cryoprotectant toxicity. Cryobiology 86 (2019) 95-102.

P. Czechura, R.Y. Tam, E. Dimitrijevic, A.V. Murphy, and R.N. Ben, The importance of hydration for inhibiting ice recrystallization with C-linked antifreeze glycoproteins. J. Am. Chem. Soc. 130 (2008) 2928-2929.

I.A. de Graaf, A.L. Draaisma, O. Schoeman, G.M. Fahy, G.M. Groothuis, and H.J. Koster, Cryopreservation of rat precision-cut liver and kidney slices by rapid freezing and vitrification. Cryobiology 54 (2007) 1-12.

R. de Vries, S.N. Tessier, P.D. Banik, S. Ozer, S.E.J. Crorin, S. Nagpal, H. Yeh, and K. Uygun, Extending the Human Liver Preservation Time for Transplantation by Supercooling. Transplantation 102 (2018) S396.

R.J. de Vries, C.A. Pendexter, S.E.J. Cronin, B. Marques, E.O.A. Hafiz, A. Muzikansky, T.M. van Gulik, J.F. Markmann, S.L. Stott, H. Yeh, M. Toner, K. Uygun, and S.N. Tessier, Cell release during perfusion reflects cold ischemic injury in rat livers. Sci Rep 10 (2020) 1102.

R.J. de Vries, S.N. Tessier, P.D. Banik, S. Nagpal, S.E. Cronin, S. Ozer, E.O. Hafiz, T.M. van Gulik, M.L. Yarmush, and J.F. Markmann, Supercooling extends preservation time of human livers. Nat Biotechnol 37 (2019) 1131-1136.

R.V. Devireddy, and J.C. Bischof, Measurement of water transport during freezing in mammalian liver tissue: Part II—The use of differential scanning calorimetry. (1998) 559-569.

R.V. Devireddy, P.R. Barratt, K.B. Storey, and J.C. Bischof, Liver freezing response of the freeze-tolerant wood frog, Rana sylvatica, in the presence and absence of glucose. I. Experimental measurements. Cryobiology 38 (1999) 310-326.

A.L. DeVries, S.K. Komatsu, and R.E. Feeney, Chemical and physical properties of freezing point-depressing glycoproteins from Antarctic fishes. J Biol Chem 245 (1970) 2901-8.

A.L. Devries, and Y. Lin, Structure of a peptide antifreeze and mechanism of adsorption to ice. Biochim Biophys Acta 495 (1977) 388-92.

K. Diller, Intracellular freezing: Effect of extracellular supercooling. Cryobiology 12 (1975) 480-485.

K. Diller, and J. Raymond, Water transport through a multicellular tissue during freezing-a network thermodynamic modeling analysis. Cryo-Letters 11 (1990) 151-162.

K.R. Diller, Intracellular freezing of glycerolized red cells. Cryobiology 16 (1979) 125-31.

R. Dittrich, T. Maltaris, A. Mueller, A. Dimmler, I. Hoffmann, F. Kiesewetter, and M.W. Beckmann, Successful uterus cryopreservation in an animal model. Horm Metab Res 38 (2006) 141-5.

Y.S. Djikaev, A. Tabazadeh, P. Hamill, and H. Reiss, Thermodynamic Conditions for the Surface-Stimulated Crystallization of Atmospheric Droplets. J Phys Chem A 106 (2002) 10247-10253.

M.T. Donato, L. Tolosa, and M.J. Gómez-Lechón, Culture and functional characterization of human hepatoma HepG2 cells, Protocols in In Vitro Hepatocyte Research, Springer, 2015, pp. 77-93.

D. Donhowe, R. Hartel, and R. Bradley, Ice crystallization processes during manufacture and storage of ice cream. J Dairy Sci 74 (1991) 3334-3344.

D.P. Donhowe, and R.W. Hartel, Recrystallization of ice during bulk storage of ice cream. Int Dairy J 6 (1996) 1209-1221.

D.P. Donhowe, and R.W. Hartel, Recrystallization of ice in ice cream during controlled accelerated storage. Int Dairy J 6 (1996) 1191-1208.

J.G. Duman, Factors involved in overwintering survival of the freeze tolerant beetle, Dendroides canadensis. J Comp Phys 136 (1980) 52-59.

J.G. Duman, Insect antifreezes and ice-nucleating agents. Cryobiology 19 (1982) 613-627.

J.G. Duman, K.L. Horwarth, A. Tomchaney, and J.L. Patterson, Antifreeze agents of terrestrial arthropods. Comparative Biochemistry and Physiology Part A: Physiology 73 (1982) 545-555.

P. Echlin, Freeze Substitution and Low-Temperature Embedding. in: P. Echlin, (Ed.), Low-Temperature Microscopy and Analysis, Springer US, Boston, MA, 1992, pp. 223-264.

B. Elford, and C. Walter, Effects of electrolyte composition and pH on the structure and function of smooth muscle cooled to− 79° C in unfrozen media. Cryobiology 9 (1972) 82-100.

A. Eniade, M. Purushotham, R.N. Ben, J. Wang, and K. Horwath, A serendipitous discovery of antifreeze protein-specific activity in C-linked antifreeze glycoprotein analogs. Cell Biochem Biophys 38 (2003) 115-124.

E.A. Eren, N. Latchana, E. Beal, D. Hayes Jr, B. Whitson, and S.M. Black, Donations after circulatory death in liver transplant. MESOT 14 (2016) 463.

D. Eshmuminov, D. Becker, L. Bautista Borrego, M. Hefti, M.J. Schuler, C. Hagedorn, X. Muller, M. Mueller, C. Onder, R. Graf, A. Weber, P. Dutkowski, P. Rudolf von Rohr, and P.A. Clavien, An integrated perfusion machine preserves injured human livers for 1 week. Nat Biotechnol 38 (2020) 189-198.

D. Everett, The thermodynamics of frost damage to porous solids. J Chem Soc Faraday Trans 57 (1961) 1541-1551.

G. Fahy, Cryoprotectant toxicity-Biochemical or osmotic. Cryo-Letters 5 (1984) 79-90.

G. Fahy, The role of nucleation in cryopreservation. Biological Ice Nucleation and its Applications, APS Press, St. Paul (1995) 315-336.

G. Fahy, and A. Karow Jr, Ultrastructure-function correlative studies for cardiac cryopreservation. V. Absence of a correlation between electrolyte toxicity and cryoinjury in the slowly frozen, cryoprotected rat heart. Cryobiology 14 (1977) 418-427.

G.M. Fahy, Cryoprotectant toxicity neutralization. Cryobiology 60 (2010) S45-53.

G.M. Fahy, The relevance of cryoprotectant "toxicity" to cryobiology. Cryobiology 23 (1986) 1-13.

G.M. Fahy, D. Levy, and S. Ali, Some emerging principles underlying the physical properties, biological actions, and utility of vitrification solutions. Cryobiology 24 (1987) 196-213.

G.M. Fahy, T.H. Lilley, H. Linsdell, M.S. Douglas, and H.T. Meryman, Cryoprotectant toxicity and cryoprotectant toxicity reduction: in search of molecular mechanisms. Cryobiology 27 (1990) 247-68.

G.M. Fahy, D.R. MacFarlane, C.A. Angell, and H.T. Meryman, Vitrification as an approach to cryopreservation. Cryobiology 21 (1984) 407-426.

G.M. Fahy, B. Wowk, J. Wu, and S. Paynter, Improved vitrification solutions based on the predictability of vitrification solution toxicity. Cryobiology 48 (2004) 22-35.

G.M. Fahy, B. Wowk, J. Wu, J. Phan, C. Rasch, A. Chang, and E. Zendejas, Cryopreservation of organs by vitrification: perspectives and recent advances. Cryobiology 48 (2004) 157-78.

J. Farrant, Mechanism of cell damage during freezing and thawing and its prevention. Nature 205 (1965) 1284-1287.

J. Farrant, and G.J. Morris, Thermal shock and dilution shock as the causes of freezing injury. Cryobiology 10 (1973) 134-140.

J. Farrant, C.A. Walter, H. Lee, and L.E. McGann, Use of two-step cooling procedures to examine factors influencing cell survival following freezing and thawing. Cryobiology 14 (1977) 273-286.

A.H. Fischer, K.A. Jacobson, J. Rose, and R. Zeller, Hematoxylin and eosin staining of tissue and cell sections. CSH Protocols 2008 (2008) pdb. prot4986.

A.H. Fischer, K.A. Jacobson, J. Rose, and R. Zeller, Paraffin embedding tissue samples for sectioning. CSH Protocols 2008 (2008) pdb. prot4989.

R. Fujisawa, M. Mizuno, H. Katano, K. Otabe, N. Ozeki, K. Tsuji, H. Koga, and I. Sekiya, Cryopreservation in 95% serum with 5% DMSO maintains colony formation and chondrogenic abilities in human synovial mesenchymal stem cells. BMC musculoskeletal disorders 20 (2019) 316-316.

B. Gaber, I. Chandrasekhar, and N. Pattiabiraman, Molecular Modeling of the Interaction of Trehalose with the Phospholipid-Bilayer, Biophysical Journal, BIOPHYSICAL SOCIETY 9650 ROCKVILLE PIKE, BETHESDA, MD 20814-3998, 1986, pp. A435-A435.

S. Giwa, J.K. Lewis, L. Alvarez, R. Langer, A.E. Roth, G.M. Church, J.F. Markmann, D.H. Sachs, A. Chandraker, J.A. Wertheim, M. Rothblatt, E.S. Boyden, E. Eidbo, W.P.A. Lee, B. Pomahac, G. Brandacher, D.M. Weinstock, G. Elliott, D. Nelson, J.P. Acker, K. Uygun, B. Schmalz, B.P. Weegman, A. Tocchio, G.M. Fahy, K.B. Storey, B. Rubinsky, J. Bischof, J.A.W. Elliott, T.K. Woodruff, G.J. Morris, U. Demirci, K.G.M. Brockbank, E.J. Woods, R.N. Ben, J.G. Baust, D. Gao, B. Fuller, Y. Rabin, D.C. Kravitz, M.J. Taylor, and M. Toner, The promise of organ and tissue preservation to transform medicine. Nat Biotechnol 35 (2017) 530-542.

N. Guan, S.A. Blomsma, G.M. Fahy, G.M. Groothuis, and I.A. de Graaf, Analysis of gene expression changes to elucidate the mechanism of chilling injury in precision-cut liver slices. Toxicol In Vitro 27 (2013) 890-9.

E.E. Guibert, L.L. Almada, M.E. Mamprin, C. Bellarosa, M.D. Pizarro, C. Tiribelli, and J.V. Rodriguez, Subzero nonfreezing storage of rat hepatocytes using UW solution and 1, 4-butanediol. II-functional testing on rewarming and gene expression of urea cycle enzymes. Ann Hepatol 8 (2009) 129-133.

A.A. Gurtovenko, and J. Anwar, Modulating the structure and properties of cell membranes: the molecular mechanism of action of dimethyl sulfoxide. J Phys Chem B 111 (2007) 10453-60.

F. Guttman, A. Khalessi, B. Huxley, R. Lee, and G. Savard, Whole organ preservation: I. A technique for in vivo freezing canine intestine using intraarterial helium and ambient nitrogen. Cryobiology 6 (1969) 32-36.

F. Guttman, N. Segal, and J. Borzone, Cryopreservation of canine kidneys with dimethyl sulphoxide: further studies, Organ Preservation II, Churchill Livingstone Edinburgh, 1979, pp. 185.

F.M. Guttman, J. Lizin, P. Robitaille, H. Blanchard, and C. Turgeon-Knaack, Survival of canine kidneys after treatment with dimethyl-sulfoxide, freezing at− 80° C, and thawing by microwave illumination. Cryobiology 14 (1977) 559-567.

T. Hagiwara, R.W. Hartel, and S. Matsukawa, Relationship between recrystallization rate of ice crystals in sugar solutions and water mobility in freeze-concentrated matrix. Food Biophys 1 (2006) 74-82.

R. Hamilton, H.I. Holst, and H.B. Lehr, Successful preservation of canine small intestine by freezing. J Surg Res 14 (1973) 313-8.

T. Hansen, Glycerol content and cold-hardiness in freeze tolerant insects. Eesti. NSV. Tead. Akad. Tiom. Biol 29 (1980) 113-118.

C.L. Harris, M. Toner, A. Hubel, E.G. Cravalho, M.L. Yarmush, and R.G. Tompkins, Cryopreservation of isolated hepatocytes: Intracellular ice formation under various chemical and physical conditions. Cryobiology 28 (1991) 436-444.

M. Hasan, A.E. Fayter, and M.I. Gibson, Ice Recrystallization Inhibiting Polymers Enable Glycerol-Free Cryopreservation of Microorganisms. Biomacromolecules 19 (2018) 3371-3376.

P.H. Hayashi, D.A. Axelrod, J. Galanko, P.R. Salvalaggio, and M. Schnitzler, Regional differences in deceased donor liver transplantation and their implications for organ utilization and allocation. Clinical transplantation 25 (2011) 156-163.

J. Hey, and D. MacFarlane, Crystallization of ice in aqueous solutions of glycerol and dimethyl sulfoxide. 1. A comparison of mechanisms. Cryobiology 33 (1996) 205-216.

J.M. Hey, and D.R. Macfarlane, Crystallization of ice in aqueous solutions of glycerol and dimethyl sulfoxide 2: Ice crystal growth kinetics. Cryobiology 37 (1998) 119-130.

A.Z. Higgins, and J.O. Karlsson, Effects of intercellular junction protein expression on intracellular ice formation in mouse insulinoma cells. Biophys J 105 (2013) 2006-15.

P.V. Hobbs, Ice physics, Oxford university press, 2010.

H. Huang, M.L. Yarmush, and O.B. Usta, Long-term deep-supercooling of large-volume water and red cell suspensions via surface sealing with immiscible liquids. Nat Commun 9 (2018) 3201.

R.C. Huebert, and V.H. Shah, Hepatic Sinusoidal Endothelial Cells. in: J.-F. Dufour, and P.-A. Clavien, (Eds.), Signaling Pathways in Liver Diseases, Springer Berlin Heidelberg, Berlin, Heidelberg, 2010, pp. 79-91.

Z.E. Hughes, A.E. Mark, and R.L. Mancera, Molecular dynamics simulations of the interactions of DMSO with DPPC and DOPC phospholipid membranes. J Phys Chem B 116 (2012) 11911-23.

C. Hunt, Studies on cellular structure and ice location in frozen organs and tissues: the use of freeze-substitution and related techniques. Cryobiology 21 (1984) 385-402.

D. Irimia, and J.O. Karlsson, Kinetics and mechanism of intercellular ice propagation in a micropatterned tissue construct. Biophys J 82 (2002) 1858-68.

H. Ishiguro, and B. Rubinsky, Mechanical interactions between ice crystals and red blood cells during directional solidification. Cryobiology 31 (1994) 483-500.

N. Ishine, B. Rubinsky, and C.Y. Lee, A histological analysis of liver injury in freezing storage. Cryobiology 39 (1999) 271-7.

N. Ishine, B. Rubinsky, and C.Y. Lee, Transplantation of mammalian livers following freezing: vascular damage and functional recovery. Cryobiology 40 (2000) 84-9.

C. J, M. Doshi, and R. N, Ice Recrystallization Inhibitors: From Biological Antifreezes to Small Molecules, 2013.

K. Jackson, and B. Chalmers, Freezing of liquids in porous media with special reference to frost heave in soils. Journal of Applied Physics 29 (1958) 1178-1181.

S.W. Jacob, Studies in organ preservation by actual freezing and reduction of the freezing point. Cryobiology 1 (1964) 176-80.

I.A. Jacobsen, and D.E. Pegg, Cryopreservation of organs: a review. Cryobiology 21 (1984) 377-84.

I.A. Jacobsen, D.E. Pegg, H. Starklint, J. Chemnitz, C. Hunt, P. Barfort, and M.P. Diaper, Effect of cooling and warming rate on glycerolized rabbit kidneys. Cryobiology 21 (1984) 637-53.

S. Jahan, M.K. Adam, J.K. Manesia, E. Doxtator, R.N. Ben, and N. Pineault, Inhibition of ice recrystallization during cryopreservation of cord blood grafts improves platelet engraftment. Transfusion 60 (2020) 769-778.

I. Jochmans, C. Moers, J.M. Smits, H.G. Leuvenink, J. Treckmann, A. Paul, A. Rahmel, J.P. Squifflet, E. van Heurn, D. Monbaliu, R.J. Ploeg, and J. Pirenne, Machine perfusion versus cold storage for the preservation of kidneys donated after cardiac death: a multicenter, randomized, controlled trial. Ann Surg 252 (2010) 756-64.

J.O. Karlsson, Effects of solution composition on the theoretical prediction of ice nucleation kinetics and thermodynamics. Cryobiology 60 (2010) 43-51.

J.O. Karlsson, E.G. Cravalho, I.H. Borel Rinkes, R.G. Tompkins, M.L. Yarmush, and M. Toner, Nucleation and growth of ice crystals inside cultured hepatocytes during freezing in the presence of dimethyl sulfoxide. Biophys J 65 (1993) 2524-36.

J.O.M. Karlsson, Effects of solution composition on the theoretical prediction of ice nucleation kinetics and thermodynamics. Cryobiology 60 (2010) 43-51.

J.O.M. Karlsson, and M. Toner, Long-term storage of tissues by cryopreservation: Critical issues. Biomaterials (1996).

K. Khosla, L. Zhan, A. Bhati, A. Carley-Clopton, M. Hagedorn, and J. Bischof, Characterization of Laser Gold Nanowarming: A Platform for Millimeter-Scale Cryopreservation. Langmuir 35 (2019) 7364-7375.

P. Klinmalai, M. Shibata, and T. Hagiwara, Recrystallization of ice crystals in trehalose solution at isothermal condition. Food Biophysics 12 (2017) 404-411.

C.A. Knight, and J.G. Duman, Inhibition of recrystallization of ice by insect thermal hysteresis proteins: A possible cryoprotective role. Cryobiology 23 (1986) 256-262.

C.A. Knight, J. Hallett, and A. DeVries, Solute effects on ice recrystallization: an assessment technique. Cryobiology 25 (1988) 55-60.

C.A. Knight, D. Wen, and R.A. Laursen, Nonequilibrium antifreeze peptides and the recrystallization of ice. Cryobiology 32 (1995) 23-34.

B. Korniski, and A. Hubel, A model of low-temperature water transport for hepatocyte spheroids. Ann N Y Acad Sci 858 (1998) 183-90.

E. Kristiansen, and K.E. Zachariassen, The mechanism by which fish antifreeze proteins cause thermal hysteresis, 2005.

S. Kubota, F. Graham, B.G. Crabo, R.C. Lillehei, and R.H. Dietman, The effect of freeze rate, duration of phase transition, and warming rate on survival of frozen canine kidneys. Cryobiology 13 (1976) 455-62.

A. Larese, J. Acker, K. Muldrew, H. Yang, and L. McGann, Antifreeze proteins induce intracellular nucleation. Cryo-Letters 17 (1996) 175-182.

A. Larese, H. Yang, A. Petrenko, and L. McGann, Intracellular ice formation is affected by cell-to-cell contact. Cryobiology 29 (1992) 728.

L. Lautner, N. William, and J.P. Acker, High subzero cryofixation: A technique for observing ice within tissues. Cryobiology 95 (2020) 116-122.

J.R. Layne, Jr., J.P. Costanzo, and R.E. Lee, Jr., Freeze duration influences postfreeze survival in the frog Rana sylvatica. J Exp Zool 280 (1998) 197-201.

J.R. Layne Jr, and R.E. Lee Jr, Freeze tolerance and the dynamics of ice formation in wood frogs (Rana sylvatica) from southern Ohio. Can J Zool 65 (1987) 2062-2065.

R.E. Lee, G.J. Warren, and L.V. Gusta, Biological ice nucleation and its applications, APS Press, St. Paul, Minn., 1995.

R. Levin, E. Cravalho, and C. Huggins, Water transport in a cluster of closely packed erythrocytes at subzero temperatures. Cryobiology 14 (1977) 549-558.

J.K. Lewis, J.C. Bischof, I. Braslavsky, K.G. Brockbank, G.M. Fahy, B.J. Fuller, Y. Rabin, A. Tocchio, E.J. Woods, B.G. Wowk, J.P. Acker, and S. Giwa, The Grand Challenges of Organ Banking: Proceedings from the first global summit on complex tissue cryopreservation. Cryobiology 72 (2016) 169-82.

I.M. Lifshitz, and V.V. Slyozov, The kinetics of precipitation from supersaturated solid solutions. J Phys Chem Sol 19 (1961) 35-50.

S. Liu, and R.N. Ben, C-linked galactosyl serine AFGP analogues as potent recrystallization inhibitors. Organic letters 7 (2005) 2385-2388.

W.P. Liu, A.L. Humphries, Jr., R. Russell, L.D. Stoddard, and W.H. Moretz, 48-hour storage of canine kidneys after brief perfusion with Collins' solution. Ann Surg 173 (1971) 748-57.

X. Liu, G. Zhao, Z. Shu, D. Niu, Z. Zhang, P. Zhou, Y. Cao, and D. Gao, Quantification of intracellular ice formation and recrystallization during freeze–thaw cycles and their relationship with the viability of pig iliac endothelium cells. Biopres Biobank 14 (2016) 511-519.

H. Lodish, A. Berk, S.L. Zipursky, P. Matsudaira, D. Baltimore, and J. Darnell, Intracellular ion environment and membrane electric potential, Molecular Cell Biology. 4th edition, WH Freeman, 2000.

S.H. Loomis, Seasonal changes in the freezing tolerance of the intertidal pulmonate gastropod Melampus bidentatus Say. Can J Zool 63 (1985) 2021-2025.

P.A. Lotke, and M.F. Dolan, Thermoelectric cooler for whole organ freezing and thawing. Cryobiology 1 (1965) 289-91.

J.E. Lovelock, Het mechanism of the protective action of glycerol against haemolysis by freezing and thawing. Bioch Biophys Acta 11 (1953) 28-36.

J.E. Lovelock, and M.W. Bishop, Prevention of freezing damage to living cells by dimethyl sulphoxide. Nature 183 (1959) 1394-5.

C.H. Lowe, P.J. Lardner, and E.A. Halpern, Supercooling in reptiles and other vertebrates. Comp Biochem Physiol A 39 (1971) 125-35.

B. Luyet, D. Rasmussen, and C. Kroener, Successive crystallization and recrystallization, during rewarming, of rapidly cooled solutions of glycerol and ethylene glycol. Biodynamica 10 (1966) 53-60.

F. Lv, B. Liu, W. Li, and G.K. Jaganathan, Devitrification and recrystallization of nanoparticle-containing glycerol and PEG-600 solutions. Cryobiology 68 (2014) 84-90.

D. MacArthur, and J. Dandy, Physiological aspects of overwintering in the boreal chorus frog (Pseudacris triseriata maculata). Comp Biochem Physiol A 72 (1982) 137-141.

A. MacKenzie, Death of frozen yeast in the course of slow warming, Ciba Foundation Symposium-The Frozen Cell, Wiley Online Library, 1970, pp. 89-96.

N. Manuchehrabadi, Z. Gao, J. Zhang, H.L. Ring, Q. Shao, F. Liu, M. McDermott, A. Fok, Y. Rabin, K.G. Brockbank, M. Garwood, C.L. Haynes, and J.C. Bischof, Improved tissue cryopreservation using inductive heating of magnetic nanoparticles. Sci Transl Med 9 (2017) eaah4586.

V. Marin, G. Kaplanski, S. Gres, C. Farnarier, and P. Bongrand, Endothelial cell culture: protocol to obtain and cultivate human umbilical endothelial cells. J Immunol Methods 254 (2001) 183-90.

M.N. Martino, and N.E. Zaritzky, Ice recrystallization in a model system and in frozen muscle tissue. Cryobiology 26 (1989) 138-48.

J. Matheny, A.M. Karow Jr, and O. Carrier Jr, Toxicity of dimethyl sulfoxide and magnesium as a function of temperature. Eur J Pharmacol 5 (1969) 209-212.

S.F. Mathias, F. Franks, and R.H. Hatley, Preservation of viable cells in the undercooled state. Cryobiology 22 (1985) 537-46.

N. Matsumoto, H. Yoshizawa, H. Kagamu, T. Abe, N. Fujita, S. Watanabe, H. Kuriyama, T. Ishiguro, J. Tanaka, and E. Suzuki, Successful liquid storage of peripheral blood stem cells at subzero non-freezing temperature. Bone Marrow Transplant 30 (2002) 777-784.

P. Mazur, 2. Roles of intracellular ice formation, vitrification of cell water, and recrystallization of intracellular ice on the survival of mouse embryos and oocytes. Cryobiology 65 (2012) 339.

P. Mazur, Causes of Injury in Frozen and Thawed Cells. Fed Proc 24 (1965) S175-82.

P. Mazur, Cryobiology: The freezing of biological systems. Science (1970) 403-506

P. Mazur, Equilibrium, quasi-equilibrium, and nonequilibrium freezing of mammalian embryos. Cell Biophys 17 (1990) 53-92.

P. Mazur, Freezing of living cells: mechanisms and implications. Am J Physiol 247 (1984) C125-42.

P. Mazur, Kinetics of water loss from cells at subzero temperatures and the likelihood of intracellular freezing. J Gen Physiol 47 (1963) 347-69.

P. Mazur, Physical-chemical basis of injury from intracellular freezing in yeast. Cellular Injury and Resistance in Freezing Organisms : proceedings 2 (1967) 171-189.

P. Mazur, Principles of cryobiology. Life in the frozen state (1984).

P. Mazur, The role of cell membranes in the freezing of yeast and other single cells. Ann N Y Acad Sci 125 (1965) 658-76.

P. Mazur, The role of intracellular freezing in the death of cells cooled at supraoptimal rates. Cryobiology 14 (1977) 251-272.

P. Mazur, and K.W. Cole, Influence of cell concentration on the contribution of unfrozen fraction and salt concentration to the survival of slowly frozen human erythrocytes. Cryobiology 22 (1985) 509-536.

P. Mazur, S.P. Leibo, and E.H. Chu, A two-factor hypothesis of freezing injury. Evidence from Chinese hamster tissue-culture cells. Exp Cell Res 71 (1972) 345-55.

P. Mazur, and R.H. Miller, Survival of frozen-thawed human red cells as a function of the permeation of glycerol and sucrose. Cryobiology 13 (1976) 523-536.

P. Mazur, W.F. Rall, and N. Rigopoulos, Relative contributions of the fraction of unfrozen water and of salt concentration to the survival of slowly frozen human erythrocytes. Biophys J 36 (1981) 653-75.

P. Mazur, and N. Rigopoulos, Contributions of unfrozen fraction and of salt concentration to the survival of slowly frozen human erythrocytes: influence of warming rate. Cryobiology 20 (1983) 274-89.

L.E. McGann, Differing actions of penetrating and nonpenetrating cryoprotective agents. Cryobiology 15 (1978) 382-90.

H. Mergental, M.T. Perera, R.W. Laing, P. Muiesan, J.R. Isaac, A. Smith, B.T. Stephenson, H. Cilliers, D.A. Neil, S.G. Hubscher, S.C. Afford, and D.F. Mirza, Transplantation of Declined Liver Allografts Following Normothermic Ex-Situ Evaluation. Am J Transplant 16 (2016) 3235-3245.

H.T. Meryman, Cryopreservation of living cells: principles and practice. Transfusion 47 (2007) 935-45.

H.T. Meryman, Osmotic stress as a mechanism of freezing injury. Cryobiology 8 (1971) 489-500.

E. Metzen, M. Wolff, J. Fandrey, and W. Jelkmann, Pericellular PO2 and O2 consumption in monolayer cell cultures. Respir Physiol 100 (1995) 101-6.

M. Milenkovic, C. Diaz-Garcia, A. Wallin, and M. Brannstrom, Viability and function of the cryopreserved whole rat ovary: comparison between slow-freezing and vitrification. Fertil Steril 97 (2012) 1176-82.

L. Miller, and J. Smith, Production of threitol and sorbitol by an adult insect: association with freezing tolerance. Nature 258 (1975) 519-520.

L.K. Miller, and J.S. Smith, Production of threitol and sorbitol by an adult insect: association with freezing tolerance. Nature 258 (1975) 519-20.

R.H. Miller, and P. Mazur, Survival of frozen-thawed human red cells as a function of cooling and warming velocities. Cryobiology 13 (1976) 404-414.

C. Moers, J. Pirenne, A. Paul, R.J. Ploeg, and G. Machine Preservation Trial Study, Machine perfusion or cold storage in deceased-donor kidney transplantation. N Engl J Med 366 (2012) 770-1.

C. Moers, J.M. Smits, M.H. Maathuis, J. Treckmann, F. van Gelder, B.P. Napieralski, M. van Kasterop-Kutz, J.J. van der Heide, J.P. Squifflet, E. van Heurn, G.R. Kirste, A. Rahmel, H.G. Leuvenink, A. Paul, J. Pirenne, and R.J. Ploeg, Machine perfusion or cold storage in deceased-donor kidney transplantation. N Engl J Med 360 (2009) 7-19.

G. Moray, S. Sevmis, F. Karakayali, S. Gorur, and M. Haberal, Comparison of histidine-tryptophan-ketoglutarate and University of Wisconsin in living-donor liver transplantation, Transplantation proceedings, Elsevier, 2006, pp. 3572-3575.

G.S. Moss, P. Reed, and A.G. Riddell, Observations on the effects of glycerol on the cold storage of the canine liver. J Surg Res 6 (1966) 147-51.

K. Muldrew, M. Hurtig, K. Novak, N. Schachar, and L.E. McGann, Localization of freezing injury in articular cartilage. Cryobiology 31 (1994) 31-8.

K. Muldrew, and L.E. McGann, Mechanisms of intracellular ice formation. Biophys J 57 (1990) 525-32.

K. Muldrew, and L.E. McGann, The osmotic rupture hypothesis of intracellular freezing injury. Biophys J 66 (1994) 532-41.

K. Muldrew, K. Novak, H. Yang, R. Zernicke, N.S. Schachar, and L.E. McGann, Cryobiology of articular cartilage: ice morphology and recovery of chondrocytes. Cryobiology 40 (2000) 102-9.

D.J. Murphy, Freezing resistance in intertidal invertebrates. Annu Rev Physiol 45 (1983) 289-99.

T. Nei, Mechanism of hemolysis of erythrocytes by freezing at near-zero temperatures: I. Microscopic observation of hemolyzing erythrocytes during the freezing and thawing process. Cryobiology 4 (1967) 153-156.

N. Nikon, Elements Advanced Research, 2014. User's Guide-ver 4.

J. O'Brien, I. Wilson, T. Orton, and F. Pognan, Investigation of the Alamar Blue (resazurin) fluorescent dye for the assessment of mammalian cell cytotoxicity. Eur J Biochem 267 (2000) 5421-6.

J.M. O'Callaghan, S.R. Knight, R.D. Morgan, and P.J. Morris, Preservation solutions for static cold storage of kidney allografts: a systematic review and meta-analysis. Am J Transplant 12 (2012) 896-906.

L.L. Olijve, K. Meister, A.L. DeVries, J.G. Duman, S. Guo, H.J. Bakker, and I.K. Voets, Blocking rapid ice crystal growth through nonbasal plane adsorption of antifreeze proteins. Proc Nat Acad Sci 113 (2016) 3740-3745.

E.S. Orman, M.E. Mayorga, S.B. Wheeler, R.M. Townsley, H.H. Toro-Diaz, P.H. Hayashi, and A.S.t. Barritt, Declining liver graft quality threatens the future of liver transplantation in the United States. Liver Transpl 21 (2015) 1040-50.

E. Ozcinar, E.N. Okatan, E. Tuncay, S. Eryilmaz, and B. Turan, Improvement of functional recovery of donor heart following cold static storage with doxycycline cardioplegia. Cardiovasc Toxicol 14 (2014) 64-73.

P.V. Pazhayannur, and J.C. Bischof, Measurement and simulation of water transport during freezing in mammalian liver tissue. J Biomech Eng 119 (1997) 269-77.

D.E. Pegg, Ice crystals in tissues and organs, The biophysics of organ cryopreservation, Springer, 1987, pp. 117-140.

D.E. Pegg, -Principles of Cryopreservation, Preservation of Human oocytes, CRC Press, 2009, pp. 34-46.

D.E. Pegg, The relevance of ice crystal formation for the cryopreservation of tissues and organs. Cryobiology 60 (2010) S36-44.

D.E. Pegg, M.P. Diaper, H.L. Skaer, and C.J. Hunt, The effect of cooling rate and warming rate on the packing effect in human erythrocytes frozen and thawed in the presence of 2 M glycerol. Cryobiology 21 (1984) 491-502.

D.E. Pegg, C.J. Green, and C.A. Walter, Attempted canine renal cryopreservation using dimethyl sulphoxide helium perfusion and microwave thawing. Cryobiology 15 (1978) 618-626.

D.E. Pegg, I.A. Jacobsen, M.P. Diaper, and J. Foreman, The effect of cooling and warming rate on cortical cell function of glycerolized rabbit kidneys. Cryobiology 21 (1984) 529-35.

D.E. Pegg, and A.M. Karow Jr, The biophysics of organ cryopreservation, Springer Science & Business Media, 2012.

D.E. Pegg, L. Wang, and D. Vaughan, Cryopreservation of articular cartilage. Part 3: the liquidus-tracking method. Cryobiology 52 (2006) 360-8.

D.E. Pegg, L. Wang, D. Vaughan, and C.J. Hunt, Cryopreservation of articular cartilage. Part 2: mechanisms of cryoinjury. Cryobiology 52 (2006) 347-359.

J.S. Poisson, J.P. Acker, J.G. Briard, J.E. Meyer, and R.N. Ben, Modulating Intracellular Ice Growth with Cell-Permeating Small-Molecule Ice Recrystallization Inhibitors. Langmuir 35 (2018) 7452-7458.

J.S. Poisson, J.G. Briard, T.R. Turner, J.P. Acker, and R.N. Ben, Hydroxyethyl Starch Supplemented with Ice Recrystallization Inhibitors Greatly Improves Cryopreservation of Human Red Blood Cells. Bioproc J 15 (2016).

C. Polge, A.U. Smith, and A.S. Parkes, Revival of spermatozoa after vitrification and dehydration at low temperatures. Nature 164 (1949) 666.

G.A. Pollock, D.E. Pegg, and I.R. Hardie, An isolated perfused rat mesentery model for direct observation of the vasculature during cryopreservation. Cryobiology 23 (1986) 500-511.

P. Popovic, and V. Popovic, Survival of newborn ground squirrels after supercooling or freezing. Am J Physiol 204 (1963) 949-52.

M.J. Powell-Palm, Y. Zhang, J. Aruda, and B. Rubinsky, Isochoric conditions enable high subfreezing temperature pancreatic islet preservation without osmotic cryoprotective agents. Cryobiology 86 (2019) 130-133.

P.D. Pudney, S.L. Buckley, C.M. Sidebottom, S.N. Twigg, M.P. Sevilla, C.B. Holt, D. Roper, J.H. Telford, A.J. McArthur, and P.J. Lillford, The physico-chemical characterization of a boiling stable antifreeze protein from a perennial grass (Lolium perenne). Arch Biochem Biophys 410 (2003) 238-45.

E. Puschmann, C. Selden, S. Butler, and B. Fuller, Liquidus tracking: controlled rate vitrification for the cryopreservation of larger volumes and tissues. Cryo Letters 35 (2014) 345-55.

E. Puschmann, C. Selden, S. Butler, and B. Fuller, Liquidus Tracking: Large scale preservation of encapsulated 3-D cell cultures using a vitrification machine. Cryobiology 76 (2017) 65-73.

C. Puts, T. Berendsen, B. Bruinsma, S. Ozer, M. Luitje, O.B. Usta, M. Yarmush, and K. Uygun, Polyethylene glycol protects primary hepatocytes during supercooling preservation. Cryobiology 71 (2015) 125-129.

P.J. Quinn, A lipid-phase separation model of low-temperature damage to biological membranes. Cryobiology 22 (1985) 128-46.

A.T. Rahman, T. Arai, A. Yamauchi, A. Miura, H. Kondo, Y. Ohyama, and S. Tsuda, Ice recrystallization is strongly inhibited when antifreeze proteins bind to multiple ice planes. Sci Rep 9 (2019) 1-9.

W.F. Rall, and J. Farrant, Slow warming injury to mouse embryos: Dissociation between the formation of intracellular ice and injury. Cryobiology 16 (1979) 589-589.

W.F. Rall, D.S. Reid, and J. Farrant, Innocuous biological freezing during warming. Nature 286 (1980) 511-514.

G. Rapatz, L. Menz, and B. Luyet, Anatomy of the freezing process in biological materials. Cryobiology 3 (1966) 139-162.

D.H. Rasmussen, M.N. Macaulay, and A.P. MacKenzie, Supercooling and nucleation of ice in single cells. Cryobiology 12 (1975) 328-39.

F. Riemann, M. Schrage, and H. Farke, High freezing tolerance of marine nematodes from intertidal sediments of the German Bight. Nematologica 30 (1984) 452-456.

J.V. Rodríguez, L.L. Almada, M.E. Mamprin, E.E. Guibert, and G. Furno, Subzero nonfreezing storage of rat hepatocytes using modified University of Wisconsin solution (mUW) and 1, 4-butanediol. I-effects on cellular metabolites during cold storage. Ann Hepatol 8 (2009) 57-62.

B. Rubinsky, A. Arav, and G.L. Fletcher, Hypothermic protection - A fundamental property of "Antifreeze" proteins. Biochem Biophys Res Comm 180 (1991) 566-571.

B. Rubinsky, A. Arav, J.S. Hong, and C.Y. Lee, Freezing of mammalian livers with glycerol and antifreeze proteins. Biochem Biophys Res Commun 200 (1994) 732-741.

B. Rubinsky, A. Arav, M. Mattioli, and A.L. Devries, The effect of antifreeze glycopeptides on membrane potential changes at hypothermic temperatures. Biochem Biophys Res Commun 173 (1990) 1369-1374.

B. Rubinsky, E.G. Cravalho, and B. Mikic, Thermal stresses in frozen organs. Cryobiology 17 (1980) 66-73.

B. Rubinsky, and M. Ikeda, A cryomicroscope using directional solidification for the controlled freezing of biological material. Cryobiology 22 (1985) 55-68.

B. Rubinsky, C.Y. Lee, J. Bastacky, and G. Onik, The process of freezing and the mechanism of damage during hepatic cryosurgery. Cryobiology 27 (1990) 85-97.

B. Rubinsky, M. Mattioli, A. Arav, B. Barboni, and G.L. Fletcher, Inhibition of Ca2+ and K+ currents by "antifreeze" proteins. Am J Physiol 262 (1992) R542-5.

B. Rubinsky, D. Pegg, and R.Y. Calne, A mathematical model for the freezing process in biological tissue. Proceedings of the Royal Society of London. Series B. Biological Sciences 234 (1988) 343-358.

B. Rubinsky, and D.E. Pegg, A mathematical model for the freezing process in biological tissue. Proc R Soc Lond B Biol Sci 234 (1988) 343-58.

B. Rubinsky, S. Wong, J. Hong, J. Gilbert, M. Roos, and K.B. Storey, 1H magnetic resonance imaging of freezing and thawing in freeze-tolerant frogs. m J Physiol Regul Integr Comp Physiol 266 (1994) R1771-R1777.

A.S. Rudolph, and J.H. Crowe, Membrane stabilization during freezing: the role of two natural cryoprotectants, trehalose and proline. Cryobiology 22 (1985) 367-77.

A.S. Rudolph, J.H. Crowe, and L.M. Crowe, Effects of three stabilizing agents—proline, betaine, and trehalose—on membrane phospholipids. Arch Biochem Biophys 245 (1986) 134-143.

T. Rutt, N. Eskandari, M. Zhurova, J.A. Elliott, L.E. McGann, J.P. Acker, and J.A. Nychka, Thermal expansion of substrate may affect adhesion of Chinese hamster fibroblasts to surfaces during freezing. Cryobiology 86 (2019) 134-139.

A. Sakai, Some factors contributing to the survival of rapidly cooled plant cells. Cryobiology 8 (1971) 225-234.

A. Sakai, and K. Otsuka, Survival of plant tissue at super-low temperatures v. An electron microscope study of ice in cortical cells cooled rapidly. Plant Physiol 42 (1967) 1680-94.

O.Y. Sally, A. Brown, A.J. Middleton, M.M. Tomczak, V.K. Walker, and P.L. Davies, Ice restructuring inhibition activities in antifreeze proteins with distinct differences in thermal hysteresis. Cryobiology 61 (2010) 327-334.

J.D. Scandling, S. Busque, J.A. Shizuru, E.G. Engleman, and S. Strober, Induced immune tolerance for kidney transplantation. N Engl J Med 365 (2011) 1359-60.

W.D. Schmid, Survival of frogs in low temperature. Science 215 (1982) 697-8.

G.J. Schwartz, and K.R. Diller, Intracellular freezing of human granulocytes. Cryobiology 21 (1984) 654-60.

S. Seki, and P. Mazur, Effect of warming rate on the survival of vitrified mouse oocytes and on the recrystallization of intracellular ice. Biol Reprod 79 (2008) 727-37.

R.A. Shaw, A.J. Durant, and Y. Mi, Heterogeneous surface crystallization observed in undercooled water. J Phys Chem B 109 (2005) 9865-8.

A. Sicular, and F.D. Moore, The postmortem survival of tissues: the effect of time and temperature on the survival of liver as measured by glucose oxidation rate. J Surg Res 1 (1961) 16-22.

L. Sømme, Supercooling and winter survival in terrestrial arthropods. Comparative Biochemistry and Physiology Part A: Physiology 73 (1982) 519-543.

Y.C. Song, Y.H. An, Q.K. Kang, C. Li, J.M. Boggs, Z. Chen, M.J. Taylor, and K.G. Brockbank, Vitreous preservation of articular cartilage grafts. J Invest Surg 17 (2004) 65-70.

Y.C. Song, P.O. Hagen, F.G. Lightfoot, M.J. Taylor, A.C. Smith, and K.G. Brockbank, In vivo evaluation of the effects of a new ice-free cryopreservation process on autologous vascular grafts. J Invest Surg 13 (2000) 279-88.

Y.C. Song, B.S. Khirabadi, F. Lightfoot, K.G. Brockbank, and M.J. Taylor, Vitreous cryopreservation maintains the function of vascular grafts. Nat Biotechnol 18 (2000) 296-9.

J.P. Stegemann, H. Hong, and R.M. Nerem, Mechanical, biochemical, and extracellular matrix effects on vascular smooth muscle cell phenotype. J Appl Physiol (1985) 98 (2005) 2321-7.

R. Steinbrecht, Recrystallization and ice-crystal growth in a biological specimen, as shown by a simple freeze substitution method. J Microsc 140 (1985) 41-46.

P. Steponkus, and M. Dowgert, Phenomenology of intracellular ice nucleation in isolated protoplasts. Plant Physiol 67 (1981) S, 58.

P.L. Steponkus, Role of the plasma membrane in freezing injury and cold acclimation. Annual Review of Plant Physiology 35 (1984) 543-584.

P.L. Steponkus, M.F. Dowgert, and W.J. Gordon-Kamm, Destabilization of the plasma membrane of isolated plant protoplasts during a freeze-thaw cycle: the influence of cold acclimation. Cryobiology 20 (1983) 448-65.

J.M. Storey, and K.B. Storey, Triggering of cryoprotectant synthesis by the initiation of ice nucleation in the freeze tolerant frog, Rana sylvatica. J Comp Phys B 156 (1985) 191-195.

K.B. Storey, Freeze tolerance in the frog,Rana sylvatica. Experientia 40 (1984) 1261-1262.

K.B. Storey, J. Bischof, and B. Rubinsky, Cryomicroscopic analysis of freezing in liver of the freeze-tolerant wood frog. Am J Physiol 263 (1992) R185-94.

K.B. Storey, and J.M. Storey, Freeze tolerance in animals. Physiol Rev 68 (1988) 27-84.

K.B. Storey, and J.M. Storey, Freeze tolerant frogs: cryoprotectants and tissue metabolism during freeze–thaw cycles. Can J Zool 64 (1986) 49-56.

K.B. Storey, and J.M. Storey, Natural Freezing Survival in Animals. Annual Review of Ecology and Systematics 27 (1996) 365-386.

S.L. Stott, and J.O.M. Karlsson, 29. Cell perimeter modulates the kinetics of intracellular ice formation and frequency of paracellular ice formation in micropatterned endothelial cells. Cryobiology 53 (2006) 379-380.

S.L. Stott, and J.O.M. Karlsson, Visualization of intracellular ice formation using high-speed video cryomicroscopy. Cryobiology 58 (2009) 84-95.

R.L. Sutton, A. Lips, G. Piccirillo, and A. Sztehlo, Kinetics of ice recrystallization in aqueous fructose solutions. Journal of food science 61 (1996) 741-745.

E.A. Szurek, and A. Eroglu, Comparison and avoidance of toxicity of penetrating cryoprotectants. PLoS One 6 (2011) e27604.

R.Y. Tam, S.S. Ferreira, P. Czechura, R.N. Ben, and J.L. Chaytor, Hydration index-a better parameter for explaining small molecule hydration in inhibition of ice recrystallization. Journal of the American Chemical Society (2008).

R.Y. Tam, S.S. Ferreira, P. Czechura, J.L. Chaytor, and R.N. Ben, Hydration index-a better parameter for explaining small molecule hydration in inhibition of ice recrystallization. J Am Chem Soc 130 (2008) 17494-17501.

M. Taylor, and D. Pegg, The effect of ice formation on the function of smooth muscle tissue following storage at− 21 C and− 60 C. Cryobiology 20 (1982) 36-40.

M. Taylor, Y. Song, K. Brockbank, B. Fuller, N. Lane, and E. Benson, 22 Vitrification in Tissue Preservation: New Developments. Life in the Frozen State, BJ Fuller, N. Lane, and EE Benson, eds., CRC Press, Boca Raton, FL (2004) 604-641.

M.J. Taylor, B.P. Weegman, S.C. Baicu, and S.E. Giwa, New Approaches to Cryopreservation of Cells, Tissues, and Organs. Transfusion medicine and hemotherapy : offizielles Organ der Deutschen Gesellschaft fur Transfusionsmedizin und Immunhamatologie 46 (2019) 197-215.

S.N. Tessier, S.E.J. Cronin, C.A. Pendexter, S. Özer, R.J. de Vries, S. Nagpal, P.D. Banik, K. Uygun, and M. Toner, Partial freezing: A nature-inspired strategy for organ banking. Cryobiology 81 (2018) 220.

S.N. Tessier, L. Weng, W.D. Moyo, S.H. Au, K.H.K. Wong, C. Angpraseuth, A.E. Stoddard, C. Lu, L.T. Nieman, R.D. Sandlin, K. Uygun, S.L. Stott, and M. Toner, Effect of Ice Nucleation and Cryoprotectants during High Subzero-Preservation in Endothelialized Microchannels. ACS Biomater Sci Eng 4 (2018) 3006-3015.

W. Thomson, LX. On the equilibrium of vapour at a curved surface of liquid. The London, Edinburgh, and Dublin Philosophical Magazine and Journal of Science 42 (2009) 448-452.

R.M.F. Tomas, T.L. Bailey, M. Hasan, and M.I. Gibson, Extracellular Antifreeze Protein Significantly Enhances the Cryopreservation of Cell Monolayers. Biomacromolecules 20 (2019) 3864-3872.

M. Toner, E.G. Cravalho, and M. Karel, Thermodynamics and kinetics of intracellular ice formation during freezing of biological cells. J App Phys 67 (1990) 1582-1593.

J. Treckmann, C. Moers, J.M. Smits, A. Gallinat, M.H. Maathuis, M. van Kasterop-Kutz, I. Jochmans, J.J. Homan van der Heide, J.P. Squifflet, E. van Heurn, G.R. Kirste, A. Rahmel, H.G. Leuvenink, J. Pirenne, R.J. Ploeg, and A. Paul, Machine perfusion versus cold storage for preservation of kidneys from expanded criteria donors after brain death. Transpl Int 24 (2011) 548-54.

R.G. Van Buskirk, Viability and functional assays used to assess preservation efficacy: the multiple endpoint/tier approach. Advances in Biopreservation (2006) 123-141.

J. van der Elsken, J. Dings, and J.C.F. Michielsen, The freezing of supercooled water. J Mol Struct 250 (1991) 245-251.

M. Verheijen, M. Lienhard, Y. Schrooders, O. Clayton, R. Nudischer, S. Boerno, B. Timmermann, N. Selevsek, R. Schlapbach, H. Gmuender, S. Gotta, J. Geraedts, R. Herwig, J. Kleinjans, and F. Caiment, DMSO induces drastic changes in human cellular processes and epigenetic landscape in vitro. Sci Rep 9 (2019) 4641.

C. Wagner, Theorie der alterung von niederschlägen durch umlösen (Ostwald-reifung). Zeitschrift für Elektrochemie, Berichte der Bunsengesellschaft für physikalische Chemie 65 (1961) 581-591.

J.A. Wahlberg, J.H. Southard, and F.O. Belzer, Development of a cold storage solution for pancreas preservation. Cryobiology 23 (1986) 477-82.

K.R. Walters, Jr., A.S. Serianni, Y. Voituron, T. Sformo, B.M. Barnes, and J.G. Duman, A thermal hysteresis-producing xylomannan glycolipid antifreeze associated with cold tolerance is found in diverse taxa. J Comp Physiol B 181 (2011) 631-40.

L. Wang, D.E. Pegg, J. Lorrison, D. Vaughan, and P. Rooney, Further work on the cryopreservation of articular cartilage with particular reference to the liquidus tracking (LT) method. Cryobiology 55 (2007) 138-147.

Z. Wang, B. He, Y. Duan, Y. Shen, L. Zhu, X. Zhu, and Z. Zhu, Cryopreservation and replantation of amputated rat hind limbs. Eur J Med Res 19 (2014) 28.

G. Warnecke, D. Van Raemdonck, M.A. Smith, G. Massard, J. Kukreja, F. Rea, G. Loor, F. De Robertis, J. Nagendran, K.K. Dhital, F.J. Moradiellos Diez, C. Knosalla, C.A. Bermudez, S. Tsui, K. McCurry, I.W. Wang, T. Deuse, G. Leseche, P. Thomas, I. Tudorache, C. Kuhn, M. Avsar, B. Wiegmann, W. Sommer, A. Neyrinck, M. Schiavon, F. Calabrese, N. Santelmo, A. Olland, P.E. Falcoz, A.R. Simon, A. Varela, J.C. Madsen, M. Hertz, A. Haverich, and A. Ardehali, Normothermic ex-vivo preservation with the portable Organ Care System Lung device for bilateral lung transplantation (INSPIRE): a randomised, open-label, non-inferiority, phase 3 study. Lancet Respir Med 6 (2018) 357-367.

L. Waters, R. Ben, J.P. Acker, M.P. Padula, D.C. Marks, and L. Johnson, Characterizing the ability of an ice recrystallization inhibitor to improve platelet cryopreservation. Cryobiology (2020).

C.J. Watson, V. Kosmoliaptsis, C. Pley, L. Randle, C. Fear, K. Crick, A.E. Gimson, M. Allison, S. Upponi, and R. Brais, Observations on the ex situ perfusion of livers for transplantation. Am J Transplant 18 (2018) 2005-2020.

D.A. Wharton, P.W. Wilson, J.S. Mutch, C.J. Marshall, and M. Lim, Recrystallization inhibition assessed by splat cooling and optical recrystallometry. CryoLetters 28 (2007) 61-68.

B.A. Whitson, and S.M. Black, Organ assessment and repair centers: The future of transplantation is near. World J Transplant 4 (2014) 40-2.

J.P. Wolanczyk, K.B. Storey, and J.G. Baust, Ice nucleating activity in the blood of the freeze-tolerant frog, Rana sylvatica. Cryobiology 27 (1990) 328-35.

D. Yang, M. Sax, A. Chakrabartty, and C. Hew, Crystal structure of an antifreeze polypeptide and its mechanistic implications. Nature 333 (1988) 232-237.

M.L. Yarmush, M. Toner, J.C. Dunn, A. Rotem, A. Hubel, and R.G. Tompkins, Hepatic tissue engineering. Development of critical technologies. Ann N Y Acad Sci 665 (1992) 238-52.

P. Yi, and G.C. Rutledge, Molecular origins of homogeneous crystal nucleation. Annu Rev Chem Biomol Eng 3 (2012) 157-82.

G. Yu, R. Li, and A. Hubel, Interfacial interactions of sucrose during cryopreservation detected by raman spectroscopy. Langmuir 35 (2018) 7388-7395.

S.O. Yu, A. Brown, A.J. Middleton, M.M. Tomczak, V.K. Walker, and P.L. Davies, Ice restructuring inhibition activities in antifreeze proteins with distinct differences in thermal hysteresis. Cryobiology 61 (2010) 327-34.

K.E. Zachariassen, Physiology of cold tolerance in insects. Physiol Rev 65 (1985) 799-832.

K.E. Zachariassen, The role of polyols and nucleating agents in cold-hardy beetles. J Comp Phys 140 (1980) 227-234.

A.M. Zade-Oppen, Posthypertonic hemolysis in a sucrose system. Experientia 26 (1970) 1087-8.

P.M. Zavos, and E.F. Graham, Effects of various degrees of supercooling and nucleation temperatures on fertility of frozen turkey spermatozoa. Cryobiology 20 (1983) 553-559.

P.M. Zavos, and E.F. Graham, Preservation of turkey spermatozoa by the use of emulsions and supercooling methods. Cryobiology 18 (1981) 497-505.

S.-z. Zhang, X.-y. Yu, and G.-m. Chen, Permeation of dimethyl sulfoxide into articular cartilage at subzero temperatures. Journal of Zhejiang University SCIENCE B 13 (2012) 213-220.

Y. Zhang, G. Ukpai, A. Grigoropoulos, M.J. Powell-Palm, B.P. Weegman, M.J. Taylor, and B. Rubinsky, Isochoric vitrification: An experimental study to establish proof of concept. Cryobiology 83 (2018) 48-55.

M. Zhurova, E.J. Woods, and J.P. Acker, Intracellular ice formation in confluent monolayers of human dental stem cells and membrane damage. Cryobiology 61 (2010) 133-41.

B. Zobrist, C. Marcolli, T. Peter, and T. Koop, Heterogeneous ice nucleation in aqueous solutions: the role of water activity. J Phys Chem A 112 (2008) 3965-75.

Appendix A Transient Loss of Membrane Integrity Following Intracellular Ice Formation in Dimethyl Sulfoxide-Treated Hepatocyte and Endothelial Monolayers

A.1 Introduction

Avoidance of intracellular ice formation (IIF) continues to be guiding principle in modern cryobiology, despite an abundance of literature characterizing conditions that render it innocuous [2; 3; 4; 5; 11; 12; 14; 16; 18; 22; 23; 26; 31]. Minimizing IIF is commonly achieved through the use of permeating cryoprotectants (CPAs), non-permeating CPAs, high nucleation temperatures, slow cooling rates, or sub-zero isothermal holding steps [8; 17; 18]. Each of these methods serve to limit the degree of intracellular supercooling such that equilibration of chemical potential is achieved through osmotic dehydration rather than a cytoplasmic phase transition.

The feasibility of minimizing supercooling is largely dependent on the type of cell as well as the configuration in which it is frozen during cryopreservation. Mammalian cells with a high activation energy for transmembrane water transport, such as hepatocytes and granulocytes, undergo limited freeze-induced dehydration at high sub-zero temperatures following extracellular nucleation [27; 30]. Cell-cell contacts in spheroids, single cell colonies, confluent monolayers, tissue constructs, and complex tissues, can decrease the effective surface area for water transport, which can similarly impose limits on osmotic dehydration [7]. As a result, emphasizing IIF avoidance in these cases may promote injury due to biochemical toxicity bought forth by high concentrations of permeating CPAs or excessive cellular dehydration. Thus, the intrinsic presumption that IIF is lethal becomes problematic when the strategies necessary to avoid IIF are themselves damaging. Such strategies may particularly prove unnecessary when freezing configurations with cell-cell contacts, which have proven to render IIF innocuous [1; 2].

The aim of the present study is to further tackle to the prevailing notion that IIF must be avoided by evaluating if immediate post-thaw assessment of membrane integrity, one of the most commonly used markers for post-thaw cell survival, can underestimate survival outcomes under conditions that promote IIF. There has historically been debate as to whether membrane failure occurs pre- or post-nucleation of intracellular ice [17; 20; 28]. Under the presumption that membrane damage occurs prior to IIF, cases of innocuous IIF would suggest that a ruptured membrane is capable of resealing. Previous studies have demonstrated that this does not in fact occur; however, these evaluations were conducted in the absence of dimethyl sulfoxide (DMSO), a commonly used permeating CPA known to promote thinning and fluidity of the lipid bilayer [1; 13].

A.2 Methods

A.2.1 HepG2 and HUVEC Culture and Monolayer Preparation

HepG2 cells and human umbilical vein endothelial cells (HUVEC), which are respectively used for evaluation of vascular disease and drug toxicity, were utilized for the purposes of this study [10; 15]. HepG2 cells (HB8065, ATCC, Manassas, VA, USA) were cultured in Dulbecco's modified eagle medium (DMEM; Sigma-Aldrich, D1145) supplemented with 10% fetal bovine serum (FBS; F1015, Gibco, Billings, MT, USA) and HUVECs (C2519A, LONZA®, Walkersville, MD, USA) were cultured in endothelial cell growth medium-2 (EGM-2; CC-3162, LONZA®) using previously described culture protocols [10; 15]. Upon reaching 80% confluency, HepG2's were seeded at a density of 40,000 cells/cm^2 onto 12 mm glass coverslips (89015-725, VWR, Radnor, PA, USA) coated with 200 µg/mL type I collagen (5006, Sigma-Aldrich, Oakville, ON, Canada) for 1 h at 22 °C, while HUVECs were seeded at a density of 25,000 cells/cm^2 onto the same type of coverslip coated instead with 2.5 µg/mL of fibronectin (F-1141, Sigma-Aldrich) for 30 min at 22 °C. HepG2 monolayers were cultured for six days to reach 70% - 80% confluency, while HUVECs were cultured for four days to reach 85% confluency. These levels of confluency enabled the formation of cell-cell contacts in both cell types and culture conditions were kept consistent for all experiments in order to limit differences in cell-cell adhesion molecule expression as this is known to affect IIF patterns [1]. Cell passage numbers were 6 for HepG2 cells and 3 for HUVEC cells.

A.2.2 Treatment and Freezing Protocol

Monolayers were incubated with 1.4 M DMSO (CP-100, OriGen Biomedical, Austin, TX, USA) prepared in 1X Dulbecco's phosphate buffered saline (1X DPBS; 14190235, Gibco) for 10 min at 22 °C, while untreated controls were incubated under these same conditions in 1X DPBS. Following treatment, monolayers were transferred to a Linkam BCS196 cryostage (Linkam Scientific Instruments, Tadworth, England) set up on a Nikon Eclipse 80i inverted microscope (Nikon, Tokyo, Japan). Freezing conditions that induced both 100% IIF and 0% IIF were implemented to effectively differentiate between damage caused by IIF and that caused by the extracellular unfrozen fraction. To promote 100% IIF, monolayers were nucleated at -25 °C after being frozen at a rate of 90 °C/min from 4 °C. They were then held for 1 min and thawed at 90 °C/min to 37 °C. This freezing profile was the same for DMSO-treated and untreated conditions;

however, the 0% IIF freezing profiles had to be varied between the treatment conditions due to DMSO-mediated depression of the freezing point. DMSO-treated monolayers were nucleated at -6 °C and held for 1 min to allow the latent heat of fusion to dissipate. They were subsequently frozen at a rate of 5 °C/min to -25 °C, held for 1 min at -25 °C, and then thawed at a rate of 90 °C/min to 37 °C. The untreated condition was instead nucleated at -2 °C and frozen at a rate of 2 °C/min to -25 °C. Nucleation of untreated monolayers below -2 °C promoted IIF in both cell types and nucleation at temperatures above -6 °C did not enable formation of extracellular ice following treatment with 1.4 M DMSO.

A.2.3 Membrane Integrity and Metabolic Activity Assessment

Upon thawing, monolayers were placed into individual wells of a 24-well plate containing 0.5 mL of 1X DPBS for CPA removal. They were then processed for the immediate post-thaw membrane integrity assessments or incubated under standard culture conditions for 24 h. Membrane integrity was evaluated both immediately and 24 h post-thaw through dual fluorescent staining with 50 μM SYTO 13 (S7575, Molecular Probes, Eugene, OR, USA) and 20 μM ethidium bromide (E1385, Molecular Probes) diluted in 1 X DPBS . Staining was performed in the dark for 10 min at 22 °C using 0.15 mL of solution. Coverslips were observed under fluorescence on a Nikon Eclipse 80i inverted microscope (Nikon) and images were captured at 10X magnification using a Hamamatsu digital camera (C4742-80, Hamamatsu, Japan) and NIS elements AR 3.22.14 software (Nikon). Twelve Images were captured at random for each coverslip and processed using the Viability3 program (custom software: Version 3.2, Great Canadian Computer Company, Spruce Grove, AB, Canada) for automated cell counting in order to quantify the number of green and red cells in each given image. Membrane integrity was calculated to determine survival relative to the unfrozen control using equation A.1 (absolute viability) as well as the relative number of live (green) to dead (red) cells using equation A.2.

$$\text{Absolute Viability} = \frac{\text{total number of green cells in experimental condition}}{\text{total number of green cell in unfrozen control}} \times 100 \quad \text{Eq. A.1}$$

$$\text{Relative Viability} = \frac{\text{total number of green cells}}{\text{total number of red cells}} \times 100 \quad \text{Eq. A.2}$$

The alamarBlue™ metabolic activity assay was performed 24 h post-thaw to serve as a more definitive measure of cell survival. In brief, the commercial stock solution was diluted 10-fold

using the growth medium for each respective cell type. 0.6 mL of this working solution was added to each well of the 24-well plate. Absorbance measurements were carried out after a 3 h incubation period by transferring three 0.15 mL aliquots from each well of the 24-well plate to a 96-well plate. A SpectraMax 364 Microplate Reader using SoftMax Pro 5.2.4 software was used to measure absorbance of alamarBlue^{TM} at λ = 570 nm and λ = 600 nm. % reduction of alamarBlue^{TM} was calculated using equation A.3 and normalized to the unfrozen control using equation A.4 [21].

$$\%\ \text{alamarBlue Reduction} = \frac{[(117216)A570nm-(80586)A600nm]\ \text{Experimental Conditions or Positive Control}}{[(155677)A600nm-(14652)A570nm]\ \text{Negative Control}} \quad \text{Eq A.3}$$

$$\text{Normalized Metabolic Activity} = \frac{\%\ \text{alamarBlue Reduction of Experimental Condition}}{\%\ \text{alamarBlue reduction of Positive Control}} \times 100 \quad \text{Eq A.4}$$

A.4 Results and Discussion

Fig. A.1 depicts images taken from representative fields of view, which highlight a profound underestimation of cell survival when conducting immediate post-thaw membrane integrity assessments in confluent HUVEC and HepG2 monolayers treated with 1.4 M DMSO and frozen under conditions that form 100% IIF. Quantifying images taken from three independent replicates revealed the 24 h post-thaw culture period facilitated significant recovery of membrane integrity based on both the absolute ($p < 0.0001$ for both cell types) and relative viability calculations ($p < 0.0001$ for both cell types) (Fig A.2). The levels of survival indicated through this 24 h post-thaw membrane integrity assessment was consistent with the metabolic activity results (Fig. A.3). Interestingly, HUVEC monolayers demonstrated recovery of membrane integrity following the 24 h culture period in the +DMSO -IIF condition ($p < 0.0001$). This requires further investigation as previous literature has indicated that a failure to capture underlying apoptosis combined with a peak in apoptosis and necrosis 12-24 h post-thaw, together facilitate an overestimation of cell survival when performing immediate post-thaw assessments of membrane integrity under freezing conditions that preclude IIF [6].

While it is possible that immediate post-thaw assessment of membrane integrity can underestimate survival in DMSO-treated cells frozen under conditions that preclude IIF, our results implicate both DMSO-treatment and IIF as the main causal factors leading to this erroneous uptake of membrane impermeable dyes (Fig. A.1-A.2). The recovery of membrane integrity in the +DMSO +IIF conditions (increase in absolute viability: 78.5% ± 5.83%; increase in relative viability: 87.8% ± 2.26%) in HUVECs was substantially greater than that seen in the +DMSO -IIF condition

(increase in absolute viability: 53.4% ± 3.01%; increase in relative viability: 26.9% ± 2.25%) (Fig. A.1-A.2). Furthermore, the data suggests a lack of membrane recovery for the +DMSO -IIF condition in HepG2s (absolute viability: $p = 0.14$; relative viability: $p > 0.99$) (Fig. A.2). Both cell types additionally yielded zero membrane intact cells during the pre- and post-culture evaluations for the -DMSO +IIF condition and viability of the -DMSO -IIF conditions did not differ significantly between these two evaluations (Fig. A.1-A.2). While, there was an increase in the relative viability for the HepG2 -DMSO -IIF condition ($p < 0.0001$), the absence of a corresponding increase in absolute viability suggests this increase is primarily due to detachment of dead cells ($p = 0.1063$) (Fig. A.2).

Permeating CPAs, such as DMSO, are known to protect cells from damage that takes place at sub-optimal cooling rates. Thus, it is not surprising that treatment with 1.4 M DMSO significantly enhanced pre- and post-culture membrane integrity of both cell types frozen in the absence of IIF ($p < 0.0001$ for HUVEC absolute and relative viability, HepG2 absolute viability; HepG2 relative viability: $p = 0.0004$). There is, however, generally a lack of clarity regarding the impact of permeating CPAs on the recovery of cells frozen under conditions that promote IIF, with prior evidence indicating both deleterious and beneficial outcomes resulting from their inclusion [9; 25]. Our results indicate a clear benefit to the addition of 1.4 M DMSO under conditions that form 100% IIF in HUVC and HepG2 monolayers as there was no survival in the absence of DMSO (Fig. A.1-A.3). Post-culture assessment of membrane integrity in both HUVECs and HepG2s revealed no significant difference in relative viability between the +DMSO +IIF and +DMSO -IIF conditions. However, the +DMSO +IIF condition saw a significant reduction in absolute viability relative to the +DMSO -IIF condition which infers nucleation of 100% IIF promoted cell detachment (HUVEC: $p = 0.0099$; HepH2: $p = 0.002$). A mismatch between the thermal expansion coefficients of borosilicate glass and ice has proven to promote cell detachment in monolayers frozen with 100% IIF, therefore, modification of the monolayer substrate may minimize this issue [24]. Metabolic activity did not pick up this difference in absolute viability, likely due to a lack of resolution in the assay (HUVEC: $p = 0.51$; HepG2: $p = 0.95$) (Fig. A.3).

The clear protection that DMSO treatment afforded to both HUVEC and HepG2 monolayers that underwent 100% IIF may primarily be the result of a colligative increase in the intra- and extracellular unfrozen fractions, leading to a corresponding decrease in osmotic stress associated

with IIF at any given nucleation temperature [19; 20]. Thus, the protective effect of DMSO in the context of IIF may be a virtue of its ability to render IIF innocuous at increasingly lower nucleation temperatures. Accurate measurements of the intra- and extracellular unfrozen fraction as a function of DMSO concentration and nucleation temperature, followed by assessments to correlate the unfrozen fraction with recovery are warranted to determine if this is the case. Furthermore, a reduction in the degree of intra- and extracellular supercooling at any given temperature would promote ice crystal stability, thus minimizing subsequent damage associated with recrystallization injury [22].

Further investigation of the conditions that cause immediate post-thaw evaluations of membrane integrity to underestimate cell survival is warranted as the ease and efficiency of these evaluations justifies their continued use. Oftentimes this is not problematic considering that DNA integrity, metabolic activity, or functional evaluations would additionally be performed. However, it is easy envision how researchers would turn to optimizing cryopreservation protocols rather than conducting more complex viability assessments when confronted with diminished immediate post-thaw membrane integrity, particularly under the premise that this evaluation typically yields survival overestimates. Considering our results appear to implicate both DMSO treatment and IIF as responsible for promoting a transient loss in membrane integrity, it is valuable to assess whether this occurs in the presence of other commonly used permeating CPAs as well as whether it differs based on CPA concentration. Such evaluations may warrant more quantitative evaluation of the extent of membrane damage using electrometric methods to assess electrolyte leakage or assessment of lactate dehydrogenase release [29]. Conducting a post-thaw time course assessment to evaluate when the membrane regains its semipermeable properties could additionally inform the extent to which the membrane is damaged. Given that this transient loss of membrane integrity is not specific to the cell types, treatment conditions, and freezing conditions implemented in this study, it is it is not unreasonable to assume that this may have helped foster the notion that cryopreservation protocols should consistently be designed to avoid IIF.

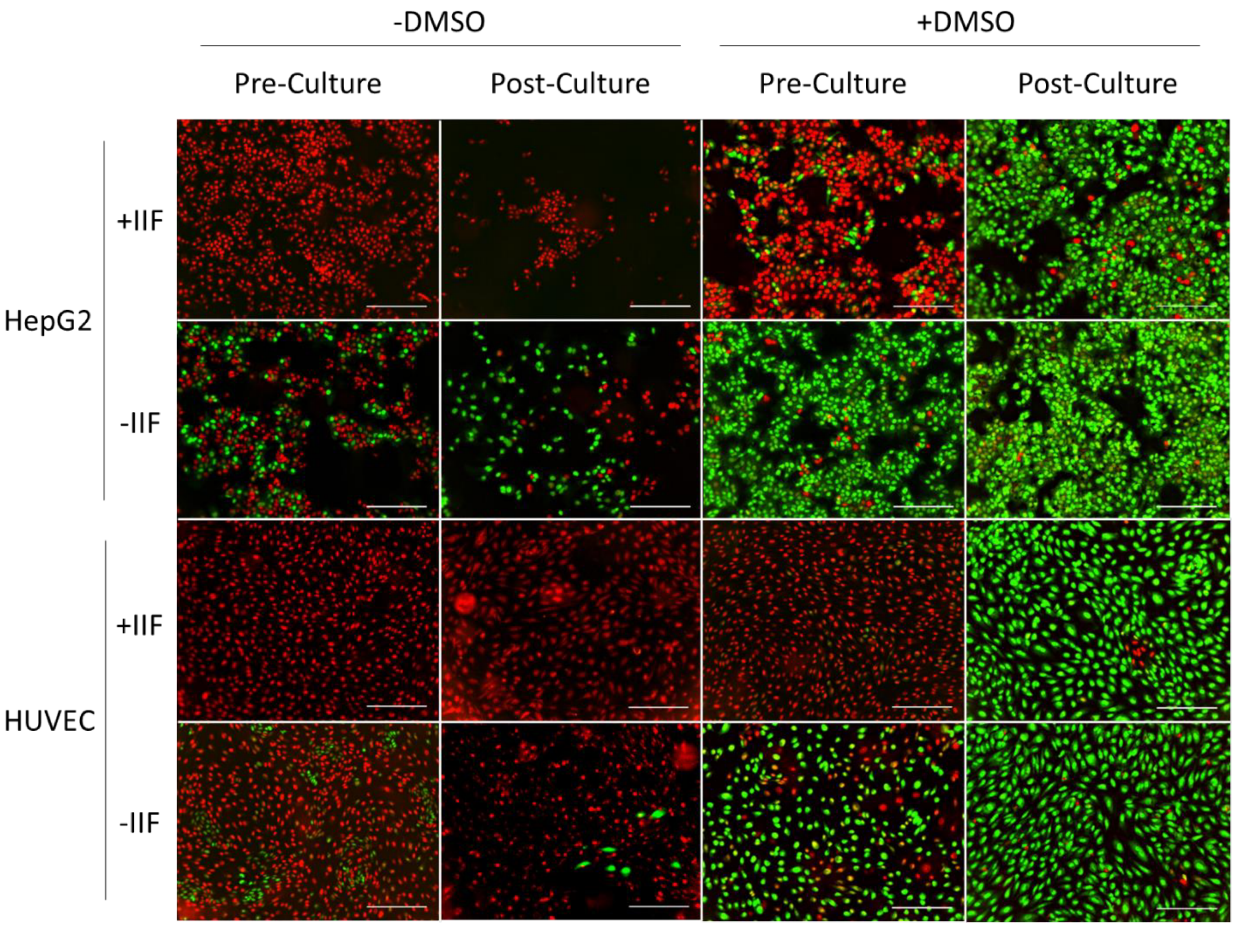

Figure A.1 Post-thaw sample images of HUVEC and HepG2 monolayers. Staining performed with SYTO 13 and EB both immediately after thawing (pre-culture) and after a 24 h period under culture conditions (post-culture). Scale bar = 100 μm

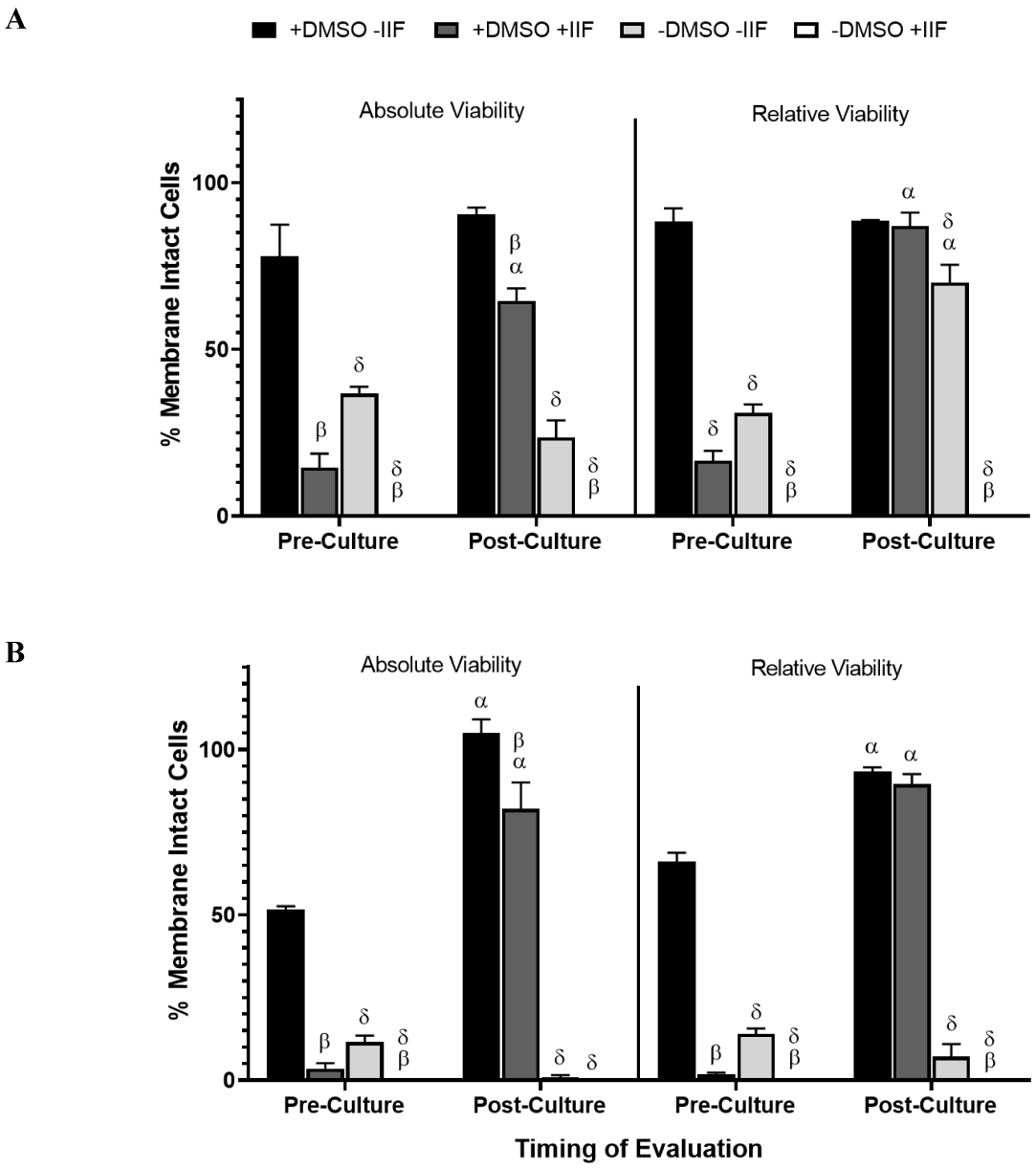

Figure A.2 Quantified pre- and post-culture membrane integrity of (A) HUVEC and (B) HepG2 monolayers treated either with or without 1.4 M DMSO and frozen to -25 °C under conditions that formed either 0% or 100% IIF. Three independent replicates were assessed for each experimental condition with 12 images taken at random per replicate (n = 3). Error bars represent the standard error of the mean between replicates. Significance was calculated using a one-way ANOVA followed by a Tukey's post-hoc test: α – significant difference from pre-culture assessment ($p < 0.05$); β – significant difference from +IIF condition ($p < 0.05$); δ - significant difference from +DMSO condition ($p < 0.05$).

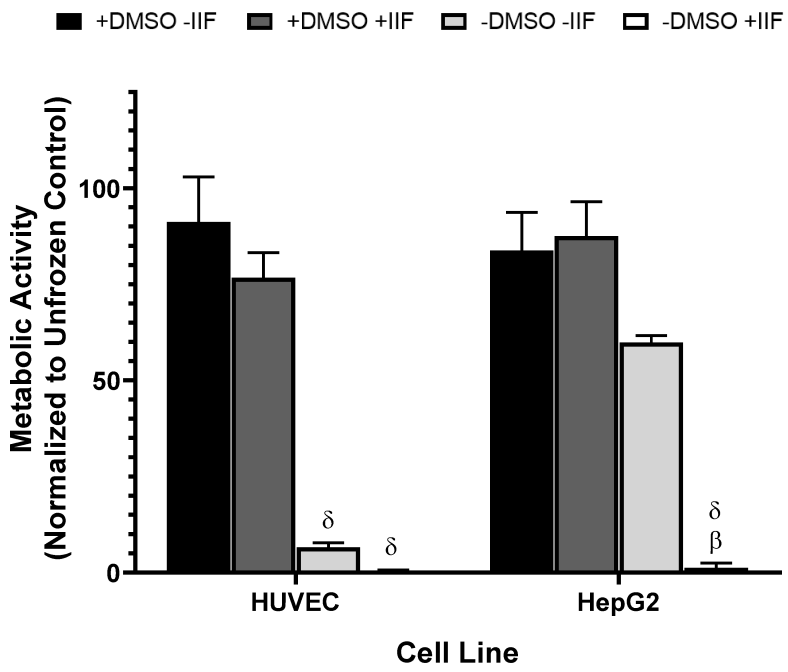

Figure A.3 Metabolic activity of HUVEC and HepG2 monolayers treated either with or without 1.4 M DMSO and frozen to -25 °C under conditions that formed either 0% or 100% IIF. Percent alamarBlue™ reduction for each condition was calculated and values were normalized to an unfrozen control. Error bars represent the standard error of the mean of three samples per condition (n = 3). Significance was calculated using a one-way ANOVA followed by a Tukey's post-hoc test: β – significant difference from +IIF condition ($p < 0.05$); δ - significant difference from +DMSO condition ($p < 0.05$).

A.6 References

[1] J.P. Acker, Innocuous intracellular ice formation : mechanisms and implications [Dissertation], Edmonton, AB: University of Alberta, 2000.

[2] J.P. Acker, and L.E. McGann, Cell-cell contact affects membrane integrity after intracellular freezing. Cryobiology 40 (2000) 54-63.

[3] J.P. Acker, and L.E. McGann, Innocuous intracellular ice improves survival of frozen cells. Cell Transplant 11 (2002) 563-71.

[4] J.P. Acker, and L.E. McGann, Protective effect of intracellular ice during freezing? Cryobiology 46 (2003) 197-202.

[5] E. Asahina, K. Shimada, and Y. Hisada, A stable state of frozen protoplasm with invisible intracellular ice crystals obtained by rapid cooling. Exp Cell Res 59 (1970) 349-358.

[6] J.M. Baust, M.J. Vogel, R. Van Buskirk, and J.G. Baust, A molecular basis of cryopreservation failure and its modulation to improve cell survival. Cell Transplant 10 (2001) 561-71.

[7] J.C. Bischof, C.M. Ryan, R.G. Tompkins, M.L. Yarmush, and M. Toner, Ice formation in isolated human hepatocytes and human liver tissue. ASAIO J 43 (1997) 271-8.

[8] K. Diller, Intracellular freezing: Effect of extracellular supercooling. Cryobiology 12 (1975) 480-485.

[9] K.R. Diller, Intracellular freezing of glycerolized red cells. Cryobiology 16 (1979) 125-31.

[10] M.T. Donato, L. Tolosa, and M.J. Gómez-Lechón, Culture and functional characterization of human hepatoma HepG2 cells, Protocols in In Vitro Hepatocyte Research, Springer, 2015, pp. 77-93.

[11] J. Farrant, and G.J. Morris, Thermal shock and dilution shock as the causes of freezing injury. Cryobiology 10 (1973) 134-140.

[12] J. Farrant, C.A. Walter, H. Lee, and L.E. McGann, Use of two-step cooling procedures to examine factors influencing cell survival following freezing and thawing. Cryobiology 14 (1977) 273-286.

[13] A.A. Gurtovenko, and J. Anwar, Modulating the structure and properties of cell membranes: the molecular mechanism of action of dimethyl sulfoxide. J Phys Chem B 111 (2007) 10453-60.

[14] A. MacKenzie, Death of frozen yeast in the course of slow warming, Ciba Foundation Symposium-The Frozen Cell, Wiley Online Library, 1970, pp. 89-96.

[15] V. Marin, G. Kaplanski, S. Gres, C. Farnarier, and P. Bongrand, Endothelial cell culture: protocol to obtain and cultivate human umbilical endothelial cells. J Immunol Methods 254 (2001) 183-90.

[16] P. Mazur, Equilibrium, quasi-equilibrium, and nonequilibrium freezing of mammalian embryos. Cell Biophys 17 (1990) 53-92.

[17] P. Mazur, Kinetics of water loss from cells at subzero temperatures and the likelihood of intracellular freezing. J Gen Physiol 47 (1963) 347-69.

[18] P. Mazur, The role of intracellular freezing in the death of cells cooled at supraoptimal rates. Cryobiology (1977).

[19] P. Mazur, W.F. Rall, and N. Rigopoulos, Relative contributions of the fraction of unfrozen water and of salt concentration to the survival of slowly frozen human erythrocytes. Biophys J 36 (1981) 653-75.

[20] K. Muldrew, and L.E. McGann, The osmotic rupture hypothesis of intracellular freezing injury. Biophys J 66 (1994) 532-41.

[21] J. O'Brien, I. Wilson, T. Orton, and F. Pognan, Investigation of the Alamar Blue (resazurin) fluorescent dye for the assessment of mammalian cell cytotoxicity. Eur J Biochem 267 (2000) 5421-6.

[22] W.F. Rall, and J. Farrant, Slow warming injury to mouse embryos: Dissociation between the formation of intracellular ice and injury. Cryobiology 16 (1979) 589-589.

[23] W.F. Rall, D.S. Reid, and J. Farrant, Innocuous biological freezing during warming. Nature 286 (1980) 511-514.

[24] T. Rutt, N. Eskandari, M. Zhurova, J.A. Elliott, L.E. McGann, J.P. Acker, and J.A. Nychka, Thermal expansion of substrate may affect adhesion of Chinese hamster fibroblasts to surfaces during freezing. Cryobiology 86 (2019) 134-139.

[25] A. Sakai, Some factors contributing to the survival of rapidly cooled plant cells. Cryobiology 8 (1971) 225-234.

[26] A. Sakai, and K. Otsuka, Survival of plant tissue at super-low temperatures v. An electron microscope study of ice in cortical cells cooled rapidly. Plant Physiol 42 (1967) 1680-94.

[27] G.J. Schwartz, and K.R. Diller, Intracellular freezing of human granulocytes. Cryobiology 21 (1984) 654-60.

[28] M. Toner, E.G. Cravalho, and M. Karel, Thermodynamics and kinetics of intracellular ice formation during freezing of biological cells. J App Phys 67 (1990) 1582-1593.

[29] R.G. Van Buskirk, Viability and functional assays used to assess preservation efficacy: the multiple endpoint/tier approach. Advances in Biopreservation (2006) 123-141.

[30] M.L. Yarmush, M. Toner, J.C. Dunn, A. Rotem, A. Hubel, and R.G. Tompkins, Hepatic tissue engineering. Development of critical technologies. Ann N Y Acad Sci 665 (1992) 238-52.

[31] M. Zhurova, E.J. Woods, and J.P. Acker, Intracellular ice formation in confluent monolayers of human dental stem cells and membrane damage. Cryobiology 61 (2010) 133-41.